Disentangling human degradation from environmental constraints: macroecological insights into the structure of coral reef fish and benthic communities

by

James Robinson
B.Sc., University of Glasgow, 2010
M.Res., University of St. Andrews, 2011

A Dissertation Submitted in Partial Fulfillment of the Requirements for the Degree of

DOCTOR OF PHILOSOPHY

in the Department of Biology

Supervisory Committee

Disentangling human degradation from environmental constraints: macroecological insights into the structure of coral reef fish and benthic communities

by

James Robinson
B.Sc., University of Glasgow, 2010
M.Res., University of St. Andrews, 2011

Supervisory Committee

Dr. Julia Baum, Co-Supervisor
Department of Biology

Dr. Francis Juanes, Co-Supervisor
Department of Biology

Dr. Andrew Edwards, Member
Fisheries & Oceans Canada

Dr. Brian Starzomski, Outside Member
School of Environmental Studies

Dr. Ivor Williams, Outside Member
Pacific Islands Fisheries Science Center

Abstract

Testing ecological theory at macroecological scales may be useful for disentangling abiotic influences from anthropogenic disturbances, and thus provide insights into fundamental processes that structure ecological communities. In tropical coral reef systems, our understanding of community structure is limited to small-scale studies conducted in moderately degraded regions, while larger regional or ocean scale analyses have typically focused on identifying human drivers of reef degradation. In this thesis, my collaborators and I combined stable isotope specimens, underwater visual censuses, and remote sensing data from 43 Pacific islands and atolls in order to examine the relative roles of natural environmental variation and anthropogenic pressures in structuring coral reef fish and benthic communities. First, at unexploited sites on Kiritimati Atoll (Kiribati), isotope estimates indicated that trophic level increased with body size across species and individuals, while negative abundance ~ body size relationships (size spectra) revealed distinct energetic constraints between energy-competing carnivores and energy-sharing herbivores. After demonstrating size structuring of reef fish communities in the absence of humans, we then examined evidence for size-selective exploitation impacts on coral reefs across the Pacific Ocean. Size spectra 'steepened' as human population density increased and proximity to market center decreased, reflecting decreases in large-bodied fish abundance, biomass, turnover rate, and mean trophic level. Depletion of large fish abundances likely diminishes functions such as bioerosion by grazers and food chain connectivity by top predators, further degrading reef community resilience. Next, we considered the relative strengths of abiotic, biotic and anthropogenic influences in determining reef benthic state across spatial scales. We found that from fine (0.25 km^2) to coarse (1,024 km^2) grain scales the phase shift index (a multivariate metric of the relative cover of hard coral and macroalgal) was primarily predicted by local

abiotic and bottom-up influences, such that coral-dominated reefs occurred in warm, productive regions at sites exposed to low wave energy, irrespective of grazing or human impacts. Our size-based analyses of reef fish communities revealed novel exploitation impacts at ocean-basin scales, and provide a foundation for delineating energetic pathways and feeding interactions in complex tropical food webs. Furthermore, we demonstrate that abiotic constraints underpin natural variation among fish and benthic communities of remote uninhabited reefs, emphasizing the importance of accounting for local environmental conditions when developing quantitative baselines for coral reef ecosystems.

Table of Contents

List of Tables

List of Figures

Acknowledgements

Many people have contributed to this work, from mentors and collaborators to colleagues and friends. First, I would like to express my sincere gratitude to Julia Baum for taking me on as a PhD student and guiding my development as a scientist over the past 4 years. Julia's dedicated and hard-working approach towards scientific research has been a constant source of inspiration, and I have benefited greatly from her encouragement and advice on concise writing, critical thinking, and sound (open) science.

It has been a privilege to work with so many talented researchers, who repeatedly challenged me to meet their high standards of ecological research. Ivor Williams is a dependably insightful coral reef collaborator, and I have appreciated his calm, common-sense approach towards analyzing data and writing papers. Andrew Edwards has been a pleasure to learn from and work with, and is a constant reminder that the pursuit of academia is not incompatible with mountain biking. Thanks to Brian Starzomski for providing a terrestrial ecologists' perspective, Lauren Yeager for her reassuring post-doc advice, and Francis Juanes for his down-to-earth academic manner and continued interest in my research and personal well-being.

I would like to acknowledge the efforts of field biologists and coding aces in collecting the data used in this thesis: Kiritimati Island 2011-13 field teams for collecting isotope and census data, particularly Scott Clark, Rowan Trebilco, Adrian Burrill, Jonatha Giddens, Sheila Walsh, Mary-Ann Watson, and Logan Wiwchar; the researchers and staff of the NOAA Coral Ecosystem Program for collecting and sharing Pacific fish and benthic data, particularly Adel Heenan; Jana McPherson and Lauren Yeager for environmental predictor data and important coauthor contributions; Mairin Deith and Jill Dunic for managing isotope and functional trait data; Jamie McDevitt-Irwin and Danielle Claar for git skills and reproducible science inspiration.

I am grateful to have shared workspaces and pub bars with numerous past and present Baum and Juanes lab members. Special mentions to Cameron Freshwater, Mauricio Carrasquilla, Logan Wiwchar, Travis Tai, Justin Suraci, Eric Hertz, Easton White, and Tom Iwanicki for reviewing barely-digestible first drafts, sharing in conference fears, and occasionally fortifying coffee with whisky. In Victoria, thanks to the Island Orphans for adventures, particularly Ben Pacquette-Struger, Kate Donaleshen, and Brian Salisbury.

Finally, I wouldn't have followed an academic path without inspiration and support from an elder generation. Thanks to Richard Robinson, Jean Gordon, Peter Buckle, Jonathan Adams, Diane Williams, and Ken McCulloch for showing me it's not all about the PhD.

To Jean and Richard,

for raising me on Scottish shores and introducing me to foreign ones

Chapter 1 - Introduction

"*Without bold, regular patterns in nature, ecologists do not have anything very interesting to explain.*" Lawton, 1996.

Ecologists have long endeavoured to uncover universal patterns in how individuals and species are organised within communities (Elton 1927; Sheldon et al. 1972; Damuth 1981), among ecosystems (Hutchinson & MacArthur 1959; Peters 1983; Brown 1984) and across biomes (Wallace 1876; Fischer 1961). Numerous fundamental patterns have been described, from the latitudinal diversity gradient (Hillebrand 2004) to species body size distributions (Blackburn & Gaston 1994), and yet many of these phenomena can be explained by multiple competing mechanisms (Rohde 1992; Lawton 1996), while others may be specific to certain systems (Brown & Maurer 1989) or scales (Rahbek 2005; Fisher et al. 2010). Macroecology, the study of species distributions and abundances across large spatial and temporal scales, was developed to address these inconsistencies (Brown & Maurer 1989; Brown 1995). By adopting a 'pseudo-experimental approach' (Kerr et al. 2007) in which statistical associations between ecological patterns across gradients in abiotic and biotic drivers are evaluated in space and time, macroecology aims to unite the linked but distinct processes that determine ecological patterns at local, regional and global scales (Gaston & Blackburn 1999; Lawton 1999). In this way, macroecology may provide insights into the mechanisms underlying fundamental ecological patterns.

As a field, macroecology is represented by a collection of large-scale patterns that can be broadly categorised into species abundance distributions, community and trophic structures, diversity gradients and biogeography, and allometric body size scaling

relationships (Brown 1995; Witman & Roy 2009). Of these patterns, size-based approaches to understanding community and food web structures have proven particularly useful in identifying generalities across terrestrial and aquatic systems (Trebilco et al. 2013; Hatton et al. 2015). Body size is a fundamental ecological trait that, owing to its strong link with individual energetic requirements (Kleiber 1932; Gillooly et al. 2001), underpins numerous allometric size scaling relationships, including physiological rates (Peters 1983), population demography (Savage et al. 2004), and abundance distributions (Damuth 1981; Brown & Gillooly 2003, White et al. 2007). Such patterns in body size allometry have provided a foundation for process-based conceptual models of community organisation (e.g. Brown et al. 2004) that can be applied across ecosystems. Characterizing community structure from a size-based perspective is particularly appropriate in aquatic systems in which gape limitation and ontogenetic niche shifts underpin a strong association between body size and trophic position (Jennings et al. 2001; Riede et al. 2011). Thus, since Sheldon et al.'s (1972) empirical study of plankton size distributions and subsequent prediction that abundance might decrease consistently 'from bacteria to whales', attempts to understand how individuals, species, and assemblages are organised in aquatic systems have typically adopted a size-based approach (e.g. Cyr et al. 1997; Jennings & Blanchard 2004; Yvon-Durocher et al. 2011a). Regular and consistent proliferation of such patterns across ecosystems provide an empirical basis for understanding universalities in community structure, while deviations from predictions present opportunities for understanding mechanisms of abiotic, biotic and anthropogenic control.

By spanning substantial gradients in abiotic conditions, macroecological studies

can be used to identify environmental mechanisms that structure ecosystems. For example, the latitudinal diversity gradient is often linked to an underlying influence of temperature on speciation rates (Rohde 1992), while species distributions are often predicted using bioclimate envelopes that represent a species' fundamental niche (Pearson & Dawson 2003). Consequently, abiotic controls on species biogeographic patterns at regional scales are widely acknowledged (McGill 2010), providing a foundation for understanding how environmental variation also influences species interactions and thus determines higher levels of community organisation (Rooney et al. 2008; Kissling & Schleuning 2015). However, general patterns in community structure, such as size-structured biomass pyramids, are often considered irrespective of abiotic conditions (Peters 1983; Cyr et al. 1997; Reuman et al. 2008; Trebilco et al. 2013; Hatton et al. 2015), despite experimental (Yvon-Durocher et al. 2011b; Dossena et al. 2012) and theoretical (Gilbert et al. 2014; Bruno et al. 2015) studies that suggest both size structure and consumer ~ resource biomass ratios respond strongly to abiotic variation. Empirical studies which link abiotic variation to community-level properties, such as size structure, will address this gap and advance our understanding of environmental constraints on community structure.

In addition to abiotic control, today's ecosystems are influenced by anthropogenic disturbances that operate at large-scales, such as global environmental change (Gaston & Blackburn 1999; Kuhn et al. 2008), habitat fragmentation (Hoekstra et al. 2004), and hunting (Jensen et al. 2012, Darimont et al. 2016). Consequently, macroecological approaches have provided invaluable insights into the impacts of anthropogenic activities on natural systems (Kerr et al. 2007). For example, in the marine realm, dramatic

reductions in the standing stock biomass of marine fishes have provoked shifts in community composition (Myers & Worm 2003; Worm et al. 2005) and trophic control (Worm & Myers 2003; Frank et al. 2005) due to long-term exploitation. Extension of metabolic theory to macroecological scales through size-based models has also identified historic declines in fisheries productivity (Jennings & Blanchard 2004) while revealing mechanisms of energy flux and compartmentation in marine food webs (Jennings et al. 2007; Blanchard et al. 2009). Assessment of exploitation impacts through a theoretical framework has guided the development of size-based indicators for detecting fishing effects across regions and ecosystem types (Bianchi et al. 2000; Jennings & Dulvy 2005; Shin et al. 2005; Nash & Graham 2016) and, more generally, has demonstrated the utility of macroecological tools for evaluating human threats across systems.

As different ecological processes are manifested at specific temporal or spatial scales our interpretation of ecological patterns is implicitly linked to the scale of study. Correspondingly, fine-scale patterns are unlikely to scale up to broad-scale generalisations (Brown & Maurer 1989). For example, biogeographic patterns in species distributions (e.g. Rahbek & Graves 2000) and experimental studies of trophic control (e.g. Paine 1966) indicate that abiotic influences are generally dominant over large spatial and temporal scales whereas biotic influences - interactions between species and individuals - operate over shorter time scales in smaller localities (Wiens 1989; Levin 1992; McGill 2010). Fine-grain local processes can be isolated from large-grain regional processes by combining remote sensing data with large ecological monitoring datasets to assess the relative roles of abiotic and biotic drivers (Wiens 1989; Rahbek 2005; Cohen et al. 2016). Recently, several such empirical analyses of bird assemblage distributions have

suggested that biotic influences remain important at large spatial scales (Gotelli et al. 2010; Belmaker et al. 2015) though, crucially, scale-dependence of specific biotic processes such as competition or predation remains unclear. Such studies provide motivation for further consideration of the strength of biotic influences across regions. Similar debate over the relative roles of global and local anthropogenic impacts in altering community composition (Vellend et al. 2013; Dornelas et al. 2014; Bruno & Valdivia 2016) can be addressed by examining associations between human activities and ecological communities at a range of spatial scales.

Our understanding of the processes that structure coral reef fish and benthic communities is particularly tightly linked to the scale of observation. Experimental and observational studies have provided insights into the small-scale processes that structure fish and benthic communities where, for example, grazing control by herbivorous fishes influences benthic state (Mumby et al. 2007; Burkepile & Hay 2008), large predators link pelagic and benthic food chains (McCauley et al. 2012), and coral architectural complexity mediates survival of small-bodied fish species (Alvarez-Filip et al. 2011). At broader spatial scales, syntheses of small-scale datasets have enabled ecologists to adopt a macroecological approach to understanding coral reef ecology. For reef fishes, large-scale studies have identified spatial differences in assemblage diversity between biogeographic regions (Parravicini et al. 2013; Mouillot et al. 2014; Bender et al. 2016), quantified metabolic scaling relationships (Barneche et al. 2014), and predicted extinction risks (Graham et al. 2011). For reef benthic organisms, cross-region analyses have revealed major biophysical influences on coral and algal abundances (Jouffray et al. 2015; Williams et al. 2015b), and provided new perspectives on the resilience of

Caribbean and Indo-Pacific systems (Roff & Mumby 2012). Thus, large-scale reef monitoring datasets provide opportunities for understanding environmental controls on community organisation by expanding small-scale community-level patterns up to regional and ocean-basin scales.

In addition to spanning abiotic gradients, macroecological reef datasets often encompass substantial gradients in anthropogenic presence, ranging from remote, pristine atolls to heavily-degraded reefs. Human impacts are pervasive and damaging in reef ecosystems (Hughes et al. 2003; Bellwood et al. 2004; Harborne et al. 2017) and, consequently, particular attention is devoted to studies understanding the drivers of coral reef degradation. Spatial or temporal comparisons of site-level data within historically-exploited regions provide substantial evidence that human-associated reefs support depleted levels of fish biomass (Mora 2008; McClanahan & Graham 2005), lower coral cover (Hughes 1994; Hughes et al. 2003; Wilson et al. 2010), flattened structural complexity (Alvarez-Filip et al. 2009) loss of top predator species (Newman et al. 2006; Ward-Paige et al. 2010b), and potentially transition from coral- to algal-dominated benthic states (Hughes 1994; Bellwood et al. 2006).

Though these patterns are somewhat typical across coral reef regions, macroecological approaches can offer insights into meaningful baselines of reef ecosystem health by accounting for spatial variation in exploitation histories and natural abiotic variability simultaneously (Knowlton & Jackson 2008). For example, global syntheses have provided quantitative predictions of unexploited biomass levels (MacNeil et al. 2015) and assessed degradation in benthic community states across regions (Bruno et al. 2009; Bruno & Valdivia 2016). However, as these studies are often focused on

documenting ongoing human-associated declines in reef condition, the relative contributions of abiotic and biotic factors to regional variability have generally remained unexplored. Furthermore, despite several recent global and ocean-basin analyses of patterns in total fish biomass (Mora 2008; MacNeil et al. 2015; Williams et al. 2015a; Cinner et al. 2016), our understanding of impacts on aspects of community and trophic structure is largely limited to analyses across small islands chains or groups (Graham et al. 2005; Wilson et al. 2010) or within regions (Mora 2008; McClanahan et al. 2011, 2015). Thus, nuanced understanding of human impacts requires a disentangling of local stressors from global patterns, which may be achieved by accounting for differences in abiotic conditions and biotic influences.

Thus, despite recent macroecological advances, our understanding of large-scale patterns of reef fish and benthic communities is lacking in several key areas. First, our understanding of macroecological patterns in reef fish community structure rarely extends beyond analyses of variation in total fish biomass (Mora et al. 2011; MacNeil et al. 2015) or the biomass of major trophic groups (McClanahan et al. 2015; Williams et al. 2015a). As a result, subtler shifts in relative abundances of species and body sizes and associated changes to energetic and functional properties may remain undetected. Second, although the importance of abiotic drivers in determining reef biogeography (Parravicini et al. 2014) is widely acknowledged, their effect on reef fish community structure is rarely considered (though see Barneche et al. 2014 and Williams et al. 2015a). Similarly, biophysical forcing of benthic communities has been widely documented at both island (Gove et al. 2015) and regional scales (Williams et al. 2015b), but these influences have not been assessed in the context of strong anthropogenic pressures.

Underlying both of these issues is a failure to connect large-scale patterns in reef fish and benthic communities with macroecological patterns in other systems, which would contribute to our understanding of universal patterns in size distributions, abiotic control, anthropogenic influences, and scale dependence. To address these gaps, I adopt a macroecological approach to examine the relative roles of abiotic, biotic and anthropogenic influences in determining coral reef fish and benthic community structure.

In this dissertation, my collaborators and I utilise underwater visual census data collected across 43 Pacific islands to examine reef fish community size structure across pristine and exploited reefs, and determine the dominant drivers of reef benthic communities across spatial scales. In Chapter 2, we combine stable isotope samples with abundance data to examine fundamental patterns in size structuring of coral reef fish communities on Kiritimati Atoll. We show, for the first time, that reef fish abundances and trophic positions scale predictably with body size. Reef fish allometry was, however, dependent upon methods of energy acquisition: herbivores had relatively greater abundances at large body sizes than did carnivores, consistent with predicted differences in the energetic constraints on size structure between individuals sharing energy sources (i.e. herbivores) and those competing for prey (i.e. carnivores) (Brown & Gillooly 2003). By analysing data collected from a system undisturbed by human activity, we provide an empirical foundation for further application of size-based theory to reef fish communities.

In Chapter 3, we scale up from Kiritimati Atoll to the Pacific Ocean to examine the impacts of exploitation on reef fish community size structure and biomass across 38 US-affiliated islands. From uninhabited pristine atolls to degraded population centres, reef fish community size structure 'steepened' with increasing proximity to population

centre and human population density, indicating that selective exploitation of large reef fishes degrades community structure. Size-specific degradation implies that community-level traits, such as the rates of productivity and biomass turnover, are reduced in exploited reefs. Furthermore, the removal of large-bodied predators that connect pelagic and benthic ecosystems and large-bodied grazers that control algal abundances may hasten the loss of important ecosystem functions.

Ocean-basin scale links between benthic community composition and grazing populations are, however, less clear. Comparisons of protected and exploited reefs indicate that herbivorous fishes provide crucial grazing control of algal organisms that promotes coral recruitment and confers ecosystem resilience to large-scale physical disturbances (Mumby et al. 2007; Nash et al. 2015) but, recently, examination of remote-sensing data suggests that abiotic controls are also important determinants of benthic community structure (Gove et al. 2015; Williams et al. 2015b). In Chapter 4, we evaluate the relative strengths of abiotic, biotic (i.e. grazing), and anthropogenic covariates in predicting the relative cover of hard coral and macroalgae across 7 spatial scales at 42 Pacific Islands. We show that abiotic drivers are the primary influence on benthic community composition across the Pacific Ocean, irrespective of the scale of analysis. Grazing biomass of scraper and excavator functional groups also promoted shifts towards coral-dominance, but only at very low biomass levels across large spatial resolutions. In contrast, proxies for human influence on reef benthos were relatively unimportant, possibly due to our limited ability to capture anthropogenic water quality impacts with population-based disturbance metrics.

In sum, this thesis aims to provide novel insights into the processes that structure

coral reef fish and benthic communities at macroecological scales, and advance our understanding of anthropogenic impacts in these vulnerable ecosystems. In an era of unprecedented environmental change, it is critically important that ecologists generate quantitative predictions of the relative contributions of abiotic, biotic and human drivers in shaping ecological communities across scales. To that end, the macroecological approach presented here illustrates a quantitative framework for analysing large-scale monitoring datasets that may be adapted and applied to other ecosystems.

Chapter 2 – Trophic roles determine reef fish size structure

Adapted from: James P.W. Robinson[1] & Julia K. Baum[1]. (2016) *Canadian Journal of Fisheries & Aquatic Sciences*, 73(4), 496-505.

[1]Department of Biology, University of Victoria, PO BOX 1700 Station CSC, Victoria British Columbia, V8W 2Y2, Canada

Author contributions: J.K.B. conceived of, designed the study and provided the data. J.P.W.R. and J.K.B. developed the analytical methods, J.P.W.R. conducted the data analyses and wrote the manuscript with input from J.K.B.

2.1 Abstract

Relationships between abundance ~ body size and trophic position ~ body size can reveal size structuring in food webs, and test ecological theory. Although there is considerable evidence of size structuring in temperate aquatic food webs, little is known about the structure of tropical coral reef food webs. Here, we use underwater visual census data and nitrogen stable isotope analysis to test if coral reef fish communities are 1) size structured and 2) follow metabolic scaling rules. Examining individuals from over 160 species spanning four orders of magnitude in body size, we show that abundance scaled negatively with body size and, as predicted, individuals sharing energy through predation (carnivorous fishes) scaled more steeply than those individuals sharing a common energy source (herbivorous fishes). Estimated size spectra were, however, shallower than predicted by metabolic theory. Trophic position scaled positively with body size across species and across individuals, providing novel evidence of size structuring in a diverse tropical food web. Size-based approaches hold great promise for integrating the complexities of food webs into simple quantitative measures, thus providing new insights into the structure and function of aquatic ecosystems.

2.2 Introduction

Elucidating the structure of natural food webs can provide fundamental insight into ecosystem dynamics, including energy fluxes (Lindeman 1942; Rooney et al. 2008), trophic cascades (Bascompte et al. 2005; Tunney et al. 2012), and potentially the mechanisms underlying ecosystem stability (May 1973; Rooney & McCann 2012). General patterns relating to body size may be of particular importance as individual

metabolic rates and, thus, many important biological processes vary consistently with body size (Peters 1983; Brown et al. 2004). In size-structured food webs, predators are typically larger than their prey (Elton 1927; Brose et al. 2006) and abundance is predicted to scale with body size due to energetic constraints (Brown & Gillooly 2003). Specifically, when individuals share a common energy source, abundance is predicted to scale with body mass (M) as $M^{-3/4}$ (the energetic equivalence hypothesis) (Brown & Gillooly 2003), whereas when individuals compete for energy through predation at multiple trophic levels, abundance is further constrained by inefficient energy transfer across trophic levels and predicted to scale as M^{-1} (trophic transfer correction) when the predator–prey mass ratio is 104 and transfer efficiency is 10% (Jennings & Mackinson 2003; Trebilco et al. 2013). Size structuring in aquatic food webs is driven by two mechanisms that reflect size-based feeding among individuals: first, gape limitation restricts the size of prey that many aquatic species can consume (Brose et al. 2006; Barnes et al. 2010), and second, ontogenetic diet shifts often lead to increases in trophic position as individuals grow (Mittelbach & Persson 1998). As a result, trophic position is often positively related to body size in aquatic food webs both at the species level (Brose et al. 2006) and at the individual level (Jennings et al. 2001).

Size structuring of abundance and individual trophic position has been clearly demonstrated in both temperate freshwater (Mittelbach & Persson 1998; Cohen et al. 2003) and marine (Jennings et al. 2001; Jennings & Mackinson 2003) food webs. Similarly, metabolic scaling predictions (Brown & Gillooly 2003) have been broadly validated in freshwater (Reuman et al. 2008) and marine (Jennings & Mackinson 2003) food webs. However, equivalent tests of size structuring in tropical systems are few, and

tests of metabolic predictions are lacking entirely. One study of a tropical riverine food web, which found that trophic position was unrelated to body size despite a significant positive correlation between mean predator body size and prey size (Layman et al. 2005), concluded that the broad range of primary consumer body sizes in their system accounted for this difference from the structure of temperate food webs. However, community-wide analyses of tropical size structure remain relatively unexplored.

On tropical coral reefs, the application of sized-based approaches has been restricted to observations of body size distributions in degraded regions or to diet analyses of individual species. For example, size spectra — a widely used form of individual abundance – body size relationship — have been used to describe reef fish community structure along gradients of fishing effort (Dulvy et al. 2004; Wilson et al. 2010) and habitat complexity (Alvarez-Filip et al. 2011). Though consistent with size-structured abundances, size spectra have typically been fitted to narrow body size ranges (10–60 cm) and used to detect community change rather than to delineate trophic structure. Similarly, tests of ontogenetic diet shifts often focus on intraspecific relationships for single or few species (Greenwood et al. 2010; Plass-Johnson et al. 2012; Hilting et al. 2013) and thus fail to examine size-based relationships at the community level.

Attempts to infer food web structure through body size relationships should also account for distinct feeding strategies within the same community size spectrum. Metabolic theory predicts that abundance – body size relationships are dependent on how energy is utilized within a community (Brown and Gillooly 2003). For example, in the North Sea food web, the size spectrum of the benthic community that feeds on a shared

energy source is shallower than the predation-based pelagic community size spectrum (Maxwell & Jennings 2006; Blanchard et al. 2009). Distinct trophic pathways also are expected in coral reef ecosystems where, specifically, herbivorous and detritivorous fishes share benthic material (Dromard et al. 2015) while planktivorous fishes derive energy from pelagic sources (Wyatt et al. 2012). Small- to medium-sized mesopredator fishes feed on reef fish and invertebrate species, thus accessing benthic and pelagic energy sources within the reef habitat and competing across trophic levels (Rogers et al 2014), while large predatory reef fish may forage more widely than mesopredators and couple pelagic open-ocean and benthic reef habitats (McCauley et al. 2012; Frisch et al. 2014). By considering size-based patterns within the distinct trophic pathways of herbivores and carnivores, we can examine food web structure in the context of metabolic predictions.

Here, we capitalize on the opportunity to sample a minimally impacted coral reef to empirically test the hypotheses that coral reef food webs are size structured and fit predictions from metabolic theory. We combine visual-census data with stable isotope samples from Kiritimati, a remote atoll in the central equatorial Pacific Ocean, to examine the food web structure of a diverse tropical fish community spanning four orders of magnitude in body mass. We expected negative abundance – body size relationships and positive trophic position – body size relationships, consistent with size structuring. We also expected steeper body size relationships for both trophic position and abundance in a predation-based community (carnivores) relative to an energy-sharing community (herbivores).

2.3 Methods

2.3.1 Study site and data collection

We examined a minimally disturbed coral reef fish community on Kiritimati (Christmas Island) in the equatorial Pacific Ocean (Fig. 2.1). Kiritimati supports a population of at least 5500 people that is concentrated around several villages on the northwest coast (Kiribati National Statistics Office 2012). Subsistence fishing is the primary human impact on the atoll and has been associated with decreases in reef fish biomass and top predator abundance (Sandin et al. 2008). Fishing activities are, however, mostly concentrated around the villages on the northwest coast, whereas the reefs off the north, east, and south coasts are relatively undisturbed (Walsh 2010; Watson et al. 2016). The northwest coast of Kiritimati is also subject to oceanic upwelling of nutrients, but industrial and agricultural nutrient runoff is virtually nonexistent around the atoll (Walsh 2010). We enumerated and sampled coral reef fishes at 14 minimally disturbed sites on Kiritimati's north and east coasts (Fig. 2.1) to reduce potentially confounding effects of fishing and nutrient inputs on trophic structure (Post 2002).

To quantify coral reef fish community structure, fish abundance and size data were recorded during SCUBA underwater visual censuses (UVC) at shallow forereef sites (n = 14, 10–12 m depth) around Kiritimati in July and August of 2011 and 2013 (Fig. 2.1). During each census, two experienced scientific divers identified, counted, and sized (total length, to the nearest centimetre) reef fishes by swimming in tandem along 25 m long belt transects; transect bearings were determined haphazardly such that they remained within the 10–12 m depth isobath. On each transect, fishes ≥ 20 cm total length were counted along the transect in an 8 m wide strip before counting fishes < 20 cm total length along the reverse direction ina4m wide strip. Three transects, each separated by 10

m, were surveyed at each site during each UVC such that the total area surveyed per UVC was 600 m^2 (i.e., 3 × 25 × 8 m) for large fishes and 300 m^2 for small fishes. Before analyzing the UVC data, we standardized the sampling area by doubling all counts of the small fishes (< 20 cm) for each transect. Each site was surveyed once in 2011 and twice in 2013, all during daylight hours. All surveys were conducted by only four divers, with a single diver participating in every survey. To reduce observation error, for two days on Kiritimati immediately before beginning visual censuses, divers re-familiarized themselves with fish species identification, as well as with underwater size estimation, using PVC objects of fixed sizes (Bell et al. 1985); divers typically could estimate fish lengths with minimal error (e.g., ±3%). Fish length estimates were converted to body mass (grams) using published species-specific length–weight relationships (Kulbicki et al. 2005; Froese & Pauly 2014).

To quantify coral reef trophic structure, we collected specimens of the most abundant fish species on Kiritimati (as determined by UVCs conducted in 2007 (Walsh 2010) and 2009) for each of the five major putative functional groups (described below; Table 2.1). For each species, we aimed to collect individuals spanning the entire species' body size range, with a minimum of three individuals in each $\log_2$ mass bin. In July–August of 2011 and 2012, divers captured fish using a combination of custom-built microspears, pole spears, and spear guns at shallow forereef sites (n = 10, 8–12 m depth). Fish were captured opportunistically, and the number of specimens per site varied from 6 to 79 (mean = 34). Specimens were immediately put on ice until dissection later that evening (typically 4–8 h between collection and dissection). Prior to dissection, each individual was photographed, weighed, and measured to the nearest millimetre with

vernier calipers (for standard, fork, and total length). We then excised a small sample (10 g) of dorso-lateral white muscle tissue from each fish before freezing at −20 °C. Samples were kept frozen with dry ice for transport from Kiritimati to the University of Victoria and then stored at −20 °C until processing.

Each white muscle tissue sample was rinsed with de-ionized water, dried at 60 °C for 48 h, and ground to a powder with a mortar and pestle. Tissue samples were weighed to 10 mg and placed into a tin capsule before analysis of nitrogen stable isotope concentrations at the Mazumder laboratory (Department of Biology, University of Victoria, British Columbia, Canada). Relative nitrogen content was estimated by continuous flow isotope ratio mass spectrometer and reported in parts per million relative to atmospheric N^2 ($\delta^{\delta 15N}$).

2.3.2 Coral reef fish functional groups and trophic pathways

We assigned each fish species recorded in our underwater visual censuses to one of five functional groups distinguished by their diet preferences following Deith (2014) (Table 2.1). We note that species within the “herbivore” functional group can feed on both plant material and detritus. Gut content analyses of our specimens were used to confirm the functional group of each species. To account for differences in energy acquisition within the fish community, we aggregated our visual-census and isotope data into two groups, carnivores and herbivores (Table 2.1). We hypothesized that planktivores, benthic invertivores, corallivores, and piscivores compete for energy in a group that is structured by predation (as in Rogers et al. 2014), whereas herbivorous and detritivorous species compete for a shared energy source of plant material and detritus in a separate herbivore group (Choat 1991). In our UVC data, nine species were classed as

omnivores (Deith 2014). Because omnivores feed on both plant and animal material, these species did not fit into either trophic pathway and so were omitted from all analyses. Omnivores comprised only 8.4% of the numerical abundance of fishes in our UVC surveys, and their inclusion as either herbivores or carnivores did not qualitatively change our results (Appendix A).

2.3.3 Abundance – body size analyses

In aquatic systems, the relationship between individual abundance and body size (or size spectrum) has typically been estimated on a logarithmic scale as the slope of the linear regression fit to abundance data binned into body size classes (e.g., Jennings et al. 2001; Jennings & Mackinson 2003). However, recent studies have recognized that rather than forming a bivariate relationship, these types of data follow a frequency distribution (i.e., of the number of individuals at each size) and that binning-based methods yield biased slope estimates (Edwards 2008; White et al. 2008). As such, we examined the size structure of fish abundances by fitting the visual-census body mass data to a bounded power law distribution:

$$(b+1)(x_{\max}^{b+1} - x_{\min}^{b+1})^{-1} x^{b} \qquad \text{Eq. 2.1}$$

where $x_{\min}$ and $x_{\max}$ are the minimum and maximum observed body masses, respectively, and the exponent b describes the relative abundance of different body sizes (White et al. 2008). We used maximum likelihood methods to estimate b with a 95% confidence interval (CI) (Edwards et al. 2012).

Interpretations of how empirical size spectra relate to theoretical metabolic predictions can be confounded by the method used to estimate the slope. Here, we explain how our estimates of b relate to Brown and Gillooly's (2003) theoretical

predictions and to the empirical estimates of others. First, our maximum likelihood approach treats untransformed body size data as a continuous variable, whereas metabolic theory describes abundance – body mass relationships across logarithmic size bins (Brown et al. 2004). As outlined by Reuman et al. (2008), this implies that Brown & Gillooly's (2003) predicted slopes will be one unit shallower than the scaling exponent of a power law distribution (Andersen & Beyer 2006). That is, the predicted abundance – body mass scaling exponents are $b = -1.75$ under the energetic equivalence hypothesis and $b = -2$ with the trophic transfer correction (Trebilco et al. 2013) rather than -0.75 and -1, respectively. Second, size spectra slopes are typically estimated empirically using a simple logarithmic binning method that also estimates a shallower slope. Here, $b + 1$ is analogous to a size spectrum slope estimated with a regression of numerical abundance against the midpoints of size bins on a log–log scale (Reuman et al. 2008; White et al. 2008) but is an unbiased estimate of the relationship. Thus, previous empirical tests of theoretical predictions (e.g., Jennings & Mackinson 2003; Blanchard et al. 2009) can also simply be corrected (true b = slope – 1) to serve as a useful guideline for interpreting the slopes of our community size spectra.

Here, all observed body masses > 1 g were summed across visual census sites to fit the size spectrum of (i) the full reef fish community and (ii) each putative trophic pathway (carnivores and herbivores). We tested the robustness of our results in several ways (Appendix A). First, we examined the potential influences of year and observer by fitting separate size spectra for each year (2011, 2013) and for each dive team (n = 3). Second, although our survey sites were selected to minimize fishing effects on reef trophic structure, we recognize that sites on Kiritimati's north coast may experience light

fishing pressure. To test for potential fishing effects, we removed sites from the north coast that are nearest to Kiritimati's population centres and refitted spectra and also compared size spectra for North vs. East coast sites. Third, we tested the effect of fitting different body size ranges on exponent estimates, thus excluding either the smallest fishes (because our UVCs may have undersampled them) or the largest fishes (because these may be targeted by fishers).

2.3.4 Trophic position estimation

We assigned all fish specimens to $\log_2$ mass bins (grams) and converted the $\delta^{15}N$ values of each individual to trophic position. $\delta^{15}N$ of an organism's tissue reflects its diet, and given that $\delta^{15}N$ increases by a known discrimination factor ($\Delta\delta^{15}N$) between predator and prey, $\delta^{15}N$ can be used as a proxy for trophic position (Post 2002). $\Delta\delta^{15}N$ is commonly set at 3.4‰, although recent work has revealed that $\Delta\delta^{15}N$ decreases with the $\delta^{15}N$ of an organism's diet such that upper trophic positions may previously have been underestimated (Caut et al. 2009; Hussey et al. 2014). We estimated carnivore trophic position using Hussey et al.'s (2014) scaled method, which accounts for variation in $\Delta\delta^{15}N$ due to dietary $\delta^{15}N$:

$$TP_{scaled} = TP_{base} + \frac{\log(\delta^{15}N_{\lim} - \delta^{15}N_{base}) - \log(\delta^{15}N_{\lim} - \delta^{15}N_{fish})}{k} \quad \text{Eq. 2.2}$$

This method was developed in a meta-analysis of experimental isotope studies of marine and freshwater fishes in which $\delta^{15}N_{lim}$ (21.926) and k (0.315) are derived from the intercept and slope of the relationship between ΔN and dietary $\delta^{15}N$ (Hussey et al. 2014). Trophic position (TP) was estimated relative to the $\delta^{15}N$ of a baseline organism, where TPbase was set to 3 and $\delta^{15}N_{base}$ was the mean $\delta^{15}N$ of the smallest planktivore species

that we sampled on Kiritimati (*Chromis vanderbilti*, δ^{15}Nbase = 10.26, mass = 0.1 g). Herbivores are known to fractionate differently than carnivores, with recorded $\Delta\delta^{15}$N values ranging from −0.7‰ to 9.2‰ (Zanden & Rasmussen 2001). In herbivorous reef fish, substantially higher feeding and excretion rates are required to subsist on low-energy algal food sources, driving higher $\Delta\delta^{15}$N rates ranging from 2.79‰ to 7.22‰ (Mill et al. 2007). We found no evidence of herbivore $\Delta\delta^{15}$N varying with dietary δ^{15}N. Instead, we used published $\Delta\delta^{15}$N estimates (Mill et al. 2007) to calculate a mean δ^{15}N of herbivorous reef fish (4.778‰) before calculating individual trophic position with an additive approach (Eq. 2.3) following Post (2002) and Hussey et al. (2014):

$$TP_{additive} = TP_{base} + \frac{\delta^{15}N_{fish} - \delta^{15}N_{base}}{4.778} \quad \text{Eq. 2.3}$$

TP_{base} was set to 2 and $\delta^{15}N_{base}$ was the mean δ^{15}N of the smallest herbivore species (*Centropyge flavissima*, $\delta^{15}N_{base}$ = 12.21, mass = 6.5 g).

2.3.5 Trophic position – body size analyses

Although species-level predator–prey mass ratios are generally positive (Brose et al. 2006), others have suggested that when ontogenetic niche shifts are prevalent, size structuring should operate most strongly at the individual level (Jennings et al. 2001). As such, we conducted trophic position – body size analyses at the species level (i.e., "cross-species approach" *sensu* Jennings et al. 2001) and at the individual level to test the hypothesis that coral reef food webs are size structured and, if so, at what level of organization is size structuring evident. Phylogenetic patterns in trophic position – body size relationships can result in non-independence of data points that can bias analyses of community structure (Jennings et al. 2001; Romanuk et al. 2011). To account for this

non-independence, we used mixed models to fit random structures that accounted for variation shared between individuals of the same species and (or) family (detailed below). First, in the species-based analyses, we used linear mixed effects models to examine the relationship between the mean trophic position of each species and the maximum observed $\log_2$ body mass of each species across the entire community, while accounting for phylogenetic relatedness of species within families. Specifically, we fitted family as a random effect to account for non-independence of trophic position – body mass relationships within families and then used the Akaike information criterion for small sample sizes (AICc) to select the optimum random effects structure (random slope or random intercept model) (Zuur et al. 2009). Second, in the individual-based analyses, we examined the relationship between the trophic position of individual fishes and their $\log_2$ body mass class. To account for the non-independence of individual fishes within species and species within families, we included both species and family as random effects in a linear mixed effects model and again used AICc to select the optimum random effects structure. In both the species- and individual-based analyses, we tested for differences in slopes of trophic position – body mass relationships between our two putative trophic pathways, carnivores and herbivores, by assessing the significance of trophic pathway as an interaction term with AICc (Burnham & Anderson 2002). We measured the goodness-of-fit of the fixed covariates in each analysis by estimating the marginal R^2 of each model (Nakagawa & Schielzeth 2013). Finally, we conducted sensitivity analyses to test the robustness of our results to different herbivore fractionation values ($\Delta\delta^{15}N$) (Table A2.1) and different sampling locations (Figs. A2.1, A2.2, Table A2.2). We note that there are multiple families included in each trophic pathway (Table 2.1). Thus, although no family

contains individuals from both trophic pathways, it seems likely that any observed differences in slopes can be attributed to true differences between herbivores and carnivores (as opposed to being conflated with phylogeny).

All abundance – body size and trophic position – body size analyses were performed in R (version 3.0.2; R Core Team 2013) using the packages MuMIn (Barton 2013) and nlme (Pinheiro et al. 2015). The R code used in our analyses is available on Github (https://github.com/baumlab/Robinson-Baum_2016_CJFAS).

2.4 Results

2.4.1 Abundance – body size relationships

In total, 28,831 individual fish from 163 species, ranging in body mass from 1.02 g to 23.04 kg were enumerated in our underwater visual censuses. Of these, 3,602 were herbivores from 44 species that ranged in size from 1.02 g to 5.87 kg, and 25,229 were carnivores from 119 species that ranged in size from 1.03 g to 23.04 kg. Mean individual size of the herbivore group (mean mass = 230.63 g, SE = 14.72) was greater than the carnivore group (mean mass = 188.83 g, SE = 16.78). These average sizes reflect the high proportion of small planktivores in the carnivore group, rather than a disproportionate abundance of large herbivores. For example, for fishes above 20 g, mean carnivore mass was 488.74 g and mean herbivore mass was 401.89 g.

When all individual fishes from the full reef fish community were considered together, the size spectrum had a negative slope (b = -1.580, 95% CI = -1.585, -1.576), indicating a strong decrease in abundance with increasing body size, consistent with size structuring of community abundances. Size spectrum slopes were, however, distinct for herbivore and carnivore trophic pathways (Fig. 2.2), with the slope of the herbivore group

(b = -1.270, 95% CI = -1.281, -1.260) significantly shallower than that of the carnivore group (b = -1.644, 95% CI = -1.649, -1.638). In the context of metabolic predictions, the herbivore slope (b = -1.270) is shallower than predicted for species within one trophic level (~ -1.75) and the carnivore slope (b = -1.644) is shallower than predicted for species across trophic levels (~ -2) (modified from Brown & Gillooly 2003; Reuman et al. 2008). We also examined the effect of sampling bias on b by fitting spectra across different body size ranges. We found that removing the largest individuals had a minimal effect on the b estimate for carnivores but made the herbivore estimate shallower, while removing the smallest individuals steepened the slope of both carnivores and herbivores considerably (Appendix A). For example, by only including fishes > 8 g in our analyses our estimated size spectrum slopes for herbivores and carnivores were b = -1.494 and b = -1.775, respectively (Fig. A2.8). Overall, across all body size ranges sampled as well as all other sensitivity analyses (i.e. across different years, divers, and sampling locations), the herbivore spectrum was always significantly shallower than the carnivore spectrum and the slopes for herbivores and carnivores were always shallower than predicted by metabolic theory (Appendix A).

2.4.2 Trophic position – body size relationships

From twenty-three species within five functional groups, we sampled a total of 344 fish ranging in body size from 0.1 g to 6.35 kg (Table 2.1). Of these, the trophic position of herbivores ranged from 1.76 to 2.62, and that of carnivores ranged from 2.42 to 5.06. In the species-based analysis, trophic position increased significantly with maximum $\log_2$ body mass across all species (estimate = 0.12, P = 0.002) (Fig. 2.3a; Table 2.2). After aggregating individuals according to their trophic pathway, we found that the

best model (as assessed by AIC_c) was the random intercept model with family as a random effect (so accounting for similar trophic position - body mass relationships within families) and with trophic pathway (carnivore, herbivore) included as an interaction term (Fig. 2.3b; Table 2.2). The relationship between trophic position and maximum $\log_2$ body mass was positive and significant (estimate = 0.114, P = 0.002), but was not significantly different between carnivores and herbivores (estimate = -0.061, P = 0.636; Table 2.2). This form of the model did, however, account for a much greater proportion of the variability (Fig. 2.3b) than the model in which all species were aggregated (Fig. 2.3a). In the individual-based analysis, the trophic position of individual fishes also increased significantly with their $\log_2$ body mass across the community, but with a shallower slope than in the species-based analysis (estimate = 0.067, $P < 0.001$) and with very little of the variability explained (Fig. 2.3c). Once trophic pathways were included, as with the species-based analysis, the optimum individual–based model included the $\log_2$ body mass class*trophic pathway interaction term and much more of the variability was explained: the slope of the relationship between trophic position - body size was positive and significant (estimate = 0.071, P = 0.004), but again was not significantly different between carnivores and herbivores (estimate = 0.004, P = 0.943) (Fig. 2.3d, Table 2.2). In both individual-based models (i.e. with and without trophic pathways considered), AIC_c supported a random slope and intercept structure with species nested within family as the random effect, thus allowing trophic position - body mass relationships to vary between species and families. For both the species-based and individual-based models, slopes were not distinct between herbivores and carnivores for any of the random effects structures that we fitted (random slopes or random intercepts, families and/or species).

We note that, in the individual-based models, had we not taken into account non-independence between species and families we would have found significantly different slopes between carnivores and herbivores (estimate = -0.066, P = 0.022). We found no evidence that relationships were influenced by our assumed herbivore fractionation value (Table A2.1) or by sampling location (north or south coast sites) (Tables A2.2, A2.3).

2.5 Discussion

Our analyses of visual census and stable isotope data provide solid quantitative evidence that coral reef food webs are size structured. Abundance - body mass relationships were negative, indicating energetic constraints on community structure in accordance with size-based theory (Trebilco et al. 2013). Trophic position - body mass relationships were significantly positive across species and across individuals, revealing strong size-based feeding in a diverse tropical food web. We also found differences in size spectra between carnivorous and herbivorous fish species that are consistent with Brown & Gillooly's (2003) prediction that body size scaling relationships reflect differences in energy acquisition between individuals sharing energy and individuals competing across trophic levels.

2.5.1 Abundance - body size relationships

We found strong evidence that abundance scales negatively with body size in coral reef communities, for individuals spanning across four orders of magnitude in body size. Our results align with ecological theory that energetic constraints cause abundance to scale negatively with body size (Brown & Gillooly 2003; Jennings & Mackinson 2003; Trebilco et al. 2013) and, specifically, provide the first evidence that reef fish species competing across trophic levels (carnivores) have a steeper size spectrum than reef fish

species sharing energy within a trophic level (herbivores) (Brown & Gillooly 2003). Previous analyses of size spectra on coral reefs, which were focused on examining how size spectra change with fishing pressure rather than testing macroecological theory, examined data from moderately to highly degraded systems and sampled individuals from a narrower range of body sizes (~10-60 cm) (Dulvy et al. 2004; Graham et al. 2005; Wilson et al. 2010). These studies used binning-based methods and fitted size spectra with body lengths rather than masses making direct comparisons to our results difficult. Our results are more directly comparable with Ackerman et al.'s (2004) census of reef fish > 1 g that, once corrected for their binning-based slope estimate, yields a size spectrum slope of b = -1.75 ± 0.34 95% confidence interval, which is steeper than our estimate for the full community size spectrum slope (b = -1.580) but still overlaps our 95% CI. Herein, we have also extended the size spectrum approach to show that the size structuring of reef fish abundances is dependent on how energy is shared within the reef community, suggesting that the food web structure of a diverse tropical community is governed by energetic constraints on size spectra that are similar to predictions for pelagic marine ecosystems (Brown & Gillooly 2003; Blanchard et al. 2009).

Our size spectra estimates were, however, shallower than predictions from metabolic theory and size-based theory for body size scaling relationships (i.e. the energetic equivalence hypothesis, and the trophic transfer correction) (Brown & Gillooly 2003; Trebilco et al. 2013). Empirical tests of abundance - body size relationships may deviate from theory when abundance estimates fail to account for every species that shares energy within the community (Maxwell & Jennings 2006; Jennings et al. 2007). Accurately quantifying the abundance of small cryptic fish species (Bozec et al. 2011),

nocturnal fish species, and the invertebrate species that compete with small fishes (Ackerman et al. 2004) is a challenge inherent to all UVC methods, including ours on Kiritimati. By underestimating the smallest individuals that contribute to energy flux in the coral reef food web, size spectra slope estimates will be biased upwards. Indeed, we found that our estimated size spectra slopes steepened when we sequentially removed the smallest size classes from the data set, suggesting that our underwater visual censuses had not quantified all of the smallest fishes in the community. Non-instantaneous UVC methods also can overestimate or underestimate the abundance of large mobile fishes depending on fish behaviour (Ward-Paige et al. 2010a; Bozec et al. 2011), and thus bias spectra estimates upwards or downwards. However, given that large individuals are considerably lower in abundance than small individuals, and that in probabilistic spectra fitting methods each individual counted is treated equally, we expect that this bias would be quite small.

In addition to the potential bias introduced by underwater visual census methods, exploitation pressure can steepen the size spectrum by reducing the abundance of the largest size classes (Blanchard et al. 2009). We attempted to reduce any potential influence of fishing pressure on trophic structure by sampling at minimally disturbed sites on Kiritimati. However, slopes did become slightly shallower (from -1.644 and -1.270 to -1.553 and -1.223 for carnivores and herbivores, respectively) after excluding the four sites nearest to Kiritimati's villages, consistent with predicted fishing effects on the size spectrum (Appendix A). Nevertheless, the pattern we observed that herbivore size spectra were significantly shallower than carnivore size spectra was consistent across all sites and body size ranges (Appendix A), indicating that the influence of fishing on our results is

minimal.

2.5.2 Trophic position - body size relationships

We also found strong evidence that trophic position increases with body size in coral reef food webs. In contrast to previous stable isotope analyses in reef systems, our results suggest that coral reef food webs are structured by size-based feeding relationships at both the species and individual level. For example, previous tests of feeding relationships have reported positive, negative and non-significant relationships between $\delta^{15}N$ and body size within individual reef fish species (Greenwood et al. 2010). However, a lack of statistical power can prevent detection of intra-specific shifts in $\delta^{15}N$ (Galvan et al. 2010). In the only previous comparison of feeding relationships across multiple coral reef species that we are aware of, $\delta^{15}N$ - body length relationships were positive across five carnivorous species, consistent with the carnivore size structuring in our results, but non-significant across four herbivorous species (de la Morinière et al. 2003). Our finding that the trophic position of herbivorous fish increased with body size (from 1.76 to 2.62) was therefore unexpected. Enriched individual $\delta^{15}N$ may result from increased consumption of detritus and small benthic invertebrates by herbivorous surgeonfish species (*Acanthuridae*) (Carassou et al. 2008; Dromard et al. 2015). We note that, in general, understanding of trophic fractionation in herbivorous fishes remains limited (Mill et al. 2007) and assigning trophic positions to herbivorous reef fish is an area requiring further study. Nevertheless, our herbivore trophic position - body size relationships are robust to varying ΔN (Appendix A), indicating that the consumption of $\delta^{15}N$ enriched detritus and invertebrates may increase with herbivore body size.

Despite evidence from gut content analyses that fish predators are generally larger

than their prey in temperate marine systems (Barnes et al. 2010), species-based tests of size structure using stable isotopes have produced equivocal results. For example, Jennings et al.'s (2001) study found a positive trophic position - body size relationship for fishes in the Celtic Sea but a non-significant relationship for fishes in the North Sea. In a tropical stream food web, despite gut content analysis revealing size-structured feeding relationships, isotope analysis of the full food web found no relationship between predator size and trophic position (Layman et al. 2005). We caution that in size-structured communities, where an individual's ecological role is best defined by its size rather than its species, species-based tests may obscure positive relationships between trophic position and body size that are evident at the individual level, if size is not controlled for in the study design. Here, because we sampled across the size range of each species we were able to detect positive trophic position - body size relationships at both the individual and the species level.

Two additional factors that may have limited the ability of previous studies to detect positive trophic position - body size relationships are variability in trophic fractionation values between trophic positions (Hussey et al. 2014) and confounding effects of phylogeny (Romanuk et al. 2011). Romanuk et al. (2011), for example, highlighted the importance of considering evolutionary history in analyses of diverse communities where, by accounting for the non-independence of species within orders, their analysis of a global dataset of fish species found that species-based trophic position - body size relationships are positive. In contrast, if we had failed to include a random effects structure in our individual-based model, we would have identified a significant difference between the trophic position - body mass relationships of carnivore and

herbivores. Without appropriate consideration of potential errors in the conversion of $\delta^{15}N$ to trophic positions and in the statistical treatment of phylogenetic relationships, examination of trophic structure from stable isotope analyses can be misleading.

2.5.3 Trophic pathways on coral reefs

We found that carnivores and herbivores were characterized by distinct abundance - body size relationships, though they had similar trophic position - body size relationships. Only a few previous studies have examined the effect of metabolic constraints on abundance - body size relationships as we did here. Our results align well with observations that the North Sea benthic community has a shallower spectrum than the pelagic community (Maxwell & Jennings 2006; Blanchard et al. 2009). In the North Sea, the detection of size spectra based on different modes of energy acquisition provided further insights into energy flux through the food web, where Blanchard et al. (2009) examined how the energy-sharing community could be coupled to a steep predation-based community by large mobile predators to confer food web stability. Their model has since been adapted to examine the coupling of size spectra between carnivore and herbivore groups in a Caribbean reef food web (Rogers et al. 2014). Though Rogers et al. (2014) did not compare size spectrum slope estimates between groups, our analyses provide empirical support for distinct structuring of herbivore and carnivore groups.

Beyond body size relationships, analysis of trophic pathways in other systems have used carbon isotope signatures to identify distinct energy sources and thus track energy flux through food web compartments or ‘channels’ (Rooney et al. 2006). Though we did not have sufficient carbon samples for the reef fish we sampled on Kiritimati, others have identified discrete benthic (Dromard et al. 2015) and pelagic (Wyatt et al.

2012) energy sources on coral reefs, and mixed benthic-pelagic diets of large predatory fish species in these ecosystems (McCauley et al. 2012; Frisch et al. 2014). We suggest that our results provide a useful foundation for future examination of coupled food web structure in coral reef systems. Notably, theoretical models and empirical analyses suggest that coupling by mobile consumers can foster food web stability (Rooney et al. 2006; Blanchard et al. 2009; Britten et al. 2014) and, given the widespread decline in top predator abundance on reefs (Williams et al. 2010; Nadon et al. 2012), it is critical that we develop a greater understanding of how differences in energy utilization between trophic pathways may define the structure of coral reef food webs.

We present novel evidence of size structuring in a minimally impacted diverse tropical food web, spanning 163 species across four orders of magnitude in body mass. By combining visual census data with stable isotope analysis we were able to examine the scaling of body size with both abundance and trophic position. Differences in the size spectra of carnivores and herbivores reflected energetic constraints on abundance - body size relationships between individuals sharing energy and those competing across trophic levels, but did not tightly match theoretical predictions. Our analyses offer new perspectives on the structure of coral reef food webs, and we suggest that future studies strive to further delineate community structure through the lens of body size distributions. Overall, size-based approaches hold great promise for integrating the complexities of food webs into simple quantitative measures and elucidating fundamental properties of aquatic ecosystems.

	FG	Family	Species: Scientific name	Species: Common name	Body mass (g): Mean	Body mass (g): Range	$\delta^{15}N$: Mean	$\delta^{15}N$: Range	N
Carnivore	BI	Chaetodontidae	*Chaetodon auriga*	Threadfin butterflyfish	87.36	58 - 98.3	14.44	13.68 - 15.6	9
			Chaetodon ornatissimus	Ornate butterflyfish	115.84	39 - 173.1	13.38	11.98 - 15.03	21
		Lethrinidae	*Monotaxis grandoculis*	Humpnose large-eyed bream	413.38	200 - 1090.8	14.96	12.9 - 15.83	20
		Cirrhitidae	*Paracirrhites arcatus*	Arc-eye hawkfish	13.28	2.35 - 31.13	13.15	12.28 - 13.99	10
		Mullidae	*Parupeneus insularis*	Two-saddle goatfish	221.78	45 - 520	12.46	11.22 - 14.4	30
	Pi	Carangidae	*Caranx ignobilis*	Giant trevally	6350.29	-	12.23	12.23 - 12.23	1
			Caranx melampygus	Bluefin trevally	1851.62	126.6 - 3719.45	12.01	11.21 - 13.28	8
			Carangoides orthogrammus	Island trevally	1732.5	-	13.74	13.74 - 13.74	1
		Lutjanidae	*Aphareus furca*	Grey jobfish	274.47	200 - 420	11.4	10.86 - 11.98	17
			Lutjanus bohar	Two-spot red snapper	1092.67	132.7 - 4540	12.23	10.91 - 13.68	23
		Serranidae	*Cephalopholis argus*	Peacock hind	382.74	200.6 - 1100	13.74	11.71 - 15.67	18
			Cephalopholis urodeta	Darkfin hind	81.67	27.1 - 151.1	11.71	9.11 - 13.59	22
			Variola louti	Yellow-edged lyretail	1713.3	127.7 - 3405	12.9	11.73 - 14.4	6
	ZP	Caesionidae	*Caesio teres*	Yellow and blueback fusilier	213.29	6.8 - 470.5	9.59	9.02 - 10.23	19
			Pterocaesio tile	Dark-banded fusilier	57.6	3.7 - 167.2	9.08	8.5 - 9.7	11
		Pomacentridae	*Chromis vanderbilti*	Vanderbilt's chromis	0.79	0.1 - 1.8	9.68	8.91 - 10.26	7
		Serranidae	*Pseudanthias bartlettorum*	Bartlett's anthias	2.88	0.8 - 3.5	9.11	7.94 - 9.84	5
			Pseudanthias olivaceus	Olive anthias	5.93	1.2 - 14.9	9.31	8.07 - 10.32	30
Herbivore	He	Acanthuridae	*Acanthurus nigricans*	Whitecheek surgeonfish	112.53	44 - 207.06	12.43	11.04 - 13.22	6
		Pomacanthidae	*Centropyge flavissima*	Lemonpeel angelfish	14.32	5.53 - 22.2	12.58	11.14 - 13.21	10
		Scaridae	*Chlorurus sordidus*	Daisy parrotfish	309.83	43.1 - 807.3	12.93	11.99 - 14.66	20
			Scarus frenatus	Bridled parrotfish	794.22	388.2 - 1954	13.86	12.72 - 15.17	24
	De	Acanthuridae	*Ctenochaetus marginatus*	Striped-fin surgeonfish	138.28	41.9 - 258.9	13.36	12.23 - 14.37	26

Table 2.1 Body sizes, $\delta^{15}N$ values, and sample sizes (*N*) for the twenty-three fish species sampled on Kiritimati for the stable isotope analyses. Each species assigned an trophic pathway (carnivore or herbivore) based on their functional group (FG: BI = benthic invertivore, Pi = piscivore, ZP = zooplanktivore, De = detritivore, He = herbivore).

	Coefficient	Estimate	Standard error	P value	Marginal R^2	ΔAIC_c
Species-based	Intercept	2.33	0.328	< 0.001	0.17	5.45
	log_2 mass	0.12	0.029	0.002		
Species-based with trophic pathway	Intercept	2.73	0.282	< 0.001	0.62	0
	Intercept (herbivore)	-0.978	1.018	0.359		
	log_2 mass	0.114	0.028	0.003		
	log_2 mass*herbivore	-0.061	0.124	0.636		
Individual-based	Intercept	2.76	0.242	< 0.001	0.04	8.8
	log_2 mass	0.067	0.02	< 0.001		
Individual-based with trophic pathway	Intercept	3.09	0.186	< 0.001	0.45	0
	Intercept (herbivore)	-1.45	0.398	0.004		
	log_2 mass	0.071	0.024	0.005		
	log_2 mass*herbivore	0.004	0.052	0.943		

Table 2.2 Best models (as evaluated by AIC_c) for trophic position - log_2 body mass relationships. Parameter estimates presented for species-based (linear mixed effects model with family as a random effect) and individual-based (linear mixed effects model with species nested within family as a random effect) analyses.

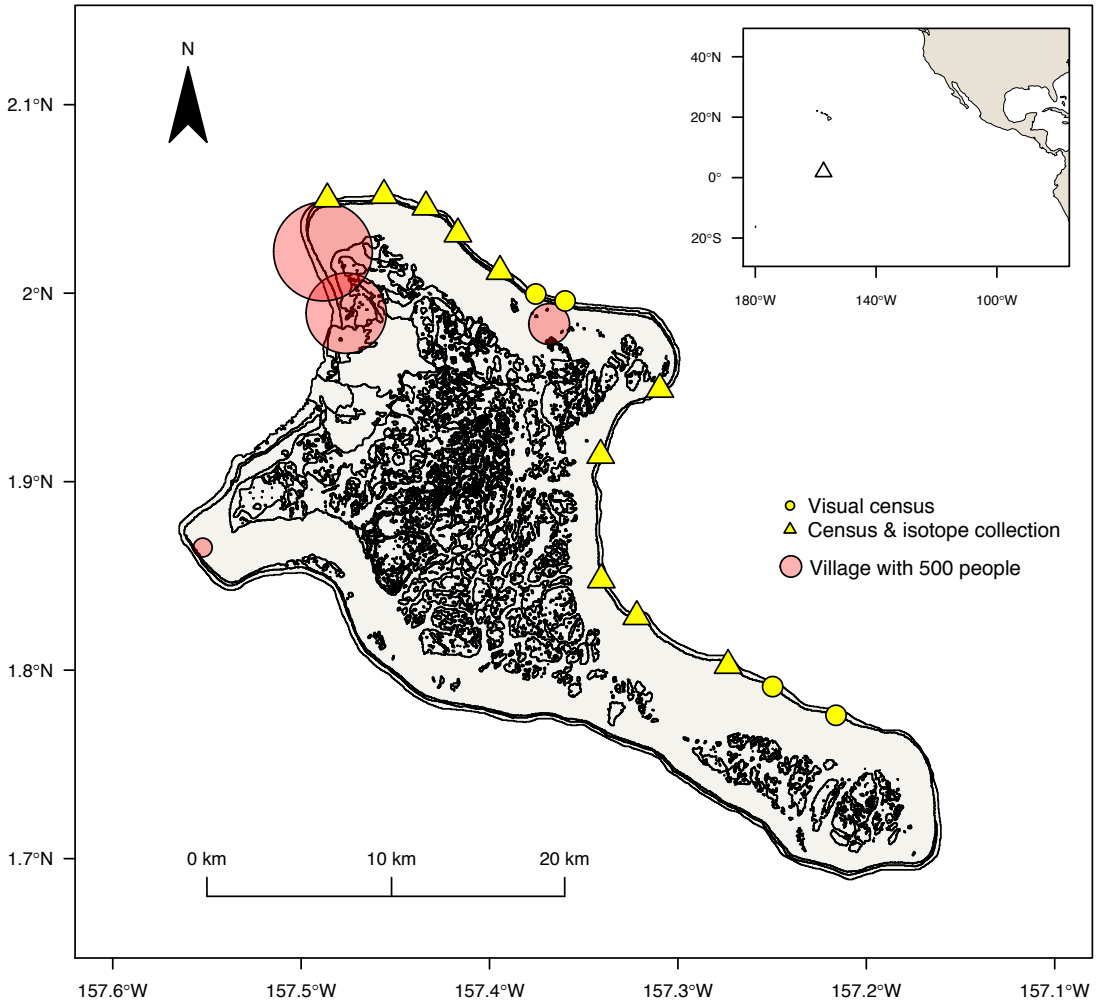

Figure 2.1 Study sites on Kiritimati, Line Islands, Republic of Kiribati. All sites have minimal fishing pressure and are located on the north and east coast of the atoll, which is outside of the upwelling zone on the leeward (lagoon facing) side. Fish specimens were collected at 10 sites in July-Aug of 2011 and 2012 (triangles). Underwater visual censuses were carried out at 14 sites in the summers of 2011 and/or 2013 (denoted by circles and triangles). Villages are marked with red circles that are scaled to their population sizes.

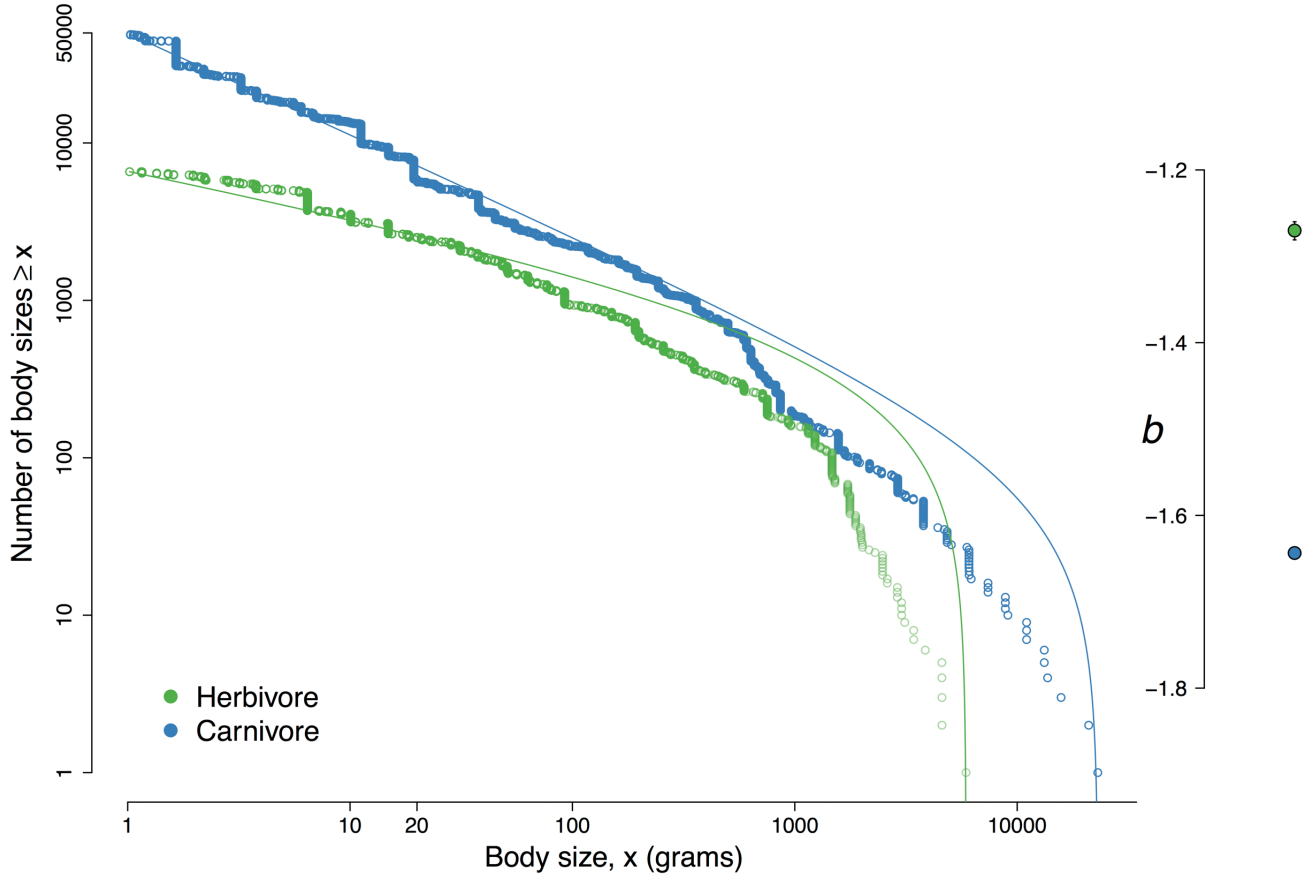

Figure 2.2 Size spectra (i.e. abundance - body size relationships) of the coral reef fish community. Left: Rank-frequency plot of reef fish body masses for carnivores (blue, n = 25,344 fish) and herbivores (green, n = 3,628 fish). Individual body masses are plotted as points and overlaid with the fitted size spectrum (i.e. bounded power law distribution). Right: size spectra slopes (*b*) with 95% confidence intervals for carnivores (blue) and herbivores (green).

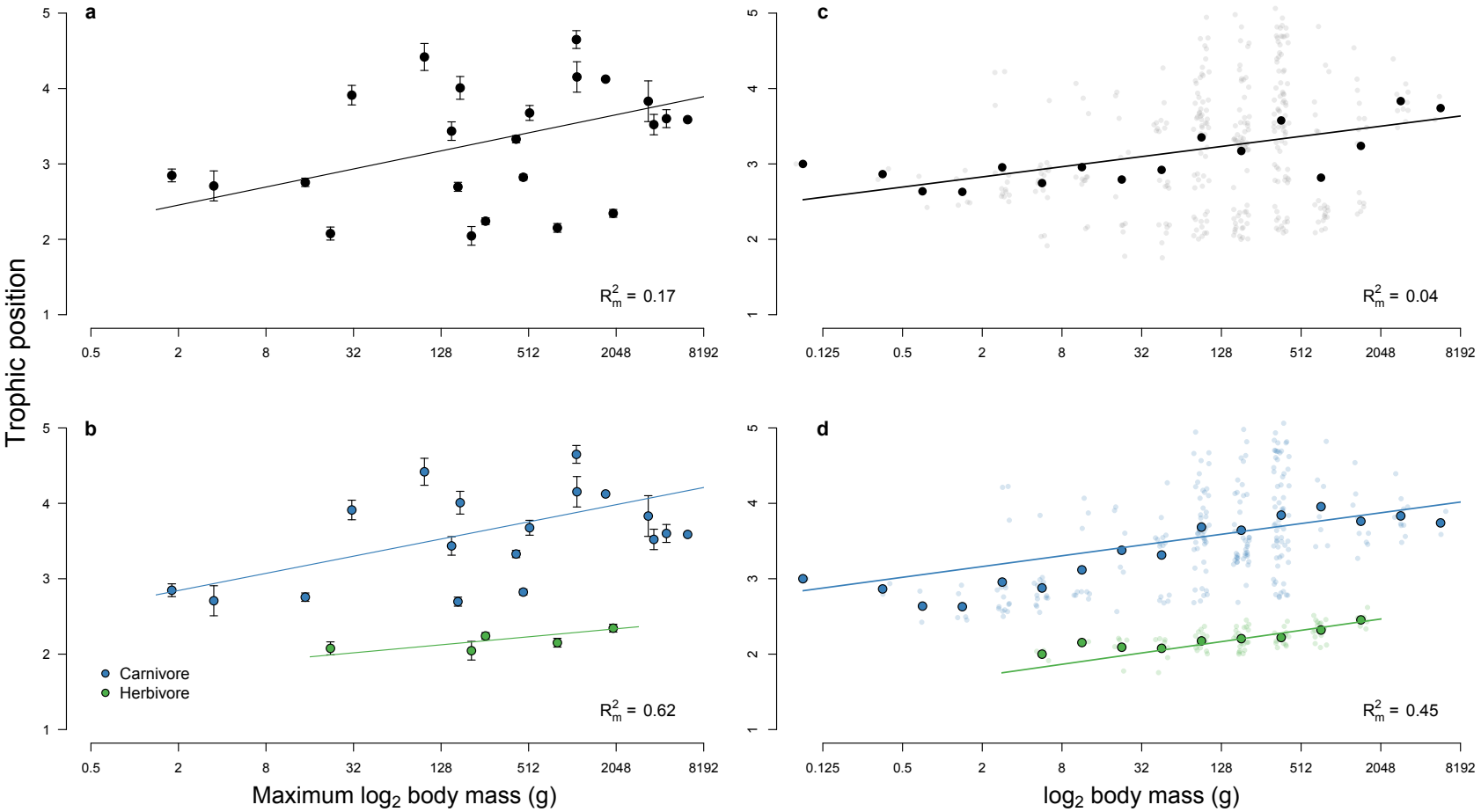
a
b
c
d
Trophic position
Maximum log2 body mass (g)
log2 body mass (g)
Carnivore
Herbivore
R2m = 0.17
R2m = 0.62
R2m = 0.04
R2m = 0.45
0.125
0.5
2
8
32
128
512
2048
8192
1
2
3
4
5

Figure 2.3 Trophic level - body size relationships a, b: Species-based analyses. Linear mixed effects models of trophic position and $\log_2$ body mass (g) in the coral reef fish community (a) across all species (n = 23), (b) for the two trophic pathways, carnivores (blue, n = 18 species) and herbivores (green, n = 5 species). For each species, the mean trophic position and 95% confidence intervals are plotted against its maximum mass. c, d: Individual-based analyses. Linear mixed effects models individual trophic position and of individual $\log_2$ body mass (g) in the coral reef fish community (c) across all individuals (n = 344) and (d) for the two trophic pathways, carnivores (blue, n = 258) and herbivores (green, n = 86). Individual trophic position estimates are plotted against body mass class (with jitter, transparent colour), and overlaid with mean trophic position (solid colour) of each body mass class.

Chapter 3 – Fishing degrades size structure of coral reef fish communities

Adapted from: James P.W. Robinson[1], Ivor D. Williams[2], Andrew M. Edwards[1,3], Jana McPherson[4,5], Lauren Yeager[6], Laurent Vigliola[7], Russell E. Brainard[2], Julia K. Baum[1]. (2016) *Global Change Biology*, DOI: 10.111/gcb.13482.

[1] Department of Biology, University of Victoria, PO BOX 1700 Station CSC, Victoria British Columbia, V8W 2Y2, Canada
[2] Coral Reef Ecosystem Program, Pacific Islands Fisheries Science Center, National Oceanic and Atmospheric Administration, 1845 Wasp Boulevard, Building 176, Honolulu, Hawaii, United States of America.
[3] Pacific Biological Station, Fisheries and Oceans Canada, 3190 Hammond Bay Road, Nanaimo, BC, V9T 6N7, Canada.
[4] Centre for Conservation Research, Calgary Zoological Society, 1300 Zoo Road NE, Calgary, AB, T2E 7V6, Canada.
[5] Department of Biological Sciences, Simon Fraser University, Burnaby, Canada
[6] National Socio-Environmental Synthesis Center, 1 Park Place Suite 300, Annapolis, Maryland 21401, United States of America.
[7] Institut de Recherche pour le Développement (IRD), UMR ENTROPIE, Laboratoire d'Excellence LABEX CORAIL, BP A5, 98848 Noumea Cedex, New Caledonia

Author contributions: J.P.W.R. and J.K.B. conceived of and designed the study. I.D.W., J.M., L.Y., R.E.B. and J.K.B. provided the data. A.M.E. and L.Y. provided R scripts and statistical advice. J.P.W.R. conducted data analysis and wrote the manuscript with input from all authors.

3.1 Abstract

Fishing pressure on coral reef ecosystems has been frequently linked to reductions of large fishes and reef fish biomass. Associated impacts on overall community structure are, however, less clear. In size-structured aquatic ecosystems, fishing impacts are commonly quantified using size spectra, which describe the distribution of individual body sizes within a community. We examined the size spectra and biomass of coral reef fish communities at 38 US-affiliated Pacific islands that ranged in human presence from near pristine to human population centres. Size spectra 'steepened' steadily with increasing human population and proximity to market due to a reduction in the relative biomass of large fishes and an increase in the dominance of small fishes. Reef fish biomass was substantially lower on inhabited islands than uninhabited ones, even at inhabited islands with the lowest levels of human presence. We found that on populated islands size spectra exponents decreased (analogous to size spectra steepening) linearly with declining biomass, whereas on uninhabited islands there was no relationship. Size spectra were steeper in regions of low sea surface temperature but were insensitive to variation in other environmental and geomorphic covariates. In contrast, reef fish biomass was highly sensitive to oceanographic conditions, being influenced by both oceanic productivity and sea surface temperature. Our results suggest that community size structure may be a more robust indicator than fish biomass to increasing human presence and that size spectra are reliable indicators of exploitation impacts across regions of different fish community compositions, environmental drivers, and fisheries types. Size-based approaches that link directly to functional properties of fish communities, and are relatively insensitive to abiotic variation across biogeographic regions, offer great potential for developing our understanding of fishing impacts in coral reef ecosystems.

3.2 Introduction

Overexploitation of marine species can cause system-wide shifts in species abundances and interactions (Bascompte et al. 2005; Britten et al. 2014), which in turn alter the structure and function of marine ecosystems (Jackson et al. 2001; Travis et al. 2014). Selective fishing of large consumers can produce trophic cascades (Bascompte et al. 2005; Baum & Worm 2009) and destabilize predator-prey dynamics (Britten et al. 2014), while sustained exploitation at lower trophic levels can collapse prey populations (Essington et al. 2015). In temperate systems, broad fishing impacts are often evaluated using complex ecosystem-based models that require high-resolution ecological and exploitation data (Thorpe et al. 2015). However, when ecosystems are characterized by high ecological diversity or limited catch data these approaches are infeasible. Instead, community-level indicators that are simple to estimate, grounded in ecological theory, and generalizable across ecosystems can provide informative assessments of fishing impacts (Rochet & Trenkel 2003; Thrush & Dayton 2010). Gaining such insights is of paramount importance for subsistence coral reef fisheries, which provide important sources of protein and livelihoods to millions of people across the world's tropical island nations (Sadovy 2005; Newton et al. 2007). Coral reef fish assemblages are highly diverse (Kulbicki et al. 2013) and their fisheries are multi-species and multi-gear (Hicks & McClanahan 2012), but catch and effort data are typically limited (Sadovy 2005; Zeller et al. 2015). As a result, exploitation impacts can be particularly difficult to quantify (McClanahan et al. 2015; Nash & Graham 2016), underscoring the need for simple community-level indicators of exploitation impacts.

In aquatic systems, trophic interactions are size-based and body size and individual trophic level are tightly linked (Jennings et al. 2001; Barnes et al. 2010). Size-based approaches that generalize across species but preserve links to community-level traits may provide significant insights into the impacts of exploitation in complex systems such as coral reefs (Nash

& Graham 2016). Body size also scales predictably with a number of important ecological processes, from metabolic rate at the individual scale (West et al. 2001) to biomass turnover at the population scale (Brown et al. 2004). Therefore, size-based approaches offer powerful methods of assessing ecological structure across distinct communities, and link directly to functional traits that are otherwise difficult to estimate in data-poor systems (Taylor et al. 2014). One metric, the size spectrum, describes the distribution of individuals across body sizes irrespective of species (White et al. 2007; Trebilco et al. 2013). The size spectrum has been used to assess fishing impacts across a range of temperate marine (Blanchard et al. 2005; Daan et al. 2005; Sweeting et al. 2009) and freshwater fish communities (Sprules 2008), where community size structure is represented by the slope of the relationship between abundance and body size on logarithmic scales (White et al. 2007). Size-selective fishing causes the spectrum slope to decrease or 'steepen' as large fishes are depleted and prey species are released from predation (Daan et al. 2005; Shin et al. 2005; Fung et al. 2013). Metabolic and size-based theory predicts that a reduction in large fishes will produce shifts in size-linked life history traits such that overexploited communities are characterized by a greater dominance of small individuals, and concomitant higher productivity and faster biomass turnover times (Jennings & Blanchard 2004; McCann et al. 2016).

In small-scale, artisanal coral reef fisheries, overexploitation is a pervasive issue that threatens the sustainability of a vital food resource for developing coastal countries (Newton et al. 2007; Cinner et al. 2009; Johnson et al. 2013). Standing stock biomass is widely used as metric of fishery health and of exploitation impacts at regional scales (Cinner et al. 2009; Cinner et al. 2013; MacNeil et al. 2015) and, although declines in the abundance of large fishes on coral reefs are well documented (Sandin et al. 2008; Williams et al. 2010), analyses of associated

impacts on coral reef fish community size structure have been infrequent (Nash & Graham 2016). Steepening of size spectra slopes due to overfishing of large fishes has thus far been detected only in Fijian small-scale reef fisheries, and across only moderate gradients in exploitation pressure (Dulvy et al. 2004; Graham et al. 2005; Wilson et al. 2010). Other direct comparisons between fished and protected areas have found that community size structure is highly variable and unrelated to exploitation, which may reflect unmeasured environmental influences (McClanahan & Graham 2005; Graham et al. 2007). As a result, it remains unclear whether degradation in overall community size structure occurs across extreme gradients in exploitation pressure, such as from pristine to overexploited reef communities, and if these patterns are dependent on the fisheries' species composition. At regional and global scales, recent macroecological analyses of coral reef fish trophic structure and life history traits indicate that biomass and ecological functions may be broadly preserved in lightly exploited communities (McClanahan et al. 2011; MacNeil et al. 2015; McClanahan et al. 2015). Similar examination of reef fish community size structure across large spatial scales and gradients in fished biomass would provide additional insights into the state of coral reef fisheries relative to unexploited ecosystems.

Here, we use a large-scale dataset of Pacific reef fish abundances spanning from remote near-pristine islands and atolls to highly populated ones, to examine how human impacts alter the size structure of reef fish communities. The reefs included in our analyses also span strong gradients in environmental covariates (Williams et al. 2015a), and differ substantially in their species compositions (Kulbicki et al. 2013) and exploitation history (Dalzell et al. 1996; Houk et al. 2012). We estimated size spectrum slopes to assess shifts in community structure across a body size range from tiny planktivores (20 g) to large piscivores (> 1 kg), and quantified the

biomass of large fishes relative to the total fish community to determine whether exploitation was size selective. To examine how changes in size structure corresponded with more conventional biomass-based indicators, we also compared trends in size spectra with trends in total community biomass.

3.3 Methods

3.3.1 Study location and survey data

We examined reef fish communities at 2,124 sites located on 38 U.S.-affiliated Pacific islands, atolls, and banks (hereafter islands) (Fig. 3.1), that were surveyed between 2010 and 2014 by the Pacific Reef Assessment and Monitoring Program (Pacific RAMP) of NOAA's Coral Reef Ecosystem Program (CREP). Surveyed islands encompass substantial gradients in biodiversity, productivity and temperature, and span human population densities from uninhabited atolls to densely populated islands supporting up to 2,235 people km^{-2} forereef habitat (Table A3.1) (Williams et al. 2015a).

The survey data (Coral Reef Ecosystem Program; Pacific Islands Fisheries Science Center 2015) consist of observations of individual fish made during underwater visual censuses (UVCs) by CREP's highly trained scientific divers. Two divers conducted stationary point counts (SPC), with each surveying one of two adjacent visually estimated 15 m diameter cylinders along a 30 m transect (survey area = 353 m^2). Each diver identified every fish species present in or transient through their cylinder, before enumerating and sizing (total length to the nearest cm) all observed fishes (Ayotte et al. 2011). CREP surveys were stratified by depth bin, into shallow (0-6 m), mid (6-18 m) and deep (18-30 m) zones, and we only examined surveys conducted on forereef habitat. The number of surveys at each island was proportional to the total

forereef area.

We considered each individual UVC survey recorded by a pair of divers (two CREP cylinders) as a unique site. To analyse fishing impacts at the community level we aggregated all sites sampled in each year across each island (n = 70 island *x* year combinations). We converted the length estimate from each individual fish to body mass (to the nearest gram) using published length-weight relationships for species or families (Kulbicki et al. 2005; Froese & Pauly 2016). Because UVC methods of coral reef fish communities can be subject to several potential biases (Bozec et al. 2011), we excluded all fish < 20 g body mass to avoid underestimating the abundance of small cryptic fishes (Ackerman & Bellwood 2000; Wilson et al. 2010). In addition, large mobile piscivores (i.e. sharks and jacks) are often overestimated in small-scale non-instantaneous underwater visual surveys (Ward-Paige et al. 2010a), and may also be attracted to divers at remote islands (Parrish et al. 2000; Richards et al. 2011). Both biases can substantially inflate biomass estimates and we therefore followed other recent large-scale studies of reef fish communities by excluding sharks and jacks from our analyses (MacNeil et al. 2015; Williams et al. 2015a).

3.3.2 Reef fish community analyses

We used size spectra to quantify reef fish community structure. The size spectrum is usually fitted to frequencies of body sizes and predicted to approximate a power law distribution (Eq. 3.1) (Vidondo et al. 1997; Andersen & Beyer 2006). Here, we used maximum likelihood estimation to estimate the size spectrum slope, *b* (Vidondo et al. 1997; Edwards 2008). We fitted body size data for individual fishes from each island, for each year, to a bounded power law distribution with probability density function:

$$f(x) = \frac{(b+1)x^b}{x_{\max}^{b+1} - x_{\min}^{b+1}} \quad \text{Eq. 3.1}$$

where x is body mass, b is the scaling exponent, and the distribution is bounded by the minimum and maximum possible body sizes ($x_{\min}$, $x_{\max}$) (White et al. 2008). Equation 3.1 is undefined for b = -1, but this value does not occur for our data. The log-likelihood of a bounded power law is:

$$\log[L(b \mid \text{data})] = n \log\left(\frac{b+1}{x_{\max}^{b+1} - x_{\min}^{b+1}} \right) + b \sum_{j=1}^{n} \log x_j \quad \text{Eq. 3.2}$$

(Edwards et al. 2017) and was numerically optimized to estimate b (Edwards 2008; Edwards et al. 2012). Unlike binning-based approaches to fitting frequency data, this method has the benefit of producing accurate estimates of b (Edwards et al. 2017). In our maximum likelihood estimation, $x_{\min}$ and $x_{\max}$ are the minimum (i.e. 20 g) and maximum observed values at each island within a single survey year (Edwards et al. 2012). In most empirical analyses of the aquatic size spectrum, binning-based methods are used to estimate b, such that the regression slope is the parameter of interest and a 'steepening spectrum' is predicted following the selective exploitation of large body sizes (i.e. the regression slope, or b, becomes more negative as the abundance of the largest size classes is depleted relative to small size classes) (Daan et al. 2005; Blanchard et al. 2005; Graham et al. 2005; Petchey & Belgrano 2010). Similarly, a 'steepening spectrum' here corresponds to the size spectrum exponent b becoming more negative. The methods previously used to calculate slopes are inaccurate, and the resulting slopes can be equivalent to either b, b+1 or b+2 depending upon the method (Edwards et al. 2017).

We used a Monte Carlo resampling procedure to correct for differences in sampling effort (i.e. number of UVCs) at each island. Size spectrum exponents were estimated for a random sample (without replacement) of 1,000 individual fish at each island in each survey year, and the size spectrum slope was the mean exponent estimate from 10,000 replicate random

samples. We used 1,000 fish as the number for the random samples to minimize bias in size spectra at low sample sizes while maximizing the number of island-survey year combinations included in our analysis (Fig. A3.1). Each island-year observation included in the analysis had at least 1,000 individual fish observations (Table A3.2) and we provide example model fits in Fig. A3.2.

In addition to size spectra, we examined two biomass–based fisheries indicators. First, we quantified overall community fish biomass (kg ha^{-1}, where 1 kg ha^{-1} = 100 kg km^{-2}) by averaging biomass across all UVCs at each island for each year. Second, to investigate the extent to which size-selective fishing was responsible for the observed patterns in size spectra exponents and overall community biomass, we estimated the proportion of large fish at each island using a large fish indicator (LFI) (Greenstreet et al. 2011). We defined the LFI as the biomass of fish > 1 kg divided by the total biomass of the fish community, averaged across all UVCs at each island for each year.

3.3.3 Explanatory covariates

We examined variation in community size spectra and fish biomass in relation to two anthropogenic and six environmental covariates (Tables 3.1, A3.1). No standard measure of fishing effort was available across all islands sampled. Instead, we estimated both human population density, expressed as number of people within a 20 km radius divided by the forereef area (Williams et al. 2015a), and distance to market (defined as the distance to provincial capital) (Cinner et al. 2013) as distal metrics of exploitation pressure on coral reef fish communities. Although human population density is often strongly correlated with a loss of reef fish biomass (Mora 2008; Williams et al. 2011; Cinner et al. 2013; Williams et al. 2015a), distance to market, which is less commonly employed, may be a more sensitive indicator of fishing intensity on

sparsely populated coral reefs (Brewer et al. 2013; Cinner et al. 2013; Maire et al. 2016). We extracted 2010 estimates of population density for a 20 km buffer (SEDAC) and divided this by the forereef area (km^2). Following Cinner et al. (2013), we estimated the shortest distance (km) from each site to the provincial capital as a proxy of market access (using ArcGIS).

For abiotic covariates, sea surface temperature (SST) and oceanic productivity can both positively influence reef fish biomass (Williams et al. 2015a), but their influence on community size structure remains unclear. We used remote sensing data to calculate time-averaged estimates of SST (°C) and oceanic productivity (mg C m^{-2} day^{-1}) at each site. We extracted the average minimum SST (°C) from the National Oceanographic Data Center's Coral Reef Temperature Anomaly Database (CoRTAD) based on AVHRR Pathfinder data on a weekly time-scale between 1982-2008 at a ~4.6 x 4.6 km resolution (http://www.nodc.noaa.gov/SatelliteData/Cortad). Net primary productivity (mg C m^{-2} day^{-1}) was modelled by NOAA CoastWatch based on satellite measurements of photosynthetically available radiation (NASA's SeaWiFS), SST (NOAA's National Climatic Data Center Reynolds Optimally-Interpolated SST), and chlorophyll a concentration (NASA Aqua MODIS) estimated every 8 days between 2002-2013 at a ~4.6 x 4.6 km resolution (http://coastwatch.pfeg.noaa.gov/erddap/griddap/erdPPbfp28day.graph). To avoid introducing bias from increased reflectance in shallow waters, we used bathymetry data from the STRM30_plus high-resolution (~1 x 1 km) bathymetry dataset (http://topex.ucsd.edu/WWW_html/srtm30_plus.html) and a focal productivity cell was excluded if any bathymetry cell within its bounds was < 30 m depth (Gove et al., 2013). We then estimated the mean SST value and mean productivity value per site by averaging SST or productivity values of the cell that included the site (if not excluded based on depth) and the

closest 3 neighbouring cells within 9.3 km of either the shoreline or site that also passed the depth filter.

In addition to oceanographic factors, coral reef fish communities may be influenced by a suite of other biophysical characteristics (Table 3.1). For example, reef area and island type have been shown to influence reef fish biomass (Cinner et al. 2013) while, at the site level, reefs of high complexity are thought to offer extensive prey refugia that support greater densities of small-bodied fish and steeper size spectra (Wilson et al. 2010; Alvarez-Filip et al. 2011; Rogers et al. 2014). We estimated land area and reef area, classified each island as an atoll (e.g. Kure, Palmyra), island with lagoon or pseudo-lagoon ('low' island, e.g. Saipan), or island without a lagoon ('high' island, e.g. Oahu) following D'Agata et al. (2014), and used *in situ* estimates of habitat complexity at each site. For land and reef area, the extent of coral reef habitat around each site was obtained by merging data from two primary sources, the Millennium Coral Reef Mapping project (data accessed from the University of South Florida Institute for Marine Remote Sensing and through the UNEP World Conservation Monitoring Centre; Andréfouët et al. 2005) and coral maps for Asian Pacific region produced under the "Coral Reef Habitat Map" project by the Japanese Ministry of the Environment (http://coralmap.coremoc.go.jp/sangomap_eng/; accessed 4/28/2011). We merged all non-land geomorphological types mapped in the Millennium data as this classification best matched the known extent of reef habitat based on the fish survey locations. Similarly, we merged all coral and associated habitats mapped in the Coral Reef Habitat Map data to best match the protocol used for the Millennium data. Using these two datasets combined, we calculated the total island reef habitat (< 30 m depth) within a 75 km buffer (~17,700 km^2) at each site (*sensu* Mellin et al. 2010). We used the Global Self-consistent, Hierarchical, High-resolution Geography Database

(http://www.soest.hawaii.edu/pwessel/gshhg/; Wessel & Smith 1996) to estimate land area (km^2) within a 75 km buffer at each site. Next, we collated large- and small-scale estimates of structural complexity. We extracted 1x1 km resolution bathymetry estimates from a global elevation model (MARSPEC) to estimate bathymetric slope (slope of reef bottom in °) at each site (Sbrocco & Barber 2013). Small-scale estimates of habitat complexity were collected in situ. At each stationary point count, CREP divers assessed structural complexity qualitatively on a scale from 1 (very low) to 5 (very high) between 2010-2011, before switching method and measuring maximum substrate height and proportion of area within substrate height bins in each point count cylinder between 2012-2014 (Williams et al. 2015a). We merged both estimates by averaging complexity estimates across all sites for each island that was sampled using both methods (n = 35), and then fitting the relationship between qualitative complexity and maximum substrate height. We used this relationship to convert qualitative complexity values to maximum substrate heights at each 2010-11 site (Williams et al. 2015a). All site-level explanatory covariates were averaged to give estimates for each island (Table A3.1).

3.3.4 Statistical modeling

Prior to analyses, we applied $\log_{10}$ transformations to distance to market (km), population density per island ($\log_{10}$(density + 1) per km^2), and reef area (km^2) to reduce skewness. We also centered and standardized all continuous covariates (Schielzeth 2010). Island type (atoll, low island, high island) was coded as two dummy variables before centering to a mean of zero. Distance to market and population density were strongly negatively correlated (r = -0.84), so to avoid collinearity issues we fitted separate models for each human covariate.

We modelled size spectra exponents and reef fish biomass estimates at the island level. Models were built separately for distance to market and human population density and the eight

environmental covariates were included in every model, producing four saturated models. The distribution of size spectra exponent estimates *b* was normal (Shapiro-Wilk normality test: W = 0.992; p = 0.934) so we used linear mixed effects models (*lme4* package in R; Bates et al. 2015) to examine variation amongst them. To account for non-independence of islands that were sampled in multiple years, survey year (*j*) was included as a random effect (ρ_j). We modeled reef fish biomass with a gamma distribution and a log link (Zuur et al. 2009), and the same fixed and random effect structure as the size spectra models. Prior to model selection procedures, we assessed evidence of collinearity with variance inflation factors (VIF), where variables with VIF > 10 were considered evidence of strong multicollinearity (Zuur et al. 2009). In the saturated size spectrum and reef fish biomass models every explanatory variable had a VIF < 6 so we retained all variables.

We used multimodel inference to examine models based on all possible subsets of our anthropogenic and environmental covariates using a dredge function (MuMIn package in R; Barton 2015). We assessed model support with the Akaike Information Criterion adjusted for small sample sizes (AIC_c) (Burnham & Anderson 2002) and found there was no single top model (i.e. in addition to the best model, there were models with $\Delta AICc < 2$). Marginal R-squared values were estimated for each model using the r.squaredGLMM function in the MuMIn package. Additionally, following Cade (2015) we examined weighted absolute t-statistic values across all subset models as a measure of covariate importance. The t-statistic, which is the parameter estimate divided by the standard error, can be used as a measure of effect size within models. We weighted each absolute t-statistic by the corresponding model probability (i.e. AIC_c weight for each model *i*, w_i), and, to generate confidence intervals, we estimated the weighted sample variance ($\sigma^2_{weighted}$) for each absolute t-value (t_i) for the weighted mean t-value (μ):

$$\sigma^2_{weighted} = \sum_{i=1}^{N} w_i (x_i - \mu)^2 \quad \text{Eq. 3.3}$$

In this way, the variables that were most important in predicting the given response (i.e., had the strongest effects in the more probable models) had the largest weighted absolute t-statistic (Cade 2015).

To visualize how the most important explanatory covariates influenced size spectra and reef fish biomass, we examined model predictions for each explanatory covariate across the range of observed values while holding all other predictor covariates at their means. We plotted the model-averaged prediction across the top model set ($\Delta AIC_c < 7$) weighted by the corresponding model probabilities (Burnham & Anderson 2002), and estimated the weighted sample variance as a measure of variability in predictions across the top model set. We visualized the predictions concerning distance to market models in the same direction as human population density by plotting predictions against the inverse of distance to market (hereafter 'proximity to market', i.e. for the scaled covariates, islands with high population estimates also had high proximity to market estimates).

We also examined if changes in size spectra corresponded with changes in reef fish biomass, and if those relationships differed between populated and uninhabited islands. We fitted linear mixed effects models to examine how size spectra changed across a gradient of reef fish biomass, treating populated and uninhabited islands separately and including survey year as a random effect. To explicitly test for size-selective fishing of large body sizes, we used the same approach to examine the relationship between size spectra and the LFI at populated and uninhabited islands (Fig. A3.3).

Finally, we conducted sensitivity analyses to test the robustness of our results to different treatments of the datasets. UVC methods provide estimates of length rather than mass, and

previous studies of reef fish communities have generally fitted length spectra (Dulvy et al. 2004; Graham et al. 2005; Wilson et al. 2010). As such, we also estimated size spectra slopes using reef fish lengths and refitted our statistical models. Model-averaged predictions and weighted mean t-statistic ratios for reef fish length spectra models were similar to results from mass spectra models (Figs. A3.4, A3.5, Table A3.5). Estimates of mass spectra facilitate comparisons with our analyses of reef fish biomass, and as a result, we decided to present mass spectra rather than length spectra as our main results.

All analyses were conducted using R version 3.2.0 (R Core Team 2015), and we provide our code at an open source repository (github.com/baumlab/robinson-reefs-spectra).

3.4 Results

3.4.1 Size spectra analyses

Reef fish community size structure varied considerably across the gradient of human impacts over the 38 Pacific islands, with size spectra slopes (b) ranging from -1.95 to -1.13 (Fig. 3.2a,b). Modeled anthropogenic and environmental variables explained a large proportion of the variation in size spectra across islands: across the top model set (all models < 7 ΔAICc), the range in R^2 was 0.55 – 0.58 and 0.58 – 0.60 for the proximity to market and human population density models, respectively (Table A3). Size spectra exponents decreased linearly with increasing proximity to market (model-averaged t-statistic = 6.77) (Fig. 3.2a) and with increasing human population density (model-averaged t-statistic = 7.83) (Fig. 3.2b). The steepest size spectra (b < -1.8) were generally observed only at reefs with high human population density, which typically also were close to market centers (Pearson correlation = 0.84), such as Guam, Hawaii, and Oahu (Fig. 3.2a,b). Regardless of the metric used, human disturbance had the strongest effect on the island-specific size spectra (Fig. 3.3a). Minimum SST (°C) had a strong

positive effect on size spectra exponents in top model sets for both proximity to market (model-averaged t-statistic = 6.18) and population density (4.84) (Fig. 3.3a), meaning that the size spectra were steeper on cooler islands. The remaining environmental and biogeographic covariates had relatively weak effects on size spectra (all model-averaged t-statistics < 2.2) (Fig. 3.3a).

3.4.2 Biomass analyses

Reef fish biomass varied across islands from an estimated 110 kg ha^{-1} to over 1770 kg ha^{-1}, and was lowest at islands with high human presence (Fig. 3.2c,d). Across the top model set, R^2 ranged from 0.69 – 0.76 and 0.67 – 0.75 for the proximity to market and human population density models, respectively (Table A3.4). As with the size spectra models, human disturbance covariates were the strongest drivers of reef fish biomass (Fig 3.3b): reef fish biomass decreased non-linearly with increasing proximity to market (Fig. 3.2c) and human population density (Fig. 3.2d), and only the remote, unpopulated islands supported biomass levels > 1000 kg ha^{-1}. The lowest biomass levels (< 200 kg ha^{-1}) were observed only at reefs with high human population density, which typically were also close to market centers (Fig. 3.2c, d). Several environmental covariates were also important drivers of reef fish biomass. Generally, islands with higher minimum SST (°C) and higher productivity supported greater biomass (Fig. 3.3b). However, the relative effects of SST and productivity on biomass differed slightly between model sets (Fig. 3.3b), with SST the stronger driver in the proximity to market model set (model-averaged t-statistic = 4.88 for proximity to market; 3.77 for human population density) and productivity the stronger in the human population density model set (2.69 and 5.60). Remaining environmental and biogeographic covariates had relatively weak effects on reef fish biomass (all model-averaged t-statistics < 2) (Fig. 3.3b).

3.4.3 Populated vs. uninhabited reef fish community structure

At the populated islands, there was a strong relationship between size spectra and reef fish biomass (slope = 0.0008, $P < 0.001$), in which reefs with the steepest size spectra and lowest reef fish biomass were those closest to market centres (Fig. 3.4). This relationship appeared to be explained by the disproportionate exploitation of large-bodied fishes, since the most negative (i.e. steepest) spectra exponents were associated with particularly low values for the large fish indicator (i.e. low relative biomass of large-bodied fish; slope = 0.9923, $P < 0.001$) (Fig. A3.3). In contrast, despite substantial variation in size spectra exponents (-1.85 to -1.13) and reef fish biomass (402 to 1774 kg ha^{-1}), both size spectra ~ biomass (Fig. 3.4; slope = 0.0002) and size spectra ~ LFI relationships (Fig. A3.3; slope = -0.204) were significantly weaker at the remote, uninhabited islands ($P < 0.001$).

3.5 Discussion

Our analyses reveal that, along a disturbance gradient from reefs of near-pristine wilderness to ones near large population centers, increasing human presence causes a degradation of coral reef fish community size structure. At populated islands, steeper size spectra were associated with a reduction in reef fish biomass and the relative biomass of large-bodied fishes. The specificity of each ecological indicator to human impacts was markedly different, such that size spectra responded solely to human presence and sea surface temperature whereas fish biomass was highly sensitive to even low levels of human presence as well as the influences of temperature and oceanic productivity.

At populated islands, steepening size spectra represent a gradual shift in body size distributions from fish communities with a high relative proportion of large fish (shallow

spectra) to ones dominated by small fishes (steep spectra). Large-bodied fishes can play important roles in maintaining reef functions, suggesting that the loss of these individuals due to size selective exploitation may have disproportionate functional impacts on coral reefs. For example, many large herbivorous fishes are important bioeroders and control algal growth (Bellwood et al. 2011; Edwards et al. 2013). More generally, large predators can control the stability of prey populations across habitats (Rooney et al. 2006; Britten et al. 2014). Size-selective exploitation of these fishes may therefore impair the ability of reefs to recover from additional disturbances such as coral bleaching and hurricane damage (Cheal et al. 2013). Size spectra analyses of moderately exploited reef fisheries in Fiji (Dulvy et al. 2004: 1-100 people per km reef front; Graham et al. 2005: 3-300 people per km reef front) previously suggested that harvesting of large-bodied fishes steepens size spectra at small spatial scales. Fishing practices across the Pacific are, however, highly variable, with the gear and associated target species varying across islands and regions (Friedlander & Parrish 1997; Craig et al. 2008; Houk et al. 2012). Our analyses encompassed regions characterized by a high diversity of fishing gears (Dalzell et al. 1996; Fenner 2012) and fish species (Kulbicki et al. 2013), and spanned a wider gradient in human population density (0 – 2,235 people per km^2 forereef area) than previous reef size spectrum studies. Moreover, our two proxies for fishing pressure performed equally well in accounting for these differences in fisheries types (although we note that for future analyses market-based metrics could provide additional information on fishing pressure (Maire et al. 2016), particularly for uninhabited reefs). Overall, our analyses suggest that size-selective exploitation is a pervasive issue on coral reefs at ocean-basin scales, which consistently alters reef community size structure.

Altered community size structure also may have important functional consequences that

extend beyond a loss of large-bodied individuals. Size structuring of trophic interactions on coral reefs (Robinson & Baum 2016) means that communities with steeper size spectra will have a lower mean trophic level (Jennings et al. 2002), consistent with evidence that the mean trophic level of reef fisheries catch is negatively correlated with human population density (Houk et al. 2012). Moreover, communities dominated by smaller individuals have faster rates of population growth (Brown et al. 2004; Blanchard et al. 2012) and biomass turnover (Jennings & Blanchard 2004), and communities with lower mean trophic level may be less stable (Blanchard et al. 2012; Rochet & Benoit 2012; Britten et al. 2014) and more sensitive to environmental change (Jennings & Blanchard 2004). Exploitation of large size classes also may release prey populations from predation pressure and thus further steepen size spectra (Daan et al. 2005). However, such cascading effects may be difficult to detect in reef systems in which predator-prey interaction strengths are dampened due to large-bodied predators feeding across large spatial scales and across trophic levels (McCauley et al. 2012; Frisch et al. 2014; Frisch et al. 2016; Roff et al. 2016). In addition, exploited reef fisheries likely also target medium- and small-bodied fishes, thus depressing any compensatory growth by prey populations. Disentangling the combined effects of trophic release of prey populations and exploitation of smaller size classes therefore remains problematic, but shifts in community size structure along human disturbance gradients may provide an early warning of impacts on functional properties at the community level.

Human-associated declines in total community biomass and large fish biomass have been documented globally across distinct coral reef regions (Roberts 1995; Mora 2008; Cinner et al. 2013; MacNeil et al. 2015; Williams et al. 2015a; Nash & Graham 2016), but the link between community size structure and biomass has not previously been examined. We found that gradual

declines in size spectra exponents along either human covariate gradient contrasted with a rapid decrease in reef fish biomass from > 1500 kg ha^{-1} at unpopulated islands to < 600 kg ha^{-1} at islands with the lowest human presence. These different patterns likely arose because biomass estimates are most strongly influenced by the number of large-bodied fish that are present (Nash & Graham 2016), whereas size spectra respond to shifts across the entire distribution of body sizes from the smallest to largest fish, and treat each individual fish equally. At the most degraded reefs where large fishes are absent, fishing of medium- and small-sized fish would further deteriorate community structure but cause less dramatic reductions in fish biomass. In contrast, the size spectra of lightly fished reefs were similar to an undisturbed size spectrum despite biomass values being typical of more heavily disturbed communities. The differential response of community size spectra and community biomass suggests that community size structure may be more resilient than fish biomass to light exploitation. These findings are consistent with patterns at coral reefs in the Indian Ocean where the functional composition of fished reefs remains partially intact at biomass levels > 600 kg ha^{-1}, despite biomass falling far below that of neighbouring unexploited sites (McClanahan et al. 2015). Although recovery of reef fish biomass towards natural baseline levels is an important conservation target that aims to restore ecosystem properties by preserving functionally important species (Knowlton & Jackson 2008; Bellwood et al. 2011; MacNeil et al. 2015), the maintenance of productive fisheries in populated regions is also a priority (Cinner et al. 2012; Zeller et al. 2015). Rebuilding community size structure in exploited regions is a realistic management target that may be achieved without implementing the fisheries closures necessary to rebuild pristine biomass (MacNeil et al. 2015). Management for the recovery of community size structure would also benefit from assessments of the influence of shark and jack populations on spectra exponents, as

these top predators likely play important roles in structuring reef food webs (Bascompte et al. 2005; Rooney et al. 2006) but are largely absent in heavily exploited regions (Roff et al. 2016).

Although human covariates were the strongest predictors of size spectra, additional variation was attributed to differences in sea surface temperature. Metabolic principles predict that, in warmer environments, increases in individual energy demands drive greater per-capita consumption rates and strengthen top-down control of prey populations (Bruno et al. 2015; DeLong et al. 2015). Therefore, in agreement with our results, warmer islands should be characterized by shallower size spectra (lower abundance of small bodied fish relative to large bodied fish). However, difficulties with UVC methods in accurately enumerating large predator populations (Ward-Paige et al. 2010a) prevented the inclusion of some groups of large predators in our size spectra analyses; our results, therefore, can provide only incomplete evidence in support of stronger top-down control. Although metabolic approaches have provided valuable insights into environmental constraints on reef fish community biomass and trophic structure (Barneche et al. 2014, 2016), theoretical predictions of the effect of temperature on reef fish size distributions are lacking. Since size spectra were robust across gradients in other environmental covariates, improved understanding of temperature control of size spectra would help the development of predictions of natural baselines for reef fish community size structure. Such understanding also is increasingly important as climate change warms reef systems and degrades fish habitat, further stressing reef fish populations (Hoegh-Guldberg et al. 2007).

We also detected a strong influence of oceanic productivity on reef fish biomass, which is consistent with previous observations that high oceanic production promotes planktivorous fish abundance (Barneche et al. 2014; Williams et al. 2015a). Subsequent increases in energy availability to upper trophic levels promote greater total community biomass (Friedlander et al.

2003; Cinner et al. 2009; Williams et al. 2015a) though, interestingly, these apparent differences in energy availability did not affect size spectra. The lack of a strong response by size spectra at the island scale suggests that the extra biomass afforded by high productivity may be evenly redistributed among all body sizes. Temperature was also a positive influence on biomass. A previous analysis of the CREP dataset detected this effect only in planktivorous fishes (Williams et al. 2015a), and other studies have variously noted positive (Richards et al. 2012) and negative (Barneche et al. 2014) effects of temperature on reef fishes, indicating that further study of the influence of temperature on biomass is warranted. We did not detect a strong influence of habitat complexity on either reef fish size spectra or biomass, despite evidence that habitat complexity enhances reef fish biomass and steepens size spectra by increasing survival rates of small-bodied fishes (Graham & Nash 2012; Rogers et al. 2014). The influence of habitat complexity on reef fish assemblages may only be detectable at smaller spatial scales than our island-scale approach (which required averaging of structural complexity estimates across survey sites) and this variable should not be overlooked in future analyses of reef fish size spectra.

The apparent lack of environmental influences on size spectra - with the exception of temperature - across islands that varied greatly in environmental setting and biogeographic context supports the utility of size spectra as a robust ecological indicator of fishing. In temperate systems, size-based indicators have proven to be powerful methods of assessing exploitation effects across communities of different compositions (Bianchi et al. 2000; Shin et al. 2005). In reef fisheries, which typically lack adequate catch and survey data (Sadovy 2005), UVC monitoring programmes can provide the body length information required for size spectra analyses (Graham et al. 2005; Nash & Graham 2016). Size-based indicators also can effectively link patterns in community structure with less tangible community-level properties such as

production and biomass turnover rates. Given their sensitivity to environmental influences and strong response at low levels of exploitation, biomass estimates may be less reliable as ecological indicators at large spatial scales.

Although we accounted for several potential sampling issues in our analyses, size spectra estimates derived from different UVC methods might vary substantially and we therefore caution against comparisons of size spectra derived from different UVC sampling methods or and from different analytical techniques (Edwards et al. 2017). Limitations of census methods can introduce error in the counts of small or large size classes (Bozec et al. 2011) that bias exponent estimates or produce non-linear size spectra (Ackerman et al. 2004). Spectra estimated with biased binning-based methods (e.g. earlier reef spectra studies (Dulvy et al. 2004; Graham et al. 2005)) can also introduce error in size spectra analyses, while subtle differences between these methods can result in spectra exponents that differ by 1 or 2 (White et al. 2008; Edwards et al. 2017). Difficulties in enumerating fishes accurately across the size spectrum suggest that it may be problematic to produce meaningful empirical estimates of baseline size spectra exponents for coral reefs, as has been done for temperate marine ecosystems (Jennings & Blanchard 2004). Importantly, by removing some of the largest fish species (the sharks and jacks) that are heavily targeted by fishers, our results are almost certainly a conservative estimate of fishing impacts on reefs and are unlikely to match metabolic predictions for size spectra in which exponents are a simple function of predator-prey mass ratio and trophic energy transfer efficiency (Brown & Gillooly 2003; Jennings & Blanchard 2004; Trebilco et al. 2013). For example, excluding sharks and jacks caused size spectra exponents to steepen slightly at most islands in the dataset, and this effect was most pronounced at islands where those species comprised a high proportion of the community abundance (Fig. A3.6). Without accurate estimates of the true relative abundances of

small, medium and large-bodied fishes, size spectra may be most informative if used to assess relative differences among communities in a space-for-time approach (as we did here) or to assess temporal changes in community size structure (Jennings & Dulvy 2005).

Across tropical Pacific coral reef ecosystems, islands with a strong human presence were characterized by degraded coral reef fish community size structure. Steepening size spectra suggest a shift in size-linked life history traits, implying that fished communities may have reduced resilience to further exploitation and future environmental change. Given comparative insensitivity to variation in environmental conditions, size spectra may prove to be effective ecological indicators of exploitation impacts on reef fisheries (Graham et al. 2005; Shin et al. 2005; Nash & Graham 2016). Extreme reductions in reef fish biomass can have potentially wide-ranging and pervasive consequences for reef ecosystems, particularly when species or trophic groups that provide key ecosystem functions are depleted (Bellwood et al. 2011; McClanahan et al. 2011; Ruttenberg et al. 2011; McClanahan et al. 2015). However, despite the loss of biomass at lightly exploited islands, we detected weaker impacts on size spectra exponents that suggest that maintenance of ecological size structure is a tangible management target that could enhance the ecological resilience of coral reef ecosystems.

Covariate	Definition	Source	Size spectrum	Fish biomass	
			-ve	+ve	-ve
Human population density	Total population within a 20 km radius divided by forereef area (km^2) (2010 estimates)	SEDAC	1, 2, 3	-	6, 7, 8, 9, 10, 11, 12
Proximity to market	Distance to nearest provincial capital (km)	ARC GIS	-	-	10, 11
Minimum SST	Mean of weekly minimum SST (°C) values over 1982-2009 at 4x4 km resolution	CoRTAD	-	12	13
Mean productivity	Weekly mean of productivity (mg C m^{-2} day^{-1}) values over 2002-2013 for at least 3 1x1 km cells	NOAA CoastWatch	-	12, 13	-
Habitat complexity	Mean substrate height within point count cylinder	CREP	3, 4, 5	12, 14, 15	-
Bathymetric slope	Bathymetric slope extent (0 – 90°) at 1x1 km resolution	MARSPEC			
Island type	Atoll, low (island with lagoon or pseudo-lagoon), high (island without lagoon)	D'Agata et al. (2014)	-	Highest at atolls (11)	
Land area	Land area within 75 km radius (km^2)	Millennium/Coral Reef Habitat Map	-	-	-
Reef area	Total reef area <30 m depth within 75 km radius (km^2)	Millennium/Coral Reef Habitat Map	-	No effect (11)	

Example references: 1. Dulvy et al. (2004); 2. Graham et al. (2005); 3. Wilson et al. (2010); 4. Alvarez-Filip et al. (2011); 5. Rogers et al. (2014); 6. Jennings et al. (1995); 7. Jennings & Polunin (1997); 8. Mora et al. (2011); 9. Williams et al. (2011); 10. Brewer et al. (2013); 11. Cinner et al. (2013); 12. Williams et al. (2015a); 13. Barneche et al. (2014); 14. Friedlander et al. (2003); 15. Graham & Nash (2012)

Table 3.1 Anthropogenic and environmental covariates included in size spectra and biomass models. Previous studies that examined the influence of each covariate on size spectra and biomass are numbered and categorized by the direction of the relationship they observed (positive, +ve; negative, -ve)

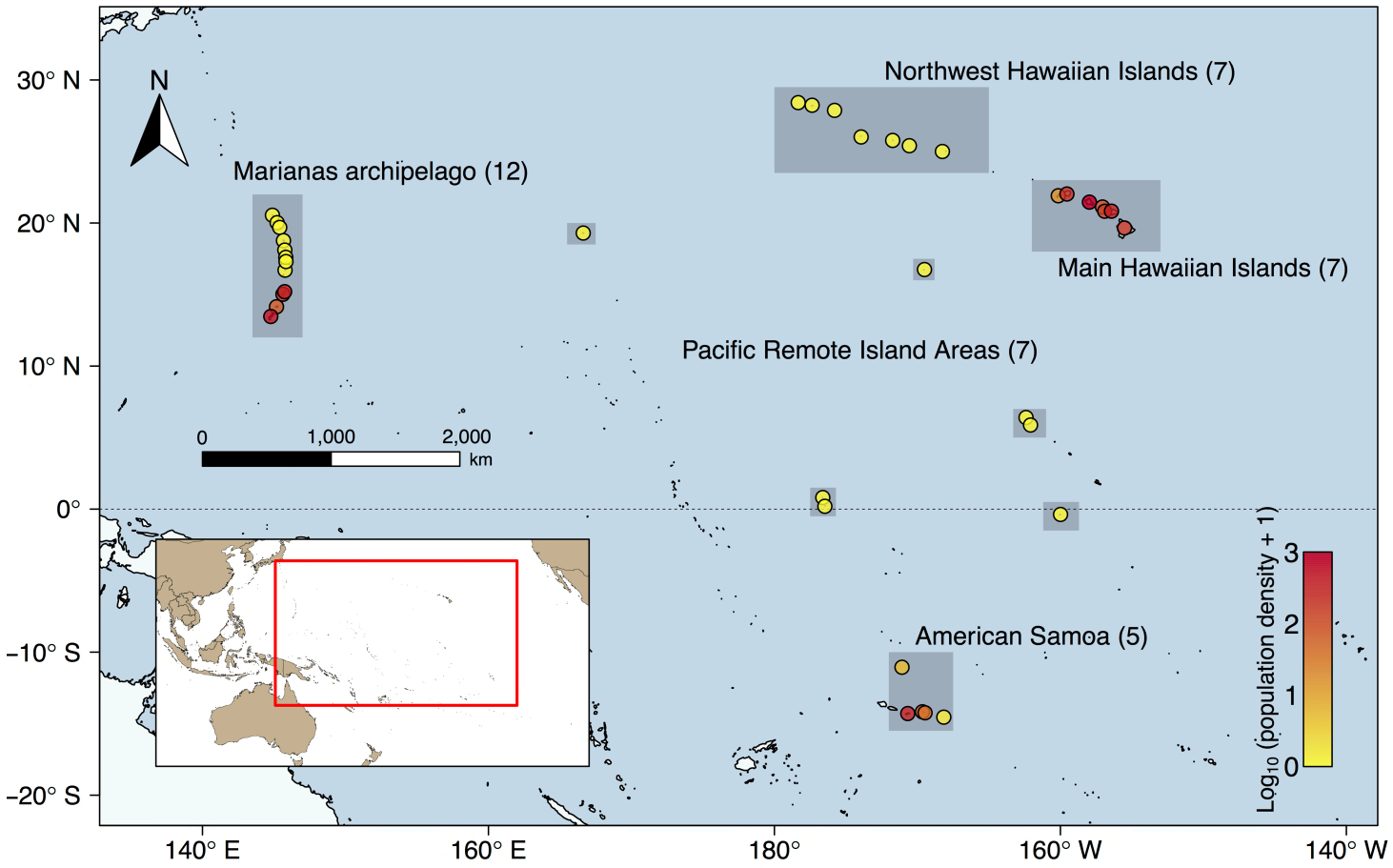

Figure 3.1 Map of Pacific islands surveyed by CREP. Each island (n = 38) is coloured by human population density (population per forereef area km^2 within a 20 km radius on a $\log_{10}$ scale).

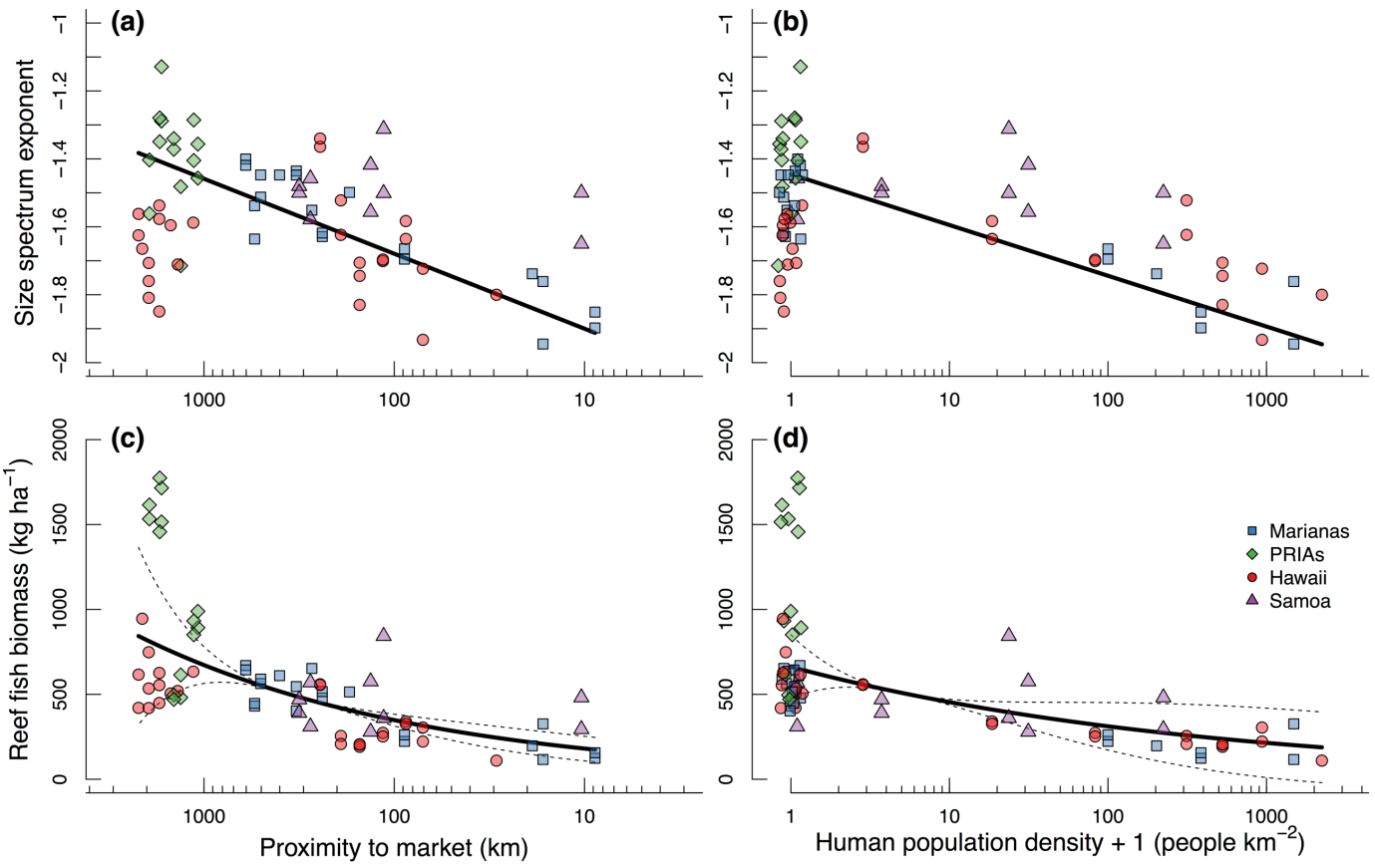

Figure 3.2 Human drivers of coral reef fish size structure and biomass (kg ha^{-1}). Size spectra (a, b) and reef fish biomass (c, d) relationships are model-averaged predictions across the standardized range of (a, c) observed $\log_{10}$ proximity to provincial capital (km) and (b, d) $\log_{10}$ (human population density per forereef area + 1) (km^2). Dashed lines are the weighted sample variance at each value of the human covariate (though these are indistinguishable from the model predictions in the size spectra analyses). For visualization purposes, we included the observed data as points plotted against the untransformed human covariates and coloured by region (blue squares = Marianas archipelago; red circles = Hawaiian archipelago, green diamonds = Pacific Remote Island Areas, purple triangles = American Samoa). Unpopulated islands have been jittered to distinguish between points with human population density = 0 (b, d).

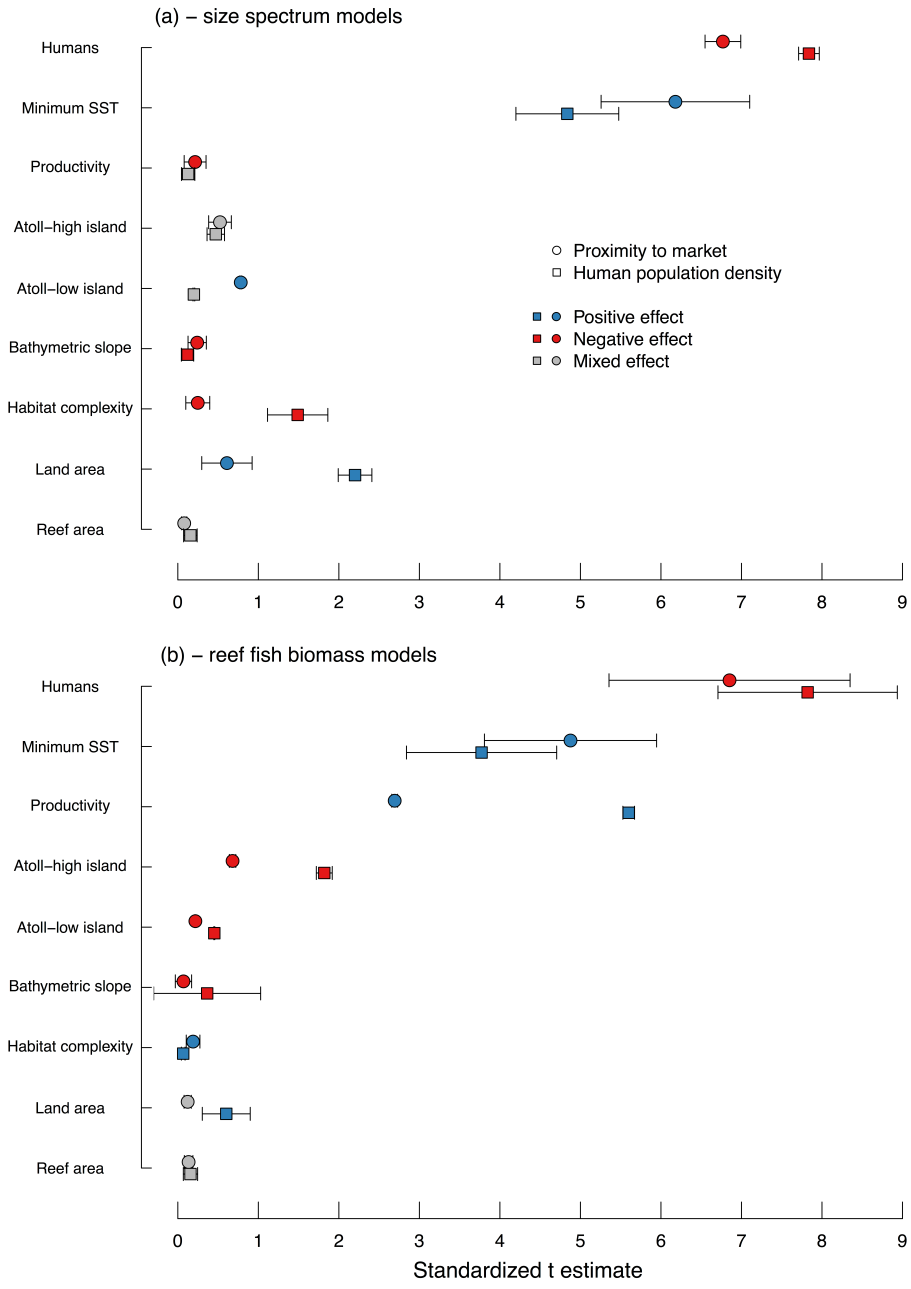

Figure 3.3 Human and environmental drivers of reef fish size structure and biomass. Size spectra (a) and reef fish biomass (b) are presented for the distance to market (circles) and human population density (squares) full model sets. Points are the weighted absolute t-values for each explanatory covariate, with weighted sample variance as error bars. T-values indicate the magnitude of each covariate effect, and colors indicate the direction of each covariate effect (blue = positive; red = negative; grey = mixed). See Tables A3.3 and A3.4 for further details.

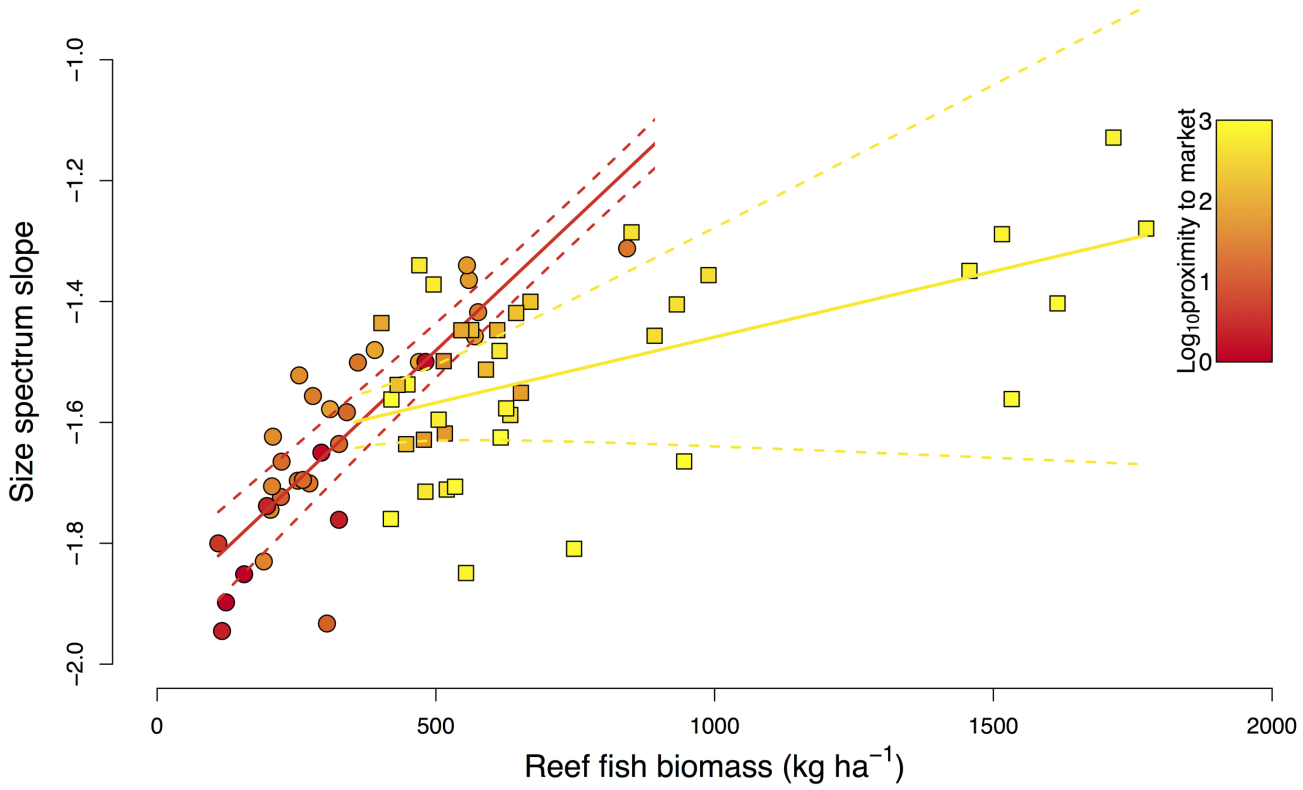

Figure 3.4 Change in size spectra across the gradient of reef fish biomass. Each point is a size spectrum exponent and biomass estimate at one island in a single survey year, colored according to $\log_{10}$ proximity to market estimates. Solid lines are parameter estimates with dashed 95% confidence intervals from a mixed effects model with habitation as an interaction effect. Size spectra ~ biomass relationships were significantly different between uninhabited (yellow line) and populated (red line) islands.

Chapter 4 - Local environmental influences and herbivore depletion determine coral reef phase shift index across scales

James P.W. Robinson[1*], Ivor D. Williams[2], Lauren Yeager[3], Jana M. McPherson[4,5], Jeanette Clark[2,6], Julia K. Baum[1].

[1]Department of Biology, University of Victoria, PO BOX 1700 Station CSC, Victoria, BC, V8W 2Y2, Canada.

[2]Coral Reef Ecosystem Program, Pacific Islands Fisheries Science Center, National Oceanic and Atmospheric Administration, 1845 Wasp Boulevard, Building 176, Honolulu, Hawaii, United States of America.

[3]Department of Marine Science, University of Texas at Austin, Port Aransas, TX, 78373, United States of America.

[4]Center for Conservation Research, Calgary Zoological Society, 1300 Zoo Road NE, Calgary, AB, T2E 7V6, Canada.

[5]Department of Biological Sciences, Simon Fraser University, Burnaby, BC, Canada

[6]Joint Institute for Marine and Atmospheric Research, University of Hawaìi at Mānoa, Honolulu, Hawaíi, United States of America.

Author contributions: J.P.W.R. conceived the study. I.D.W., J.M., L.Y., J.C. and J.K.B. provided the data. L.Y. provided R scripts and statistical advice. J.P.W.R. conducted data analysis and wrote the manuscript with input from all authors.

4.1 Abstract

The influence abiotic and biotic factors have on species' distributions varies with scale. Scale dependence arises when ecological processes are spatially heterogeneous, such that abiotic factors typically dominate at regional scales and biotic factors are influential at smaller local scales. Nonetheless, macroecological analyses have recently shown that biotic influences of competition on species occurrence patterns remain detectable at coarse grain sizes. In contrast, the strength across scales of other biotic processes, such as grazing, remains unclear. We combined underwater visual census data with remotely sensed environmental and anthropogenic data for 42 Pacific islands and atolls to empirically test the scale-dependence of abiotic, bottom-up (productivity) and top-down (grazing), and human influences on the abundances of competing hard coral and macroalgal organisms. Using boosted regression trees, we predicted a composite indicator of hard coral and macroalgal cover - the phase shift index - using a combination of abiotic, biotic, and anthropogenic covariates across 7 grain sizes (0.25 – 1,024 km^2). Temperature, oceanic productivity, and wave energy were the strongest predictors of benthic communities across all grain sizes, whereby coral cover dominated in warm, high productivity reefs at low exposure sites. Only one grazing predictor – scraper and excavator biomass – was moderately influential, but it consistently predicted transitions to algal states at low biomass levels. Weak anthropogenic impacts were predicted by human travel time covariates but not human population density covariates. For coral reefs, local environmental conditions such as temperature and productivity produce strong differences in reef benthic communities across regions which may bias expectations of healthy reef states. Maintenance of scraper and excavator biomass even at relatively low levels (~10-20 kg ha^{-1}) may also prevent transitions to algal-dominated states, providing a tractable management target for rebuilding overexploited herbivore populations. By uniting fine-scale observations with remote sensing data, we were able to

disentangle the relative influences of abiotic, biotic and anthropogenic drivers, and thus provide insights into the dominant processes that structure communities from local to regional scales.

4.2 Introduction

Ecological processes that control the distribution of species are scale-dependent (Wiens 1989; Levin 1992). Opportunities for quantitative tests of scale-dependence have emerged with the increased availability of large spatially-explicit ecological datasets (Gotelli et al. 2010; Kissling & Schleuning 2014; Belmaker et al. 2015; Cohen et al. 2016). Consequently, we understand that the climatological factors that constrain species distributions at medium to large spatial scales are mediated at smaller spatial scales by biotic factors, such as competition and predation, and physical influences (Pearson & Dawson 2003; McGill 2010; Wisz et al. 2013). Meta-analyses of studies encompassing different survey areas, for example, indicate that climate drivers of species richness gradients are strongest at scales spanning continents (Stein et al. 2014) or distances over 1000 km (Field et al. 2009). Furthermore, studies of spatially-gridded species occurrence datasets show that the drivers of species distributions shift from strong biotic influences at small cell resolutions ($\sim < 50$ km^2) to strong abiotic influences at large resolutions ($\sim > 600$ km^2) (Cohen et al. 2016).

These macroecological patterns reflect both the extent (size of the area surveyed) and grain (spatial resolution, or size of the smallest sampling unit) of a study (Wiens 1989), and changing either spatial attribute can alter the strength of different ecological drivers (Rahbek & Graves 2000; Rahbek 2005; Field et al. 2009; Chase & Knight 2013). This scale-dependence is caused by spatial heterogeneity in abiotic and biotic influences (Wiens 1989; Rahbek 2005) where, for a constant extent, increasing grain size raises within-grain spatial heterogeneity and

reduces variance between grains, potentially obscuring fine-scale physical and biotic influences (Wiens 1989; Cohen et al. 2016). Spatial scale may therefore bias our interpretation of the magnitude and direction of different ecological drivers, whereas a study with a limited extent, that does not extend completely across abiotic and biotic gradients may fail to capture patterns at ecological extremes (Rahbek 2005; Wisz et al. 2013). Similarly, a study that focuses on a single grain size may be unable to distinguish between ecological processes that operate at different spatial scales (Wiens 1989).

Despite a long-standing perception that abiotic factors predominate at large spatial scales (Pearson & Dawson 2003), there is growing evidence that biotic influences, too, can manifest at coarse grain sizes (Wisz et al. 2013). Recent analyses of species distribution models that combined remotely-sensed abiotic variables with biotic information derived from either the direction of species interactions (i.e. positive or negative) (Heikkinen et al. 2007; Belmaker et al. 2015) or, more simply, by the presence of competitors (Gotelli et al. 2010), indicate that competition can be a strong predictor of (avian) species occurrence at spatial grains as coarse as 40 km^2 (Heikkinen et al. 2007) to 100 km^2 (Gotelli et al. 2010; Belmaker et al. 2015). Theoretical simulations indicate, however, that scaling of specific biotic processes such as predation, grazing, competition, parasitism, or mutualism is dependent upon the interaction type (Araújo & Rozenfeld 2014). Unfortunately, empirical tests that explicitly examine scale-dependence are lacking for most biotic processes.

Top-down control of resources by consumers likely is a strongly scale-dependent process, given the spatial heterogeneity in the densities, mobilities, and interaction strengths of consumers and their resources (Gripenberg & Roslin 2007). Assessments of spatial variation in the abundances of consumers and their resource have, however, not yet been conducted at

macroecological scales. Furthermore, although empirical scaling studies have focused on diverse terrestrial assemblages, including invertebrates (Araujo & Luoto 2007) and vertebrates birds (van Rensburg et al. 2002; Belmaker & Jetz 2010; Gotelli et al. 2010), equivalent consideration of scale-dependence in aquatic systems is limited.

Here, we examine scale-dependence in the biotic and abiotic controls that influence benthic communities on coral reefs. Coral reef benthic communities are thought to be controlled by a combination of top-down, bottom-up, physical factors, and anthropogenic influences operating across a range of spatial scales (Hughes et al. 2003, 2010; Bellwood et al. 2004; Mumby et al. 2013). Tropical reef benthos is primarily composed of hard coral and coralline algae organisms that deposit calcium carbonate to form a structural reef architecture, and turf and macroalgal organisms which occupy coral settlement space and overgrow coral colonies (McCook et al. 2001; Hughes et al. 2010). Shifts in the relative abundance of competing hard coral and macroalgal organisms represent alternating benthic regimes or states along a gradient of coral to algal dominance (Bruno et al. 2009).

Top-down control of coral reef benthos by grazers is clearly important at small scales. Between connected reefs (tens of kilometers apart), both experimental and observational studies indicate that benthic community state is strongly linked to the biomass (Mumby et al. 2006) and diversity (Burkepile & Hay 2008; Rasher et al. 2013) of herbivorous fishes which maintain algal communities in cropped states that are likely to be relatively benign for coral growth and recruitment (Green & Bellwood 2009). The role of herbivorous fish biomass at larger scales is more uncertain, with correlative analyses providing examples of both positive (Heenan & Williams 2013; Jouffray et al. 2015) and insignificant (Carassou et al. 2013; Russ et al. 2015; Suchley et al. 2016) influences of herbivore biomass in promoting hard coral cover or controlling

macroalgal abundances across continents or island groups.

In addition to top-down control by grazers, benthic community state may also be influenced by abiotic and bottom-up factors. At small scales, natural variability in wave energy, for example, influences habitat suitability for coral growth (Gove et al. 2015) and grazer foraging ability (Bejarano et al. in press). Reefs exposed to frequent and intense physical disturbances are characterised by low hard coral cover and a benthic community dominated by algal organisms (Williams et al. 2013, 2015b). At larger scales, latitudinal gradients in the distribution of coral and macroalgal cover likely reflect positive influences of sea surface temperature and productivity on the growth rates of calcifying organisms, with coral cover declining from equatorial reefs to reefs in sub-tropical latitudes (Williams et al. 2015b; Smith et al. 2016).

Beyond spatial scale, temporal shifts from coral to algal dominance within a location are typically associated with an increase in anthropogenic disturbances, such as sedimentation, pollution, overexploitation of grazing herbivores, and habitat destruction, which can overwhelm abiotic and top-down controls (Hughes et al. 2003; Pandolfi et al. 2003; Mumby & Steneck 2008; Jouffray et al. 2015; Smith et al. 2016). Although evidence of human impacts driving phase shifts from coral to algal states has been clearly documented on some Caribbean reefs (Hughes 1994; Hughes et al. 2010) (though see Bruno & Valdivia (2016)), both community states have been observed in the absence of anthropogenic pressures across distinct regions (Vroom & Braun 2010).

Explicit tests of the relative strengths, and scale-dependence across grain sizes, of these various abiotic and biotic (i.e. bottom-up productivity and top-down grazing) influences on the reef benthos are lacking. Here, we combine underwater visual census data with remotely sensed environmental data to test the scale-dependence of abiotic, bottom-up, and top-down influences

on the abundances of competing hard coral and macroalgal organisms at 42 Pacific islands and atolls. Surveyed islands display substantial spatial heterogeneity in abiotic conditions and grazing strength, ranging from warm equatorial reefs to cool sub-tropical reefs (Williams et al. 2015b) characterized by substantial intra-island (Gove et al. 2015) and inter-island variability in wave energy (Gove et al. 2013), and encompassing distinct island groups that each support similar gradients in fishing pressure and herbivore biomass (Williams et al. 2015a; Heenan et al. 2016). In the Pacific, reefs with low coral and high macroalgal cover typically occur either in highly-degraded (Smith et al. 2016) or high-latitude regions (Vroom & Braun 2010; Smith et al. 2016), whereas high-coral low-macroalgal cover reefs tend to be found at lower latitudes in minimally-disturbed sites (Williams et al. 2015b) with low wave exposure (Gove et al. 2015). We quantified the relative importance of 2 abiotic variables, oceanic productivity, 4 grazing variables, and 4 anthropogenic variables in predicting a composite indicator of reef benthic state (the phase shift index, Bruno et al. (2009)) across spatial scales, altering grain size from 0.25 to 1,024 km^2 over the extent of the Central Pacific Ocean (~43° latitude x 61° longitude). We hypothesised that benthic community states would be predicted by physical (e.g. wave energy) and grazing influences at small and medium spatial grains but, because our analysis was at a large ocean-basin extent, that oceanographic influences (e.g. temperature, productivity) would be apparent at every spatial grain size. We also considered how these scale-dependent patterns may bias expectations of natural baselines for reef benthic community states, and how they can inform management strategies for promoting herbivore grazing function.

4.3 Methods

4.3.1 Coral reef data

Data on benthic cover and herbivorous fish assemblages were collected between 2010-2014 by trained scientific divers as part of the Coral Reef Ecosystem Program (CREP) of NOAA's Pacific Island Fisheries Science Center. Underwater visual censuses (UVC) were carried out at 42 US-affiliated tropical Pacific islands and atolls, encompassing the Hawaiian and Marianas archipelagoes, American Samoa, and the Pacific Remote Island Areas (PRIAs), that span strong gradients in human population density, sea surface temperature, and oceanic productivity (Fig. 4.1, Table A4.1) (Coral Reef Ecosystem Program; Pacific Islands Fisheries Science Center 2015). UVCs were conducted at unreplicated sites stratified across three depth bins (shallow, 0-6 m; medium, 6-18 m; deep, 18-30 m) on the forereef habitat. The fish community was surveyed using stationary point counts in which paired divers surveyed two adjacent 7.5 m radius cylinders centered at 7.5 and 22.5 m on a 30 m transect positioned along a depth contour (2 x 7.5 m radius cylinders = 353.4 m^2 area surveyed per site). For the first five survey minutes each diver compiled a species list of all fishes observed in their cylinder, before then sizing (total length to nearest cm) and enumerating each recorded species on that list. Each diver then visually assessed benthic cover by recording the percent cover of hard coral, crustose coralline algae (CCA), fleshy macroalgae, and turf algae in their cylinder, and quantified habitat complexity by estimating the mean substrate height. CREP survey procedures are described in further detail by Ayotte et al. (2015).

To characterize the state of the coral reef benthic community, we calculated the phase shift index (PSI), an integrated measure of reef benthic state. Developed by Bruno et al. (2009), the PSI is the first component of a principal component analysis of UVC site-level hard coral and fleshy macroalgae cover estimates, with negative values indicating coral-dominated sites and

positive values indicating algal-dominated sites (Fig. A4.1). Although our goal is not to assess evidence for or against phase shifts, the PSI quantifies the natural continuum of coral-algal dominance whose drivers we seek to analyze. We centered hard coral and macroalgal cover estimates to a mean of zero and scaled them to have unit variance prior to analysis. Turf and CCA cover estimates were not included in our analyses.

4.3.2 Predictor variables

Our biotic grazing predictor, herbivorous fish grazing pressure, was represented by site-level biomass estimates that we compiled from the UVC fish observations. Extensive observations of their feeding mechanisms and behaviors have been used to classify herbivorous reef fishes into a number of broad functional groups representing distinct grazing functions (Green & Bellwood 2009; Cheal et al. 2010; Bellwood et al. 2011; Nash et al. 2015). Following Deith (2014) and Green & Bellwood (2009), we classified herbivorous fish species as: 1) croppers, which feed on turf algal assemblages, including detritus, with minimal impacts to the coral substrate; 2) scrapers and excavators, which consume turf, detritus and coral by scraping or removing the upper layer of the reef substrate; 3) browsers that primarily feed on macroalgae and do not impact coral substrate (Table A4.2). Herbivore biomass was used as a proximate measure of the strength of herbivory (Bellwood et al. 2011; Nash et al. 2015), either for the entire herbivore community or each functional group individually. Individual length observations were converted to masses using published length ~ weight relationships (Kulbicki et al. 2005, Froese & Pauly 2016), before generating site-level biomass estimates (kg ha^{-1}) by summing fish masses observed by both divers in each UVC survey and dividing by the area surveyed. Small juvenile fishes likely only have minimal contributions to grazing, bioerosion and sedimentation processes on coral reefs (Lokrantz et al. 2008) and may also be underestimated in visual surveys (Bozec et

al. 2011). Consequently, we excluded fish < 10 cm from our analyses. Infrequent sightings of large herbivore schools that are difficult to count accurately can produce exceptionally high biomass estimates that are not reflective of the grazing biomass at a single site. To prevent these observations from having a disproportionate influence on our predictive models we capped site-level biomass outliers at 95% of the interquartile range, treating each island group separately (Heenan et al. 2016).

To examine abiotic and bottom-up influences on benthic community structure, we compiled remote sensing data for three covariates that have previously been shown to influence benthic community composition across the Pacific Ocean (Table 4.1). Average weekly minimum SST (°C) estimates were extracted from the National Oceanographic Data Center's Coral Reef Temperature Anomaly Database (CoRTAD) based on AVHRR Pathfinder data between 1982-2008 at a ~4.6 x 4.6 km resolution (http://www.nodc.noaa.gov/SatelliteData/Cortad) (Yeager et al. in press). Net primary productivity (mg C m^{-2} day^{-1}) estimates were extracted from NOAA CoastWatch based on satellite measurements of photosynthetically available radiation (NASA's SeaWiFS), SST (NOAA's National Climatic Data Center Reynolds Optimally-Interpolated SST) and chlorophyll a concentration (NASA Aqua MODIS), and were estimated every 8 days between 2002-2013 at a ~4.6 x 4.6 km resolution (http://coastwatch.pfeg.noaa.gov/erddap/griddap/erdPPbfp28day.graph) (Behrenfield & Falkowski 1997; Yeager et al. in press). To avoid introducing bias associated with increased reflectance in shallow water areas, cells < 30 m depth were excluded from SST and productivity estimates (Gove et al. 2013). We estimated the mean SST value and mean productivity value per UVC site by averaging SST or productivity values across the cell containing the site and the closest 3 neighbouring cells within 9.3 km of either the shoreline or site (if not excluded based

on depth) (Yeager et al. in press). For wave energy, we extracted wave power hourly estimates from the global Wave Watch III model (Tolman 2014) at a 50 km resolution, forced with hindcast winds from 1979-2010 (Durrant et al. 2010). For each UVC site, we created radial lines in 1° bins unobstructed by land for at least 100 km to give a site's incident wave swath (e.g. Ekebom et al. 2003; Burrows et al. 2008; Chollett & Mumby 2012), and calculated wave power in each degree bin by summing annual wave power values of the closest Wave Watch III pixel with the same direction as the degree bin. Site-level cumulative wave power estimates were calculated by integrating wave power for each degree bin over the entire incident wave swath, and averaging annual sums across 1979-2010 (KWhr m^{-1}).

In lieu of direct spatially-consistent measures of fishing pressure and water quality, most coral reef macroecological analyses have had to rely on indirect measures of 'human impact' using some form of human population density (Table 4.1). Recently, estimates of travel time or linear distance to 'market centers' (national or provincial capitals, or major cities) have been linked with the health of reef fish communities (Brewer et al. 2012; Brewer et al. 2013; Maire et al. 2016; Robinson et al. 2016). These metrics may provide more refined estimates of local human impacts because they capture subtle differences in reef accessibility that may exist between sites with similar local human population sizes (Maire et al. 2016), and account for market pressures that reflect socioeconomic drivers of exploitation more accurately than population density (Brewer et al. 2013). As such, we compiled site-level estimates of both human population density and travel time. Human population estimates for 2010 were extracted at each UVC site for buffers at 5 and 20 km radii (SEDAC, Center for International Earth Science Information Network) (Robinson et al. 2016; Yeager et al. in press). Travel time was estimated as the linear travel time (hours) to 1) the nearest human settlement (any populated cell

at 1 km^2 resolution) and 2) the nearest major market (any national or provincial capital, major population center, or landmark city), after accounting for differences in travel speeds across 24 landscape types (e.g. road, track, ocean), with sites in populated cells assigned a travel time of 1 minute (Maire et al. 2016). Estimates of travel time were extracted by E. Maire for each UVC site at a 1 km^2 cell resolution.

4.3.3 Spatial grain and boosted regression tree analyses

Spatial scale is defined by the size of the smallest sampling unit (grain) and the total area surveyed (extent) (Wiens 1989; Belmaker et al. 2015). We examined the spatial dependence of environmental and grazing drivers of benthic state by aggregating our response and predictor covariates at different grain sizes and examining the relative strength of each covariate as a predictor of the PSI. Reefs were patchily distributed across the Pacific with each island group differing substantially in area and, as such, we were unable to systematically shift extent. Grains were produced by aggregating UVC sites into a gridded network of varying cell (i.e. grain) sizes produced from a WGS84 projection system. Our smallest spatial scale was a 0.25 km^2 grid, which we increased by quadrupling each grid area to give seven total grains (0.25, 1, 4, 16, 64, 256, 1,024 km^2). For each spatial grain, we averaged the PSI and all 11 predictor covariates across every UVC site contained in each cell and then used these data to fit our predictive models (Figs. 4.1, A4.2, A4.3, A4.4, Table A4.1). Every UVC site was included in each spatial grain analysis. Note that grain sizes below 16 km^2 are finer than the resolution of our environmental covariates; implications for the interpretation of our analyses are highlighted in the discussion. Pairwise correlations among predictor covariates indicated moderate collinearity between related covariates ($r > 0.5$; e.g. population density at 5 and 20 km, travel time to market and settlement) but only rare instances of strong collinearity that might bias our model

predictions (e.g. $r > 0.7$ for 15 of 385 total pairwise correlations) (Dormann et al. 2013).

Next, we used boosted regression trees (BRTs) to examine the relative strength of each covariate in predicting the PSI at each spatial scale. BRT models are regression tree ensembles constructed by building trees sequentially where, at each step, the next tree attempts to minimise the deviance of the residuals of the previous tree (Elith et al. 2008). Thus, boosting improves model predictive performance and robustness of single trees. BRTs provide a flexible method of modelling relationships between variables that can incorporate complex interaction effects and account for missing predictor values with minimal loss of predictive power, while also modelling non-linear relationships (Elith et al. 2008) which have been detected in related macroecological analyses of spatial variation in reef benthic cover (Heenan and Williams 2013; Jouffray et al. 2015). BRTs were fitted with the 'gbm' package in R (Elith et al. 2008), and BRT performance was optimised by adjusting three model parameters: tree complexity (tc), which sets the number of nodes in each tree; learning rate (lr), which sets the importance of each tree added and so influences the number of trees included in each model; bag-fraction, which sets the proportion of the data utilised at each step. We fitted models to all combinations of parameter values across tc (1-2-3-4-5), lr (0.01, 0.001, 0.0001) and bag-fraction (0.25, 0.5, 0.75, 0.9), and selected the parameter set with the lowest mean predictive deviance as our final fitted model (Richards et al. 2012; Jouffray et al. 2015) (Table A4.3). The PSI was normally distributed at every spatial scale and so we fitted BRTs to a normal distribution. We assessed relative strengths of grazing, productivity, abiotic, and anthropogenic influences at each spatial scale by extracting the gbm measure of relative importance, which is scaled between 0% (weak influence) and 100% (strong influence) (Elith et al. 2008), and relationships between PSI and predictors were visualised using partial dependency plots that show the fitted function while holding the effect of other predictors

at their mean (Elith et al. 2008). Relative model performance across spatial scales was assessed by comparing the overall deviance explained and mean predictive deviance for each optimal model.

Finally, we conducted two sensitivity analyses to examine potential bias introduced by low sample replication at small grain sizes. First, because the number of cells sampled was directly linked to spatial grain size (decreasing from n = 1,680 for 0.25 km^2 cells to n = 99 for 1,024 km^2 cells), we attempted to separate the effects of scale and cell sample size by standardising our sample size across grain size to that of the largest grain size (i.e. n = 99). To maintain extent in the sensitivity analyses we ensured that each island group was equally represented in each subsample by randomly sampling 25 cells from each of the four island groupings. Second, because the number of UVC represented per cell was directly linked to spatial grain size (78.9% of 0.25 km^2 cells represented by 1 UVC, whereas 79.8% of 1,024 km^2 cells represented by > 5 UVCs) (Fig. A4.4), we attempted to identify bias introduced by low UVC replication by standardizing all grain cells to contain a single UVC. For each grain size, a bootstrap sample was generated by randomly sampling a single UVC site from each grid cell. In each sensitivity analysis, we then followed the same BRT fitting procedure as our main analysis to determine the optimal BRT model for each bootstrap sample at each spatial grain size, and extracted the relative importance of each predictor, overall deviance explained, and mean predictive deviance. The process was repeated for 100 replicates.

All analyses were conducted using R version 3.3.1 (R Core Team 2016), and we provide our code at an open source repository (github.com/baumlab/robinson-benthic-scale).

4.4 Results

4.4.1 Phase shift index across reefs

At 2,199 UVC sites across 42 islands and atolls spanning ~ 43° latitude by ~ 61° longitude, reef benthic states ranged from coral-dominated (228 sites at 31 islands with > 50% hard coral cover and -3.1 < PSI < -0.3) to macroalgal-dominated (88 at 24 islands with > 50% macroalgal cover and 0.7 < PSI < 4.5) (Table A4.1). As expected, variability in the PSI was highest at the smallest spatial scales, such that every island encompassed at least one coral-dominated and one macroalgal-dominated 0.25 km^2 grid cell. Variation in PSI values decreased as grid cell size increased and, at the largest spatial scale (1,024 km^2), grids with the lowest PSI (< -0.75; coral cover > 30%) were on islands in the main Hawaiian archipelago and PRIAs, whereas grids with the highest PSI (> 0.75; macroalgal cover > 25%) were on uninhabited islands in the Northwestern Hawaiian archipelago and inhabited islands in the Marianas archipelago (Figs. 4.1, A4.2, A4.3).

4.4.2 Abiotic and bottom-up influences

Abiotic and bottom-up covariates were the dominant predictors of reef PSI values, with increases in SST and oceanic productivity, and decreases in wave energy, associated with lower PSI values (i.e. higher coral cover relative to macroalgal cover) at every spatial grain (Figs. 4.2a, 4.3). SST was consistently ranked as an important predictor (relative importance > 8.9%), and was most influential at the smallest and largest grains (relative importance > 13.9%) (Fig. 4.2a). Occurrence of algal-dominated reefs (PSI > 0.5) was predicted at the lowest temperatures (< 21°C), which transitioned towards greater coral dominance (PSI < 0.2) between 22-24°C and then remained relatively constant to PSI values of ~ 0 at the warmest grids (> 25 °C) (Fig. 4.3a,e,k,m). Oceanic productivity had an equally strong influence on the PSI with high importance values at small (0.25-1 km^2; ≥ 14.5%) and large (1,024 km^2; 22.2%) grains, but

lower values at intermediate scales (≤ 11.9 %). Algal-dominated reefs occurred in grids with the lowest oceanic productivity values (< 300 mg C m^2day^{-1}), beyond which the PSI gradually decreased to ~0 with increasing productivity (600-700 mg C m^2day^{-1}) to then remain constant as productivity estimates reached their maximum (800-1,000 mg C m^2day^{-1}) (Fig. 4.3b,g,n). Wave energy also had a strong influence across all spatial grains, increasing in relative importance with grain size (12.9-24.9%) before dropping to 13.7% at the largest grain size (Fig. 4.2a). The PSI and wave energy were weakly and negatively related at small spatial grains, such that coral dominance was maximized at low wave energy. This relationship was most pronounced at large spatial grains where, at 64 and 256 km^2, the PSI transitioned sharply towards coral dominance at wave energy < ~ 25,000 KWhr m^{-1} (Fig. 4.3c,f,i).

4.4.3 Biotic grazing influences

Although grazing biomass was generally a weak predictor of the PSI across spatial grains (mean relative importance of all herbivore biomass covariates = 6.8%) (Fig. 4.2b), the importance of different functional groups varied strongly among grain sizes. Across grain sizes, scraper and excavator biomass had the strongest influence of any herbivore covariate and steadily increased in importance with grain size, from 9.9% at 0.25 km^2 to 19.8% at 1,024 km^2. In contrast, cropper, browser and total herbivore biomass were weak predictors at all spatial grains (< 10%) (Fig. 4.2b), although croppers were moderately important at the smallest grain size (9.9% at 0.25 km^2). For any grazing covariate, the PSI ~ biomass relationships were non-linear and characterized by a shift to algal-dominated values (PSI > 0) at extremely low biomass estimates (< 10 kg ha^{-1}) but remained relatively constant above these thresholds at a PSI of ~0 (Fig. 4.3d,g,j,o). The scraper and excavator biomass threshold increased at 256-1,024 km^2, with the PSI steadily increasing towards algal-dominated values below a threshold of ~20-60 kg ha^{-1}.

4.4.4 Anthropogenic influences

The influence of anthropogenic covariates on the reef PSI varied between the travel time and population metrics where travel time was consistently more important than population density across all spatial grains (Fig. 4.2c). Travel time to nearest settlement increased in importance with spatial grain, reaching 16.3% at 256 km^2, while travel time to nearest market center was only important at small grain sizes (0.25-16 km^2; 6.4-11%). Population density estimates were consistently poor predictors of PSI values and remained below 5.8% across all grain sizes. Relative to abiotic and grazing influences, anthropogenic covariates were generally not important predictors of the PSI and, as such, the PSI was largely invariant across the range of human influence. However, travel time to nearest settlement was moderately influential at large scales, and predicted slight shifts towards algal grids (PSI > 0) at the highest (> 3000 hours; i.e. most remote grids) and lowest (< 2000 hours; i.e. most accessible grids) travel times but a PSI of ~ 0 in the middle of that range (Fig. A4.5).

4.4.5 Model fitting and sensitivity analyses

Our modelling approach was most accurate at predicting fine-scale patterns in the PSI, such that overall deviance explained decreased steadily with increasing spatial grain, from 43% at 0.25 km^2 to 32% at 1,024 km^2 (Fig. A4.6). Mean predictive deviance also decreased with increasing spatial grain (0.80 at 0.25 km^2 to 0.55 at 1,024 km^2), indicating that our ability to predict the PSI based on abiotic and biotic variables decreased at coarser scales (Fig. A4.6). In our sensitivity analysis where sample sizes were fixed at 100 cells across each grain size, patterns in both the deviance explained and the relative importance estimates were similar to the results from the full model, though were slightly more variable at small to moderate spatial grains (0.25-64 km^2) (Figs. A4.6, A4.7). Similarly, in our sensitivity analysis where sample sizes

were fixed at one UVC site per grid cell, temperature and productivity influences remained relatively unchanged across grain sizes between the full model and the single UVC analysis. However, at large grain sizes (64 – 1,024 km^2) the importance of wave energy, browser, and scraper and excavator covariates decreased relative to the full model, while cropper, total herbivore biomass, and population density (5 and 20 km) importance increased (Fig. A4.8). Relative importance estimates of the remaining covariates were relatively unaffected at small grain sizes (0.25 – 16 km^2).

4.5 Discussion

We combined ecological data with remotely-sensed environmental and anthropogenic covariates for 42 Pacific islands to show that a composite indicator of the relative abundances of hard coral and macroalgal organisms - the phase shift index - was primarily predicted by natural variation in temperature, productivity and wave energy, such that coral-dominated reefs occurred in warm, productive regions at areas of low wave energy. In contrast, grazing by herbivorous fishes and impacts of human activity were both comparatively weak influences on benthic communities, although several of these metrics did increase in importance at coarse spatial resolutions, where areas with extremely low scraper and excavator biomass or very short or long distances to market centers shifted towards algal states. Our results add to growing evidence that biotic interactions are moderately important at coarse grain sizes and highlight the non-linear nature of grazing control. Our analyses also show, for the first time, that abiotic conditions outweigh grazing pressure as predictors of the relative abundances of hard coral and macroalgal organisms, perhaps precisely because the influence of grazing is non-linear, with grazer biomass bearing little influence above a rather low threshold.

We found that abiotic and bottom-up factors were important predictors of benthic

community state at all spatial grains. Shifts from positive (algal-dominated) to negative (coral-dominated) PSI values tracked increases in sea surface temperature (Williams et al. 2015b), representing a latitudinal gradient in coral dominance that is likely linked to energetic constraints on the growth rates of calcifying organisms (Johannes et al. 1983; Lough & Barnes 2000). The mechanisms by which bottom-up processes influence coral reef ecosystems are more complex (Gove et al. 2016). High chlorophyll-a concentrations are associated with enhanced near-shore phytoplankton (Gove et al. 2016), planktivorous fish (Williams et al. 2015a) and piscivorous fish biomass (Nadon et al. 2012), suggesting that increases in both food availability (Leichter et al. 1998) and background nutrient supply (Burkepile et al. 2013) promotes coral cover on Pacific reefs. Wave energy was as important as temperature and productivity in predicting PSI values, consistent with evidence that habitat suitability is a key influence on benthic community composition between sites (Williams et al. 2013; Gove et al. 2015) and among islands (Williams et al. 2015b) due to the vulnerability of coral and algal organisms to dislodgement, breakage and scour in high energy environments (Madin & Connolly 2006), and perhaps additionally the hindrance high wave energy poses for grazers (Bejarano et al. in press). These influences were relatively scale-invariant, and consistently stronger than biotic covariates, in agreement with recent analyses of remotely-sensed environmental covariates that have highlighted the significant roles played by biophysical factors in structuring coral reef benthic communities across scales (Madin & Connolly 2006; Williams et al. 2015b; Gove et al. 2015).

We did, however, find substantial scale-dependence among biotic covariates, with the influence of scraper and excavator biomass increasing to match that of abiotic covariates at 64 - 1,024 km^2 grains. This increase in relative importance indicates that the role of scrapers and excavators in promoting coral recruitment and controlling algal cover is detectable at coarse

grain scales, and is greater than that of cropper and browser functional groups. Excavators and scrapers tend to be large-bodied species, and large-bodied individuals are often preferentially targeted by fishers (Graham et al. 2005; Bellwood et al. 2011; Robinson et al. 2016). Because biomass estimates at the largest spatial grains were often representative of entire islands, strong differences in scraper and excavator biomass between exploited and unexploited islands may therefore explain the increased importance of these groups at large scales. However, for all grazing covariates, biotic effects were unexpectedly weak at small grains, with PSI values remaining invariant across much of the observed range in grazing biomass. These results contrast markedly with experimental site-level grazer exclusion studies that find strong effects of grazing biomass and species diversity in promoting coral cover (Mumby et al. 2006; Burkepile & Hay 2008), and with observational evidence of positive associations between site-level estimates of coral cover and herbivore biomass across islands in American Samoa (Heenan & Williams 2013) and Hawaii (Jouffray et al. 2015). However, as abiotic and productivity covariates were consistently stronger predictors of the PSI than grazing biomass, we suggest that, at oceanic extents, coral and algal composition of a given reef is primarily determined by environmental conditions rather than grazing capacity, given a minimum threshold of grazer presence.

We cannot discount the fact that weak grazing influences at smaller grain scales may reflect sampling error due to grids containing relatively few UVC surveys. Allometric scaling of herbivore foraging distances and home ranges with individual body size indicate that large herbivorous fish species - scrapers and excavators - forage across areas up to ~0.5 km^2 (Nash et al. 2013, 2015). Given that these species also typically school in large aggregations (Green & Bellwood 2009), such behaviors add uncertainty to biomass estimates when surveys are unreplicated and limited to relatively small areas of the reef. At our smallest grain sizes (0.25-1

km^2), grids often contained only one or two unreplicated UVC surveys conducted by two divers across ~ 350 m^2 and, as such, fail to fully characterize the resident fish community over longer time scales. This effect was apparent in our sensitivity analysis which showed that, for large scales where grids typically contained ≥ 2 UVC sites (64 – 1,024 km^2), constraining cells to a single site caused the importance of functional groups that were infrequently observed (scrapers, excavators, and browsers) to decrease, but the importance of groups that were regularly detected (croppers and total herbivores) to increase. These patterns suggest that our ability to detect meaningful grazing relationships at small grain scales may have been limited by sampling error and, although we somewhat controlled for variability in fine-scale biomass estimates by capping biomass outliers, larger grains may have provided a more representative measure of grazing biomass by averaging fish biomass estimates across multiple UVC sites. Given that the importance estimates of abiotic influences and productivity were robust to our sensitivity analyses, analysis of replicated ecological surveys would help resolve uncertainty in the relative influences of abiotic, bottom-up and top-down pressures on benthic state at small scales.

Relative to abiotic and biotic influences, anthropogenic covariates were weak predictors of the PSI. Weak site-level relationships between human population density and benthic states have been documented at global and regional scales, indicative of both the inability of population density to capture local impacts as well as overriding influences of global stressors (Bruno & Valdivia 2016). We did, however, find novel evidence of a link between the PSI and travel time to settlement centers, reflecting slight shifts towards algal dominance at the most accessible locations. By directly measuring human access to coral reefs, travel time metrics may supersede human population density as a metric of local stressors (e.g. fishing, sedimentation, pollution). We caution that these metrics may be misleading when used to compare isolated reefs that span

environmental gradients where, for example, an apparent link between increased algal abundances at the most remote grid cells (> 3,500 hours travel time) reflected influences of temperature and productivity at uninhabited Northwestern Hawaiian Islands rather than human impacts. Indeed, given that grazing covariates provided stronger predictive power than human metrics at the largest spatial grains, grazing biomass may provide a more accurate reflection of anthropogenic disturbance than population density and travel time metrics. Combining herbivore biomass with fine-scale indices of terrestrial pollution that predict local anthropogenic impacts at smaller spatial scales (e.g. Jouffray et al. 2015) may facilitate a scaled-up approach to predicting human influences on coral reefs at global scales.

Understanding how the relative strengths of abiotic, biotic, and anthropogenic factors shift over spatial scales can provide insights into when mechanisms of promoting reef resilience are most effective. Our results suggest that abiotic context is likely key in controlling the competitive balance between coral and macroalgae and thus is a primary determinant of reef state at macroecological scales. Some remote sub-tropical coral reefs, for example, support many algal-dominated sites, irrespective of grazer biomass (Vroom & Braun 2010). Alternatively, in warm and productive regions, healthy and diverse grazing communities confer resilience to loss of coral cover following disturbance events (Cheal et al. 2013; Graham et al. 2015; Nash et al. 2015). Such distinctions highlight the difficulties associated with evaluating grazing function across reef regions. Indeed, the importance of abiotic and bottom-up influences in controlling reef state may explain the lack of observed phase shifts on many degraded coral reefs globally (Bruno et al. 2009), and inform debates about the generality of phase shifts across reef regions (Roff & Mumby 2012). Irrespective of environmental conditions, non-linearities in benthic ~ grazing relationships show that areas of extremely low herbivore biomass are characterised by

algal-dominated states, consistent with evidence of thresholds in reef benthic state at low grazer biomass (Graham et al. 2015; Jouffray et al. 2015). Currently, the effectiveness of management strategies that aim to protect reef benthos by promoting herbivorous grazing in marine protected areas is disputed, with examples of coral recovery (Mumby et al. 2007; Rasher et al. 2012) at odds with studies reporting no effect of protection status on benthic state (Kramer & Heck Jr. 2007; Russ et al. 2015), although perceived management ineffectiveness may also arise when herbivore populations fail to recover (Huntington et al. 2011; Carassou et al. 2013). Our results suggest that restoring grazing function of scraper and excavator species at heavily-exploited reef sites that support very low herbivore populations and, in less degraded regions, preventing depletion of grazer populations below a threshold ~10-20 kg ha^{-1} may be effective management strategies.

By focusing on two broad benthic community states - coral or algal dominance - we excluded contributions of other major taxonomic groups on reefs that influence the strength of coral ~ algal competition where, for example, CCA act as important mediators in competition between hard coral and macroalgae (Price 2010) and turf algae can cause substantial coral mortality (Arnold et al. 2010). Consideration of these additional influences on reef benthic community composition and their contribution to alternative reef states (Jouffray et al. 2015) will improve our understanding of abiotic and biotic drivers in reef ecosystems. We also stress that our space-for-time approach is distinct from the original definition of a phase shift as a temporal change in reef benthic state (Hughes 1994; Nystrom et al. 2008) but, instead, we utilized the PSI in order to characterize spatial differences in benthic community composition rather than identify drivers or examples of Pacific phase shifts.

More broadly, we were also limited by the spatial resolution of two of our remotely

sensed covariates, by our measurement of wave energy, and by our inability to vary extent in addition to grain. First, temperature and productivity estimates were extracted at coarser resolutions than our smallest grain sizes (i.e. at ~21 km^2), and thus neighboring cells at small grains were likely to be assigned identical environmental conditions. However, given that gradients in temperature and productivity generally extended latitudinally across the Pacific Ocean, these covariates are unlikely to vary substantially at fine-scales. As such, this resolution mismatch likely had a minimal influence on our predictive models. Second, our time-integrated method of estimating long-term mean wave energy was unsuitable for quantifying the frequency and magnitude of extreme wave events which are major physical influences on reef benthic structure (Gove et al. 2015; Williams et al. 2015b). Although high-resolution maximum wave energy data have been developed for individual Pacific islands (Gove et al. 2015), equivalent data were unavailable for the full CREP dataset; we recommend further investigation of the relative roles of average and anomalous wave events across scales to improve our understanding of physical processes on reefs. Third, although our analysis encompassed large gradients of abiotic and biotic covariates, reefs were patchily distributed across the Pacific with each island group differing substantially in area and, as such, we were unable to systematically shift extent. Similarly, as coral reef ecosystems are among the smallest marine ecosystems by area, our maximum grain size (1,024 km^2) was often smaller than equivalent terrestrial approaches that have extended grain sizes to 100,000 km^2, often spanning different habitat types and ecosystems (Rahbek & Graves 2000; Araujo & Luoto 2007; Cohen et al. 2016). Nevertheless, as 1,024 km^2 generally represented entire islands, our spatial resolution was ecologically relevant for examining processes structuring coral reef benthic communities. Thus, although there is no single correct grain or extent, utilising macroecological datasets to systematically shift grain and

extent will develop our understanding of spatial scaling rules in particular ecosystems (Rahbek 2005; Wisz et al. 2013) and, consequently, improve models of species abundance distributions (Heikkinen et al. 2007). Furthermore, where the importance of biotic factors at coarse scales has previously been revealed by analysing occupancy patterns derived from breeding bird checklist surveys (Heikkinen et al. 2007; Gotelli et al. 2010; Belmaker et al. 2015), the addition of abundance estimates allowed us to examine how a specific biotic process - grazing - scaled in space. Moving forward, further consideration of biotic scaling in the context of species abundances will offer insights into how the strength of trophic processes and species interactions varies spatially, and thus link more directly to concepts of ecosystem function (Brose & Hillebrand 2016) and resilience to global environmental change (Van der Putten et al. 2010).

In coral reef systems, the role of abiotic, biotic and anthropogenic drivers have typically been considered independently where, for example, variation in Pacific reef benthic cover has been examined in the context of biophysical forces (Williams et al. 2015b), human presence (Smith et al. 2016), or grazing biomass (Heenan & Williams 2013), but rarely for all three components or across different spatial scales. Our results provide a foundation for a unified understanding of scale-dependence in the strength of abiotic and biotic controls on reef benthic communities across scales, and demonstrate, for the first time, that abiotic factors are primary determinants of the coral reef phase shift index across the Pacific Ocean. Our multi-scale approach may help to resolve debate on the importance of bottom-up or top-down processes for promoting healthy reef states across regions (Roff & Mumby 2012), and stimulate discussion about meaningful baselines for reefs that are naturally dominated by algal organisms (Vroom & Braun 2010). Beyond coral reef systems, understanding the scales at which biotic interactions overcome abiotic constraints can be advanced by combining remotely-sensed abiotic data with

ecological observations collected at large spatial scales. Such macroecological approaches facilitate quantitative examination of scale-dependence among specific biotic processes that will advance our understanding of how species interactions structure ecological communities.

					Grain		*Extent*			
Driver	Pattern	Hard coral	Macroalgae	Mechanism	Site	Reef	Reef	Reef archipelago/shelf	Ocean-basin	Geographic region
Abiotic										
SST	Hard coral cover increases with SST	+	-	Coral calcification rates reduced at low temperatures		1			1	Pacific[1]
Wave energy	Hard coral and macroalgal cover decrease with increasing wave action	-	-	High wave energy increases coral colony damage and removal, reduces larval settlement, and removes established macroalgal organisms.	2,3	1	2,3		1	Pacific[1,2,3]
Latitude	Higher latitudes associated with decrease in calcifying organisms and increase prevalence of algal communities	-	+	Proxy for temperature	4			4		Hawaiian archipelago[4]
		-	0			5			5	Pacific[5]
Biotic – bottom-up										
Oceanic productivity	Hard coral cover maximised at islands with high mean chlorophyll-a values, and macroalgal cover highest at the lowest mean chlorophyll-a values	+	-	Increased nutrient supply represents higher energy flux into system, promotes coral growth		1			1	Pacific[1]
	Macroalgal cover increased with a water quality index (proxy for dissolved nutrient and chlorophyll concentrations)	0	+	Macroalgal growth increases with level of dissolved nutrients	6			6		GBR[6]

Biotic – top-down									
Herbivore biomass	Total herbivore biomass and/or biomass of key functional groups is positively correlated with coral cover and negatively correlated with macroalgal cover	+	-	Grazing promotes coral recruitment, reduces macroalgae	4,8	7	4,7,8		Hawaiian archipelago[4], Caribbean[7], American Samoa[8]
	Increased herbivore biomass correlated with lower macroalgal cover, but unrelated to hard coral cover	0	-	colonisation rates and abundance.	9			9	Caribbean[9]
	Herbivorous fish biomass not associated with macroalgal cover	*Not tested*	0	No impact of fishing on herbivorous fish biomass	10		10		Pacific[10]
Anthropogenic									
Population density	Coral reef benthic state unrelated to local impacts when measured by human population density	0	0	Fishing and pollution have weak effects on benthic cover, or those effects are superseded by global stressors such as climate change, or population density is a poor proxy for local impacts	11	1	11	1,11	Pacific[1], Global[11]
		0	+		4		4		Hawaiian archipelago[4]
Effluent	Reduced hard coral cover at higher effluent levels	-	0	Proxy for sedimentation and pollution impact on coral growth	4		4		Hawaiian archipelago[4]

References: 1. Williams et al. (2015b); 2. Williams et al. (2013); 3. Gove et al. (2015); 4. Jouffray et al. (2015); 5. Smith et al. (2016); 6. Fabricius et al. (2005); 7. Williams & Polunin (2001); 8. Heenan & Williams (2013); 9. Newman et al. (2006); 10. Carassou et al. (2013); 11. Bruno & Valdivia (2016)

Table 4.1 Major abiotic and biotic drivers of hard coral and macroalgae cover detected by observational studies conducted at different spatial grains and extents. Relationships were either positive (+), negative (-), insignificant (0), or not tested, and approximate grain and extent values were extracted from map figures and methods section of each paper, where grain was the smallest sampling unit analysed and extent was the latitudinal and longitudinal range of the study. Both spatial attributes were then aggregated into grains of site (< 0.5 km^2) or reef areas (0.5 - 500 km^2, equivalent to an atoll or island), and extents of an island, reef archipelago/continental shelf, or ocean basin.

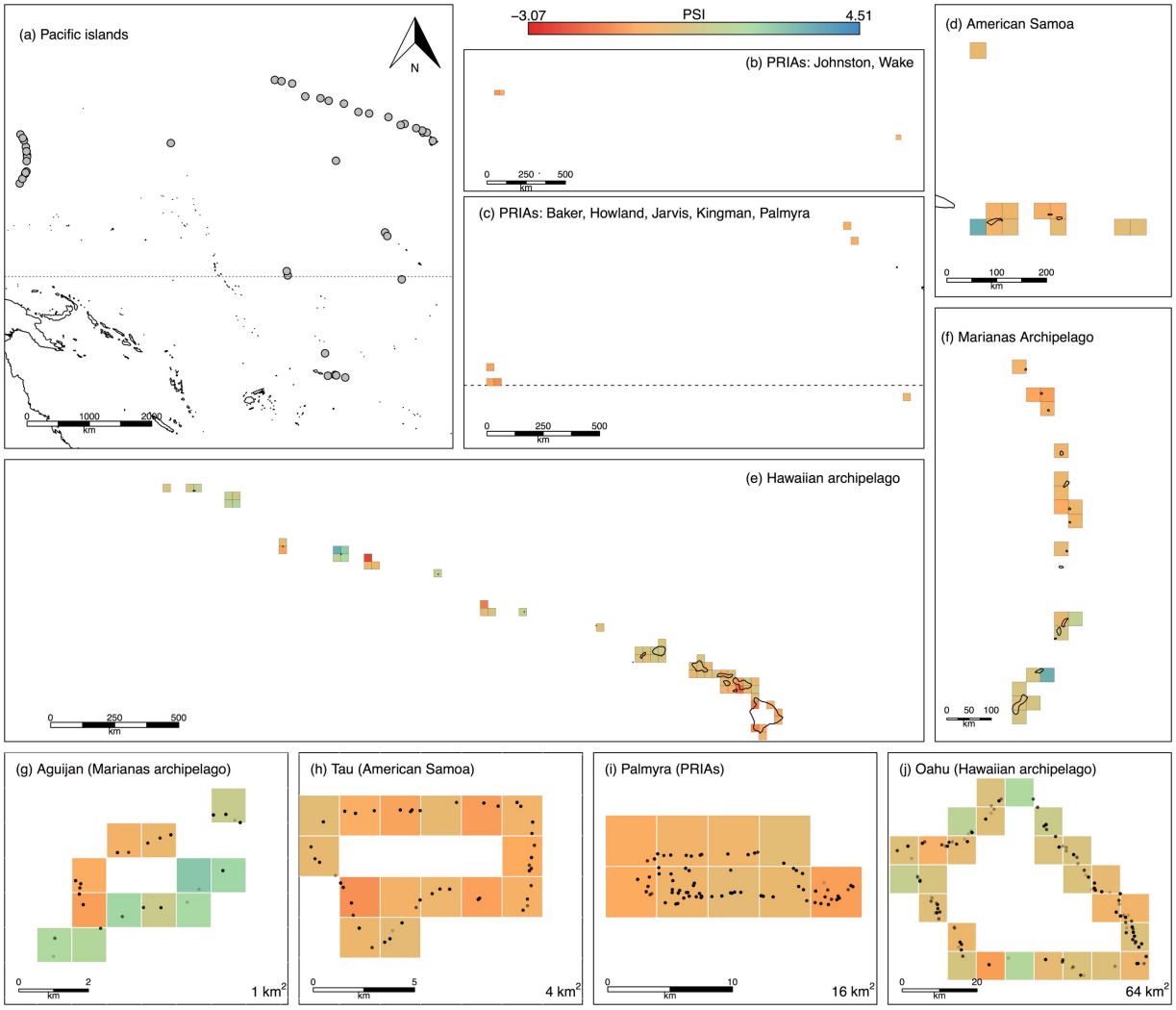

Figure 4.1 Spatial variation in reef benthic community composition across 42 Pacific islands and atolls. Across each island group (a), cells are colored by its PSI value (red = coral-dominated; blue = algal-dominated) at the 1,024 km^2 grain scale for the Pacific Remote Island Areas (PRIAs, n = 7) (b,c), American Samoa (n = 5) (d), Hawaiian archipelago (n = 17) (e) and Marianas archipelago (n = 13) (f). Examples of smaller grain scales shown for Aguijan at 1 km^2 (g), Tau at 4 km^2 (h), Palmyra at 16 km^2 (i), and Oahu at 64 km^2 (j), overlaid by black points that indicate UVC site locations.

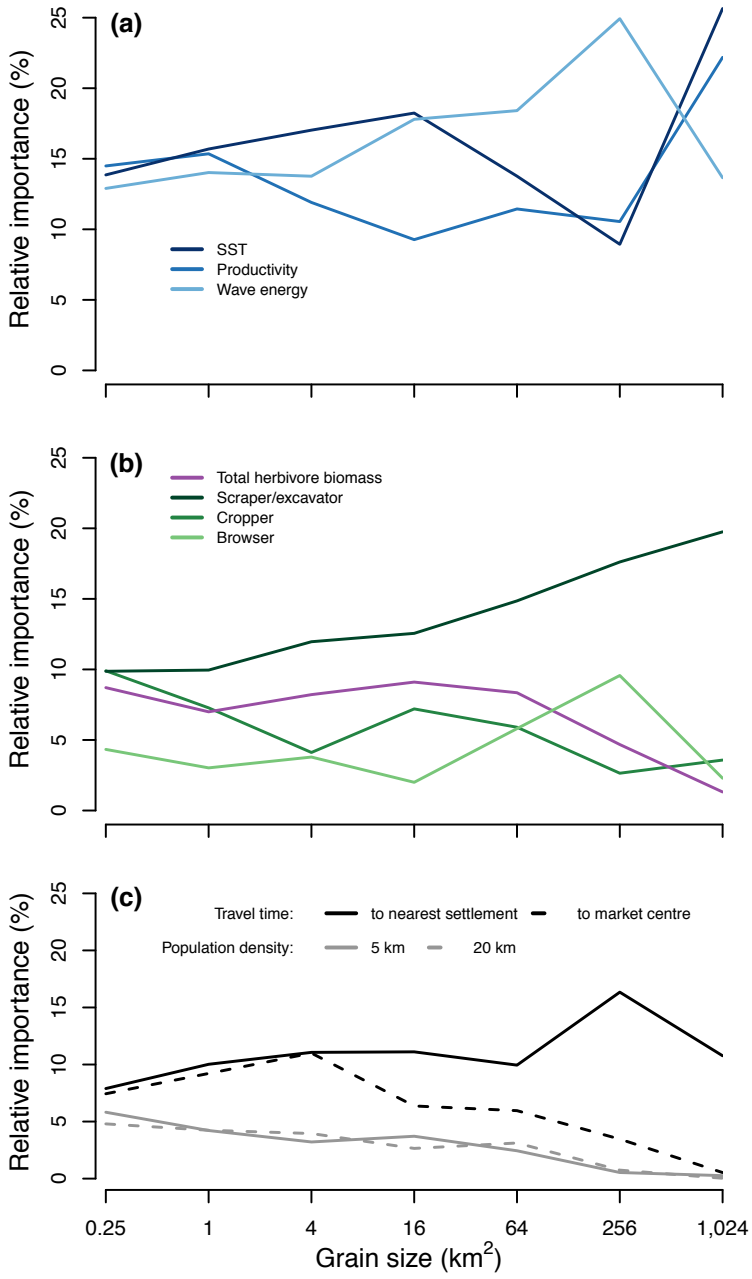

Figure 4.2 Relative importance (%) of abiotic, biotic, and anthropogenic covariates in explaining variation in PSI values. Covariates are coloured and separated into abiotic and bottom-up (a, blues), biotic grazing (b, greens and purple) and anthropogenic (c, black and grey) across 0.25 to 1,024 km^2 grain scales.

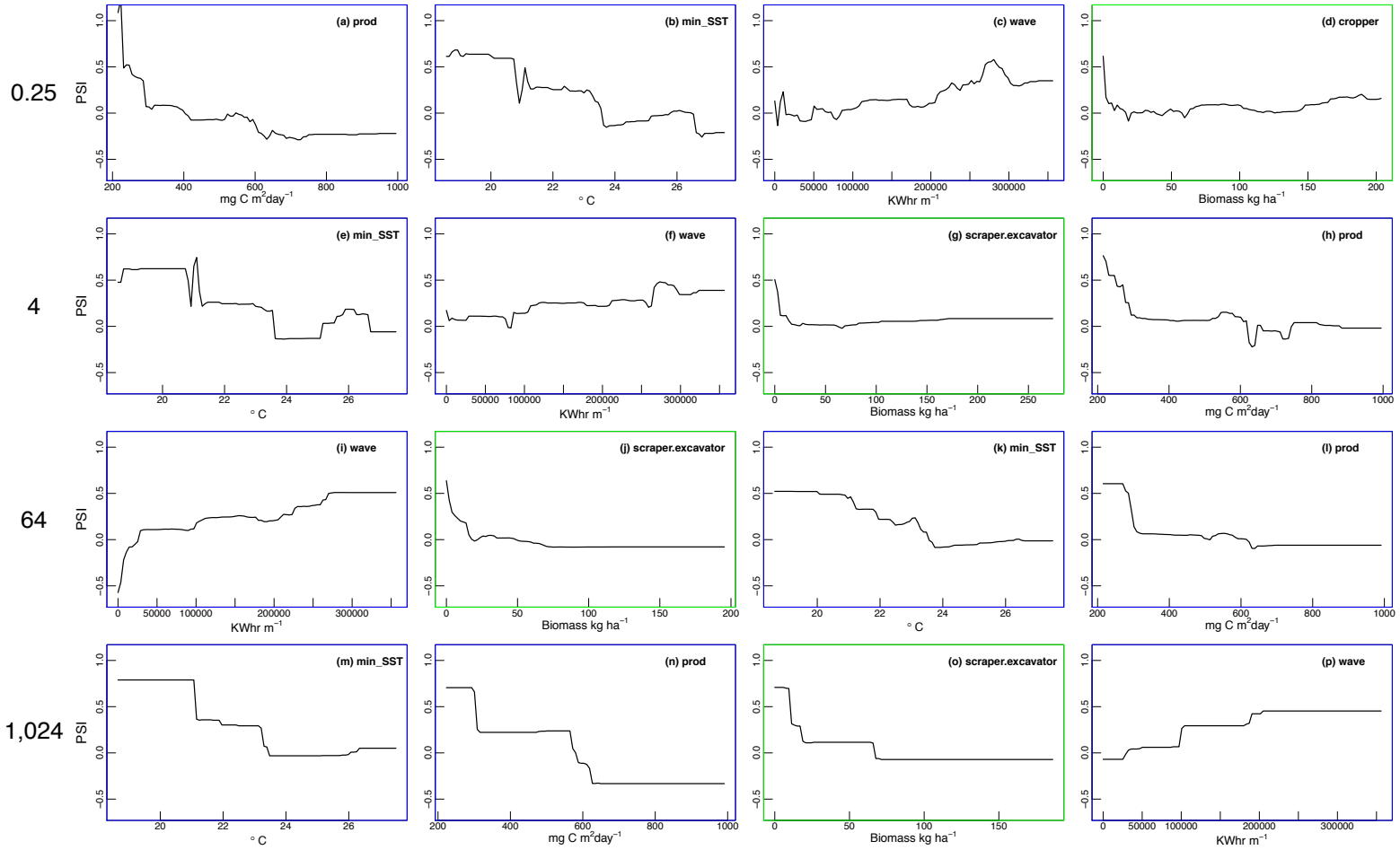

Figure 4.3 Partial dependence plots for the four most important covariates in predicting PSI values. Across selected grain scales, 0.25 (a - d), 4 (e - h), 64 (i - l), and 1,024 km^2 (m - p) (i.e. each row), covariate importance decreases across columns from left (most important covariate) to right (4th ranked covariate). Plot borders are colored to distinguish between abiotic/bottom-up (blue) and biotic (green) covariates, and annotated with each covariate name (min_SST = minimum SST; prod = oceanic productivity; wave = wave energy; total_herb = total herbivore biomass; scraper = scraper biomass; excavator = excavator biomass). Partial dependence plots for the top four covariates at all grain scales are shown in Fig. S4.5.

Chapter 5 – Discussion

Empirical tests of general ecological patterns conducted at broad spatial scales and in different ecosystems provide opportunities for validating ecological theory (Marquet et al. 2005) and gaining insights into the drivers of global environmental degradation (Kerr et al. 2007). The work presented in this thesis utilises data collected across the tropical Pacific Ocean to test macroecological predictions of body size allometry in reef fishes against gradients in abiotic factors and exploitation pressure, and quantify scale dependence in the drivers of reef benthic community structure. At pristine sites on Kiritimati Atoll, positive trophic position ~ body size and negative abundance ~ body size relationships provided novel evidence of size structuring in coral reef fish communities (Fig. 2.2), and supported theoretical predictions that allometric scaling relationships were dependent on modes of energy acquisition (Fig. 2.3) (Brown & Gillooly 2003). Across the Pacific, macroecological patterns in reef fish community size structure provided novel evidence of size-selective exploitation in reef fisheries (Fig. 3.2), and revealed that fish biomass was highly sensitive to environmental variation. Finally, regional variation in hard coral and macroalgal cover was shown to be primarily determined by local environmental conditions, rather than herbivore biomass or human presence (Figs. 4.2, 4.3).

5.1 Abiotic control of coral reefs

Abiotic factors were important influences on fish (Chapter 3) and benthic community (Chapter 4) structure at macroecological scales. Sea surface temperature had a strong effect on size spectrum slopes (Fig. 3.3a,b) and reef fish biomass (Fig. 3.3c,d), as well mediating relative dominance of hard coral and macroalgal organisms (Fig 4.3).

These patterns highlight the importance of incorporating temperature effects in regional comparisons of reef communities (e.g. Williams et al. 2015a, Williams et al. 2015b), which may improve estimates of natural baselines for fish (e.g. Sandin et al. 2008) and benthic community structure (e.g. Bruno et al. 2014). Although the role of energetic constraints in limiting growth rates of calcifying organisms and mediating coral-algal competition is well-documented (Lough & Barnes 2000; Williams et al. 2015b; Gove et al. 2016), mechanistic explanations for temperature control of fish assemblages were less clear. Predator-prey mass ratio and trophic transfer efficiency are predicted controls on size structure (Brown & Giloolly 2003; Andersen & Beyer 2000; Brown et al. 2004), but these rules do not accommodate extensions to metabolic theory that also predict temperature control of community biomass, trophic structure, and the strength of consumer-resource interactions (Bruno et al. 2015). We hypothesised that steepening spectra in cooler regions might be caused by a reduction in top-down control (Chapter 3), though we were unable to test this empirically owing to confounding influences such as covariation of temperature with productivity, historical exploitation, and energetic subsidies to top predators (Barneche et al. 2014). Nevertheless, by confirming general patterns in community size structure at Kiritimati Atoll (Figs. 2.2, 2.3), we were then able to scale up and describe real differences in reef fish community structure across the Pacific that revealed novel temperature control of size distributions (Fig. 3.3). Thus, by examining patterns in fish and benthic communities across gradients in local environmental conditions, we provided insights into the abiotic mechanisms that structure coral reef systems.

5.2 Human degradation

We detected anthropogenic degradation of coral reef ecosystems across the Pacific Ocean. For fishes, size-specific exploitation caused community size spectra to steepen at sites on Kiritimati that were more accessible to fishers (Fig. A2.10) and at US-affiliated islands that were heavily populated or close to provincial capitals (Fig. 3.2a,b). Until now, small-scale analyses of UVC data had identified weak exploitation impacts on specific size classes, but in sites that were historically exploited and on islands with similar fisheries types and fish community compositions (Dulvy et al. 2004; Graham et al. 2005). By developing and applying improved size-spectra fitting methods (Edwards et al. 2017) and examining a wider disturbance gradient that encompassed diverse fisheries (Dalzell 1996) in distinct biogeographic regions (Kulbicki et al. 2013) our results indicated that exploitation degrades fish community size structure. Size-selective fishing increases the relative abundance of smaller-bodied fishes and correspondingly increases rates of growth and biomass turnover and decreases mean trophic level, mirroring exploitation impacts in temperate fisheries (e.g. Bianchi et al. 2000; Blanchard et al. 2005; Blanchard et al. 2009).

Size-based theory offers a powerful framework for understanding exploitation, and recent examples of length-based stock assessment models (Nadon et al. 2015) and size-structured food web models (Rogers et al. 2014) are promising avenues for future research in reef systems. Here, we showed that total fish biomass was a poor indicator of fishing pressure owing to its disproportionate response to light levels of size-selective fishing and relative sensitivity to temperature and productivity (Fig 3.3). Simple indicators that provide meaningful measures of community-level properties, such as size spectra, can complement coarse indicators such as fish biomass, and are particularly

useful in data-limited systems such as coral reefs (Sadovy 2005; Nash & Graham 2016).

Although exploitation impacts on reef fish communities were detected on Kiritimati Atoll and across Pacific regions, reef benthic community composition was only weakly associated with human presence. Ongoing loss of hard coral cover and associated phase shifts towards algal-dominated states are critical issues on coral reefs which reflect synergistic impacts of habitat destruction, thermal bleaching events, physical disturbances, pollution, and overexploitation of grazing fishes (Hughes et al. 2003; Bellwood et al. 2004). The population and travel time proxies that we compiled are likely poor representations of all these threats (Bruno & Valdivia 2016), and development of high-resolution data on anthropogenic pressures such as water quality (e.g. Jouffray et al. 2015) would improve benthic analyses at macroscales. We did, however, identify a scraper and excavator grazing biomass threshold at ~10-20 kg ha^{-1} below which reefs transitioned sharply towards algal-dominated PSI values. Such non-linear grazing effects suggest that targeting recovery of heavily-exploited herbivore populations may be an effective strategy for promoting coral cover on degraded reefs.

However, for moderately-degraded or near-pristine systems, our finding that environmental influences are primary controls of reef benthic state underlines the importance of maintaining a local perspective when comparing reefs across distinct regions. For example, management strategies for maximising coral cover are more relevant for exploited Hawaiian Islands (e.g. Williams et al. 2016) and disturbance-prone equatorial reefs (e.g. Nash et al. 2015) than for remote reefs in the Northwest Hawaiian Islands (Vroom & Braun 2010). Difficulties associated with sampling in remote locations mean that our understanding of ecological processes on human-dominated reefs is far

more comprehensive than it is for pristine systems (Knowlton & Jackson 2008). By surveying minimally-disturbed reef sites, the CREP dataset addresses this gap and enabled us to demonstrate how environmental influences underpin spatial variation in the coral ~ algal composition of uninhabited Pacific islands.

5.3 Caveats and Limitations

Despite utilising such a spatially-extensive dataset, our statistical analyses were limited by our ability to replicate patterns at small scales and to accurately quantify local human impacts with remotely-sensed predictors. The lack of temporal replication at the UVC scale was particularly problematic for fitting size distributions (Chapters 2, 3) and comparing patterns generated across spatial grains (Chapter 4). Although we utilised a suite of sensitivity analyses (Appendices A-C) to assess and account for any potential biases produced by unequal sampling effort, data were most reliable when aggregated at reef or island scales and, consequently, important site-level relationships, such as the influence of habitat complexity on fish size structure at smaller spatial scales (e.g. Alvarez-Filip et al. 2011; Wilson et al. 2010), were overlooked.

At any scale, our ability to identify meaningful relationships was further limited by our reliance on combining covariates that were measured at different scales. Habitat complexity, for example, was measured both *in situ* (UVC level) and remotely (1 km^2 resolution), while remotely-sensed SST and productivity estimates were extracted at a 4.6 km^2 resolution but assigned to individual UVCs. Abiotic drivers such as temperature can vary substantially among depths, seasons and sites (Leichter et al. 2006) and, consequently, this scale mismatch reduced our ability to detect scale-dependency among abiotic drivers of reef benthos. Similarly, many explanatory covariates were coarse

proxies for unmeasured processes, such as human population density for exploitation pressure or benthic degradation, and radiation and chlorophyll concentrations for primary productivity. As a result, many of the unexpected patterns we detected in the CREP dataset (such as weak human influences on the PSI) likely reflect our inability to quantify fine-scale processes on reefs, such as the energetic contribution of plankton biomass to reef food webs or the impact of effluent run-off on coral cover. Development of fine-scale abiotic (e.g. *in situ* oceanographic data; Gove et al. 2015) and human covariates (e.g. GIS-derived human-use variables; Jouffray et al. 2015) will substantially improve our understanding of the mechanisms that structure reef fish and benthic communities.

Isolating natural stochasticity from sampling biases is a concern for any macroecological study (Beck et al. 2012). More broadly, our ability to infer mechanistic relationships was limited by two other general critiques of macroecology. First, given that long-term, large-scale datasets are often unavailable, macroecology predominantly adopts a space-for-time approach that implicitly assumes temporal variation is minimal (Kerr et al. 2007; Fisher et al. 2010). Our datasets spanned 2 (Kiritimati Atoll) and 4 years (CREP) and, although potential year effects were assessed with sensitivity analyses (Chapter 2) or accounted for in mixed effects models (Chapter 3), these time periods are insufficient in length to detect temporal trends in fish populations (e.g. Mellin et al. 2010).

5.4 Future Directions

Extending the spatial differences described here over larger time scales might provide useful avenues for future research. For example, examining temporal trends in coral and macroalgal cover would inform our understanding of reef health in sub-tropical

algal reefs (Vroom & Braun 2010) and provide novel perspectives on resilience processes that control reef benthic regimes (Graham et al. 2015). Such temporal analyses have uncovered resilience mechanisms in frequently-disturbed Seychelles (Graham et al. 2015; Nash et al. 2015) and Australian reefs (Cheal et al. 2013), but the importance of these processes for other reef regions remains unclear (Roff & Mumby 2012). Similarly, replicated surveys on fished reefs would allow tests of the interaction between coral habitat loss, size-selective exploitation, and fisheries productivity (Rogers et al. 2014; Bozec et al. 2016), and could also be leveraged to quantify the link between grazing function, herbivore size structure (e.g. Nash et al. 2015), and fishing.

In any system, strong inference of ecological mechanisms from correlative relationships often requires patterns to be validated by process-based models (Gaston & Blackburn 1999; McGill 2003; Kerr et al. 2007). Linking the empirical size spectra presented here to size-based models of coral reef food webs (Rogers et al. 2014) would help to disentangle direct fisheries effects on large- bodied herbivores from indirect effects of predation release (Blanchard et al. 2009), and provide a mechanistic basis for understanding the influence of temperature on top-down control in complex food webs (Petchey et al. 2010).

Finally, temperature was a pervasive influence on both reef and benthic communities. Given that rising temperatures are predicted to degrade habitat, alter species interactions and dispersal patterns, and reduce primary productivity (Munday et al. 2008), it is imperative that we develop quantitative predictions for how community-level properties respond to warming. Metabolic approaches can provide theoretical predictions of the structure of fish communities under warming scenarios (e.g. Barneche

et al. 2014) which are underpinned with empirical support from replicated surveys of bleached fish and benthic communities (e.g. Graham et al. 2015).

5.6 Conclusion

Standardized ecological monitoring programmes such as CREP provide invaluable fine-grained ecological data collected across large extents (Beck et al. 2012) that, combined with remote-sensing technologies, present unique opportunities for testing ecological theories across scales. By scaling up from sites to islands, this thesis provides empirical evidence of size-based constraints on reef fish community structure that are mediated by temperature and degraded by anthropogenic activities, and reveals that the strength of abiotic controls on benthic community composition outweigh both grazing and human-associated influences. Anchoring our size- based analyses with expectations from theoretical process-based models enabled us to examine the relative roles of abiotic, biotic and anthropogenic influences in producing fundamental patterns of community organisation. In this way, our results underline the importance of incorporating abiotic effects when comparing communities across scales and ecosystems, while documenting wide-ranging exploitation impacts from island to ocean-basin scales that increase the vulnerability of coral reef ecosystems (Bellwood et al. 2004). Ultimately, macroecology provides invaluable insights into the influence of abiotic and biotic processes in determining different levels of ecological organisation, and provide important predictive tools that can be used to identify mechanisms by which human stressors degrade ecosystems.

Bibliography

Ackerman, J.L. & Bellwood, D.R. (2000). Reef fish assemblages: A re-evaluation using enclosed rotenone stations. *Mar. Ecol. Prog. Ser.*, **206**, 227–237.

Ackerman, J.L., Bellwood, D.R. & Brown, J.H. (2004). The contribution of small individuals to density-body size relationships: Examination of energetic equivalence in reef fishes. *Oecologia*, **139**, 568–571.

Alvarez-Filip, L., Dulvy, N.K., Gill, J.A., Côté, I.M. & Watkinson, A.R. (2009). Flattening of Caribbean coral reefs: Region-wide declines in architectural complexity. *Proc. R. Soc. B*, **276**, 3019–3025.

Alvarez-Filip, L., Gill, J.A. & Dulvy, N.K. (2011). Complex reef architecture supports more small-bodied fishes and longer food chains on Caribbean reefs. *Ecosphere*, **2**, 1–17.

Andersen, K.H. & Beyer, J.E. (2006). Asymptotic size determines species abundance in the marine size spectrum. *Am. Nat.*, **168**, 54–61.

Andréfouët S, Muller-Karger FE, Robinson JA, Kranenburg, CJ, Torres-Pulliza, D, Spraggins, SA, Murch, B (2005). Global assessment of modern coral reef extent and diversity for regional science and management applications: a view from space. In: *Proceedings of 10th International Coral Reef Symposium (eds Y. Suzuki, T. Nakamori, M. Hidaka, H. Kayanne, B. E. Casareto, K. Nadaoka, H. Yamano, M. Tsuchiya, and K. Yamazato)*, pp. 1732-1745, Japanese Coral Reef Society, Okinawa, Japan.

Araújo, M.B. & Luoto, M. (2007). The importance of biotic interactions for modelling species distributions under climate change. *Glob. Ecol. Biogeogr.*, **16**, 743–753.

Araújo, M.B. & Rozenfeld, A. (2014). The geographic scaling of biotic interactions. *Ecography*, **37**, 406–415.

Arnold, S.N., Steneck, R.S. & Mumby, P.J. (2010). Running the gauntlet: Inhibitory effects of algal turfs on the processes of coral recruitment. *Mar. Ecol. Prog. Ser.*, **414**, 91–105.

Ayotte, P., K. McCoy, I. Williams, and J. Zamzow. (2011). *Coral Reef Ecosystem Division standard operating procedures: data collection for Rapid Ecological Assessment fish surveys.* Pacific Islands Fish. Sci. Cent., Natl. Mar. Fish. Serv., NOAA, Honolulu, HI 96822-2396. Pacific Islands Fish. Sci. Cent. Admin. Rep. H-11-08, 24 p.

Ayotte, P., K. McCoy, A. Heenan, I. Williams, and J. Zamzow. (2015). *Coral reef ecosystem program standard operating procedures: data collection for rapid ecological assessment fish surveys*. Pacific Islands Fish. Sci. Cent., Natl. Mar. Fish. Serv., NOAA, Honolulu, HI 96818-5007. Pacific Islands Fish. Sci. Cent. Admin. Rep. H-15-07, 33 p. doi:10.7289/V5SN06ZT.

Barneche, D.R., Kulbicki, M., Floeter, S.R., Friedlander, A.M. & Allen, A.P. (2016). Energetic and ecological constraints on population density of reef fishes. *Proc. R. Soc. B*, **283**, 20152186.

Barneche, D.R., Kulbicki, M., Floeter, S.R., Friedlander, A.M., Maina, J. & Allen, A.P. (2014). Scaling metabolism from individuals to reef-fish communities at broad spatial scales. *Ecol. Lett.*, **17**, 1067–1076.

Barnes, C., Maxwell, D., Reuman, D.C. & Jennings, S. (2010). Global patterns in predator-prey size relationships reveal size dependency of trophic transfer efficiency. *Ecology*, **91**, 222–232.

Bartoń, K. (2013). MuMIn: Multi-model inference. *R package version*, **1**, 18.

Bascompte, J., Melián, C.J. & Sala, E. (2005). Interaction strength combinations and the overfishing of a marine food web. *Proc. Natl. Acad. Sci. U.S.A.*, **102**, 5443–5447.

Baum, J.K. & Worm, B. (2009). Cascading top-down effects of changing oceanic predator abundances. *J. Anim. Ecol.*, **78**, 699–714.

Beck, J., Ballesteros-Mejia, L., Buchmann, C.M., Dengler, J., Fritz, S.A., Gruber, B., Hof, C., Jansen, F., Knapp, S., Kreft, H., Schneider, A.-K., Winter, M. & Dormann, C.F. (2012). What's on the horizon for macroecology? *Ecography*, **35**, 673–683.

Behrenfield, M.J. & Falkowski, P.G. (1997). A consumer's guide to phytoplankton primary productivity models. *Limnol. Oceanogr.*, **42**, 1479–1491.

Bejarano, S., Jouffray, J.-B., Chollett, I., Allen, R., Roff, G., Marshell, A., Steneck, R., Ferse, S. & Mumby, P.J. (In press). The shape of success in a turbulent world: Wave exposure filtering of coral reef herbivory. *Funct. Ecol.*

Bell, J.D., Craik, G.J.S., Pollard, D.A. & Russell, B.C. (1985). Estimating length frequency distributions of large reef fish underwater. *Coral Reefs*, **4**, 41–44.

Bellwood, D.R., Hoey, A.S. & Hughes, T.P. (2011). Human activity selectively impacts the ecosystem roles of parrotfishes on coral reefs. *Proc. R. Soc. B*, **279**, 1621–1629.

Bellwood, D.R., Hoey, A.S., Ackerman, J.L. & Depczynski, M. (2006). Coral bleaching, reef fish community phase shifts and the resilience of coral reefs. *Glob. Chang. Biol.*, **12**, 1587–1594.

Bellwood, D.R., Hughes, T.P., Folke, C. & Nyström, M. (2004). Confronting the coral reef crisis. *Nature*, **429**, 827–833.

Belmaker, J. & Jetz, W. (2010). Cross-scale variation in species richness-environment associations. *Glob. Ecol. Biogeogr.*, **20**, 464–474.

Belmaker, J., Zarnetske, P., Tuanmu, M.-N., Zonneveld, S., Record, S., Strecker, A. & Beaudrot, L. (2015). Empirical evidence for the scale dependence of biotic interactions. *Glob. Ecol. Biogeogr.*, **24**, 750–761.

Bender, M.G., Leprieur, F., Mouillot, D., Kulbicki, M., Parravicini, V., Pie, M.R., Barneche, D.R., Oliveira-Santos, L.G.R. & Floeter, S.R. (2016). Isolation drives taxonomic and functional nestedness in tropical reef fish faunas. *Ecography*, **39**, 001–011.

Bianchi, G., Gislason, H., Graham, K., Hill, L., Jin, X., Koranteng, K., Manickchand-Heileman, S., Payá, I., Sainsbury, K., Sanchez, F. & Zwanenburg, K. (2000). Impact of fishing on size composition and diversity of demersal fish communities. *ICES J. Mar. Sci.*, **57**, 558–571.

Blackburn, T.M. & Gaston, K.J. (1994). Animal body size distributions: Patterns, mechanisms and implications. *Trends Ecol. Evol.*, **9**, 471–474.

Blanchard, J.L., Dulvy, N.K., Jennings, S., Ellis, J.R., Pinnegar, J.K., Tidd, A. & Kell, L.T. (2005). Do climate and fishing influence size-based indicators of celtic sea fish community structure? *ICES J. Mar. Sci.*, **62**, 405–411.

Blanchard, J.L., Jennings, S., Holmes, R., Harle, J., Merino, G., Allen, J.I., Holt, J., Dulvy, N.K. & Barange, M. (2012). Potential consequences of climate change for primary production and fish production in large marine ecosystems. *Phil. Trans. R. Soc. B*, **367**, 2979–2989.

Blanchard, J.L., Jennings, S., Law, R., Castle, M.D., McCloghrie, P., Rochet, M.-J. & Benoît, E. (2009). How does abundance scale with body size in coupled size-structured food webs? *J. Anim. Ecol.*, **78**, 270–280.

Bozec, Y.-M., Kulbicki, M., Laloë, F., Mou-Tham, G. & Gascuel, D. (2011). Factors affecting the detection distances of reef fish: Implications for visual counts. *Mar. Biol.*, **158**, 969–981.

Bozec, Y.-M., O'Farrell, S., Bruggermann, J.H., Luckhurst, B.E. & Mumby, P.J. (2016). Tradeoffs between fisheries harvest and the resilience of coral reefs. *Proc. Natl. Acad. Sci. U.S.A.*, **113**, 4536–4541.

Brewer, T.D., Cinner, J.E., Fisher, R., Green, A. & Wilson, S.K. (2012). Market access, population density, and socioeconomic development explain diversity and functional group biomass of coral reef fish assemblages. *Glob. Environ. Change*, **22**, 399–406.

Brewer, T.D., Cinner, J.E., Green, A. & Pressey, R.L. (2013). Effects of human population density and proximity to markets on coral reef fishes vulnerable to extinction by fishing. *Conserv. Biol.*, **27**, 443–452.

Britten, G.L., Dowd, M., Minto, C., Ferretti, F., Boero, F. & Lotze, H.K. (2014). Predator decline leads to decreased stability in a coastal fish community. *Ecol. Lett.*, **17**, 1518–1525.

Brose, U. & Hillebrand, H. (2016). Biodiversity and ecosystem functioning in dynamic landscapes. *Phil. Trans. R. Soc. B*, **371**, 20150267.

Brose, U., Jonsson, T., Berlow, E.L., Warren, P., Banasek-Richter, C., Bersier, L.-F., Blanchard, J.L., Brey, T., Carpenter, S.R., Blandenier, M.-F.C., Cushing, L., Dawah, H.A., Dell, T., Edwards, F., Harper-Smith, S., Jacob, U., Ledger, M.E., Martinez, N.D., Memmott, J., Mintenbeck, K., Pinnegar, J.K., Rall, B.C., Rayner, T.S., Reuman, D.C., Ruess, L., Ulrich, W., Williams, R.J., Woodward, G. & Cohen, J.E. (2006). Consumer-resource body-size relationships in natural food webs. *Ecology*, **87**, 2411–2417.

Brown, J.H. (1995). *Macroecology*. University of Chicago Press.

Brown, J.H. (1984). On the relationship between abundance and distribution of species. *Am. Nat.*, **124**, 255–279.

Brown, J.H. & Gillooly, J.F. (2003). Ecological food webs: High-quality data facilitate theoretical unification. *Proc. Natl. Acad. Sci. U.S.A.*, **100**, 1467–1468.

Brown, J.H. & Maurer, B.A. (1989). Macroecology: The division of food and space among species on continents. *Science*, **243**, 1145–1150.

Brown, J.H., Gillooly, J.F., Allen, A.P., Savage, V.M. & West, G.B. (2004). Toward a metabolic theory of ecology. *Ecology*, **85**, 1771–1789.

Bruno, J.F. & Valdivia, A. (2016). Coral reef degradation is not correlated with local human population density. *Sci. Rep.*, **6**, 29778.

Bruno, J.F., Carr, L.A. & O'Connor, M.I. (2015). Exploring the role of temperature in the ocean through metabolic scaling. *Ecology*, **96**, 3126–3140.

Bruno, J.F., Precht, W.F., Vroom, P.S. & Aronson, R.B. (2014). Coral reef baselines: How much macroalgae is natural? *Mar. Pollut. Bull.*, **80**, 24–29.

Bruno, J.F., Sweatman, H., Precht, W.F., Selig, E.R. & Schutte, V.G.W. (2009). Assessing evidence of phase shifts from coral to macroalgal dominance on coral reefs. *Ecology*, **90**, 1478–1484.

Burkepile, D.E. & Hay, M.E. (2008). Herbivore species richness and feeding complementarity affect community structure and function on a coral reef. *Proc. Natl. Acad. Sci. U.S.A.*, **105**, 16201–16206.

Burkepile, D.E., Allgeier, J.E., Shantz, A.A., Pritchard, C.E., Lemoine, N.P., Bhatti, L.H. & Layman, C.A. (2013). Nutrient supply from fishes facilitates macroalgae and suppresses corals in a Caribbean coral reef ecosystem. *Sci. Rep.*, **3**, 1493.

Burnham, K.P., and Anderson, D.R. 2002. *Model Selection and Multimodel Inference: A Practical Information-Theoretic Approach.* 2nd edition. Springer, New York.

Burrows, M. T., Harvey, R., and Robb, L. 2008. Wave exposure indices from digital coastlines and the prediction of rocky shore community structure. *Marine Ecology Progress Series* **353**: 1-12.

Cade, B.S. (2015). Model averaging and muddled multimodel inference. *Ecology*, **96**, 2370–2382.

Carassou, L., Kulbicki, M., Nicola, T.J.R. & Polunin, N.V.C. (2008). Assessment of fish trophic status and relationships by stable isotope data in the coral reef lagoon of new caledonia, southwest pacific. *Aquat. Living Resour.*, **21**, 1–12.

Carassou, L., Léopold, M., Guillemot, N., Wantiez, L. & Kulbicki, M. (2013). Does herbivorous fish protection really improve coral reef resilience? A case study from new caledonia (south pacific). *PLoS One*, **8**, e60564.

Caut, S., Angulo, E. & Courchamp, F. (2009). Variation in discrimination factors (Δ 15N and Δ 13C): The effect of diet isotopic values and applications for diet reconstruction. *J. Appl. Ecol.*, **46**, 443–453.

Chase, J.M. & Knight, T.M. (2013). Scale-dependent effect sizes of ecological drivers on biodiversity: Why standardised sampling is not enough. *Ecol. Lett.*, **16**, 17–26.

Cheal, A.J., Aaron MacNeil, M., Cripps, E., Emslie, M.J., Jonker, M., Schaffelke, B. & Sweatman, H. (2010). Coral–macroalgal phase shifts or reef resilience: Links with

diversity and functional roles of herbivorous fishes on the great barrier reef. *Coral Reefs*, **29**, 1005–1015.

Cheal, A.J., Emslie, M., Aaron, M.M., Miller, I. & Sweatman, H. (2013). Spatial variation in the functional characteristics of herbivorous fish communities and the resilience of coral reefs. *Ecol. Appl.*, **23**, 174–188.

Choat, J.H. 1991. The Biology of Herbivorous Fishes on Coral Reefs. *In The Ecology of Fishes on Coral Reefs*. Edited by P.F. Sale. Academic Press, San Diego, California. pp. 120–155.

Chollett, I. & Mumby, P.J. (2012). Predicting the distribution of montastraea reefs using wave exposure. *Coral Reefs*, **31**, 493–503.

Cinner, J.E., Graham, N.A.J., Huchery, C. & Macneil, M.A. (2013). Global effects of local human population density and distance to markets on the condition of coral reef fisheries. *Conserv. Biol.*, **27**, 453–458.

Cinner, J.E., Huchery, C., Aaron MacNeil, M., Graham, N.A.J., McClanahan, T.R., Maina, J., Maire, E., Kittinger, J.N., Hicks, C.C., Mora, C., Allison, E.H., D'Agata, S., Hoey, A., Feary, D.A., Crowder, L., Williams, I.D., Kulbicki, M., Vigliola, L., Wantiez, L., Edgar, G., Stuart-Smith, R.D., Sandin, S.A., Green, A.L., Hardt, M.J., Beger, M., Friedlander, A., Campbell, S.J., Holmes, K.E., Wilson, S.K., Brokovich, E., Brooks, A.J., Cruz-Motta, J.J., Booth, D.J., Chabanet, P., Gough, C., Tupper, M., Ferse, S.C.A., Rashid Sumaila, U. & Mouillot, D. (2016). Bright spots among the world's coral reefs. *Nature*, **535**, 416–419.

Cinner, J.E., McClanahan, T.R., Daw, T.M., Graham, N.A.J., Maina, J., Wilson, S.K. & Hughes, T.P. (2009). Linking social and ecological systems to sustain coral reef fisheries. *Curr. Biol.*, **19**, 206–212.

Cinner, J.E., McClanahan, T.R., MacNeil, M.A., Graham, N.A.J., Daw, T.M., Mukminin, A., Feary, D.A., Rabearisoa, A.L., Wamukota, A., Jiddawi, N., Campbell, S.J., Baird, A.H., Januchowski-Hartley, F.A., Hamed, S., Lahari, R., Morove, T. & Kuange, J. (2012). Comanagement of coral reef social-ecological systems. *Proc. Natl. Acad. Sci. U.S.A.*, **109**, 5219–5222.

Cocheret de la Morinière, E., Pollux, B., Nagelkerken, I., Hemminga, M.A., Huiskes, A. & Velde, G. van der. (2003). Ontogenetic dietary changes of coral reef fishes in the mangrove-seagrass-reef continuum: Stable isotopes and gut-content analysis. *Mar. Ecol. Prog. Ser.*, **246**, 279–289.

Cohen, J.M., Civitello, D.J., Brace, A.J., Feichtinger, E.M., Ortega, C.N., Richardson, J.C., Sauer, E.L., Liu, X. & Rohr, J.R. (2016). Spatial scale modulates the strength of ecological processes driving disease distributions. *Proc. Natl. Acad. Sci. U.S.A.*, **113**, E3359–64.

Cohen, J.E., Jonsson, T. & Carpenter, S.R. (2003). Ecological community description using the food web, species abundance, and body size. *Proc. Natl. Acad. Sci. U.S.A.*, **100**, 1781–1786.

Coral Reef Ecosystem Program; Pacific Islands Fisheries Science Center (2015) National Coral Reef Monitoring Program: Stratified Random surveys (StRS) of Reef Fish, including Benthic Estimate Data of the U.S. Pacific Reefs since 2007. NOAA National Centers for Environmental Information. Unpublished Dataset. Available at: https://inport.nmfs.noaa.gov/inport/item/24447 (accessed 30 October 2015).

Craig, P., Green, A. & Tuilagi, F. (2008). Subsistence harvest of coral reef resources in the outer islands of american samoa: Modern, historic and prehistoric catches. *Fish. Res.*, **89**, 230–240.

Cyr, H., Peters, R.H. & Downing, J.A. (1997). Population density and community size structure: Comparison of aquatic and terrestrial systems. *Oikos*, **80**, 139–149.

D'Agata, S., Mouillot, D., Kulbicki, M. & Andréfouët, S. (2014). Human-mediated loss of phylogenetic and functional diversity in coral reef fishes. *Curr. Biol.* **24,** 555–560.

Daan, N., Gislason, H., G. Pope, J. & C. Rice, J. (2005). Changes in the north sea fish community: Evidence of indirect effects of fishing? *ICES J. Mar. Sci.*, **62**, 177–188.

Dalzell, P., Adams, T.J.H. & Polunin, N.V.C. (1996). Coastal fisheries in the pacific islands. *Oceanography and Marine Biology: an Annual Review*, **5**, 395–531.

Damuth, J. (1981). Population density and body size in mammals. *Nature*, **290**, 699–700.

Darimont, C. T., Fox, C.H., Bryan, H.M., Reimchen, T.E. (2015). The unique ecology of human predators. *Science*, **349**, 858–860.

Deith, M.D. 2014. Is an ecosystem driven by its species or their traits? Taxonomic and functional diversity in Pacific coral reef fish communities. Honours thesis, Department of Biology, University of Victoria, Victoria, B.C.

DeLong, J.P., Gilbert, B., Shurin, J.B., Savage, V.M., Barton, B.T., Clements, C.F., Dell, A.I., Greig, H.S., Harley, C.D.G., Kratina, P., McCann, K.S., Tunney, T.D., Vasseur, D.A. & O'Connor, M.I. (2015). The body size dependence of trophic cascades. *Am. Nat.*, **185**, 354–366.

Dormann, C.F., Elith, J., Bacher, S., Buchmann, C., Carl, G., Carré, G., Marquéz, J.R.G., Gruber, B., Lafourcade, B., Leitão, P.J., Münkemüller, T., McClean, C., Osborne, P.E.,

Reineking, B., Schröder, B., Skidmore, A.K., Zurell, D. & Lautenbach, S. (2013). Collinearity: A review of methods to deal with it and a simulation study evaluating their performance. *Ecography*, **36**, 27–46.

Dornelas, M., Gotelli, N.J., McGill, B., Shimadzu, H., Moyes, F., Sievers, C. & Magurran, A.E. (2014). Assemblage time series reveal biodiversity change but not systematic loss. *Science*, **344**, 296–299.

Dossena, M., Yvon-Durocher, G., Grey, J., Montoya, J.M., Perkins, D.M., Trimmer, M. & Woodward, G. (2012). Warming alters community size structure and ecosystem functioning. *Proc. R. Soc. B*, **279**, 3011–3019.

Dromard, C.R., Bouchon-Navaro, Y., Harmelin-Vivien, M. & Bouchon, C. (2015). Diversity of trophic niches among herbivorous fishes on a Caribbean reef (Guadeloupe, Lesser Antilles), evidenced by stable isotope and gut content analyses. *J. Sea Res.*, **95**, 124–131.

Dulvy, N.K., Polunin, N.V.C., Mill, A.C. & Graham, N.A.J. (2004). Size structural change in lightly exploited coral reef fish communities: Evidence for weak indirect effects. *Can. J. Fish. Aquat. Sci.*, **61**, 466–475.

Durrant, T., Hemer, M., Trenham, C., and Greenslade, D. 2013. CAWCR Wave Hindcast 1979-2010. v7. CSIRO. Data Collection. http://doi.org/10.4225/08/523168703DCC5.

Edwards, A.M. (2008). Using likelihood to test for lévy flight search patterns and for general power-law distributions in nature. *J. Anim. Ecol.*, **77**, 1212–1222.

Edwards, A.M., Freeman, M.P., Breed, G.A. & Jonsen, I.D. (2012). Incorrect likelihood methods were used to infer scaling laws of marine predator search behaviour. *PLoS One*, **7**, e45174.

Edwards, C.B., Friedlander, A.M., Green, A.G., Hardt, M.J., Sala, E., Sweatman, H.P., Williams, I.D., Zgliczynski, B., Sandin, S.A. & Smith, J.E. (2014). Global assessment of the status of coral reef herbivorous fishes: Evidence for fishing effects. *Proc. Biol. Sci.*, **281**, 20131835.

Edwards, A.M., Robinson, J.P.W., Plank, M.J., Baum, J.K. & Blanchard, J.L. (2017). Testing and recommending methods for fitting size spectra to data. *Methods Ecol. Evol.*, **8**, 57–67.

Ekebom, J., Laihonen, P. & Suominen, T. (2003). A GIS-based step-wise procedure for assessing physical exposure in fragmented archipelagos. *Estuar. Coast. Shelf Sci.*, **57**, 887–898.

Elith, J., Leathwick, J.R. & Hastie, T. (2008). A working guide to boosted regression trees. *J. Anim. Ecol.*, **77**, 802–813.

Elton, C.S. (1927). *Animal ecology*. University of Chicago Press.

Essington, T.E., Moriarty, P.E., Froehlich, H.E., Hodgson, E.E., Koehn, L.E., Oken, K.L., Siple, M.C. & Stawitz, C.C. (2015). Fishing amplifies forage fish population collapses. *Proc. Natl. Acad. Sci. U.S.A.*, **112**, 6648–6652.

Estes, J.A., Terborgh, J., Brashares, J.S., Power, M.E., Berger, J., Bond, W.J., Carpenter, S.R., Essington, T.E., Holt, R.D., Jackson, J.B.C., Marquis, R.J., Oksanen, L., Oksanen, T., Paine, R.T., Pikitch, E.K., Ripple, W.J., Sandin, S.A., Scheffer, M., Schoener, T.W., Shurin, J.B., Sinclair, A.R.E., Soulé, M.E., Virtanen, R. & Wardle, D.A. (2011). Trophic downgrading of planet earth. *Science*, **333**, 301–306.

Fabricius, K., De'ath, G., McCook, L., Turak, E. & Williams, D.M. (2005). Changes in algal, coral and fish assemblages along water quality gradients on the inshore great barrier reef. *Mar. Pollut. Bull.*, **51**, 384–398.

Fenner, D. (2012). Challenges for managing fisheries on diverse coral reefs. *Diversity*, **4**, 105–160.

Field, R., Hawkins, B.A., Cornell, H.V., Currie, D.J., Diniz-Filho, J.A.F., Guégan, J.-F., Kaufman, D.M., Kerr, J.T., Mittelbach, G.G., Oberdorff, T., O'Brien, E.M. & Turner, J.R.G. (2009). Spatial species-richness gradients across scales: A meta-analysis. *J. Biogeogr.*, **36**, 132–147.

Fischer, A.G. (1961). Latitudinal variations in organic diversity. *Am. Sci.*, **49**, 50–74.

Fisher, J.A.D., Frank, K.T. & Leggett, W.C. (2010). Dynamic macroecology on ecological time-scales. *Glob. Ecol. Biogeogr.*, **19**, 1–15.

Frank, K.T., Petrie, B., Choi, J.S. & Leggett, W.C. (2005). Trophic cascades in a formerly cod-dominated ecosystem. *Science*, **308**, 1621–1623.

Friedlander, A.M. & Parrish, J.D. (1997). Fisheries harvest and standing stock in a Hawaiian bay. *Fish. Res.*, **32**, 33–50.

Friedlander, A.M., Brown, E.K., Jokiel, P.L., Smith, W.R. & Rodgers, K.S. (2003). Effects of habitat, wave exposure, and marine protected area status on coral reef fish assemblages in the Hawaiian archipelago. *Coral Reefs*, **22**, 291–305.

Frisch, A.J., Ireland, M. & Baker, R. (2014). Trophic ecology of large predatory reef fishes: Energy pathways, trophic level, and implications for fisheries in a changing climate. *Mar. Biol.*, **161**, 61–73.

Frisch, A.J., Ireland, M., Rizzari, J.R., Lönnstedt, O.M., Magnenat, K.A., Mirbach, C.E. & Hobbs, J.-P.A. (2016). Reassessing the trophic role of reef sharks as apex predators on coral reefs. *Coral Reefs*, **35**, 459–472.

Froese, R. & Pauly, D. (*Editors*) (2014) FishBase. version (01/2014). Available at: http://www.fishbase.org (accessed 1 January 2014).

Froese, R. & Pauly, D. (*Editors*) (2016) FishBase. version (01/2016). Available at: http://www.fishbase.org (accessed 1 January 2016).

Fung, T., Farnsworth, K.D., Shephard, S., Reid, D.G. & Rossberg, A.G. (2013). Why the size structure of marine communities can require decades to recover from fishing. *Mar. Ecol. Prog. Ser.*, **484**, 155–171.

Galván, D.E., Sweeting, C.J. & Reid, W. (2010). Power of stable isotope techniques to detect size-based feeding in marine fishes. *Mar. Ecol. Prog. Ser.*, **407**, 271–278.

Gaston, K.J. & Blackburn, T.M. (1999). A critique for macroecology. *Oikos*, **84**, 353–368.

Gilbert, B., Tunney, T.D., McCann, K.S., DeLong, J.P., Vasseur, D.A., Savage, V., Shurin, J.B., Dell, A.I., Barton, B.T., Harley, C.D.G., Kharouba, H.M., Kratina, P., Blanchard, J.L., Clements, C., Winder, M., Greig, H.S. & O'Connor, M.I. (2014). A bioenergetic framework for the temperature dependence of trophic interactions. *Ecol. Lett.*, **17**, 902–914.

Gillooly, J.F., Brown, J.H., West, G.B., Savage, V.M. & Charnov, E.L. (2001). Effects of size and temperature on metabolic rate. *Science*, **293**, 2248–2251.

Gotelli, N.J., Graves, G.R. & Rahbek, C. (2010). Macroecological signals of species interactions in the danish avifauna. *Proc. Natl. Acad. Sci. U.S.A.*, **107**, 5030–5035.

Gove, J.M., McManus, M.A., Neuheimer, A.B., Polovina, J.J., Drazen, J.C., Smith, C.R., Merrifield, M.A., Friedlander, A.M., Ehses, J.S., Young, C.W., Dillon, A.K. & Williams, G.J. (2016). Near-island biological hotspots in barren ocean basins. *Nat. Commun.*, **7**, 10581.

Gove, J.M., Williams, G.J., McManus, M.A., Clark, S.J., Ehses, J.S. & Wedding, L.M. (2015). Coral reef benthic regimes exhibit non-linear threshold responses to natural physical drivers. *Mar. Ecol. Prog. Ser.*, **522**, 33–48.

Gove, J.M., Williams, G.J., McManus, M.A., Heron, S.F., Sandin, S.A., Vetter, O.J. & Foley, D.G. (2013). Quantifying climatological ranges and anomalies for pacific coral reef ecosystems. *PLoS One*, **8**, e61974.

Graham, N.A.J. & Nash, K.L. (2012). The importance of structural complexity in coral reef ecosystems. *Coral Reefs*, **32**, 315–326.

Graham, N.A.J., Chabanet, P., Evans, R.D., Jennings, S., Letourneur, Y., Aaron Macneil, M., McClanahan, T.R., Ohman, M.C., Polunin, N.V.C. & Wilson, S.K. (2011). Extinction vulnerability of coral reef fishes. *Ecol. Lett.*, **14**, 341–348.

Graham, N., Dulvy, N.K., Jennings, S. & Polunin, N. (2005). Size-spectra as indicators of the effects of fishing on coral reef fish assemblages. *Coral Reefs*, **24**, 118–124.

Graham, N.A.J., Jennings, S., MacNeil, M.A., Mouillot, D. & Wilson, S.K. (2015). Predicting climate-driven regime shifts versus rebound potential in coral reefs. *Nature*, **518**, 94–97.

Graham, N.A.J., Wilson, S.K., Jennings, S., Polunin, N.V.C., Robinson, J., Bijoux, J.P. & Daw, T.M. (2007). Lag effects in the impacts of mass coral bleaching on coral reef fish, fisheries, and ecosystems. *Conserv. Biol.*, **21**, 1291–1300.

Green, A.L. & Bellwood, D.R. (2009). *Monitoring functional groups of herbivorous reef fishes as indicators of coral reef resilience - a practical guide for coral reef managers in the asia pacific region*. IUCN working group on Climate Change; Coral Reefs, Gland, Switzerland.

Greenstreet, S.P.R., Rogers, S.I., Rice, J.C., Piet, G.J., Guirey, E.J., Fraser, H.M. & Fryer, R.J. (2011). Development of the EcoQO for the north sea fish community. *ICES J. Mar. Sci.*, **68**, 1–11.

Greenwood, N.D.W., Sweeting, C.J. & Polunin, N.V.C. (2010). Elucidating the trophodynamics of four coral reef fishes of the solomon islands using δ15N and δ13C. *Coral Reefs*, **29**, 785–792.

Gripenberg, S. & Roslin, T. (2007). Up or down in space? Uniting the bottom-up versus top-down paradigm and spatial ecology. *Oikos*, **116**, 181–188.

Harborne, A.R., Rogers, A., Bozec, Y.-M. & Mumby, P.J. (2017). Multiple stressors and the functioning of coral reefs. *Ann. Rev. Mar. Sci.*, **9**, 445–468.

Hatton, I.A., McCann, K.S., Fryxell, J.M., Davies, T.J., Smerlak, M., Sinclair, A.R.E. & Loreau, M. (2015). The predator-prey power law: Biomass scaling across terrestrial and aquatic biomes. *Science*, **349**, aac6284.

Heenan, A. & Williams, I.D. (2013). Monitoring herbivorous fishes as indicators of coral reef resilience in american samoa. *PLoS One*, **8**, e79604.

Heenan, A., Hoey, A.S., Williams, G.J. & Williams, I.D. (2016). Natural bounds on herbivorous coral reef fishes. *Proc. R. Soc. B*, **283**, 20161716.

Heikkinen, R.K., Luoto, M., Virkkala, R., Pearson, R.G. & Körber, J.-H. (2007). Biotic interactions improve prediction of boreal bird distributions at macro-scales. *Glob. Ecol. Biogeogr.*, **16**, 754–763.

Hicks, C.C. & McClanahan, T.R. (2012). Assessing gear modifications needed to optimize yields in a heavily exploited, multi-species, seagrass and coral reef fishery. *PLoS One*, **7**, e36022.

Hillebrand, H. (2004). On the generality of the latitudinal diversity gradient. *Am. Nat.*, **163**, 192–211.

Hilting, A.K., Currin, C.A. & Kosaki, R.K. (2013). Evidence for benthic primary production support of an apex predator–dominated coral reef food web. *Mar. Biol.*, **160**, 1681–1695.

Hoegh-Guldberg, O., Mumby, P.J., Hooten, A.J., Steneck, R.S., Greenfield, P., Gomez, E., Harvell, C.D., Sale, P.F., Edwards, A.J., Caldeira, K., Knowlton, N., Eakin, C.M., Iglesias-Prieto, R., Muthiga, N., Bradbury, R.H., Dubi, A. & Hatziolos, M.E. (2007). Coral reefs under rapid climate change and ocean acidification. *Science*, **318**, 1737–1742.

Hoekstra, J. M., Boucher, T.M., Ricketts, T.H. & Roberts, C. (2005). Confronting a biome crisis: global disparities of habitat loss and protection. *Ecol. Lett.*, **8**, 23–29.

Houk, P., Rhodes, K., Cuetos-Bueno, J., Lindfield, S., Fread, V. & McIlwain, J.L. (2012). Commercial coral-reef fisheries across micronesia: A need for improving management. *Coral Reefs*, **31**, 13–26.

Hughes, T.P. (1994). Catastrophes, phase shifts, and large-scale degradation of a Caribbean coral reef. *Science*, **265**, 1547–1551.

Hughes, T.P., Baird, A.H., Bellwood, D.R., Card, M., Connolly, S.R., Folke, C., Grosberg, R., Hoegh-Guldberg, O., Jackson, J.B.C., Kleypas, J., Lough, J.M., Marshall, P.,

Nyström, M., Palumbi, S.R., Pandolfi, J.M., Rosen, B. & Roughgarden, J. (2003). Climate change, human impacts, and the resilience of coral reefs. *Science*, **301**, 929–933.

Hughes, T.P., Graham, N.A.J., Jackson, J.B.C., Mumby, P.J. & Steneck, R.S. (2010). Rising to the challenge of sustaining coral reef resilience. *Trends Ecol. Evol.*, **25**, 633–642.

Huntington, B.E., Karnauskas, M. & Lirman, D. (2011). Corals fail to recover at a Caribbean marine reserve despite ten years of reserve designation. *Coral Reefs*, **30**, 1077–1085.

Hussey, N.E., Macneil, M.A., McMeans, B.C., Olin, J.A., Dudley, S.F.J., Cliff, G., Wintner, S.P., Fennessy, S.T. & Fisk, A.T. (2014). Rescaling the trophic structure of marine food webs. *Ecol. Lett.*, **17**, 239–250.

Hutchinson, G.E. & MacArthur, R.H. (1959). A theoretical ecological model of size distributions among species of animals. *Am. Nat.*, **93**, 117.

Jackson, J.B., Kirby, M.X., Berger, W.H., Bjorndal, K.A., Botsford, L.W., Bourque, B.J., Bradbury, R.H., Cooke, R., Erlandson, J., Estes, J.A., Hughes, T.P., Kidwell, S., Lange, C.B., Lenihan, H.S., Pandolfi, J.M., Peterson, C.H., Steneck, R.S., Tegner, M.J. & Warner, R.R. (2001). Historical overfishing and the recent collapse of coastal ecosystems. *Science*, **293**, 629–637.

Jennings, S. & Blanchard, J.L. (2004). Fish abundance with no fishing: Predictions based on macroecological theory. *J. Anim. Ecol.*, **73**, 632–642.

Jennings, S. & Dulvy, N.K. (2005). Reference points and reference directions for size-based indicators of community structure. *ICES J. Mar. Sci.*, **62**, 397–404.

Jennings, S. & Mackinson, S. (2003). Abundance-body mass relationships in size-structured food webs. *Ecol. Lett.*, **6**, 971–974.

Jennings, S. & Polunin, N.V.C. (1996). Effects of fishing effort and catch rate upon the structure and biomass of fijian reef fish communities. *J. Appl. Ecol.*, **33**, 400–412.

Jennings, S., De Oliveira, J.A.A. & Warr, K.J. (2007). Measurement of body size and abundance in tests of macroecological and food web theory. *J. Anim. Ecol.*, **76**, 72–82.

Jennings, S., Grandcourt, E.M. & Polunin, N.V.C. (1995). The effects of fishing on the diversity, biomass and trophic structure of seychelles' reef fish communities. *Coral Reefs*, **14**, 225–235.

Jennings, S., Greenstreet, S., Hill, L., Piet, G., Pinnegar, J. & Warr, K.J. (2002). Long-term trends in the trophic structure of the north sea fish community: Evidence from stable-isotope analysis, size-spectra and community metrics. *Mar. Biol.*, **141**, 1085–1097.

Jennings, S., Pinnegar, J.K., Polunin, N.V.C. & Boon, T.W. (2001). Weak cross-species relationships between body size and trophic level belie powerful size-based trophic structuring in fish communities. *J. Anim. Ecol.*, **70**, 934–944.

Jensen, O.P., Branch, T.A. & Hilborn, R. (2012). Marine fisheries as ecological experiments. *Theor. Ecol.*, **5**, 3–22.

Johannes, R.E., Wiebe, W.J., Crossland, C.J., Rimmer, D.W. & Smith, S.V. (1983). Latitudinal limits of coral reef growth. *Mar. Ecol. Prog. Ser.*, **11**, 105–111.

Johnson, A.E., Cinner, J.E., Hardt, M.J., Jacquet, J., McClanahan, T.R. & Sanchirico, J.N. (2013). Trends, current understanding and future research priorities for artisanal coral reef fisheries research. *Fish Fish*, **14**, 281–292.

Jouffray, J.-B., Nyström, M., Norström, A.V., Williams, I.D., Wedding, L.M., Kittinger, J.N. & Williams, G.J. (2015). Identifying multiple coral reef regimes and their drivers across the Hawaiian archipelago. *Phil. Trans. R. Soc. B*, **370**, 20130268.

Kerr, J.T., Kharouba, H.M. & Currie, D.J. (2007). The macroecological contribution to global change solutions. *Science*, **316**, 1581–1584.

Kiribati National Statistics Office 2012. Kiribati 2010 Census Volume 1 & 2. Secretariat of the Pacific Community. Statistics for Development Programme, Noumea, New Caledonia.

Kissling, W.D. & Schleuning, M. (2015). Multispecies interactions across trophic levels at macroscales: Retrospective and future directions. *Ecography*, **38**, 346–357.

Kissling, W.D., Dormann, C.F., Groeneveld, J., Hickler, T., Kühn, I., McInerny, G.J., Montoya, J.M., Römermann, C., Schiffers, K., Schurr, F.M., Singer, A., Svenning, J.-C., Zimmermann, N.E. & O'Hara, R.B. (2012). Towards novel approaches to modelling biotic interactions in multispecies assemblages at large spatial extents. *J. Biogeogr.*, **39**, 2163–2178.

Kleiber, M. (1932). Body size and metabolism. *Hilgardia*, **6**, 315–353.

Knowlton, N. & Jackson, J.B.C. (2008). Shifting baselines, local impacts, and global change on coral reefs. *PLoS Biol.*, **6**, e54.

Kramer, K.L. & Heck, K.L., Jr. (2007). Top-down trophic shifts in florida keys patch reef marine protected areas. *Mar. Ecol. Prog. Ser.*, **349**, 111–123.

Kulbicki, M., Guillemot, N. & Amand, M. (2005). A general approach to length-weight relationships for new caledonian lagoon fishes. *Cybium*, **29**, 235–252.

Kulbicki, M., Parravicini, V., Bellwood, D.R., Arias-Gonzàlez, E., Chabanet, P., Floeter, S.R., Friedlander, A., McPherson, J., Myers, R.E., Vigliola, L. & Mouillot, D. (2013). Global biogeography of reef fishes: A hierarchical quantitative delineation of regions. *PLoS One*, **8**, e81847.

Kühn, I., Böhning-Gaese, K., Cramer, W. & Klotz, S. (2008). Macroecology meets global change research. *Glob. Ecol. Biogeogr.*, **17**, 3–4.

Lawton, J.H. (1999). Are there general laws in ecology? *Oikos*, **84**, 177–192.

Lawton, J.H. (1996). Patterns in ecology. *Oikos*, **75**, 145–147.

Layman, C.A., Winemiller, K.O., Arrington, D.A. & Jepsen, D.B. (2005). Body size and trophic position in a diverse tropical food web. *Ecology*, **86**, 2530–2535.

Leichter, J.J., Shellenbarger, G., Genovese, S.J. & Wing, S.R. (1998). Breaking internal waves on a florida (USA) coral reef:a plankton pump at work? *Mar. Ecol. Prog. Ser.*, **166**, 83–97.

Levin, S.A. (1992). The problem of pattern and scale in ecology. *Ecology*, **73**, 1943–1967.

Lindeman, R.L. (1942). The trophic-dynamic aspect of ecology. *Ecology*, **23**, 399–417.

Lokrantz, J., Nyström, M., Thyresson, M. & Johansson, C. (2008). The non-linear relationship between body size and function in parrotfishes. *Coral Reefs*, **27**, 967–974.

Lough, J.M. & Barnes, D.J. (2000). Environmental controls on growth of the massive coral porites. *J. Exp. Mar. Bio. Ecol.*, **245**, 225–243.

MacNeil, M.A., Graham, N.A.J., Cinner, J.E., Wilson, S.K., Williams, I.D., Maina, J., Newman, S., Friedlander, A.M., Jupiter, S., Polunin, N.V.C. & McClanahan, T.R. (2015). Recovery potential of the world's coral reef fishes. *Nature*, **520**, 341–344.

Madin, J.S. & Connolly, S.R. (2006). Ecological consequences of major hydrodynamic disturbances on coral reefs. *Nature*, **444**, 477–480.

Maire, E., Cinner, J., Velez, L., Huchery, C., Mora, C., Dagata, S., Vigliola, L., Wantiez, L., Kulbicki, M. & Mouillot, D. (2016). How accessible are coral reefs to people? A global assessment based on travel time. *Ecol. Lett.*, **19**, 351–360.

Marquet, P.A., Quiñones, R.A., Abades, S., Labra, F., Tognelli, M., Arim, M. & Rivadeneira, M. (2005). Scaling and power-laws in ecological systems. *J. Exp. Biol.*, **208**, 1749–1769.

Maxwell, T.A.D. & Jennings, S. (2006). Predicting abundance-body size relationships in functional and taxonomic subsets of food webs. *Oecologia*, **150**, 282–290.

May, R.M. (1973). Qualitative stability in model ecosystems. *Ecology*, **54**, 638–641.

McCann, K.S., Gellner, G., McMeans, B.C., Deenik, T., Holtgrieve, G., Rooney, N., Hannah, L., Cooperman, M. & Nam, S. (2016). Food webs and the sustainability of indiscriminate fisheries. *Can. J. Fish. Aquat. Sci.*, **73**, 656–665.

McCauley, D.J., Young, H.S., Dunbar, R.B., Estes, J.A., Semmens, B.X. & Micheli, F. (2012). Assessing the effects of large mobile predators on ecosystem connectivity. *Ecol. Appl.*, **22**, 1711–1717.

McClanahan, T.R. & Graham, N. (2005). Recovery trajectories of coral reef fish assemblages within kenyan marine protected areas. *Mar. Ecol. Prog. Ser.*, **294**, 214–248.

McClanahan, T.R., Graham, N.A.J., MacNeil, M.A. & Cinner, J.E. (2015). Biomass-based targets and the management of multispecies coral reef fisheries. *Conserv. Biol.*, **29**, 409–417.

McClanahan, T.R., Graham, N.A.J., MacNeil, M.A., Muthiga, N.A., Cinner, J.E., Bruggemann, J.H. & Wilson, S.K. (2011). Critical thresholds and tangible targets for ecosystem-based management of coral reef fisheries. *Proc. Natl. Acad. Sci. U.S.A.*, **108**, 17230–17233.

McCook, L., Jompa, J. & Diaz-Pulido, G. (2001). Competition between corals and algae on coral reefs: A review of evidence and mechanisms. *Coral Reefs*, **19**, 400–417.

McGill, B.J. (2010). Matters of scale. *Science*, **328**, 575–576.

McGill, B. (2003). Strong and weak tests of macroecological theory. *Oikos*, **102**, 679–685.

Mellin, C., Huchery, C., Caley, M.J., Meekan, M.G. & Bradshaw, C.J.A. (2010). Reef size and isolation determine the temporal stability of coral reef fish populations. *Ecology*, **91**, 3138–3145.

Mill, A.C., Pinnegar, J.K. & Polunin, N.V.C. (2007). Explaining isotope trophic-step fractionation: Why herbivorous fish are different. *Funct. Ecol.*, **21**, 1137–1145.

Mittelbach, G.G. & Persson, L. (1998). The ontogeny of piscivory and its ecological consequences. *Can. J. Fish. Aquat. Sci.*, **55**, 1454–1465.

Mora, C. (2008). A clear human footprint in the coral reefs of the Caribbean. *Proc. R. Soc. B*, **275**, 767–773.

Mora, C., Aburto-Oropeza, O., Ayala Bocos, A., Ayotte, P.M., Banks, S., Bauman, A.G., Beger, M., Bessudo, S., Booth, D.J., Brokovich, E., Brooks, A., Chabanet, P., Cinner, J.E., Cortés, J., Cruz-Motta, J.J., Cupul Magaña, A., Demartini, E.E., Edgar, G.J., Feary, D.A., Ferse, S.C.A., Friedlander, A.M., Gaston, K.J., Gough, C., Graham, N.A.J., Green, A., Guzman, H., Hardt, M., Kulbicki, M., Letourneur, Y., López Pérez, A., Loreau, M., Loya, Y., Martinez, C., Mascareñas-Osorio, I., Morove, T., Nadon, M.-O., Nakamura, Y., Paredes, G., Polunin, N.V.C., Pratchett, M.S., Reyes Bonilla, H., Rivera, F., Sala, E., Sandin, S.A., Soler, G., Stuart-Smith, R., Tessier, E., Tittensor, D.P., Tupper, M., Usseglio, P., Vigliola, L., Wantiez, L., Williams, I., Wilson, S.K. & Zapata, F.A. (2011). Global human footprint on the linkage between biodiversity and ecosystem functioning in reef fishes. *PLoS Biol.*, **9**, e1000606.

Mouillot, D., Villéger, S., Parravicini, V., Kulbicki, M., Arias-González, J.E., Bender, M., Chabanet, P., Floeter, S.R., Friedlander, A., Vigliola, L. & Bellwood, D.R. (2014).

Functional over-redundancy and high functional vulnerability in global fish faunas on tropical reefs. *Proc. Natl. Acad. Sci. U.S.A.*, **111**, 13757–13762.

Mumby, P.J. & Steneck, R.S. (2008). Coral reef management and conservation in light of rapidly evolving ecological paradigms. *Trends Ecol. Evol.*, **23**, 555–563.

Mumby, P.J., Dahlgren, C.P., Harborne, A.R., Kappel, C.V., Micheli, F., Brumbaugh, D.R., Holmes, K.E., Mendes, J.M., Broad, K., Sanchirico, J.N., Buch, K., Box, S., Stoffle, R.W. & Gill, A.B. (2006). Fishing, trophic cascades, and the process of grazing on coral reefs. *Science*, **311**, 98–101.

Mumby, P.J., Harborne, A.R., Williams, J., Kappel, C.V., Brumbaugh, D.R., Micheli, F., Holmes, K.E., Dahlgren, C.P., Paris, C.B. & Blackwell, P.G. (2007). Trophic cascade facilitates coral recruitment in a marine reserve. *Proc. Natl. Acad. Sci. U.S.A.*, **104**, 8362–8367.

Mumby, P.J., Steneck, R.S. & Hastings, A. (2013). Evidence for and against the existence of alternate attractors on coral reefs. *Oikos*, **122**, 481–491.

Munday, P. L., Jones, G.P., Pratchett, M.S. & Williams, A.J. (2008). Climate change and the future for coral reef fishes. *Fish & Fisheries*, **9**, 261–285.

Myers, R.A. & Worm, B. (2003). Rapid worldwide depletion of predatory fish communities. *Nature*, **423**, 280–283.

Nadon, M.O., Ault, J.S., Williams, I.D., Smith, S.G. & DiNardo, G.T. (2015). Length-based assessment of coral reef fish populations in the main and Northwestern Hawaiian islands. *PLoS One*, **10**, e0133960.

Nadon, M.O., Baum, J.K., Williams, I.D., McPherson, J.M., Zgliczynski, B.J., Richards, B.L., Schroeder, R.E. & Brainard, R.E. (2012). Re-creating missing population baselines for pacific reef sharks. *Conserv. Biol.*, **26**, 493–503.

Nakagawa, S. & Schielzeth, H. (2013). A general and simple method for obtaining R2 from generalized linear mixed-effects models. *Methods Ecol. Evol.*, **4**, 133–142.

Nash, K.L. & Graham, N.A.J. (2016). Ecological indicators for coral reef fisheries management. *Fish Fish*, **17**, 1029–1054.

Nash, K.L., Graham, N. & Bellwood, D.R. (2013). Fish foraging patterns, vulnerability to fishing and implications for the management of ecosystem function across scales. *Ecol. Appl.*, **23**, 1632–1644.

Nash, K. L., Graham, N. A. J., Jennings, S., Wilson, S. K. & Bellwood, D. R. (2015). Herbivore cross-scale redundancy supports response diversity and promotes coral reef resilience. *J. Appl. Ecol.*, **53**, 646–655.

Newman, M.J.H., Paredes, G.A., Sala, E. & Jackson, J.B.C. (2006). Structure of Caribbean coral reef communities across a large gradient of fish biomass. *Ecol. Lett.*, **9**, 1216–1227.

Newton, K., Côté, I.M., Pilling, G.M., Jennings, S. & Dulvy, N.K. (2007). Current and future sustainability of island coral reef fisheries. *Curr. Biol.*, **17**, 655–658.

Nyström, M., Graham, N.A.J., Lokrantz, J. & Norström, A.V. (2008). Capturing the cornerstones of coral reef resilience: Linking theory to practice. *Coral Reefs*, **27**, 795–809.

Paine, R.T. (1966). Food web complexity and species diversity. *Am. Nat.*, **100**, 65–75.

Pandolfi, J.M., Bradbury, R.H., Sala, E., Hughes, T.P., Bjorndal, K.A., Cooke, R.G., McArdle, D., McClenachan, L., Newman, M.J.H., Paredes, G., Warner, R.R. & Jackson,

J.B.C. (2003). Global trajectories of the long-term decline of coral reef ecosystems. *Science*, **301**, 955–958.

Parravicini, V., Kulbicki, M., Bellwood, D.R., Friedlander, A.M., Arias-Gonzalez, J.E., Chabanet, P., Floeter, S.R., Myers, R., Vigliola, L., D'Agata, S. & Mouillot, D. (2013). Global patterns and predictors of tropical reef fish species richness. *Ecography*, **36**, 1254–1262.

Parrish, F.A., Craig, M.P., Ragen, T.J., Marshall, G.J. & Buhleier, B.M. (2000). Identifying diurnal foraging habitat of endangered Hawaiian monk seals using a seal-mounted video camera. *Mar. Mamm. Sci.*, **16**, 392–412.

Pearson, R.G. & Dawson, T.P. (2003). Predicting the impacts of climate change on the distribution of species: Are bioclimate envelope models useful? *Glob. Ecol. Biogeogr.*, **12**, 361–371.

Petchey, O.L. & Belgrano, A. (2010). Body-size distributions and size-spectra: Universal indicators of ecological status? *Biol. Lett.*, **6**, 434–437.

Petchey, O.L., Brose, U. & Rall, B.C. (2010). Predicting the effects of temperature on food web connectance. *Phil. Trans. R. Soc. B*, **365**, 2081–2091.

Peters, R.H. (1983). *The ecological implications of body size*. Cambridge University Press, Cambridge.

Pinheiro J., Bates D., DebRoy S., Sarkar D., and R Core Team 2015. *nlme: Linear and Nonlinear Mixed Effects Models*. R package version 3.1-120.

Plass-Johnson, J.G., McQuaid, C.D. & Hill, J.M. (2012). Stable isotope analysis indicates a lack of inter- and intra-specific dietary redundancy among ecologically important coral reef fishes. *Coral Reefs*, **32**, 429–440.

Post, D.M. (2002). Using stable isotopes to estimate trophic position: Models, methods, and assumptions. *Ecology*, **83**, 703–718.

Price, N. (2010). Habitat selection, facilitation, and biotic settlement cues affect distribution and performance of coral recruits in french polynesia. *Oecologia*, **163**, 747–758.

Rahbek, C. (2005). The role of spatial scale and the perception of large-scale species-richness patterns. *Ecol. Lett.*, **8**, 224–239.

Rahbek, C. & Graves, G.R. (2000). Detection of macro-ecological patterns in south american hummingbirds is affected by spatial scale. *Proc. R. Soc. Lond. B*, **267**, 2259–2265.

R Core Team (2013) R: A Language and Environment for Statistical Computing. R Foundation for Statistical Computing, Vienna, Austria.

R Core Team (2015) R: A Language and Environment for Statistical Computing. R Foundation for Statistical Computing, Vienna, Austria.

R Core Team (2016) R: A Language and Environment for Statistical Computing. R Foundation for Statistical Computing, Vienna, Austria.

Rasher, D.B., Engel, S., Bonito, V., Fraser, G.J., Montoya, J.P. & Hay, M.E. (2012). Effects of herbivory, nutrients, and reef protection on algal proliferation and coral growth on a tropical reef. *Oecologia*, **169**, 187–198.

Rasher, D.B., Hoey, A.S. & Hay, M.E. (2013). Consumer diversity interacts with prey defenses to drive ecosystem function. *Ecology*, **94**, 1347–1358.

Rensburg, B.J. van, Chown, S.L. & Gaston, K.J. (2002). Species richness, environmental correlates, and spatial scale: A test using south african birds. *Am. Nat.*, **159**, 566–577.

Reuman, D.C., Mulder, C., Raffaelli, D. & Cohen, J.E. (2008). Three allometric relations of population density to body mass: Theoretical integration and empirical tests in 149 food webs. *Ecol. Lett.*, **11**, 1216–1228.

Richards, B.L., Williams, I.D., Nadon, M.O. & Zgliczynski, B.J. (2011). A towed-diver survey method for mesoscale fishery-independent assessment of large-bodied reef fishes. *Bull. Mar. Sci.*, **87**, 55–74.

Richards, B.L., Williams, I.D., Vetter, O.J. & Williams, G.J. (2012). Environmental factors affecting large-bodied coral reef fish assemblages in the mariana archipelago. *PLoS One*, **7**, e31374.

Riede, J.O., Brose, U., Ebenman, B., Jacob, U., Thompson, R., Townsend, C.R. & Jonsson, T. (2011). Stepping in elton's footprints: A general scaling model for body masses and trophic levels across ecosystems. *Ecol. Lett.*, **14**, 169–178.

Roberts, C.M. (1995). Effects of fishing on the ecosystem structure of coral reefs. *Conserv. Biol.*, **9**, 988–995.

Robinson, J.P.W. & Baum, J.K. (2016). Trophic roles determine coral reef fish community size structure. *Can. J. Fish. Aquat. Sci.*, **73**, 496–505.

Robinson, J.P.W., Williams, I.D., Edwards, A.M., McPherson, J., Yeager, L., Vigliola, L., Brainard, R.E. & Baum, J.K. (2016). Fishing degrades size structure of coral reef fish communities. *Glob. Chang. Biol.* doi: 10.1111/gcb.13482.

Rochet, M.-J. & Benoît, E. (2012). Fishing destabilizes the biomass flow in the marine size spectrum. *Proc. R. Soc. B*, **279**, 284–292.

Rochet, M.-J. & Trenkel, V.M. (2003). Which community indicators can measure the impact of fishing? A review and proposals. *Can. J. Fish. Aquat. Sci.*, **60**, 86–99.

Roff, G. & Mumby, P.J. (2012). Global disparity in the resilience of coral reefs. *Trends Ecol. Evol.*, **27**, 404–413.

Roff, G., Doropoulos, C., Rogers, A., Bozec, Y.-M., Krueck, N.C., Aurellado, E., Priest, M., Birrell, C. & Mumby, P.J. (2016). The ecological role of sharks on coral reefs. *Trends Ecol. Evol.*, **31**, 395–407.

Rogers, A., Blanchard, J.L. & Mumby, P.J. (2014). Vulnerability of coral reef fisheries to a loss of structural complexity. *Curr. Biol.*, **24**, 1000–1005.

Rohde, K. (1992). Latitudinal gradients in species diversity: The search for the primary cause. *Oikos*, **65**, 514–527.

Romanuk, T.N., Hayward, A. & Hutchings, J.A. (2011). Trophic level scales positively with body size in fishes. *Glob. Ecol. Biogeogr.*, **20**, 231–240.

Rooney, N. & McCann, K.S. (2012). Integrating food web diversity, structure and stability. *Trends Ecol. Evol.*, **27**, 40–46.

Rooney, N., McCann, K.S. & Moore, J.C. (2008). A landscape theory for food web architecture. *Ecol. Lett.*, **11**, 867–881.

Rooney, N., McCann, K., Gellner, G. & Moore, J.C. (2006). Structural asymmetry and the stability of diverse food webs. *Nature*, **442**, 265–269.

Russ, G.R., Questel, S.-L.A., Rizzari, J.R. & Alcala, A.C. (2015). The parrotfish–coral relationship: Refuting the ubiquity of a prevailing paradigm. *Mar. Biol.*, **162**, 2029–2045.

Ruttenberg, B.I., Hamilton, S.L., Walsh, S.M., Donovan, M.K., Friedlander, A., DeMartini, E., Sala, E. & Sandin, S.A. (2011). Predator-induced demographic shifts in coral reef fish assemblages. *PLoS One*, **6**, e21062.

Sadovy, Y. (2005). Trouble on the reef: The imperative for managing vulnerable and valuable fisheries. *Fish Fish*, **6**, 167–185.

Sandin, S.A., Smith, J.E., Demartini, E.E., Dinsdale, E.A., Donner, S.D., Friedlander, A.M., Konotchick, T., Malay, M., Maragos, J.E., Obura, D., Pantos, O., Paulay, G., Richie, M., Rohwer, F., Schroeder, R.E., Walsh, S., Jackson, J.B.C., Knowlton, N. & Sala, E. (2008). Baselines and degradation of coral reefs in the northern line islands. *PLoS One*, **3**, e1548.

Savage, V.M., Gillooly, J.F., Woodruff, W.H. & others. (2004). The predominance of quarter-power scaling in biology. *Funct. Ecol.*, **18**, 257–282.

Sbrocco, E.J. & Barber, P.H. (2013). MARSPEC: Ocean climate layers for marine spatial ecology. *Ecology*, **94**, 979–979.

Schielzeth, H. (2010). Simple means to improve the interpretability of regression coefficients. *Methods Ecol. Evol.*, **1**, 103–113.

Sheldon, R.W., Prakash, A. & Sutcliffe, W.H. (1972). The size distribution of particles in the ocean. *Limnol. Oceanogr.*, **17**, 327–340.

Shin, Y.-J., Rochet, M.-J., Jennings, S., Field, J.G. & Gislason, H. (2005). Using size-based indicators to evaluate the ecosystem effects of fishing. *ICES J. Mar. Sci.*, **62**, 384–396.

Smith, J.E., Brainard, R., Carter, A., Grillo, S., Edwards, C., Harris, J., Lewis, L., Obura, D., Rohwer, F., Sala, E., Vroom, P.S. & Sandin, S. (2016). Re-evaluating the health of coral reef communities: Baselines and evidence for human impacts across the Central Pacific. *Proc. R. Soc. B*, **283**, 20151985.

Sprules, W.G. (2008). Ecological change in great lakes communities-a matter of perspective. *Can. J. Fish. Aquat. Sci.*, **65**, 1–9.

Stein, A., Gerstner, K. & Kreft, H. (2014). Environmental heterogeneity as a universal driver of species richness across taxa, biomes and spatial scales. *Ecol. Lett.*, **17**, 866–880.

Suchley, A., McField, M.D. & Alvarez-Filip, L. (2016). Rapidly increasing macroalgal cover not related to herbivorous fishes on mesoamerican reefs. *PeerJ*, **4**, e2084.

Sweeting, C.J., Badalamenti, F., D'Anna, G., Pipitone, C. & Polunin, N.V.C. (2009). Steeper biomass spectra of demersal fish communities after trawler exclusion in sicily. *ICES J. Mar. Sci.*, **66**, 195–202.

Taylor, B.M., Houk, P., Russ, G.R. & Choat, J.H. (2014). Life histories predict vulnerability to overexploitation in parrotfishes. *Coral Reefs*, **33**, 869–878.

Thorpe, R.B., Le Quesne, W.J.F., Luxford, F., Collie, J.S. & Jennings, S. (2015). Evaluation and management implications of uncertainty in a multispecies size-structured model of population and community responses to fishing. *Methods Ecol. Evol.*, **6**, 49–58.

Thrush, S.F. & Dayton, P.K. (2010). What can ecology contribute to ecosystem-based management? *Ann. Rev. Mar. Sci.*, **2**, 419–441.

Tolman, H. L. 2014. User manual and system documentation of WAVEWATCH III version 4.18. NOAA / NWS / NCEP / MMAB Technical Note 316, 194 pp.+ Appendices.

Travis, J., Coleman, F.C., Auster, P.J., Cury, P.M., Estes, J.A., Orensanz, J., Peterson, C.H., Power, M.E., Steneck, R.S. & Wootton, J.T. (2014). Integrating the invisible fabric of nature into fisheries management. *Proc. Natl. Acad. Sci. U.S.A.*, **111**, 581–584.

Trebilco, R., Baum, J.K., Salomon, A.K. & Dulvy, N.K. (2013). Ecosystem ecology: Size-based constraints on the pyramids of life. *Trends Ecol. Evol.*, **28**, 423–431.

Tunney, T.D., McCann, K.S., Lester, N.P. & Shuter, B.J. (2012). Food web expansion and contraction in response to changing environmental conditions. *Nat. Commun.*, **3**, 1105.

Van der Putten, W.H., Macel, M. & Visser, M.E. (2010). Predicting species distribution and abundance responses to climate change: Why it is essential to include biotic interactions across trophic levels. *Phil. Trans. R. Soc. B*, **365**, 2025–2034.

Vander Zanden, M. & Rasmussen, J.B. (2001). Variation in δ15N and δ13C trophic fractionation: Implications for aquatic food web studies. *Limnol. Oceanogr.*, **46**, 2061–2066.

Vellend, M., Baeten, L., Myers-Smith, I.H., Elmendorf, S.C., Beauséjour, R., Brown, C.D., De Frenne, P., Verheyen, K. & Wipf, S. (2013). Global meta-analysis reveals no net change in local-scale plant biodiversity over time. *Proc. Natl. Acad. Sci. U.S.A.*, **110**, 19456–19459.

Vidondo, B., Prairie, Y.T., Blanco, J.M. & Duarte, C.M. (1997). Some aspects of the analysis of size spectra in aquatic ecology. *Limnol. Oceanogr.*, **42**, 184–192.

Vroom, P.S. & Braun, C.L. (2010). Benthic composition of a healthy subtropical reef: Baseline species-level cover, with an emphasis on algae, in the Northwestern Hawaiian islands. *PLoS One*, **5**, e9733.

Wallace, A.R. (1876). *The geographical distribution of animals: With a study of the relations of living and extinct faunas as elucidating the past changes of the earth's surface*. London, Macmillan & Co.

Walsh, S.M. (2010). Ecosystem-scale effects of nutrients and fishing on coral reefs. *J. Mar. Biol.*, **2011**, 1–13.

Ward-Paige, C., Mills Flemming, J. & Lotze, H.K. (2010a). Overestimating fish counts by non-instantaneous visual censuses: Consequences for population and community descriptions. *PLoS One*, **5**, e11722.

Ward-Paige, C.A., Mora, C., Lotze, H.K., Pattengill-Semmens, C., McClenachan, L., Arias-Castro, E. & Myers, R.A. (2010b). Large-scale absence of sharks on reefs in the Greater-Caribbean: A footprint of human pressures. *PLoS One*, **5**, e11968.

Watson, M.S., Claar, D.C. & Baum, J.K. (2016). Subsistence in isolation: Fishing dependence and perceptions of change on kiritimati, the world's largest atoll. *Ocean Coast. Manag.*, **123**, 1–8.

Wessel, P. & Smith, W. (1996). A global, self-consistent, hierarchical, high-resolution shoreline database. *J. Geophys. Res.*, **101**, 8741–8743.

West, G.B., Brown, J.H. & Enquist, B.J. (2001). A general model for ontogenetic growth. *Nature*, **413**, 628–631.

White, E.P., Enquist, B.J. & Green, J.L. (2008). On estimating the exponent of power-law frequency distributions. *Ecology*, **89**, 905–912.

White, E.P., Ernest, S.K.M., Kerkhoff, A.J. & Enquist, B.J. (2007). Relationships between body size and abundance in ecology. *Trends Ecol. Evol.*, **22**, 323–330.

Wiens, J.A. (1989). Spatial scaling in ecology. *Funct. Ecol.*, **3**, 385–397.

Williams, I. & Polunin, N. (2001). Large-scale associations between macroalgal cover and grazer biomass on mid-depth reefs in the Caribbean. *Coral Reefs*, **19**, 358–366.

Williams, I.D., Baum, J.K., Heenan, A., Hanson, K.M., Nadon, M.O. & Brainard, R.E. (2015a). Human, oceanographic and habitat drivers of Central and Western Pacific coral reef fish assemblages. *PLoS One*, **10**, e0120516.

Williams, G.J., Gove, J.M., Eynaud, Y., Zgliczynski, B.J. & Sandin, S.A. (2015b). Local human impacts decouple natural biophysical relationships on Pacific coral reefs. *Ecography*, **38**, 751–761.

Williams, I.D., Richards, B.L., Sandin, S.A., Baum, J.K., Schroeder, R.E., Nadon, M.O., Zgliczynski, B., Craig, P., McIlwain, J.L. & Brainard, R.E. (2010). Differences in reef fish assemblages between populated and remote reefs spanning multiple archipelagos across the Central and Western Pacific. *J. Mar. Biol.*, **2011**, 14.

Williams, G.J., Smith, J.E., Conklin, E.J., Gove, J.M., Sala, E. & Sandin, S.A. (2013). Benthic communities at two remote pacific coral reefs: Effects of reef habitat, depth, and wave energy gradients on spatial patterns. *PeerJ*, **1**, e81.

Williams, I.D., White, D.J., Sparks, R.T., Lino, K.C., Zamzow, J.P., Kelly, E.L.A. & Ramey, H.L. (2016). Responses of herbivorous fishes and benthos to 6 years of protection at the Kahekili Herbivore Fisheries Management Area, Maui. *PLoS One*, **11**, e0159100.

Wilson, S.K., Fisher, R., Pratchett, M.S., Graham, N.A.J., Dulvy, N.K., Turner, R.A., Cakacaka, A. & Polunin, N.V.C. (2010). Habitat degradation and fishing effects on the size structure of coral reef fish communities. *Ecol. Appl.*, **20**, 442–451.

Wisz, M.S., Pottier, J., Kissling, W.D., Pellissier, L., Lenoir, J., Damgaard, C.F., Dormann, C.F., Forchhammer, M.C., Grytnes, J.-A., Guisan, A., Heikkinen, R.K., Høye, T.T., Kühn, I., Luoto, M., Maiorano, L., Nilsson, M.-C., Normand, S., Öckinger, E., Schmidt, N.M., Termansen, M., Timmermann, A., Wardle, D.A., Aastrup, P. & Svenning, J.-C. (2013). The role of biotic interactions in shaping distributions and realised assemblages of species: Implications for species distribution modelling. *Biol. Rev.*, **88**, 15–30.

Witman, J.D. & Roy, K. (2009). *Marine macroecology*. University of Chicago Press.

Worm, B. & Myers, R.A. (2003). Meta-analysis of cod-shrimp interactions reveals top-down control in oceanic food webs. *Ecology*, **84**, 162–173.

Worm, B., Sandow, M., Oschlies, A., Lotze, H.K. & Myers, R.A. (2005). Global patterns of predator diversity in the open oceans. *Science*, **309**, 1365–1369.

Wyatt, A.S.J., Waite, A.M. & Humphries, S. (2012). Stable isotope analysis reveals community-level variation in fish trophodynamics across a fringing coral reef. *Coral Reefs*, **31**, 1029–1044.

Yeager, L., Deith, M., McPherson, J., Williams, I., and Baum, J. (In press). Scale dependence of environmental controls on the functional diversity of coral reef fish communities. *Global Ecology & Biogeography*.

Yvon-Durocher, G., Reiss, J., Blanchard, J., Ebenman, B., Perkins, D.M., Reuman, D.C., Thierry, A., Woodward, G. & Petchey, O.L. (2011a). Across ecosystem comparisons of size structure: Methods, approaches and prospects. *Oikos*, **120**, 550–563.

Yvon-Durocher, G., Montoya, J.M., Trimmer, M. & Woodward, G. (2011b). Warming alters the size spectrum and shifts the distribution of biomass in freshwater ecosystems. *Glob. Chang. Biol.*, **17**, 1681–1694.

Zeller, D., Harper, S., Zylich, K. & Pauly, D. (2015). Synthesis of underreported small-scale fisheries catch in Pacific island waters. *Coral Reefs*, **34**, 25–39.

Zuur, A.F., Ieno, E.N., Walker, N.J., Saveliev, A.A., and Smith, G.M. 2009. Mixed effects models and extensions in ecology with R. Springer Science, New York

Appendices

Appendix A: Supplemental information for Chapter 2

A2.1 Trophic position ~ body size sensitivity analyses

A2.1.1 Herbivore trophic fractionation

We estimated the trophic position of herbivores using an additive approach (Hussey et al. 2014). Herbivorous fish fractionate differently to carnivores, so we used the mean trophic fractionation ($\Delta N = 4.778‰$) of herbivorous reef fish from published estimates (Mill et al. 2007). We tested the sensitivity of our results to ΔN by estimating herbivore trophic position for ΔN values ranging from 1 to 8‰, and refitting the optimum mixed effects model for both the species-based and individual-based approaches. The trophic pathway interaction term remained insignificant for all ΔN values, indicating that herbivore slopes were not distinct from carnivore slopes (Table A2.1).

A2.1.2 Location of isotope specimen collection

We examined trophic position ~ body size relationships for specimens collected from sites on the northeast coast (n = 5) and those collected from sites in the Bay of Wrecks on the southeast coast (n = 5). Sites on the northeast coast are closer to Kiritimati's population centers than the Bay of Wrecks, and thus may experience light fishing pressure that might influence food web structure. Relationships between trophic position and body size remained positive and significant for the species-based and individual-based analyses at north and south locations, for both herbivores and carnivores (Figs. A2.1, A2.2; Table A2.2). All random effects structures were identical to those selected for the models using the full dataset (see Chapter 2 Methods, Results), except for the individual-based model at southern sites that would not converge for species nested

within family, and thus was refit with only species as a random effect.

A2.2 Size spectra sensitivity analyses

Size spectra were fit to visual census data from Kiritimati collected in 2011 and 2013 to examine size structuring and energy pathways in coral reef food webs. Herbivores had shallower slopes than carnivores, and, generally, abundance decreased with increasing body size. Sensitivity analyses were run to examine whether this result was robust to differences in year, in site location, in the size range observed, and in diver identity. We also assessed potential impacts of fishing pressure at sites near the population centers on Kiritimati.

A2.2.1 Differences in year, site, and diver

Visual censuses were carried out in 2011 and 2013, and size spectra fit to each year separately yielded the same qualitative result (Fig. A2.3). The herbivore spectrum was shallower (b = 1.18, 95% CI = 1.16, 1.19) in 2011 than in 2013 (b = 1.37, 95% CI = 1.36, 1.39) and the carnivore spectrum was slightly steeper in 2011 (b = 1.66, 95% CI = 1.65, 1.67) than 2013 (b = 1.62, 95% CI = 1.62, 1.63). We also examined differences between sites on the northeast coast (n = 7) and sites in the Bay of Wrecks on the southeast coast (n = 7). Sites on the northeast coast are closer to Kiritimati's population centers than the Bay of Wrecks, and thus may experience light fishing pressure that might influence food web structure. However, size spectra exponents were qualitatively similar between these regions, and across years (Fig. A2.4).

Visual censuses were conducted by 4 divers: Scott Clark, Jonatha Giddens, Sheila Walsh, and Rowan Trebilco. SC took part in every dive (n = 26), JG dived every site in 2013 (n = 14), and SW (n = 11) and RT (n = 2) dived in 2011. Size spectra results were

qualitatively similar across divers, dive teams, and across years (for SC) (Figs. A2.5, A2.6, Table A2.3).

Finally, we examined size spectra across visual censuses that were conducted in both years (4 sites: 3, 15 ,19, 24). Spectra fit to the observed body sizes at each site did not differ qualitatively across years (Fig. A2.7). Site 25 was also sampled in both years, but the likelihood optimization failed to estimate 95% confidence intervals for the carnivore spectrum in 2013, and so we omitted site 25 from the figure.

A2.2.2 Potential biases in counts of small- and large-bodied fishes

Underwater visual censuses of reef fish are subject to known biases that can strongly influence estimates of abundance, biomass and community structure (Ward-Paige et al. 2010a). Bozec et al. (2011) examined fish detection rates on paired-diver transects and found that estimates of small, cryptic species decreased strongly with increasing distance from the transect line, whereas large mobile fish were underestimated due to diver avoidance, though noted that large fish biases can be site- and species-specific. Conversely, Ward-Paige et al. (2010a) reported overestimation of large mobile fish in non-instantaneous underwater visual censuses (e.g. line transects) when fish move into the survey area after the survey has started. The extent of this bias decreased substantially for transect widths > 5 m. We attempted to reduce these biases in our sample design by counting small fishes in a 4 m wide strip and large fishes in an 8 m wide strip. We also conducted sensitivity analyses to test the potential effect of biases in counting small and large fish on our size spectra estimates by estimating the size spectrum exponent b for different minimum (x_{min}) and maximum (x_{max}) observed size limits (Fig. A2.8), thus removing the observations that may be subject to over- or

underestimation. Though the estimates of herbivores and carnivores changed slightly for each change in minimum/maximum observed body mass, our results remained qualitatively robust.

A2.2.3 Omnivorous species contribution to trophic pathways

Omnivorous species derive energy from benthic and pelagic resource bases and, as such, we could not confidently assign each species a trophic pathway (herbivores or carnivores). To test this issue, we removed omnivores from the main size spectra analyses. However, including omnivores as either carnivores (Fig. A2.9, top) or herbivores (Fig. A2.9, bottom) did not qualitatively affect our results: the herbivore spectrum was always shallower than the carnivore spectrum.

A2.2.4 Potential fishing pressure at north coast sites

We attempted to minimize any confounding influences of exploitation by surveying the fish communities at remote sites on the northwest coast of Kiritimati. Though most of our survey sites are generally inaccessible to subsistence fishers, we acknowledge that the sites on the north coast are nearest Kiritimati's population centers (Fig. 2.1) and so may experience light fishing pressure. We removed observations from the four north coast sites and refitted size spectra to carnivore and herbivore groups (Fig. A2.10). The exponent *b* increased slightly for both groups, suggesting that the abundance of large body sizes is depleted at north coast sites. Nevertheless, the carnivore spectrum remains steeper than the herbivore spectrum, consistent with our original predictions.

	Trophic pathway interaction term		
	Estimate	P	ΔN
Species-based	-0.042	0.746	1
	-0.051	0.694	2
	-0.057	0.654	3
	-0.063	0.623	4
	-0.068	0.598	5
	-0.071	0.578	6
	-0.075	0.561	7
	-0.078	0.546	8
Individual-based	0.031	0.559	1
	0.018	0.728	2
	0.009	0.871	3
	0.001	0.989	4
	-0.006	0.913	5
	-0.011	0.834	6
	-0.017	0.765	7
	-0.020	0.710	8

Table A2.1 Sensitivity of trophic position ~ body size analyses to varying herbivore trophic fractionation (ΔN) values. Significance value and slope of trophic pathway interaction term are reported for the optimum species-based and individual-based mixed effects models reported in the main text. ΔN ranged from 1 to 8‰.

	Coefficient	Estimate	Standard error	P value	Marginal R^2	AIC_c	Location
Species-based	Intercept	2.37	0.305	< 0.001	0.17	49.09	North
	log_2 mass	0.122	0.025	< 0.001			
Species-based with trophic pathway	Intercept	2.76	0.256	< 0.001	0.64	47.53	
	Intercept (herbivore)	-1.09	0.958	0.282			
	log_2 mass	0.118	0.024	0.001			
	log_2 mass*herbivore	-0.05	0.117	0.681			
Individual-based	Intercept	2.7	0.251	< 0.001	0.08	57.43	
	log_2 mass	0.095	0.015	< 0.001			
Individual-based with trophic pathway	Intercept	3.059	0.186	< 0.001	0.65	53.69	
	Intercept (herbivore)	-1.433	0.383	0.004			
	log_2 mass	0.097	0.017	< 0.001			
	log_2 mass*herbivore	0.008	0.036	0.817			
Species-based	Intercept	2.173	0.32	< 0.001	0.2	50.39	South
	log_2 mass	0.131	0.026	0.001			
Species-based with trophic pathway	Intercept	2.595	0.274	< 0.001	0.6	49.53	
	Intercept (herbivore)	-1.2	1.033	0.274			
	log_2 mass	0.122	0.026	0.003			
	log_2 mass*herbivore	-0.039	0.125	0.766			
Individual-based	Intercept	2.787	0.222	< 0.001	0.04	34.34	
	log_2 mass	0.067	0.022	0.012			
Individual-based with trophic pathway	Intercept	3.045	0.2	< 0.001	0.4	25.6	
	Intercept (herbivore)	-1.434	0.492	0.009			
	log_2 mass	0.06	0.023	0.011			
	log_2 mass*herbivore	0.004	0.059	0.953			

Table A2.2 Parameter estimates of the best model (as evaluated by AIC_c) for log_2 body mass ~ trophic position relationships for sites on the northeast coast (North) and in the Bay of Wrecks (South). Species-based analyses were linear mixed effects models with family as a random effect and individual-based were linear mixed effects models random structure of species nested within family as a random effect (north) and species as a random effect (south).

Diver	Year	Energy pathway	*b*	CI min	CI max
SC	2011	Carnivore	1.60	1.59	1.61
SC	2011	Herbivore	1.20	1.18	1.23
SC	2013	Carnivore	1.52	1.51	1.53
SC	2013	Herbivore	1.37	1.35	1.39
JLG	2013	Carnivore	1.80	1.78	1.81
JLG	2013	Herbivore	1.37	1.35	1.40
RT	2011	Carnivore	1.82	1.79	1.84
RT	2011	Herbivore	1.22	1.09	1.34
SMW	2011	Carnivore	1.70	1.69	1.72
SMW	2011	Herbivore	1.14	1.12	1.17

Table A2.3 Size spectra exponent estimates with 95% confidence intervals for each diver, year, and energy pathway. SC: Scott Clark; JLG: Jonatha Giddens; RT: Rowan Trebilco; SMW: Sheila Walsh.

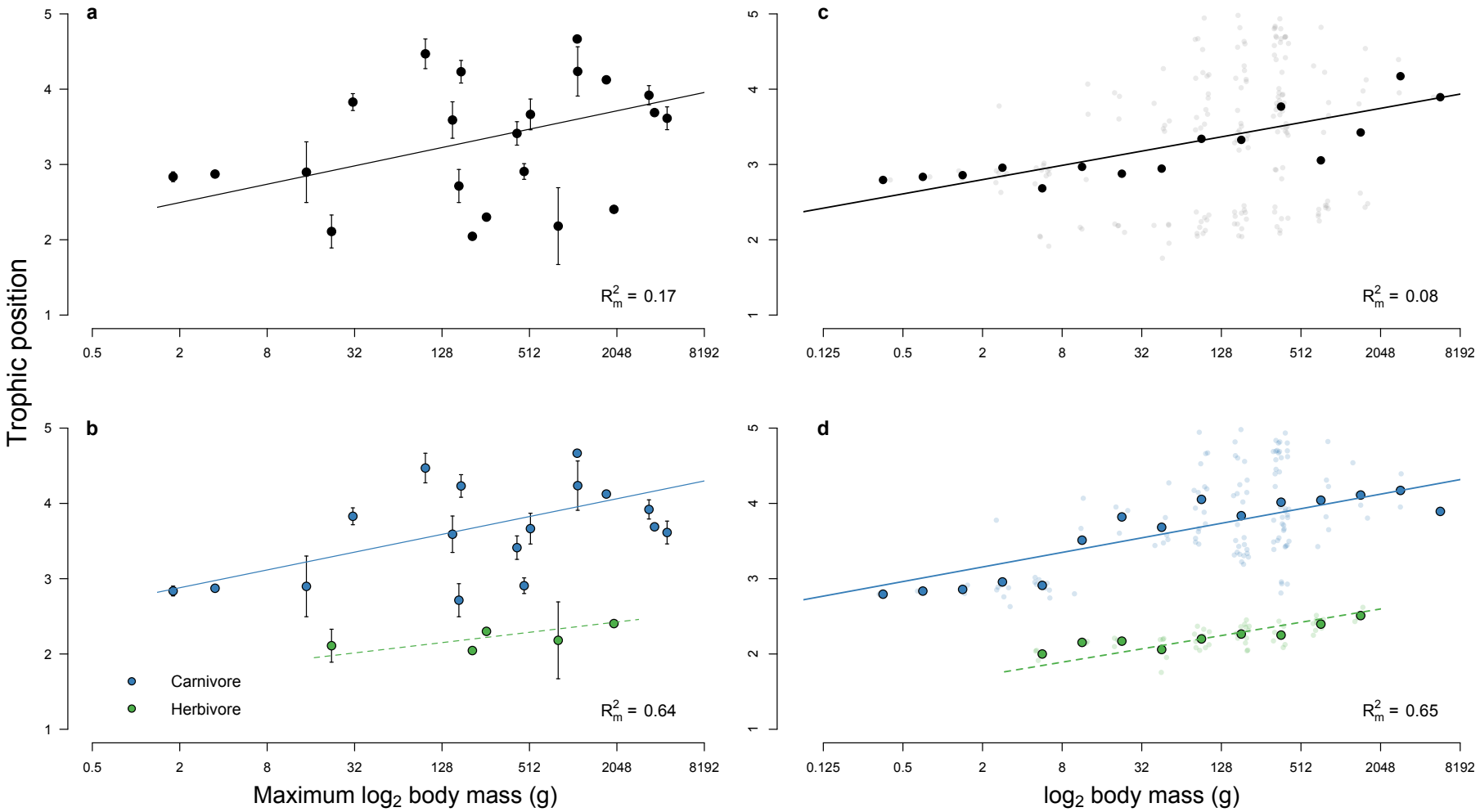
a
b
c
d
Trophic position
Maximum log2 body mass (g)
log2 body mass (g)
Carnivore
Herbivore
R2m = 0.17
R2m = 0.64
R2m = 0.08
R2m = 0.65
1
2
3
4
5
0.125
0.5
2
8
32
128
512
2048
8192

Figure A2.1 Trophic position ~ body size relationships at sites on the Northwest coast (n = 5). a, b: Species-based analyses. Linear mixed effects models of trophic position and $\log_2$ body mass (g) in the coral reef fish community (a) across all species (n = 22), (b) for the two trophic pathways, carnivores (blue, n = 17 species) and herbivores (green, n = 5 species). For each species, the mean trophic position and 95% confidence intervals are plotted against its maximum mass. **c, d:** Individual-based analyses. Linear mixed effects models individual trophic position and of individual $\log_2$ body mass (g) in the coral reef fish community (c) across all individuals (n = 184) and (d) for the two trophic pathways, carnivores (blue, n = 129) and herbivores (green, n = 55). Individual trophic position estimates (with jitter, transparent colour) are plotted against body mass class, and overlaid with mean trophic position (solid colour) of each body mass class.

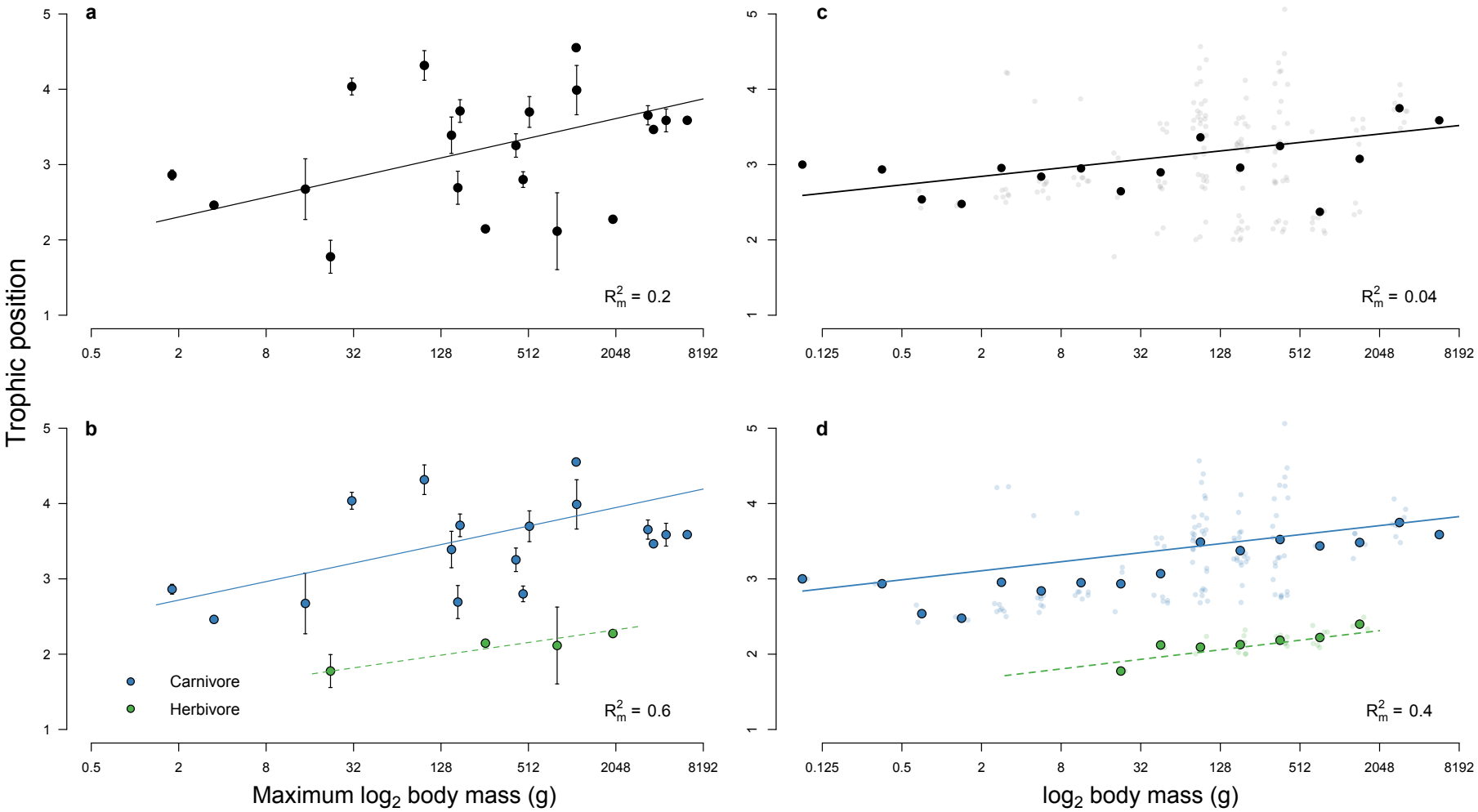
a
b
c
d
Trophic position
Maximum log2 body mass (g)
log2 body mass (g)
Carnivore
Herbivore
R2m = 0.2
R2m = 0.6
R2m = 0.04
R2m = 0.4
0.125
0.5
2
8
32
128
512
2048
8192
1
2
3
4
5

Figure A2.2 Trophic position ~ body size relationships at sites in the Bay of Wrecks (Southwest coast (n = 5)). **a, b:** Species-based analyses. Linear mixed effects models of trophic position and $\log_2$ body mass (g) in the coral reef fish community (a) across all species (n = 21), (b) for the two trophic pathways, carnivores (blue, n = 17 species) and herbivores (green, n = 4 species). For each species, the mean trophic position and 95% confidence intervals are plotted against its maximum mass. **c, d:** Individual-based analyses. Linear mixed effects models individual trophic position and of individual $\log_2$ body mass (g) in the coral reef fish community (c) across all individuals (n = 160) and (d) for the two trophic pathways, carnivores (blue, n = 129) and herbivores (green, n = 31). Individual trophic position estimates (with jitter, transparent colour) are plotted against body mass class, and overlaid with mean trophic position (solid colour) of each body mass class.

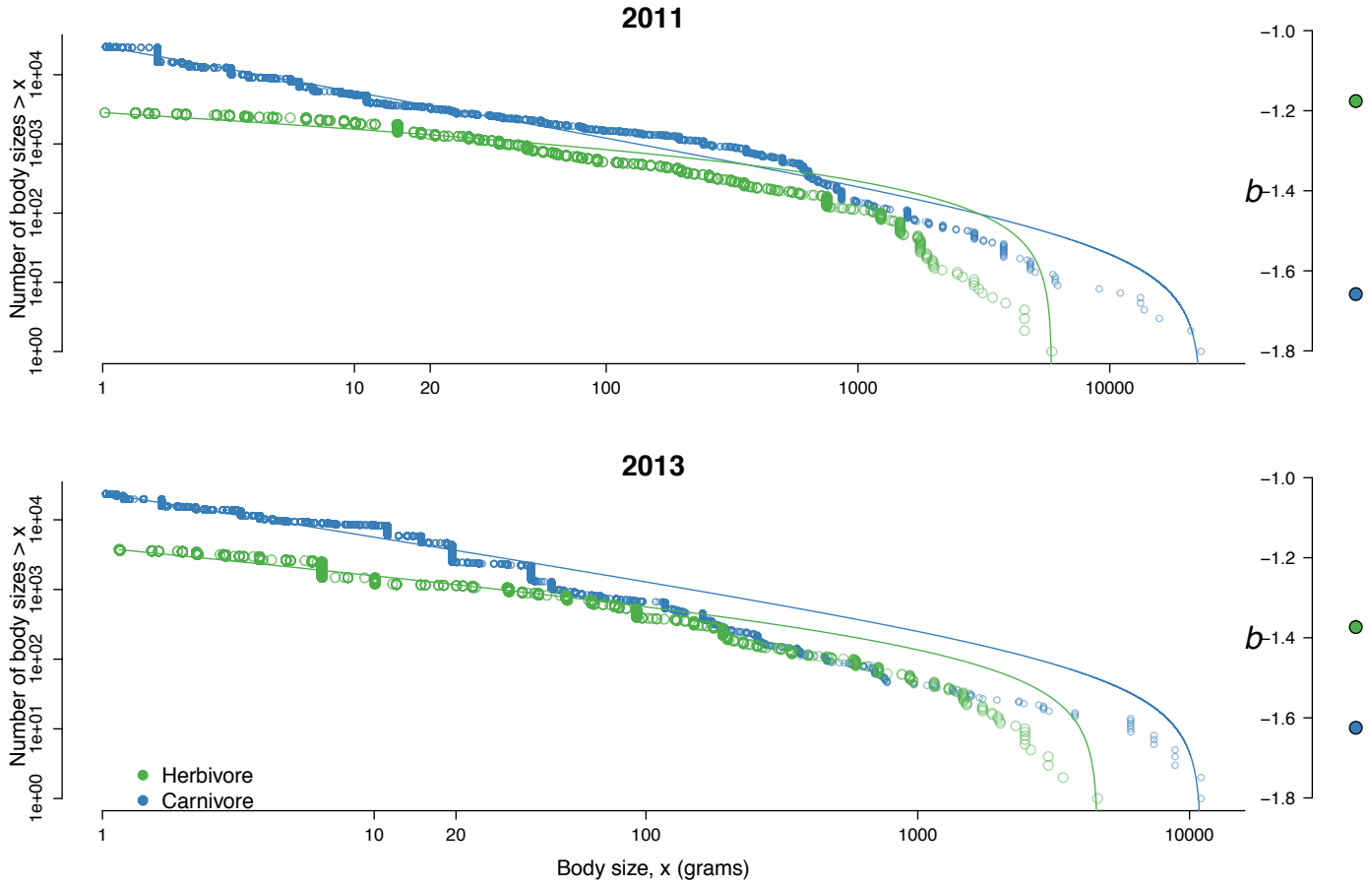

Figure A2.3 Rank-frequency plot of reef fish body masses in 2011 (top) and 2013 (bottom), with associated size spectra exponent estimates and 95% confidence intervals (right panel). Carnivore trophic pathway in blue; herbivore trophic pathway in green.

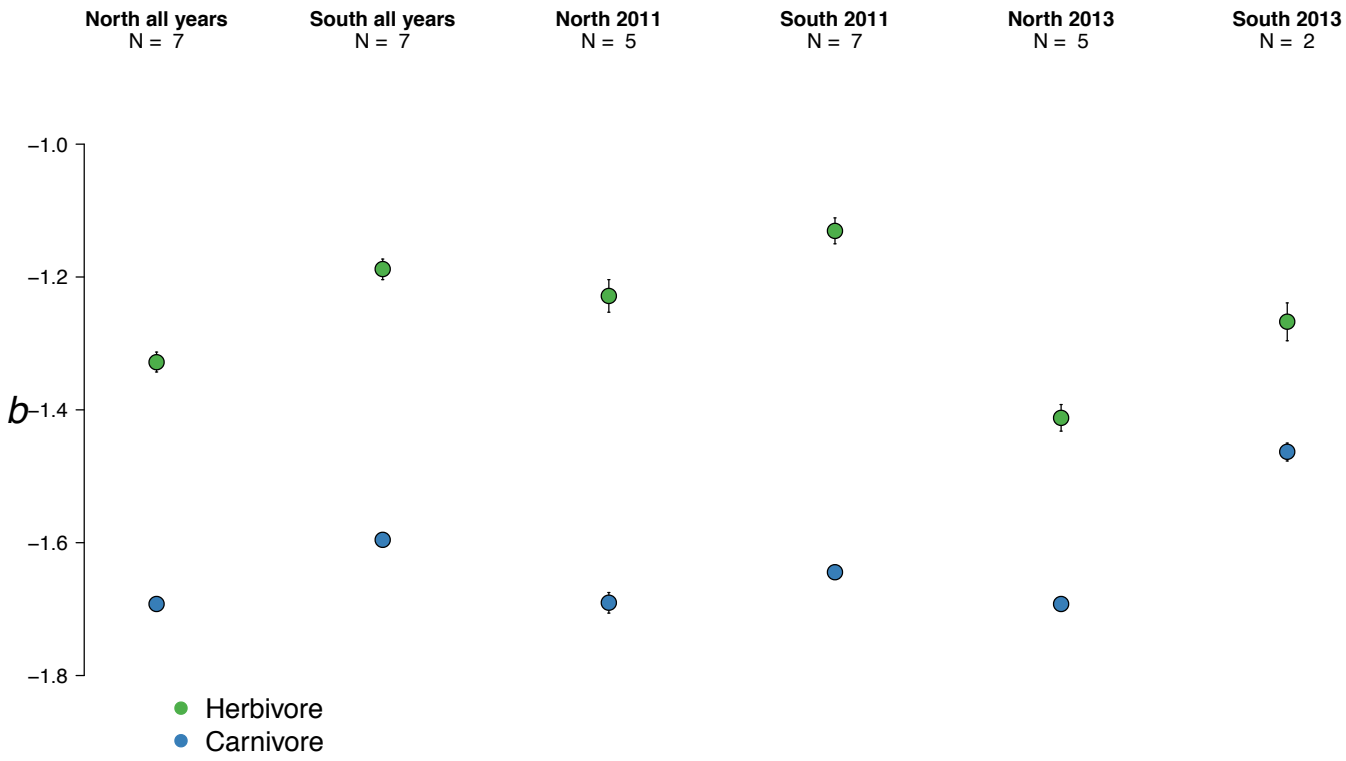

Figure A2.4 Size spectra exponent estimates with 95% confidence intervals for northeast coast sites (North, n = 7) and Bay of Wrecks sites (South, n = 7) across years. Carnivore trophic pathway in blue; herbivore trophic pathway in gree

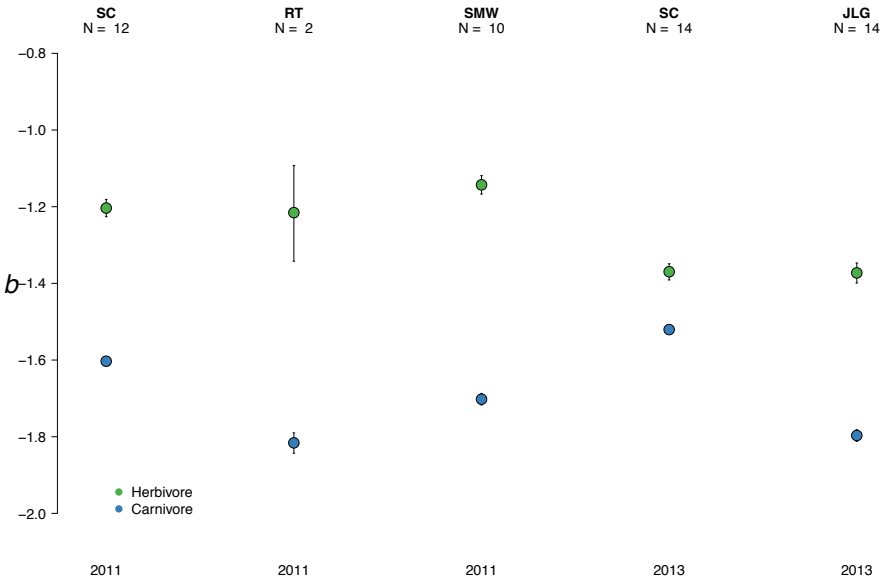

Figure A2.5 Size spectra exponent estimates with 95% confidence intervals for each diver across years. Carnivore trophic pathway in blue; herbivore trophic pathway in green.

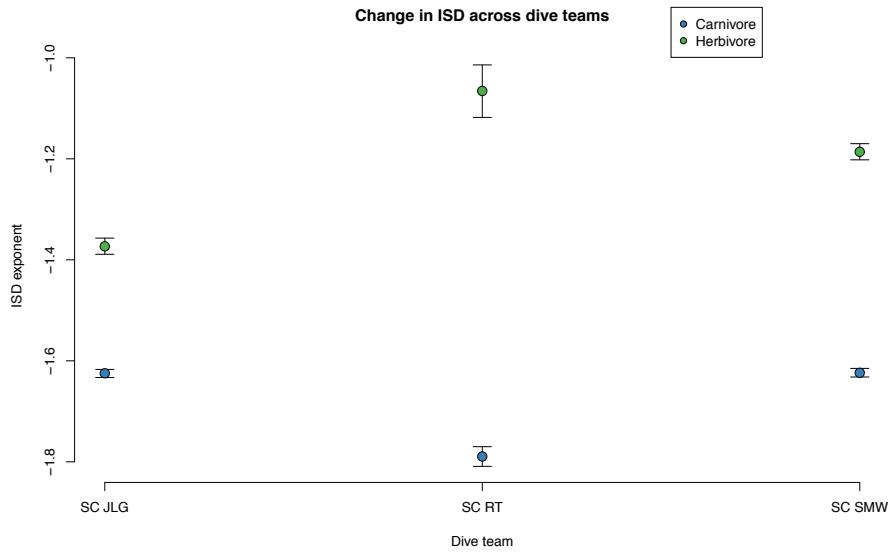

Figure A2.6 Size spectra exponent estimates with 95% confidence intervals for each dive team. Carnivore trophic pathway in blue; herbivore trophic pathway in green.

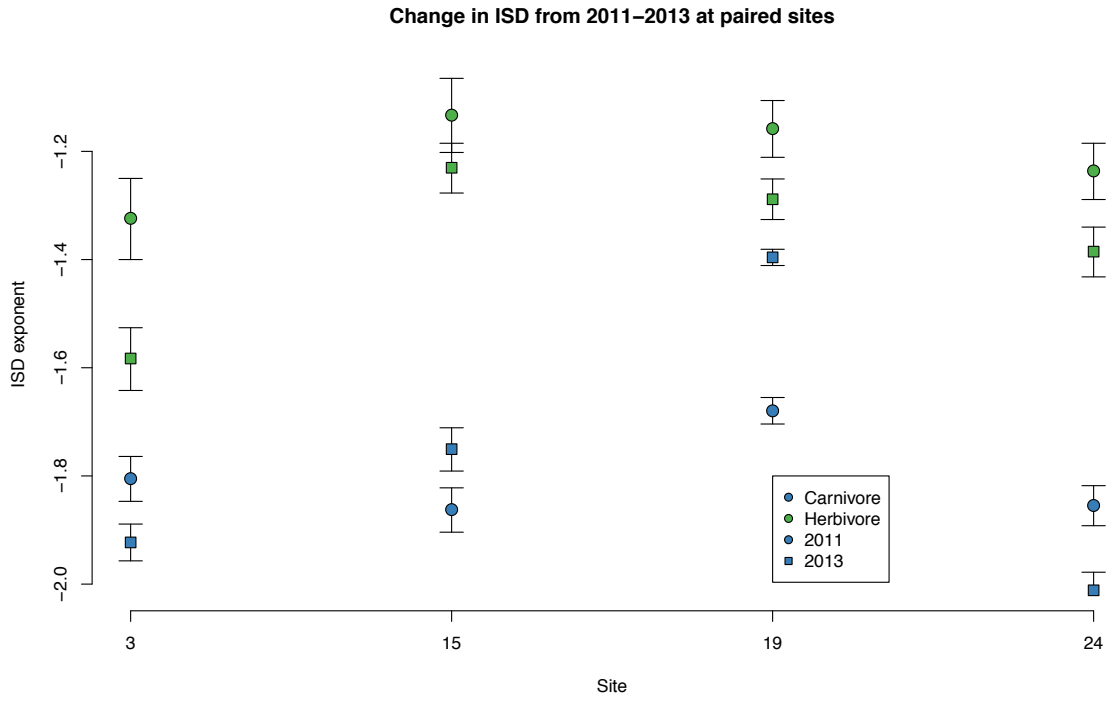

Figure A2.7 Size spectra exponent estimates with 95% confidence intervals for sites (n = 4) sampled in both 2011 (circles) and 2013 (squares). Carnivore trophic pathway in blue; herbivore trophic pathway in green.

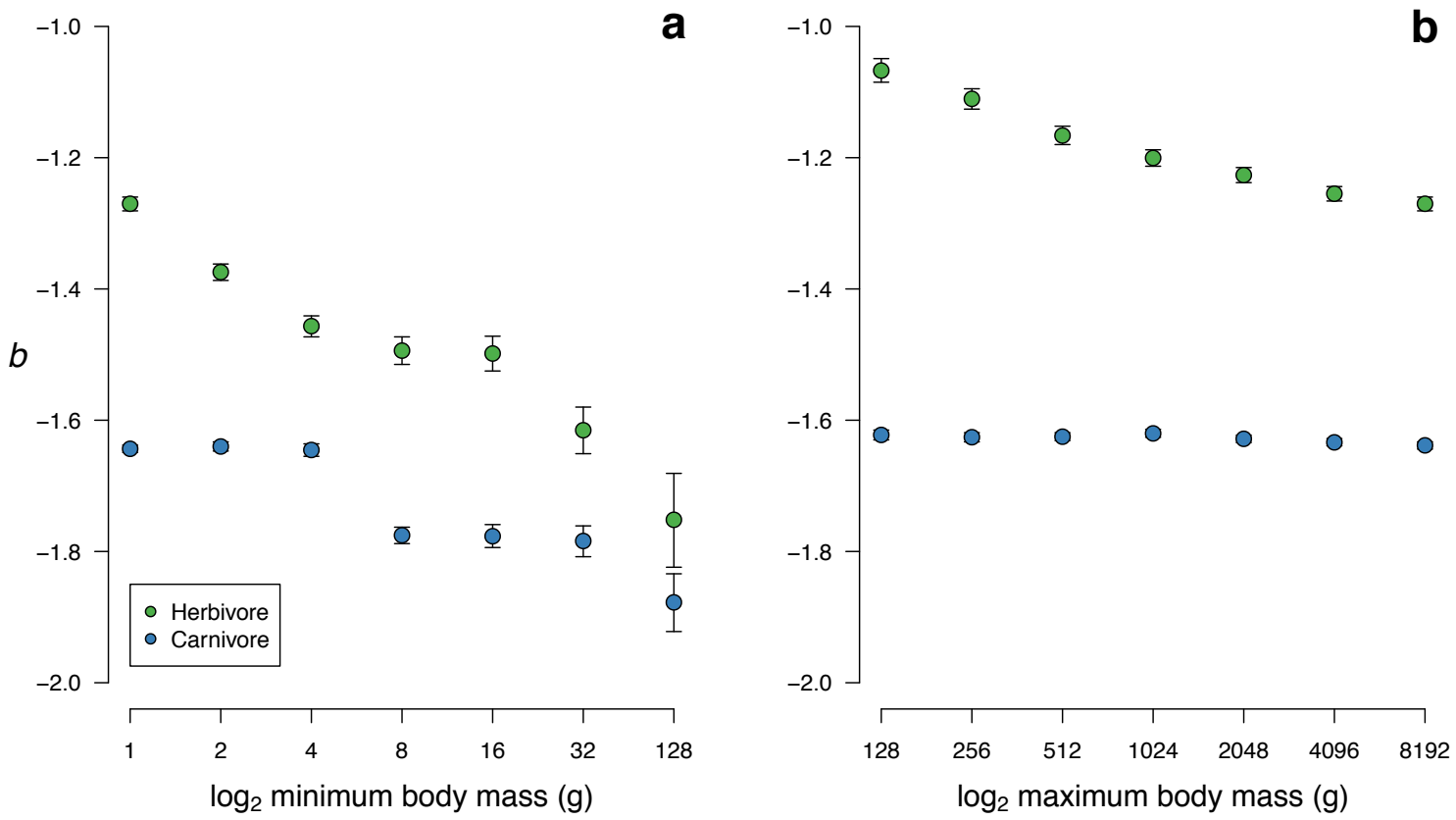

Figure A2.8 Size spectra exponent estimates with 95% confidence intervals for different minimum and maximum observed body masses. a: We estimated the exponent *b* separately for herbivores (green) and carnivores (blue) after removing the observations in the smallest $\log_2$ size categories (2, 4, 8, 16, 32, 128 g). **b**: We estimated the exponent *b* separately for herbivores (green) and carnivores (blue) after removing the observations in the largest $\log_2$ size categories (128, 256, 512, 1024, 2048, 4096, 8192 g).

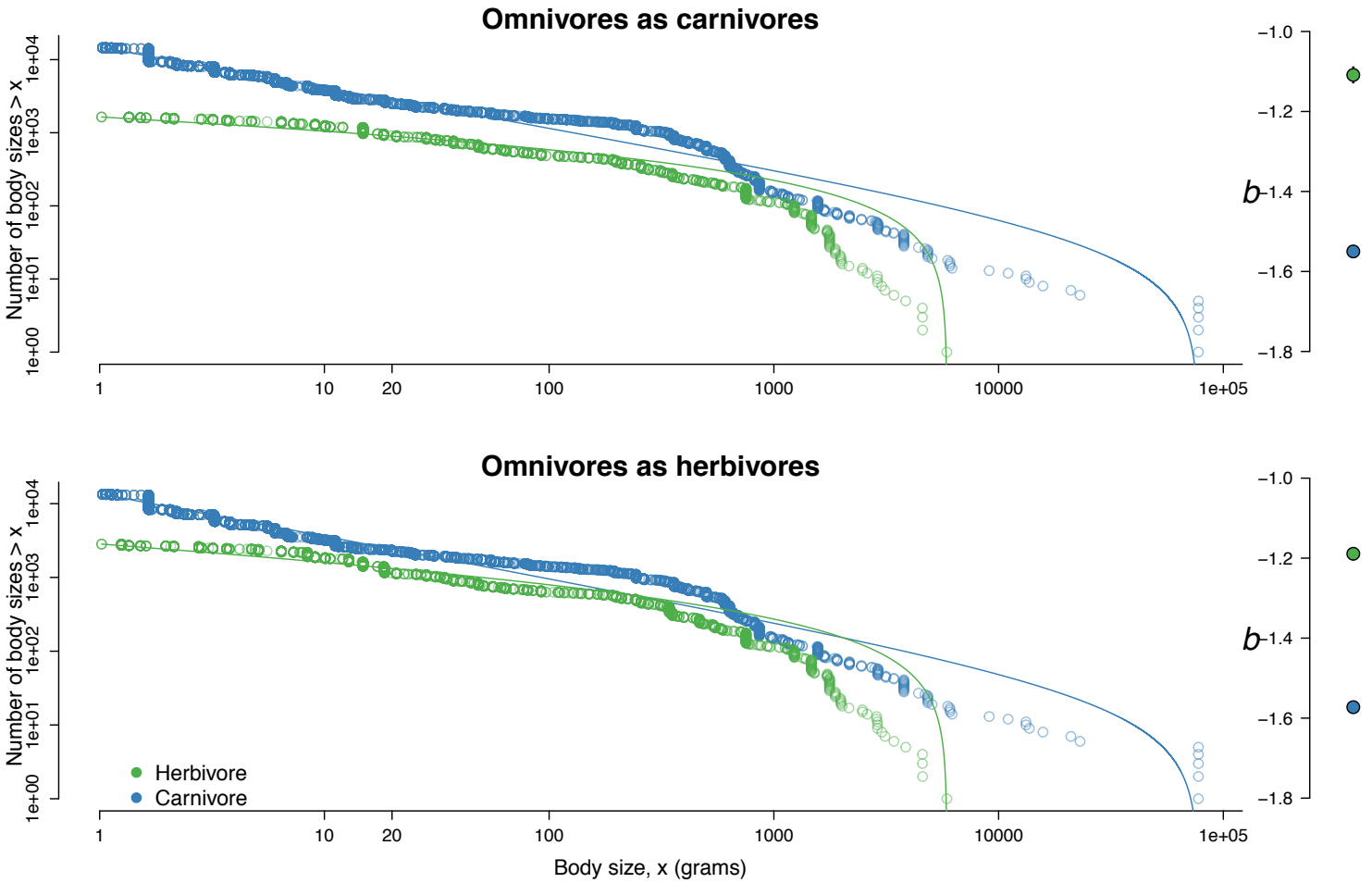

Figure A2.9 Rank-frequency plot of observed masses for carnivores (blue) and herbivores (green) and associated size spectra exponent estimates (with 95% CIs) when omnivorous species were classed as carnivores (top) or herbivores (bottom).

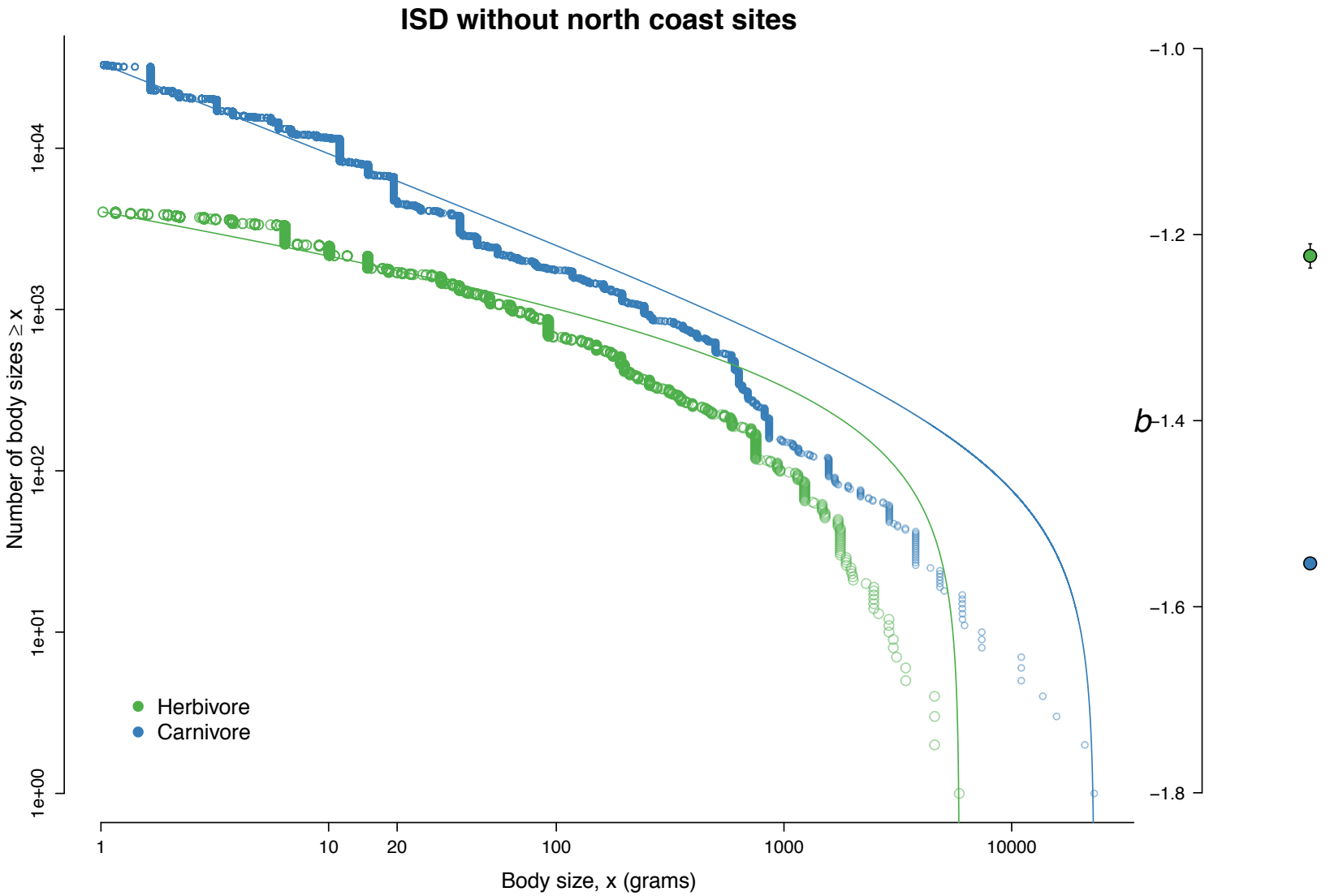

Figure A2.10 Rank-frequency plot of observed masses for carnivores (blue) and herbivores (green), and associated size spectra exponent estimates (with 95% CIs) with potentially exploited North coast sites (n = 4) removed.

Appendix B: Supplemental information for Chapter 3

Reef area		Island type	Latitude	Longitude	minimum SST (°C)	Productivity (mg C m^{-2} day^{-1})	Habitat complexity	Bathymetric slope	Reef area within 75 km radius (km^2)	Land area within 75 km radius (km^2)	Population density in 20 km radius	Population density in 20 km radius per reef area km^2	Distance to nearest provincial capital (km)	Nearest provincial capital
Gardner	Hawaiian archipelago	low	24.999	191.748	21.62	588.3	0.57	4.00	1605.3	0.1	0	0	1139	Honolulu
Hawaii		high	19.653	204.482	23.67	485.5	0.63	5.39	84.8	5604.8	17712	936	71	Hilo
Kauai		high	22.028	200.457	23.09	530.9	0.39	1.59	311.3	1616.4	22167	312	191	Honolulu
Kure		atoll	28.416	181.664	18.66	581.4	0.67	0.94	83.1	1.4	0	0	2209	Honolulu
Lanai		high	20.823	203.099	23.76	532.6	0.54	1.20	1116.8	2635.4	8336	82	115	Honolulu
Laysan		high	25.773	188.270	21.10	526.2	0.47	0.25	636.8	4.6	0	0	1498	Honolulu
Lisianski		atoll	26.016	186.065	20.87	604.1	0.83	0.25	1504.5	1.9	0	0	1718	Honolulu
Maro		atoll	25.404	189.438	21.25	652.5	0.61	0.10	1653.0	0.0	0	0	1374	Honolulu
Maui		high	20.827	203.573	23.48	537.5	0.60	1.03	555.4	2779.3	45648	527	152	Hilo
Midway		atoll	28.234	182.637	18.99	570.0	0.62	0.92	123.7	7.1	0	0	2112	Honolulu
Molokai		high	21.121	202.942	23.50	567.6	0.51	1.03	1319.1	1981.3	3678	18	87	Honolulu
Niihau		high	21.906	199.851	23.20	474.9	0.47	0.79	236.7	1133.4	163	2	245	Honolulu
Oahu		high	21.460	202.030	23.40	544.9	0.32	1.75	951.9	1713.7	261815	2235	29	Honolulu
Pearl & Hermes		atoll	27.875	184.207	19.23	634.0	0.64	1.39	485.8	0.8	0	0	1953	Honolulu
Agrihan	Marianas archipelago	high	18.769	145.666	25.57	300.0	0.63	10.64	15.5	85.0	0	0	401	Saipan
Alamagan		high	17.598	145.829	25.76	311.1	0.70	9.22	18.8	74.6	0	0	271	Saipan
Asuncion		high	19.690	145.402	25.16	313.2	0.71	9.94	7.0	10.9	0	0	504	Saipan
Farallon de Pajaros		high	20.543	144.894	24.72	322.3	0.72	10.43	5.2	5.3	0	0	604	Saipan
Guam		high	13.466	144.779	26.44	266.4	0.48	6.71	184.9	585.6	96118	1486	17	Hagatna

Guguan		high	17.307	145.841	25.93	303.3	0.73	7.92	12.0	23.3	0	0	239	Saipan
Maug		high	20.023	145.222	25.11	323.6	0.60	6.99	9.0	13.3	0	0	542	Saipan
Pagan		high	18.107	145.760	25.67	302.0	0.70	8.57	22.0	92.9	0	0	327	Saipan
Rota		high	14.145	145.178	26.41	230.3	0.56	3.29	55.9	198.8	2527	99	88	Hagatna
Saipan		low	15.199	145.747	26.24	329.5	0.46	4.71	174.1	239.0	47987	385	9	Saipan
Sarigan		high	16.703	145.777	25.77	303.0	0.74	11.39	17.0	44.4	0	0	172	Saipan
Tinian		high	15.019	145.629	26.31	294.2	0.49	4.88	174.1	239.0	19021	202	19	Saipan
Baker	Pacific Remote Island Areas	high	0.196	183.528	26.27	884.9	0.65	12.47	10.2	4.2	0	0	1077	Funafuti
Howland		high	0.807	183.382	26.29	893.5	0.64	11.32	10.2	4.2	0	0	1132	Funafuti
Jarvis		high	-0.374	200.010	25.15	991.0	0.52	8.72	6.6	4.4	0	0	1937	Pago Pago
Johnston		atoll	16.747	190.494	24.59	435.4	0.53	11.40	202.2	3.5	0	0	1326	Honolulu
Kingman		atoll	6.402	197.596	26.31	654.0	0.50	12.34	128.1	11.5	0	0	1673	Hilo
Palmyra		atoll	5.876	197.911	26.30	683.5	0.55	11.42	125.2	11.5	0	0	1709	Hilo
Wake		atoll	19.299	166.630	25.12	314.0	0.53	15.22	27.7	8.8	0	0	1441	Majuro
Ofu & Olosega	American Samoa	low	-14.171	190.351	26.64	315.9	0.66	3.43	56.0	61.7	782	23	114	Pago Pago
Rose		atoll	-14.545	191.844	26.46	374.4	0.71	21.22	8.0	0.1	1	0	276	Pago Pago
Swains		high	-11.056	188.921	27.50	350.3	0.85	16.82	6.2	4.1	17	3	316	Apia
Tau		high	-14.240	190.535	26.76	305.8	0.56	6.86	54.6	61.7	957	30	133	Pago Pago
Tutuila		high	-14.293	189.326	26.57	406.7	0.65	3.73	316.0	145.8	46993	223	10	Pago Pago

Table A3.1 Anthropogenic and environmental covariate estimates for CREP reef areas.

Region	Reef area	Latitude	Longitude	Year	Number of sites	Number of fish observed
Hawaiian archipelago	Gardner	24.999	191.748	2011	12	1662
	Hawaii	19.653	204.482	2010	43	2425
	Hawaii	19.653	204.482	2013	58	5670
	Kauai	22.028	200.457	2010	26	1224
	Kauai	22.028	200.457	2013	35	1580
	Kure	28.416	181.664	2010	16	1313
	Kure	28.416	181.664	2012	14	1298
	Lanai	20.823	203.099	2012	29	2209
	Lanai	20.823	203.099	2013	29	1833
	Laysan	25.773	188.270	2011	23	1373
	Lisianski	26.016	186.065	2010	24	1584
	Lisianski	26.016	186.065	2011	9	1078
	Lisianski	26.016	186.065	2012	25	2677
	Maro	25.404	189.438	2011	21	2097
	Maui	20.827	203.573	2010	33	1768
	Maui	20.827	203.573	2012	49	2652
	Maui	20.827	203.573	2013	34	1996
	Midway	28.234	182.637	2011	17	2820
	Molokai	21.121	202.942	2012	50	3794
	Molokai	21.121	202.942	2013	39	3322
	Niihau	21.906	199.851	2010	16	1268
	Niihau	21.906	199.851	2013	26	1898
	Oahu	21.460	202.030	2013	63	1993
	Pearl & Hermes	27.875	184.207	2010	22	1599
	Pearl & Hermes	27.875	184.207	2011	9	1327
	Pearl & Hermes	27.875	184.207	2012	15	1432
Marianas archipelago	Agrihan	18.769	145.666	2011	20	1850
	Alamagan	17.598	145.829	2014	11	1873
	Asuncion	19.690	145.402	2011	20	1597
	Asuncion	19.690	145.402	2014	21	2849
	Farallon de Pajaros	20.543	144.894	2011	12	1309
	Farallon de Pajaros	20.543	144.894	2014	11	1359
	Guam	13.466	144.779	2011	133	11812
	Guam	13.466	144.779	2014	51	2495
	Guguan	17.307	145.841	2011	10	1170
	Guguan	17.307	145.841	2014	11	1243
	Maug	20.023	145.222	2011	30	2615
	Maug	20.023	145.222	2014	40	4515
	Pagan	18.107	145.760	2011	29	2087

	Pagan	18.107	145.760	2014	43	4446
	Rota	14.145	145.178	2011	24	1508
	Rota	14.145	145.178	2014	28	1585
	Saipan	15.199	145.747	2011	30	1380
	Saipan	15.199	145.747	2014	45	2404
	Sarigan	16.703	145.777	2014	11	1060
	Tinian	15.019	145.629	2011	19	1193
Pacific Remote Island Areas	Baker	0.196	183.528	2010	21	2455
	Baker	0.196	183.528	2012	24	3608
	Howland	0.807	183.382	2010	16	1817
	Howland	0.807	183.382	2012	39	6170
	Jarvis	-0.374	200.010	2010	19	4827
	Jarvis	-0.374	200.010	2012	42	9644
	Johnston	16.747	190.494	2010	8	1021
	Johnston	16.747	190.494	2012	9	1022
	Kingman	6.402	197.596	2010	19	3469
	Kingman	6.402	197.596	2012	26	3834
	Palmyra	5.876	197.911	2010	33	3678
	Palmyra	5.876	197.911	2012	42	7311
	Wake	19.299	166.630	2011	30	2187
	Wake	19.299	166.630	2014	43	3550
American Samoa	Ofu & Olosega	-14.171	190.351	2010	30	2735
	Ofu & Olosega	-14.171	190.351	2012	30	3845
	Rose	-14.545	191.844	2010	24	1912
	Rose	-14.545	191.844	2012	33	3180
	Swains	-11.056	188.921	2010	24	1453
	Swains	-11.056	188.921	2012	38	3040
	Tau	-14.240	190.535	2010	24	1625
	Tau	-14.240	190.535	2012	22	2020
	Tutuila	-14.293	189.326	2010	105	8493
	Tutuila	-14.293	189.326	2012	85	7923

Table A3.2 Reef areas surveyed in the CREP dataset with number of survey sites and fish observed at each island in each observation year.

	Intercept	Humans	Complexity	Atoll - high	Atoll - low	Bathy. slope	Land area	Reef area	min SST	Prod.	DF	LL	AICc	ΔAICc	weight	R^2
Proximity to market	-1.57	-0.13	-	0.03	0.05	-	-	-	0.11	-	7	53.04	-90.27	0.00	0.16	0.56
	-1.57	-0.16	-	0.00	0.05	-	0.04	-	0.12	-	8	54.26	-90.15	0.12	0.15	0.58
	-1.57	-0.14	-	0.02	0.04	-0.03	-	-	0.14	-	8	53.71	-89.05	1.22	0.09	0.57
	-1.57	-0.14	-0.01	0.03	0.04	-	-	-	0.11	-	8	53.38	-88.41	1.86	0.06	0.57
	-1.57	-0.16	-	0.00	0.04	-0.02	0.03	-	0.14	-	9	54.67	-88.34	1.93	0.06	0.58
	-1.57	-0.14	-	0.03	0.05	-	-	0.02	0.12	-	8	53.31	-88.25	2.02	0.06	0.57
	-1.57	-0.14	-	0.03	0.06	-	-	-	0.11	-0.01	8	53.10	-87.84	2.44	0.05	0.56
	-1.57	-0.16	-	0.00	0.05	-	0.04	-	0.12	0.00	9	54.30	-87.60	2.67	0.04	0.58
	-1.57	-0.16	0.00	0.00	0.05	-	0.03	-	0.12	-	9	54.27	-87.53	2.74	0.04	0.58
	-1.57	-0.16	-	0.00	0.05	-	0.04	0.00	0.12	-	9	54.26	-87.52	2.75	0.04	0.58
	-1.57	-0.15	-0.01	0.02	0.04	-0.03	-	-	0.14	-	9	54.05	-87.10	3.17	0.03	0.58
	-1.57	-0.15	-	0.03	0.05	-0.03	-	-	0.13	-0.01	9	53.79	-86.58	3.69	0.02	0.57
	-1.57	-0.14	-	0.02	0.04	-0.03	-	0.00	0.14	-	9	53.71	-86.41	3.86	0.02	0.57
	-1.57	-0.15	-0.02	0.04	0.06	-	-	-	0.11	-0.02	9	53.68	-86.36	3.92	0.02	0.56
	-1.57	-0.16	-	-0.02	0.04	-0.03	0.04	-0.02	0.14	-	10	54.87	-86.02	4.25	0.02	0.59
	-1.57	-0.14	-0.01	0.03	0.05	-	-	0.01	0.12	-	9	53.49	-85.98	4.29	0.02	0.57
	-1.57	-0.17	-	0.00	0.05	-0.02	0.03	-	0.14	-0.01	10	54.77	-85.82	4.45	0.02	0.59
	-1.57	-0.15	-	0.04	0.06	-	-	0.02	0.12	-0.01	9	53.41	-85.82	4.46	0.02	0.56
	-1.57	-0.16	0.00	0.00	0.04	-0.02	0.03	-	0.14	-	10	54.70	-85.66	4.61	0.02	0.58
	-1.57	-0.16	-0.02	0.04	0.06	-0.03	-	-	0.13	-0.02	10	54.43	-85.12	5.15	0.01	0.57
	-1.57	-0.16	0.00	0.01	0.05	-	0.03	-	0.12	-0.01	10	54.33	-84.94	5.34	0.01	0.58
	-1.57	-0.17	-	0.01	0.05	-	0.03	0.00	0.12	-0.01	10	54.32	-84.90	5.37	0.01	0.58
	-1.57	-0.16	0.00	0.00	0.05	-	0.03	0.00	0.12	-	10	54.27	-84.80	5.47	0.01	0.58
	-1.57	-0.14	-0.01	0.01	0.03	-0.04	-	-0.01	0.14	-	10	54.14	-84.54	5.73	0.01	0.58
	-1.57	-0.15	-	0.03	0.05	-0.03	-	0.00	0.13	-0.01	10	53.79	-83.86	6.41	0.01	0.57

	-1.57	-0.16	-0.01	0.05	0.07	-	-	0.01	0.11	-0.02	10	53.78	-83.83	6.44	0.01	0.56
	-1.57	-0.16	-0.01	-0.02	0.03	-0.04	0.03	-0.02	0.14	-	11	54.98	-83.40	6.87	0.01	0.59
Human population density	-1.57	-0.18	-0.03	-0.01	0.01	-	0.06	-	0.08	-	9	59.20	-97.40	0.00	0.23	0.60
	-1.57	-0.17	-	-0.03	0.00	-	0.08	-	0.08	-	8	57.61	-96.86	0.54	0.18	0.59
	-1.57	-0.17	-	-0.04	0.00	-	0.08	-	0.09	0.02	9	58.05	-95.10	2.31	0.07	0.60
	-1.57	-0.18	-0.03	-0.01	0.00	-0.01	0.06	-	0.09	-	10	59.35	-94.98	2.43	0.07	0.60
	-1.57	-0.17	-0.03	-0.02	0.01	-	0.07	-0.01	0.07	-	10	59.32	-94.91	2.49	0.07	0.60
	-1.57	-0.18	-0.02	-0.01	0.01	-	0.06	-	0.08	0.00	10	59.21	-94.69	2.71	0.06	0.60
	-1.57	-0.17	-	-0.03	0.00	-0.01	0.07	-	0.09	-	9	57.67	-94.33	3.07	0.05	0.59
	-1.57	-0.17	-	-0.03	0.00	-	0.08	0.00	0.08	-	9	57.63	-94.26	3.14	0.05	0.59
	-1.57	-0.14	-0.03	0.03	0.02	-	-	-	0.08	-	8	56.27	-94.18	3.22	0.05	0.58
	-1.57	-0.17	-0.03	-0.04	-0.01	-0.03	0.07	-0.03	0.09	-	11	59.98	-93.40	4.00	0.03	0.61
	-1.57	-0.14	-0.04	0.03	0.01	-0.02	-	-	0.09	-	9	56.76	-92.52	4.89	0.02	0.59
	-1.57	-0.17	-	-0.04	-0.01	-0.01	0.08	-	0.09	0.02	10	58.10	-92.47	4.93	0.02	0.61
	-1.57	-0.17	-	-0.04	0.00	-	0.08	-0.01	0.08	0.02	10	58.10	-92.47	4.94	0.02	0.61
	-1.57	-0.18	-0.03	-0.01	0.00	-0.01	0.06	-	0.09	0.00	11	59.36	-92.16	5.24	0.02	0.61
	-1.57	-0.17	-0.03	-0.02	0.01	-	0.07	-0.01	0.07	0.00	11	59.33	-92.12	5.29	0.02	0.61
	-1.57	-0.14	-0.04	0.04	0.02	-	-	-	0.07	-0.01	9	56.43	-91.85	5.55	0.01	0.58
	-1.57	-0.17	-	-0.04	0.00	-0.02	0.08	-0.01	0.09	-	10	57.79	-91.85	5.56	0.01	0.59
	-1.57	-0.14	-0.03	0.03	0.02	-	-	0.01	0.08	-	9	56.30	-91.60	5.80	0.01	0.58
	-1.57	-0.12	-	0.02	0.01	-	-	-	0.08	-	7	53.38	-90.95	6.45	0.01	0.55
	-1.57	-0.17	-0.03	-0.04	-0.01	-0.03	0.07	-0.03	0.09	0.00	12	59.98	-90.49	6.91	0.01	0.61

Table A3.3 Parameter estimates and model fit for top size spectra model set (ΔAICc < 7). All models within 7 AIC units of the top ranked model are included (DF = degrees of freedom; LL = log-likelihood) .

				Island geomorphology					*Environmental*			*Model fit*				
	Intercept	Humans	Complexity	Atoll - high	Atoll - low	Bathy. slope	Land area	Reef area	min SST	Prod.	DF	LL	AICc	ΔAICc	weight	R^2
Distance to market	6.22	-0.44	0.13	-0.24	-0.11	-0.13	-	-	0.37	0.22	10	-464.18	952.10	0.00	0.25	0.58
	6.23	-0.39	0.14	-0.23	-0.09	-	-	-	0.26	0.24	9	-465.55	952.10	0.00	0.25	0.56
	6.22	-0.45	0.15	-0.14	-0.03	-	-	0.10	0.31	0.22	10	-464.75	953.24	1.14	0.14	0.58
	6.22	-0.42	0.15	-0.27	-0.09	-	0.07	-	0.27	0.25	10	-465.32	954.37	2.27	0.08	0.58
	6.22	-0.44	0.14	-0.26	-0.11	-0.13	0.03	-	0.37	0.23	11	-464.15	954.85	2.75	0.06	0.59
	6.22	-0.45	0.13	-0.22	-0.10	-0.12	-	0.02	0.37	0.22	11	-464.15	954.86	2.76	0.06	0.58
	6.22	-0.49	-	-0.23	-0.13	-0.15	-	-	0.38	0.18	9	-467.45	955.90	3.80	0.04	0.58
	6.22	-0.46	0.16	-0.16	-0.04	-	0.03	0.09	0.31	0.22	11	-464.72	955.99	3.89	0.04	0.58
	6.23	-0.43	-	-0.23	-0.11	-	-	-	0.25	0.19	8	-469.07	956.50	4.41	0.03	0.56
	6.23	-0.44	-	-0.17	-0.12	-0.17	-0.09	-	0.38	0.17	10	-466.90	957.54	5.44	0.02	0.56
	6.22	-0.45	0.14	-0.23	-0.10	-0.12	0.02	0.02	0.37	0.22	12	-464.13	957.74	5.64	0.01	0.59
	6.22	-0.45	-	-0.30	-0.17	-0.20	-	-0.07	0.38	0.19	10	-467.19	958.10	6.00	0.01	0.58
	6.23	-0.40	-	-0.20	-0.10	-	-0.06	-	0.23	0.19	9	-468.84	958.68	6.59	0.01	0.54
	6.22	-0.47	-	-0.19	-0.08	-	-	0.04	0.27	0.18	9	-468.92	958.83	6.73	0.01	0.56
Human population density	6.21	-0.44	0.12	-0.42	-0.23	-	0.17	-	0.21	0.33	10	-461.20	946.13	0.00	0.16	0.58
	6.22	-0.36	0.09	-0.31	-0.20	-	-	-	0.19	0.30	9	-462.65	946.30	0.16	0.14	0.53
	6.22	-0.40	-	-0.31	-0.20	-	-	-	0.17	0.27	8	-464.25	946.86	0.73	0.11	0.54
	6.22	-0.43	-	-0.32	-0.24	-0.12	-	-	0.27	0.27	9	-462.98	946.97	0.83	0.10	0.56
	6.22	-0.39	0.08	-0.33	-0.24	-0.11	-	-	0.27	0.30	10	-461.65	947.03	0.90	0.10	0.55
	6.22	-0.40	0.10	-0.25	-0.18	-	-	0.08	0.22	0.29	10	-462.01	947.75	1.61	0.07	0.55
	6.21	-0.45	0.11	-0.41	-0.25	-0.08	0.14	-	0.27	0.32	11	-460.69	947.93	1.79	0.06	0.58
	6.21	-0.46	0.12	-0.37	-0.21	-	0.15	0.05	0.23	0.32	11	-461.01	948.56	2.43	0.05	0.58
	6.21	-0.45	-	-0.36	-0.21	-	0.09	-	0.18	0.28	9	-463.83	948.65	2.52	0.04	0.56
	6.22	-0.43	-	-0.26	-0.18	-	-	0.06	0.20	0.27	9	-463.92	948.84	2.70	0.04	0.55
	6.22	-0.46	-	-0.35	-0.24	-0.11	0.06	-	0.27	0.28	10	-462.78	949.29	3.16	0.03	0.57
	6.22	-0.42	-	-0.34	-0.26	-0.14	-	-0.03	0.28	0.27	10	-462.93	949.60	3.46	0.03	0.55

6.22	-0.39	0.09	-0.31	-0.23	-0.09	-	0.02	0.27	0.29	11	-461.63	949.80	3.67	0.02	0.55
6.21	-0.45	0.11	-0.42	-0.25	-0.08	0.14	0.00	0.27	0.32	12	-460.69	950.85	4.71	0.01	0.58
6.22	-0.47	-	-0.31	-0.19	-	0.07	0.04	0.20	0.28	10	-463.69	951.10	4.97	0.01	0.56
6.22	-0.45	-	-0.41	-0.27	-0.14	0.08	-0.05	0.28	0.28	11	-462.65	951.84	5.71	0.01	0.57
6.22	-0.43	-	-0.32	-0.24	-0.12	-	-	0.27	0.27	9	-462.98	946.97	0.83	0.10	0.56
6.22	-0.39	0.08	-0.33	-0.24	-0.11	-	-	0.27	0.30	10	-461.65	947.03	0.90	0.10	0.55
6.22	-0.40	0.10	-0.25	-0.18	-	-	0.08	0.22	0.29	10	-462.01	947.75	1.61	0.07	0.55
6.21	-0.45	0.11	-0.41	-0.25	-0.08	0.14	-	0.27	0.32	11	-460.69	947.93	1.79	0.06	0.58
6.21	-0.46	0.12	-0.37	-0.21	-	0.15	0.05	0.23	0.32	11	-461.01	948.56	2.43	0.05	0.58
6.21	-0.45	-	-0.36	-0.21	-	0.09	-	0.18	0.28	9	-463.83	948.65	2.52	0.04	0.56
6.22	-0.43	-	-0.26	-0.18	-	-	0.06	0.20	0.27	9	-463.92	948.84	2.70	0.04	0.55
6.22	-0.46	-	-0.35	-0.24	-0.11	0.06	-	0.27	0.28	10	-462.78	949.29	3.16	0.03	0.57
6.22	-0.42	-	-0.34	-0.26	-0.14	-	-0.03	0.28	0.27	10	-462.93	949.60	3.46	0.03	0.55
6.22	-0.39	0.09	-0.31	-0.23	-0.09	-	0.02	0.27	0.29	11	-461.63	949.80	3.67	0.02	0.55
6.21	-0.45	0.11	-0.42	-0.25	-0.08	0.14	0.00	0.27	0.32	12	-460.69	950.85	4.71	0.01	0.58
6.22	-0.47	-	-0.31	-0.19	-	0.07	0.04	0.20	0.28	10	-463.69	951.10	4.97	0.01	0.56
6.22	-0.45	-	-0.41	-0.27	-0.14	0.08	-0.05	0.28	0.28	11	-462.65	951.84	5.71	0.01	0.57

Table A3.4 Parameter estimates and model fit for top biomass model set (ΔAICc < 7). All models within 7 AIC units of the top ranked model are included (DF = degrees of freedom; LL = log-likelihood).

				Island geomorphology					*Environmental*		*Model fit*					
	Intercept	Humans	Complexity	Atoll - high	Atoll - low	Bathy. slope	Land area	Reef area	min SST	Prod.	DF	LL	AICc	ΔAICc	weight	R^2
Proximity to market	-2.42	-0.24	-	0.11	0.10	-	0.07	-	0.15	-	8.00	12.88	-7.39	0.00	0.14	0.44
	-2.42	-0.19	-	0.16	0.09	-	-	-	0.13	-	7.00	11.50	-7.19	0.20	0.12	0.42
	-2.42	-0.21	-	0.15	0.08	-0.06	-	-	0.19	-	8.00	12.61	-6.87	0.53	0.10	0.44
	-2.42	-0.25	-	0.11	0.09	-0.05	0.06	-	0.19	-	9.00	13.65	-6.30	1.10	0.08	0.45
	-2.42	-0.22	-	0.19	0.11	-	-	0.04	0.16	-	8.00	12.11	-5.86	1.53	0.06	0.43
	-2.42	-0.25	0.03	0.10	0.10	-	0.09	-	0.15	-	9	13.29	-5.59	1.81	0.06	0.45
	-2.42	-0.25	-	0.13	0.11	-	0.06	0.02	0.16	-	9	12.97	-4.94	2.45	0.04	0.44
	-2.42	-0.24	-	0.11	0.10	-	0.07	-	0.15	0.00	9	12.88	-4.76	2.63	0.04	0.44
	-2.42	-0.19	-	0.16	0.09	-	-	-	0.13	0.00	8	11.50	-4.64	2.76	0.03	0.42
	-2.42	-0.19	0.00	0.16	0.09	-	-	-	0.13	-	8	11.50	-4.64	2.76	0.03	0.42
	-2.42	-0.22	-	0.16	0.09	-0.06	-	0.01	0.19	-	9	12.64	-4.29	3.11	0.03	0.44
	-2.42	-0.22	-	0.15	0.09	-0.07	-	-	0.19	-0.01	9	12.63	-4.26	3.13	0.03	0.44
	-2.42	-0.26	0.02	0.10	0.09	-0.05	0.08	-	0.19	-	10	13.99	-4.24	3.15	0.03	0.46
	-2.42	-0.21	0.00	0.15	0.08	-0.06	-	-	0.19	-	9	12.62	-4.23	3.16	0.03	0.44
	-2.42	-0.25	-	0.09	0.08	-0.07	0.07	-0.02	0.19	-	10	13.74	-3.75	3.65	0.02	0.46
	-2.42	-0.26	-	0.11	0.09	-0.06	0.06	-	0.19	-0.01	10	13.69	-3.65	3.74	0.02	0.45
	-2.42	-0.22	0.01	0.19	0.11	-	-	0.05	0.16	-	9	12.23	-3.46	3.94	0.02	0.43
	-2.42	-0.23	-	0.19	0.11	-	-	0.05	0.16	-0.01	9	12.15	-3.30	4.09	0.02	0.43
	-2.42	-0.25	0.03	0.12	0.11	-	0.08	0.03	0.16	-	10	13.50	-3.27	4.12	0.02	0.45
	-2.42	-0.24	0.03	0.10	0.10	-	0.09	-	0.15	0.00	10	13.31	-2.88	4.51	0.01	0.45
	-2.42	-0.25	-	0.13	0.11	-	0.06	0.02	0.16	-0.01	10	13.00	-2.27	5.12	0.01	0.44
	-2.42	-0.19	0.00	0.16	0.09	-	-	-	0.13	0.00	9	11.50	-2.00	5.39	0.01	0.42
	-2.42	-0.23	-	0.16	0.09	-0.06	-	0.01	0.19	-0.01	10	12.67	-1.62	5.78	0.01	0.44
	-2.42	-0.22	0.01	0.16	0.09	-0.05	-	0.02	0.19	-	10	12.66	-1.59	5.80	0.01	0.44
	-2.42	-0.22	0.00	0.15	0.09	-0.07	-	-	0.19	-0.01	10	12.63	-1.53	5.86	0.01	0.44
	-2.42	-0.25	0.02	0.09	0.09	-0.06	0.08	-0.01	0.19	-	11	14.00	-1.44	5.95	0.01	0.46
	-2.42	-0.26	0.02	0.10	0.09	-0.05	0.08	-	0.19	0.00	11	13.99	-1.42	5.97	0.01	0.46

	-2.42	-0.25		-	0.09	0.08	-0.07		0.07	-0.02		0.19	-0.01	11	13.75	-0.95	6.44	0.01	0.46
	-2.42	-0.22	0.01		0.19	0.11	-		-	0.05		0.16	-0.01	10	12.25	-0.76	6.63	0.00	0.43
	-2.42	-0.26	0.03		0.12	0.11	-		0.08	0.03		0.16	0.00	11	13.50	-0.45	6.95	0.00	0.45
	-2.42	-0.28		-	0.06	0.04		-	0.14	-		0.09	-	8	17.84	-17.33	0.00	0.26	0.51
	-2.42	-0.27		-	0.03	0.01	-		0.15		-	0.10	0.05	9	18.72	-16.43	0.89	0.16	0.52
	-2.42	-0.28		-	0.06	0.03	-0.04		0.13	-		0.12	-	9	18.35	-15.70	1.63	0.11	0.51
	-2.42	-0.29	-		0.08	0.04		-	0.13	0.02		0.10	-	9	18.02	-15.05	2.28	0.08	0.51
	-2.42	-0.28	-0.01		0.07	0.04	-		0.14		-	0.09	-	9	17.93	-14.86	2.47	0.07	0.51
	-2.42	-0.28		-	0.03	0.00	-0.04		0.15	-		0.13	0.04	10	19.17	-14.61	2.72	0.07	0.53
	-2.42	-0.28		-	0.04	0.02		-	0.15		0.01	0.11	0.04	10	18.78	-13.84	3.49	0.04	0.52
	-2.42	-0.27		0.01	0.01	0.00		-	0.16	-		0.11	0.06	10	18.77	-13.81	3.52	0.04	0.53
	-2.42	-0.29	-0.01		0.07	0.03		-0.04	0.13	-		0.12	-	10	18.50	-13.26	4.06	0.03	0.51
	-2.42	-0.28	-		0.06	0.03	-0.04		0.13		0.00	0.12	-	10	18.35	-12.97	4.36	0.03	0.51
	-2.42	-0.29		-0.01	0.09	0.04		-	0.13	0.02		0.10	-	10	18.08	-12.42	4.91	0.02	0.51
	-2.42	-0.27		-	0.01	-0.01	-0.05		0.15		-0.01	0.14	0.05	11	19.21	-11.87	5.46	0.02	0.53
	-2.42	-0.27		0.00	0.02	0.00	-0.04		0.15	-		0.14	0.05	11	19.18	-11.80	5.52	0.02	0.53
	-2.42	-0.27	0.01		0.03	0.01		-	0.16		0.01	0.12	0.05	11	18.84	-11.13	6.19	0.01	0.53
	-2.42	-0.19		-	0.16	0.06	-		-		-	0.08	-	7	13.27	-10.74	6.59	0.01	0.45
	-2.42	-0.28	-0.02		0.06	0.02	-0.05		0.13	-0.01		0.12	-	11	18.52	-10.48	6.85	0.01	0.51
	-2.42	-0.22		-	0.19	0.06		-	-		0.06	0.11	-	8	14.39	-10.42	6.91	0.01	0.46

Human population density

Table A3.5 Parameter estimates and model fit for top length spectra model set (ΔAICc < 7). All models within 7 AIC units of the top ranked model are included (DF = degrees of freedom; LL = log-likelihood)

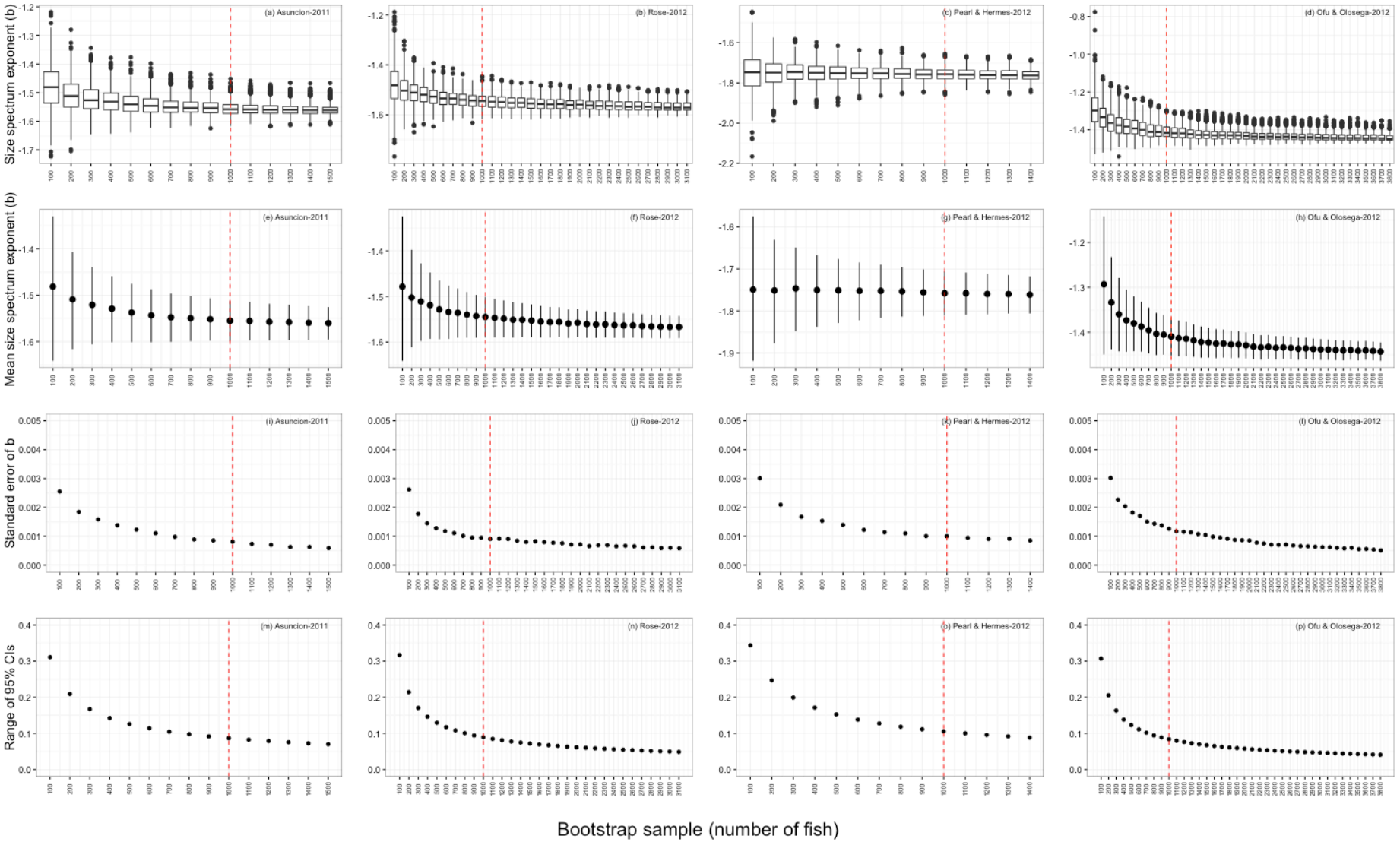
(a) Asuncion-2011
(b) Rose-2012
(c) Pearl & Hermes-2012
(d) Ofu & Olosega-2012
(e) Asuncion-2011
(f) Rose-2012
(g) Pearl & Hermes-2012
(h) Ofu & Olosega-2012
(i) Asuncion-2011
(j) Rose-2012
(k) Pearl & Hermes-2012
(l) Ofu & Olosega-2012
(m) Asuncion-2011
(n) Rose-2012
(o) Pearl & Hermes-2012
(p) Ofu & Olosega-2012
Size spectrum exponent (b)
Mean size spectrum exponent (b)
Standard error of b
Range of 95% CIs
Bootstrap sample (number of fish)

Figure A3.1 Sensitivity of size spectrum exponent to bootstrap sample size. Size spectrum exponent estimates were estimated following a bootstrap procedure in which 1,000 replicates were produced for sample sizes ranging from 100 individuals to the maximum number of individuals observed at each island-year, for increasing increments of 100 individuals. For 4 island-year combinations, we present boxplots of size spectrum exponents (a, e, i, m), mean exponents with 95% confidence intervals (b, f, j, n), standard error of exponents (c, g, k, o), and range of 95% confidence intervals (d, h, l, p), across the bootstrap sample size. Boxplots represent the median value bounded by the 25th and 95th percentiles, with lines extending to 1.5 x the distance between 25th and 75th percentiles and outliers as solid points. Bootstrap sample selected for main analysis was 1,000 individuals (red dashed line). The sample size sensitivity analysis for every island-year is available at github.com/baumlab/robinson-reefs-spectra.

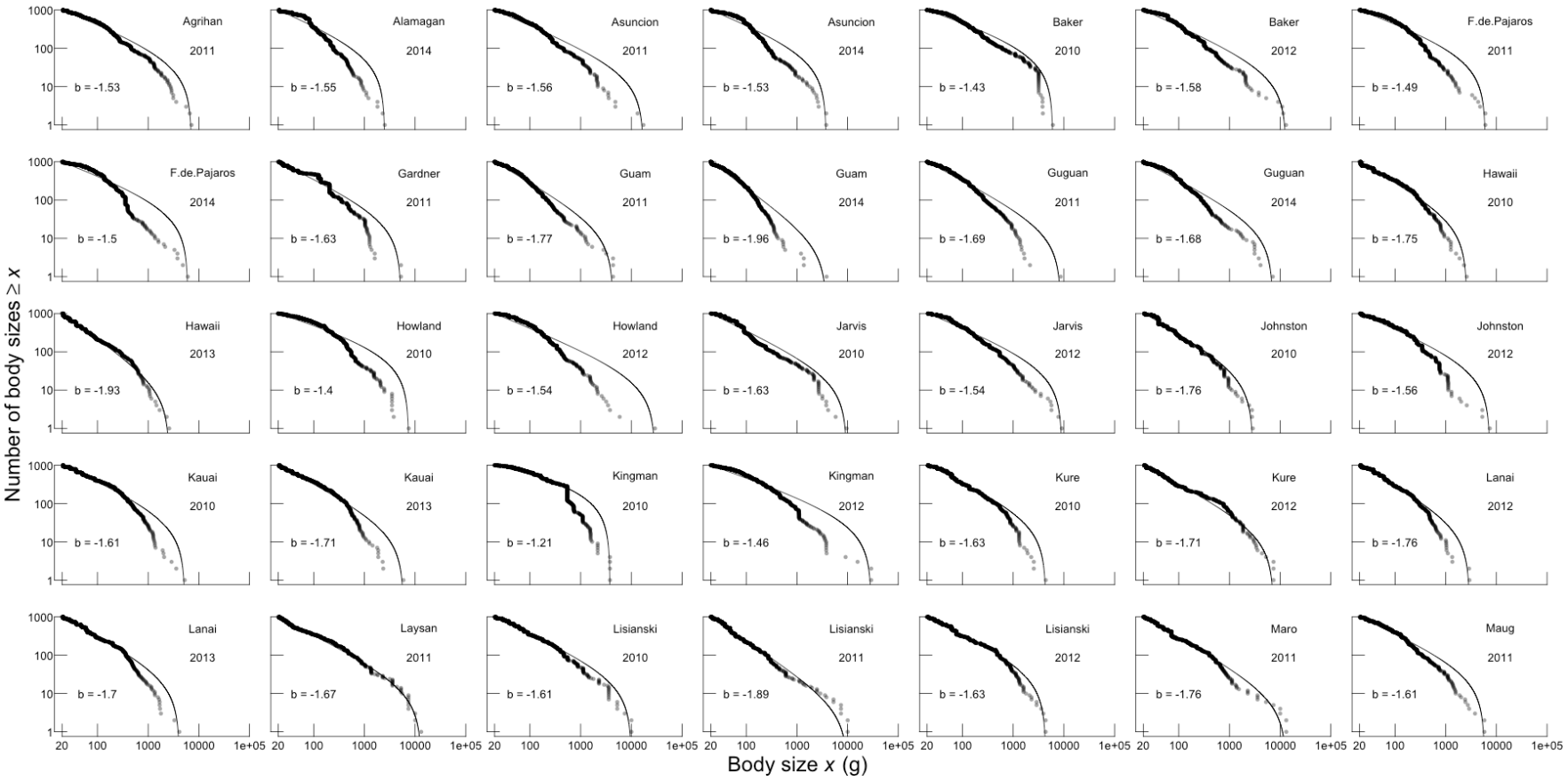
Agrihan 2011 b = -1.53
Alamagan 2014 b = -1.55
Asuncion 2011 b = -1.56
Asuncion 2014 b = -1.53
Baker 2010 b = -1.43
Baker 2012 b = -1.58
F.de.Pajaros 2011 b = -1.49
F.de.Pajaros 2014 b = -1.5
Gardner 2011 b = -1.63
Guam 2011 b = -1.77
Guam 2014 b = -1.96
Guguan 2011 b = -1.69
Guguan 2014 b = -1.68
Hawaii 2010 b = -1.75
Hawaii 2013 b = -1.93
Howland 2010 b = -1.4
Howland 2012 b = -1.54
Jarvis 2010 b = -1.63
Jarvis 2012 b = -1.54
Johnston 2010 b = -1.76
Johnston 2012 b = -1.56
Kauai 2010 b = -1.61
Kauai 2013 b = -1.71
Kingman 2010 b = -1.21
Kingman 2012 b = -1.46
Kure 2010 b = -1.63
Kure 2012 b = -1.71
Lanai 2012 b = -1.76
Lanai 2013 b = -1.7
Laysan 2011 b = -1.67
Lisianski 2010 b = -1.61
Lisianski 2011 b = -1.89
Lisianski 2012 b = -1.63
Maro 2011 b = -1.76
Maug 2011 b = -1.61
1000
100
10
1
20 100 1000 10000 1e+05
Number of body sizes ≥ x
Body size x (g)

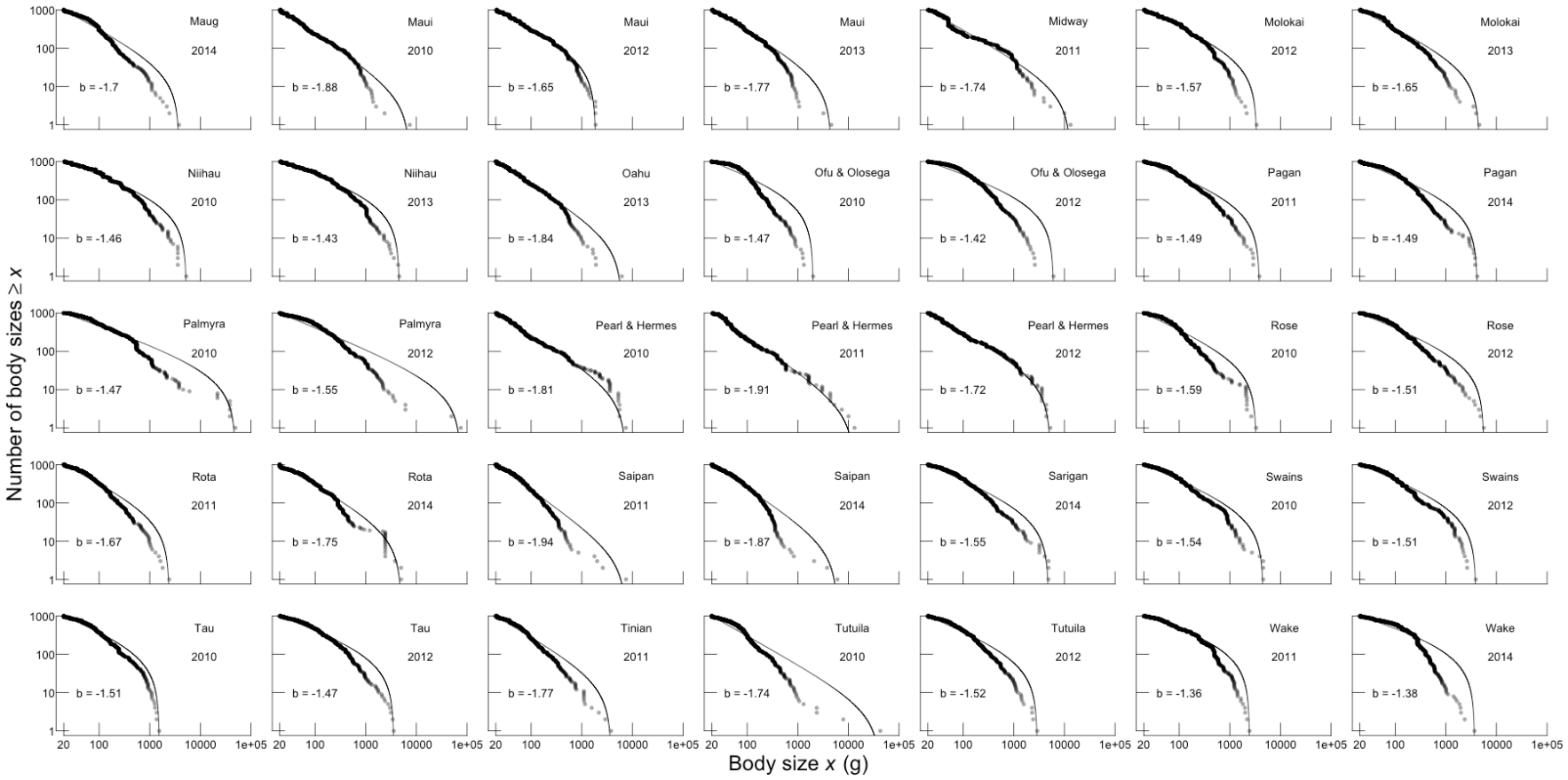

Figure A3.2 Fit of size spectrum model to reef fish data. Rank-frequency plots show the number of body sizes ≥ x against body size, where each point is the mass of an individual fish (g) and fitted size spectrum model is indicated by the solid line. Each panel is a single bootstrap sample of 1,000 fish from each island-year combination, annotated with the size spectrum exponent estimate (*b*).

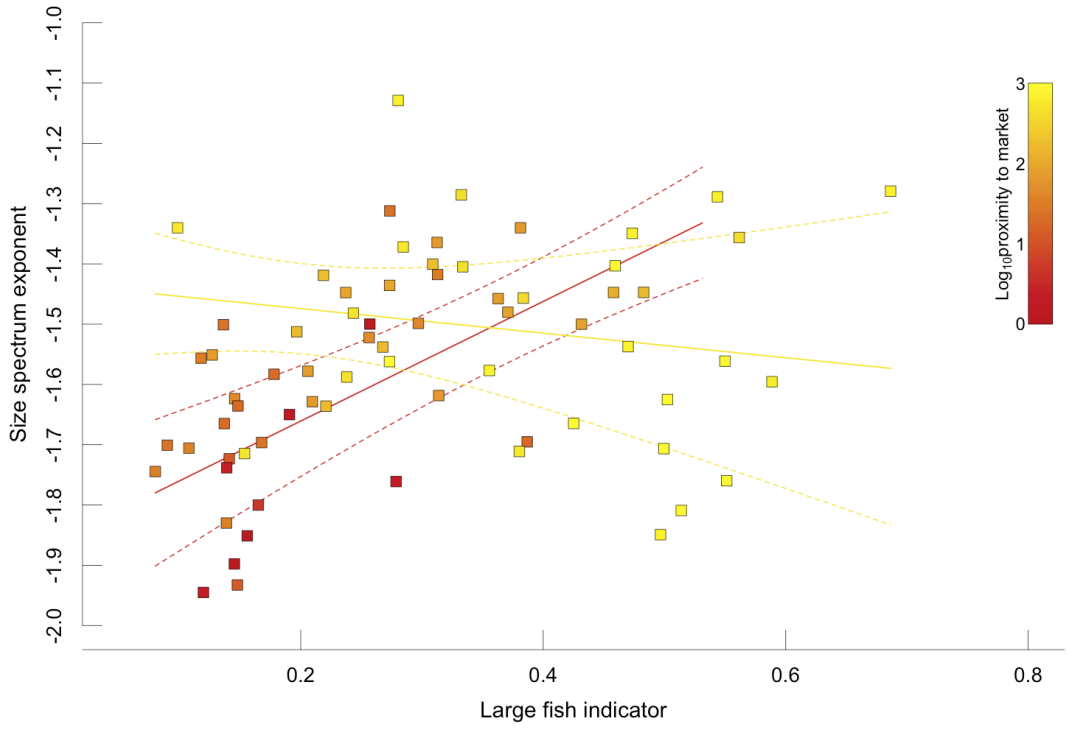

Figure A3.3 Relationship between size spectra exponents and the LFI. Each point is a size spectrum exponent and LFI (large fish indicator = biomass of fish > 1kg divided by total fish biomass) estimate at one island in a single survey year, and coloured according to $\log_{10}$ proximity to market estimates. Linear regression (solid line) and 95% confidence intervals (dashed lines) are parameter estimates from a linear mixed effects model with survey year as a random effect and habitation (unpopulated, populated) as an interaction effect. Size spectra ~ LFI relationships were significantly different between uninhabited (yellow line) and populated (red line) islands.

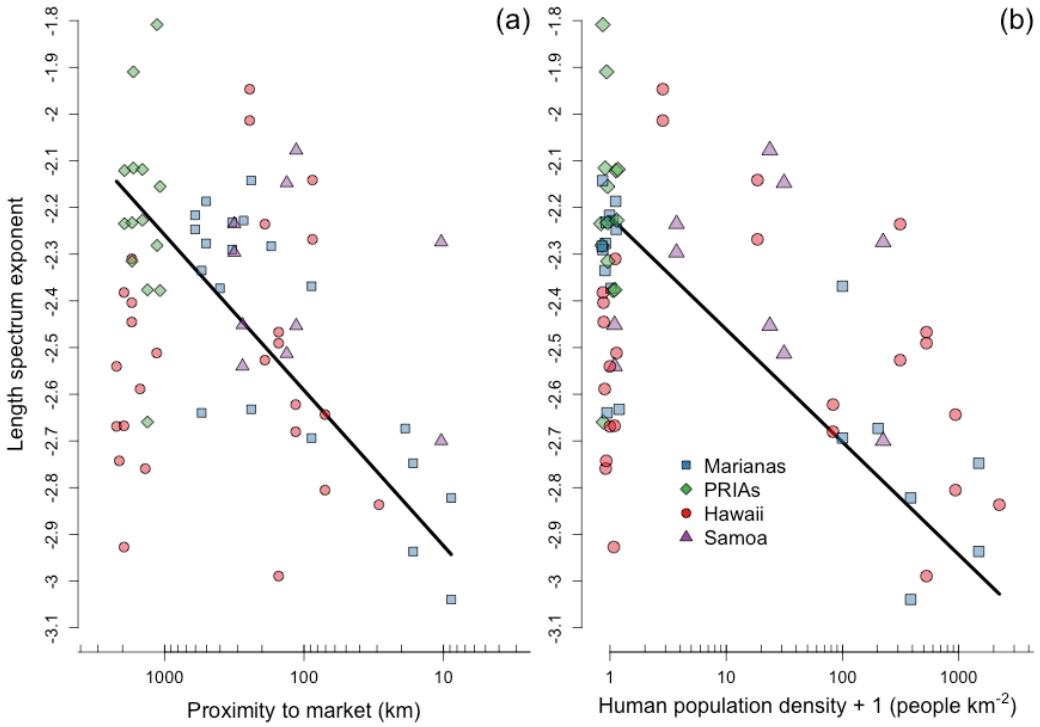

Figure A3.4 Length spectra exponents across proximity to market (a) and human population density (b). Length spectra relationships are model-averaged predictions across the standardized range of observed $\log_{10}$ proximity to provincial capital (km) and $\log_{10}$ human population density per forereef area (km^2) (a, b respectively). Predictions were made across the top model set (ΔAICc < 7) and weighted using model probabilities, while holding all other relevant covariates to their mean observed value (Table A3.5). Dashed lines are the weighted sample variance at each value of human covariate (though these are indistinguishable here from model predictions). For visualization purposes, we included the observed data as points and coloured by region (blue squares = Marianas archipelago; red circles = Hawaiian archipelago, green diamonds = Pacific Remote Island Areas, purple triangles = American Samoa). Unpopulated islands have been jittered to distinguish between points with human population density = 0 (b, d).

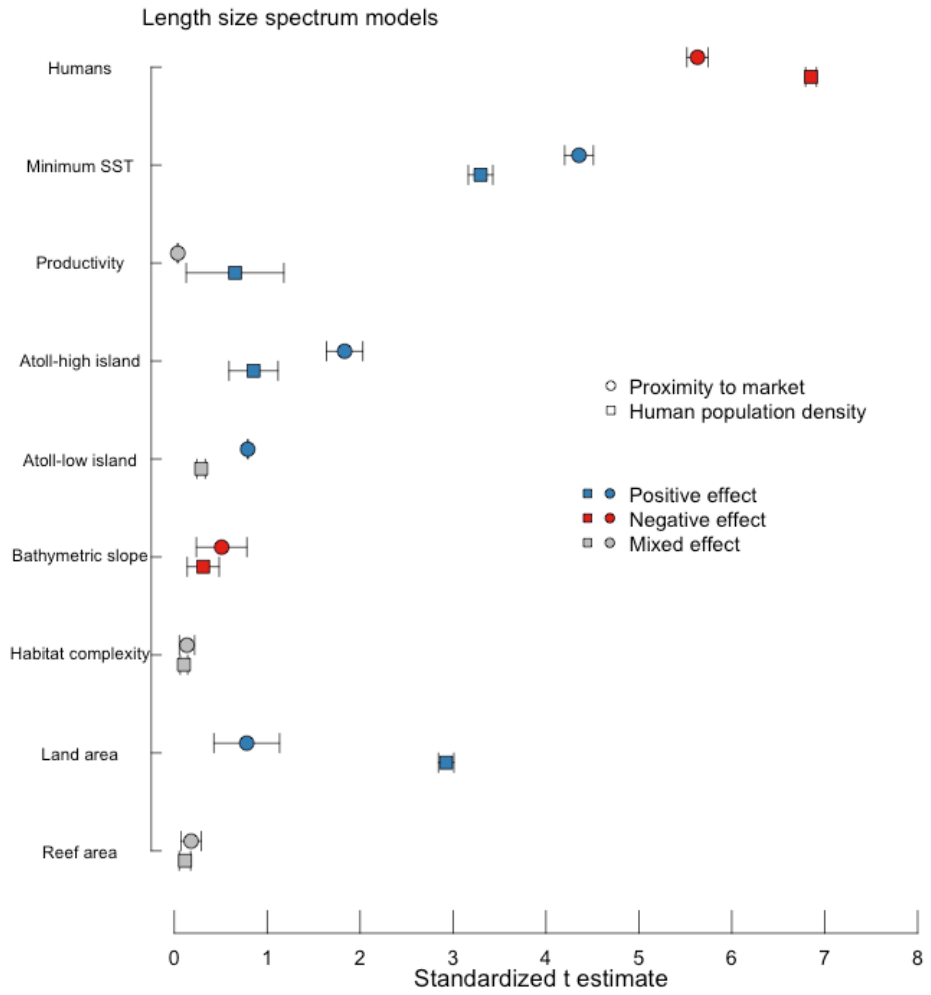

Figure A3.5 Model parameter estimates for length spectra. Length spectra are for the distance to market (circles) and human population density (squares) full model sets. Points are the weighted absolute t-values for each explanatory covariate, with weighted sample variance as error bars. T-values indicate the magnitude of each covariate effect, and colors indicate the direction of each covariate effect (blue = positive; red = negative; grey = mixed). See Table A3.5 for further details.

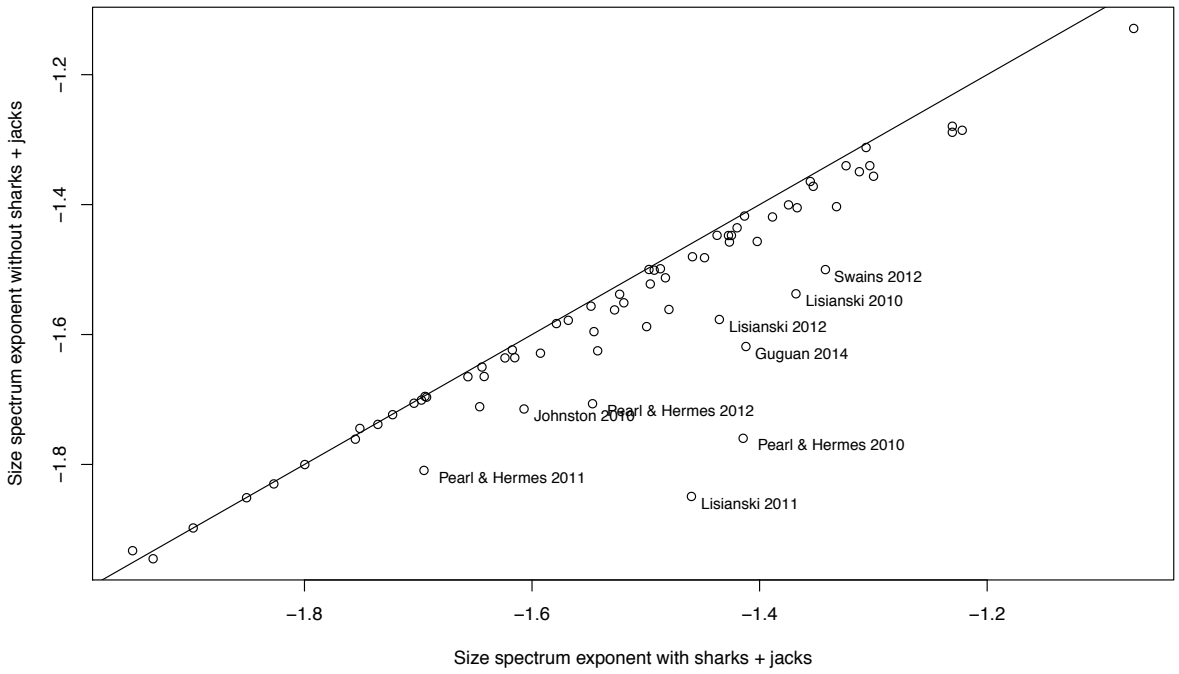

Figure A3.6 Influence of shark and jack species on size spectrum exponent. Points indicate the size spectrum exponent at each island-year, estimated with (x) and without (y) shark and jack species included. Large outliers (annotated points) were observed at islands where sharks and jacks were the highest relative abundance. All points fell below the 1:1 line, indicating that including shark and jack species would produce shallower size spectra.

Appendix C: Supplemental information for Chapter 4

			Number of grids per grain (km^2)							*PSI*			*Hard coral cover (%)*			*Macroalgal cover (%)*		
Region	Island	UVCs	0.25	1	4	16	64	256	1,024	min	mean	max	min	mean	max	min	mean	max
Hawaiian archipelago	French Frigate	15	14	12	12	8	7	6	3	-3.07	-0.57	3.24	0	30.53	90	0	10.86	60
	Gardner	10	2	3	3	2	1	1	1	0.1	1.3	3.16	0	9.39	15	0	29.16	60
	Hawaii	100	92	85	70	51	33	20	8	-2.79	-0.67	1.43	2	25.67	75	0	2.74	25
	Kauai	47	47	43	35	28	16	9	5	-0.3	0.84	2.7	1	7.42	20	0	18.74	50
	Kure	29	25	20	14	8	3	2	1	-0.76	0.61	4.19	0	17.91	40	0	21.4	80
	Lanai	69	59	45	36	17	10	5	4	-2.26	-0.06	3.77	1	23.82	75	0	12.55	75
	Laysan	16	15	15	9	6	3	2	4	0.52	1.9	4.44	0	11.17	30	5	39.05	85
	Lisianski	56	55	47	35	21	10	5	2	-2.99	-0.38	3.28	0	37.9	85	0	18.44	65
	Maro	20	20	20	18	13	8	3	3	-2.29	-0.01	3.78	5	30.66	75	1	19.64	75
	Maui	107	98	78	62	40	26	15	7	-2.86	-0.15	3.53	1	20.58	80	0	9.28	95
	Midway	17	15	13	11	11	5	2	2	0.11	1.01	4.23	0	3.33	10	0	17.66	80
	Molokai	88	84	71	46	25	15	8	4	-3.02	0	2.96	0	21.5	85	0	12.2	60
	Necker	8	6	5	3	2	2	1	1	0.31	1.07	2.13	5	8.68	15	5	23.29	50
	Nihoa	7	5	3	2	2	1	1	1	-0.04	0.29	1.3	5	6.09	7.5	0	5.4	25
	Niihau	39	38	39	27	18	8	4	4	-0.18	0.48	1.69	0	3.79	20	0	6.64	25
	Oahu	102	96	91	67	47	26	13	7	-1.46	0.39	3.57	0	13.1	60	0	13.64	75
	Pearl & Hermes	45	41	37	28	16	11	6	4	-0.94	1.27	4.46	0	6.27	40	1	31.31	90
Marianas archipelago	Agrihan	20	19	16	10	7	4	4	1	-1.36	-0.16	1.02	0	18.61	45	0	5.47	32
	Aguijan	23	18	12	6	4	2	1	1	-0.96	0.98	2.62	1	15.11	40	0	27.91	60
	Alamagan	16	15	13	7	4	4	4	2	-2.26	-0.15	0.5	1	18.08	50	0	5.03	20
	Asuncion	41	20	10	6	4	2	2	1	-1.34	-0.24	0.46	1	17.59	45	0	3.91	16.67
	Farallon de Pajaros	23	13	7	3	4	1	1	1	-0.74	-0.19	0.25	0.5	13.29	35	0	2.47	14
	Guam	179	148	118	73	37	19	8	4	-2.56	0.61	4.38	1	19.85	85	0	23.59	95
	Guguan	21	16	11	6	2	1	1	1	-1.08	-0.17	0.63	1	15.95	50	0	4.11	16.67
	Maug	70	28	15	8	4	2	2	2	-1.98	-0.68	0.52	2	27.96	56.25	0	3.8	17.5
	Pagan	70	53	42	22	12	3	1	2	-1.46	-0.02	1	1	14.36	40	0	6.47	30

	Rota	51	40	32	19	8	4	3	2	-2.18	0.99	4.51	1	11.82	77	0	23.69	90
	Saipan	74	65	53	39	19	9	4	3	-2.56	0.14	2.36	1	17.2	60	0	11.51	43
	Sarigan	20	17	11	6	4	2	2	1	-0.75	0.22	1.24	2	12.72	40	0	8.62	40
	Tinian	35	33	25	22	12	4	2	1	-1.71	0.54	3.34	2	15.7	67.5	0	17.6	70
PRIAs	Baker	45	22	9	5	3	2	1	2	-2.86	-0.99	0.17	7	37.63	85	0	3.54	15
	Howland	55	19	9	5	3	2	1	1	-2.16	-0.71	-0.1	10	29.51	60	0	5.14	11
	Jarvis	60	28	13	6	2	1	1	1	-1.86	-0.1	1.18	7.5	20.65	45	0	9.08	17.5
	Johnston	17	15	12	10	7	6	3	1	-1.57	-0.13	0.4	1	13.58	80	0	4.02	10
	Kingman	45	39	29	21	10	5	4	1	-2.18	-0.53	1.07	5	31.33	60	0	7.67	20
	Palmyra	75	57	41	19	9	3	2	1	-2.18	-0.27	1.25	5	24.56	60	0	9.92	35
	Wake	73	36	24	15	7	4	2	2	-1.38	-0.48	0.6	10	28.82	60	0	7.63	27.5
American Samoa	Ofu & Olosega	60	45	28	13	6	4	1	2	-1.72	-0.29	0.99	5	23.95	57.5	0	9.26	42
	Rose	57	22	12	6	2	1	1	2	-0.87	0.33	1.14	3	17.44	43.33	0	15.77	37.5
	Swains	62	16	12	5	3	2	1	1	-2.02	0.05	1.79	18	36.15	60	2.5	24.68	50
	Tau	46	38	27	15	9	3	2	2	-1.39	-0.3	0.64	3	23.95	50	0	8.03	29
	Tutuila	190	146	99	58	28	12	5	5	-2.04	-0.18	3.75	1	20.95	75	0	8.69	77

Table A4.1 Summary of spatial grains and PSI for each Pacific island surveyed by CREP. For each island, the total number of UVC sites and number of grids per grain scale is shown with the corresponding mean, minimum and maximum estimates for the PSI, hard coral cover, and macroalgal cover across scales.

		Grazing biomass (kg ha^{-1})							*Population density*		*Travel time (hrs)*	
Region	Island	total_herb	cropper	scraper/excavator	browser	min_SST (°C)	Prod (mg C m^{-2} day^{-1})	Wave (KWhr m^{-1})	5 km	20 km	nearest settlement	nearest market
Hawaiian archipelago	French Frigate	126.28	51.68	11.46	11.00	22.34	565	116829	0	0	1861	2568
	Gardner	182.45	142.73	0.54	13.34	21.57	642	290404	0	0	2507	3207
	Hawaii	122.59	77.64	17.00	12.39	23.68	481	40412	1320	16301	9	105
	Kauai	92.01	58.91	17.76	6.88	23.07	536	155020	3648	21890	15	468
	Kure	182.51	37.36	24.90	39.43	18.66	582	183942	0	0	4856	6418
	Lanai	115.91	55.34	23.97	14.96	23.76	535	32437	5	8438	16	272
	Laysan	148.93	83.59	6.43	20.70	21.09	533	186497	0	0	3295	4309
	Lisianski	199.64	65.70	20.61	16.28	20.86	618	198300	0	0	3554	4938
	Maro	93.38	39.28	6.19	13.76	21.24	660	86094	0	0	3120	3948
	Maui	99.16	54.60	15.54	16.70	23.44	541	56386	4053	43167	4	294
	Midway	220.71	54.24	14.29	52.99	18.99	569	146604	0	0	4660	6136
	Molokai	129.41	64.53	25.05	14.72	23.50	567	150068	404	3843	7	189
	Necker	118.13	78.13	2.09	28.98	22.38	677	196257	0	0	1544	2133
	Nihoa	220.75	138.93	5.63	46.71	22.59	514	186742	0	0	666	1245
	Niihau	181.71	86.06	36.66	35.35	23.20	475	162811	28	163	20	590
	Oahu	53.19	39.25	4.63	5.09	23.37	549	172030	21260	263101	4	38
	Pearl & Hermes	98.57	26.27	7.80	15.31	19.23	647	183982	0	0	4350	5678
Marianas archipelago	Agrihan	178.49	49.30	63.00	39.19	25.57	301	67975	0	0	1305	1422
	Aguijan	63.54	35.91	17.22	3.90	26.32	291	120177	207	1647	52	198
	Alamagan	147.91	59.37	59.12	15.64	25.76	311	66722	0	0	865	976
	Asuncion	95.52	34.46	35.02	18.78	25.15	313	92972	0	0	1613	1662
	Farallon de Pajaros	108.72	34.23	24.66	46.94	24.72	322	104387	0	0	1642	1981
	Guam	97.77	26.60	28.12	13.03	26.42	263	53324	9435	95606	11	155
	Guguan	149.93	57.32	55.96	26.37	25.92	303	77953	0	0	755	867
	Maug	117.71	26.70	44.23	37.64	25.11	324	67980	0	0	1737	1785
	Pagan	144.71	46.51	52.96	31.70	25.67	302	74667	0	0	1056	1171

	Rota	79.45	29.92	22.36	10.48	26.40	231	40218	830	2527	15	364
	Saipan	56.02	23.97	9.26	8.21	26.24	327	45044	9860	48017	7	105
	Sarigan	135.23	59.78	47.69	19.99	25.76	303	69245	0	0	539	652
	Tinian	44.96	19.52	9.71	5.94	26.31	295	39829	908	17817	15	146
PRIAs	Baker	112.34	44.04	44.57	12.38	26.27	885	121660	0	0	1794	5114
	Howland	91.11	36.97	35.58	14.51	26.31	893	110033	0	0	1982	5350
	Jarvis	266.98	109.76	129.37	6.80	25.14	991	110884	0	0	20	6108
	Johnston	223.54	90.11	29.54	24.72	24.58	429	171434	0	0	22	3758
	Kingman	176.17	35.08	58.25	3.02	26.31	653	77142	0	0	883	5391
	Palmyra	185.48	48.11	56.12	6.77	26.30	683	68336	0	0	667	5541
	Wake	123.33	22.40	38.41	19.07	25.12	314	91836	0	0	2846	4735
American Samoa	Ofu & Olosega	184.86	50.75	40.43	7.22	26.62	316	76094	229	817	12	364
	Rose	115.67	40.59	18.65	10.46	26.47	374	111590	1	1	436	806
	Swains	44.69	19.54	13.87	4.72	27.50	350	92528	17	17	31	1124
	Tau	141.75	40.49	32.07	8.23	26.76	306	97868	390	968	22	403
	Tutuila	112.99	38.92	31.22	6.54	26.58	406	81578	8006	46371	8	70

Table A4.2 Summary of predictor covariates. Island-means for each abiotic, biotic and anthropogenic predictor covariate.

Feeding group	Definition	Functional role	Families	Species (n)
Cropper	Graze on turf algae and rarely impact the reef substrate. May also gain feed upon detritus.	Prevent algal overgrowth and clear settlement space to promote coral recruitment	Acanthuridae, Pomacanthidae, Pomacentridae, Monacanthidae, Blenniidae, Siganidae	*Acanthurus achilles, Acanthurus blochii, Acanthurus dussumieri, Acanthurus guttatus, Acanthurus leucocheilus, Acanthurus leucopareius, Acanthurus lineatus, Acanthurus maculiceps, Acanthurus nigricans, Acanthurus nigricauda, Acanthurus nigrofuscus, Acanthurus nigroris, Acanthurus olivaceus, Acanthurus pyroferus, Acanthurus triostegus, Acanthurus xanthopterus, Blenniella chrysospilos, Cantherhines sandwichiensis, Centropyge bicolor, Centropyge bispinosa, Centropyge flavissima, Centropyge heraldi, Centropyge loricula, Centropyge potteri, Centropyge shepardi, Centropyge vrolikii, Cirripectes obscurus, Cirripectes polyzona, Cirripectes vanderbilti, Cirripectes variolosus, Plectroglyphidodon lacrymatus, Plectroglyphidodon sindonis, Siganus argenteus, Siganus punctatus, Siganus spinus, Stegastes albifasciatus, Stegastes aureus, Stegastes fasciolatus, Stegastes nigricans, Zebrasoma flavescens, Zebrasoma rostratum, Zebrasoma scopas, Zebrasoma veliferum (42)*
Scraper/excavator	Graze on turf algae by lightly scraping the surface of carbonate corals	Prevent algal overgrowth and clear settlement space to promote recruitment by corals and CCA. Large-bodied individuals are bioeroders that remove large portions of dead coral substrate.	Scaridae	*Calotomus carolinus, Calotomus zonarchus, Cetoscarus ocellatus, Chlorurus frontalis, Chlorurus japanensis, Chlorurus microrhinos, Chlorurus perspicillatus, Chlorurus sordidus, Hipposcarus longiceps, Scarus altipinnis, Scarus dimidiatus, Scarus dubius, Scarus festivus, Scarus forsteni, Scarus frenatus, Scarus fuscocaudalis, Scarus ghobban, Scarus globiceps, Scarus niger,*

				Scarus oviceps, Scarus psittacus, Scarus rubroviolaceus, Scarus schlegeli, Scarus sp, Scarus spinus, Scarus tricolor, Scarus xanthopleura (27)
Browser	Feed on large macroalgal organisms	Prevent overgrowth by large macroalgae	Acanthuridae, Kyphosidae	*Naso lituratus, Naso unicornis, Naso brachycentron, Naso tonganus, Kyphosus cinerascens, Kyphosus vaigiensis, Kyphosus sandwicensis (7)*

Table A4.2 Characteristics of herbivore functional feeding groups. Each herbivorous fish species observed by CREP was assigned one of three functional feeding groups, defined following established classifications. References: Bellwood et al. (2004); Cheal et al. (2013); Deith (2014); Edwards et al. (2014); Green & Bellwood (2009); Heenan & Williams (2013); Nash et al. (2016).

		Grain size (km^2)						
		0.25	1	4	16	64	256	1,024
	Optimal model parameters							
	Learning rate	0.01	0.01	0.01	0.001	0.001	0.01	0.01
	Tree complexity	5	5	5	5	5	4	1
	Bag fraction	0.5	0.9	0.9	0.75	0.5	0.9	0.75
	Deviance explained (%)	0.43	0.44	0.35	0.41	0.30	0.29	0.32
	Mean predictive deviance	0.80	0.75	0.70	0.68	0.61	0.60	0.55
	SE predictive deviance	0.03	0.04	0.04	0.08	0.09	0.16	0.19
	Relative influence (%)							
Abiotic	SST	13.86	15.69	17.03	18.24	13.77	8.94	25.64
Abiotic	Productivity	14.49	15.35	11.90	9.27	11.44	10.55	22.19
Abiotic	Wave energy	12.90	14.02	13.76	17.80	18.41	24.93	13.65
Biotic	Total herbivore	8.71	6.99	8.21	9.10	8.35	4.68	1.32
Biotic	Cropper	9.90	7.28	4.11	7.20	5.90	2.64	3.58
Biotic	Scraper/excavator	9.87	9.95	11.96	12.56	14.86	17.62	19.75
Biotic	Browser	4.33	3.02	3.79	2.00	5.81	9.57	2.29
Biotic	Population density 5 km	5.82	4.21	3.21	3.71	2.44	0.53	0.26
Biotic	Population density 20 km	4.80	4.24	3.95	2.65	3.12	0.74	0.03
Human	Travel time to market	7.44	9.22	11.00	6.37	5.96	3.46	0.53
Human	Travel time to settlement	7.89	10.02	11.06	11.11	9.95	16.34	10.77

Table A4.3 Model parameters and relative influence (%) estimates of the optimum boosted regression tree at each spatial grain. Optimal parameter settings were selected by fitting models across all combinations of tc (1-2-3-4-5), lr (0.01, 0.001, 0.0001) and bag-fraction (0.25, 0.5, 0.75, 0.9) and identifying the parameter set with the lowest mean predictive deviance.

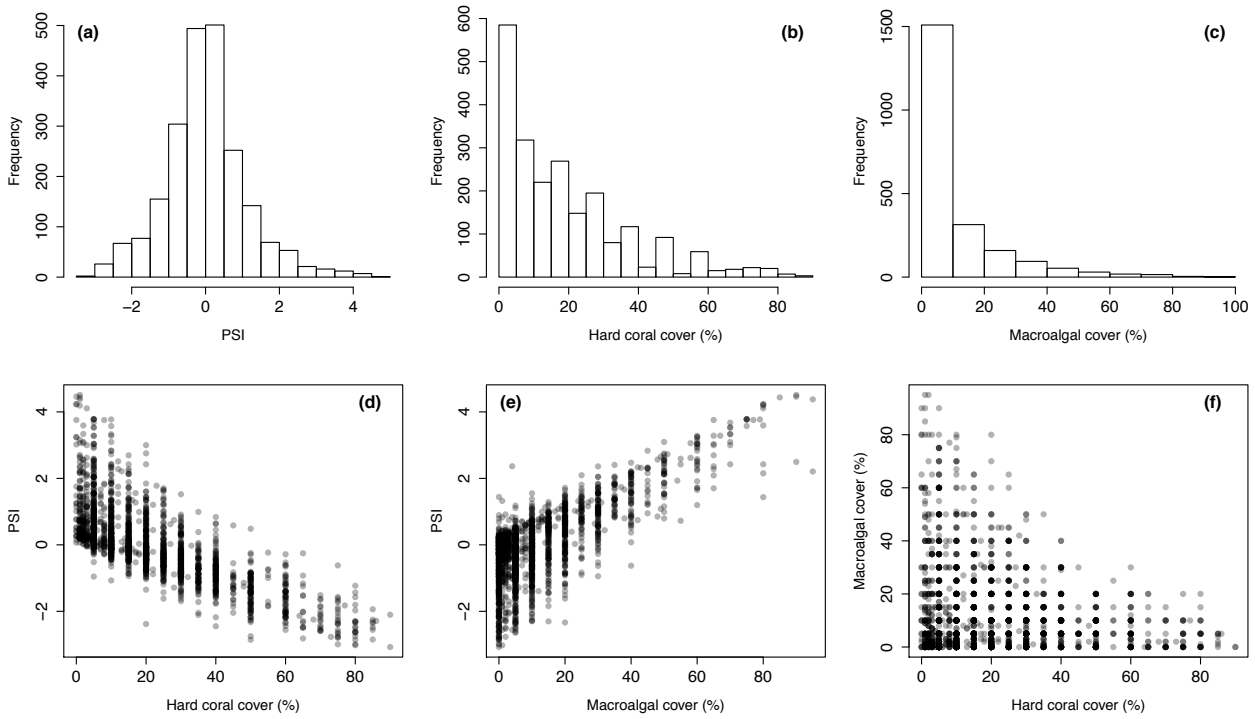

Figure A4.1 PSI, coral and macroalgal cover across UVC sites. Histograms of PSI values (a), hard coral cover (%) (b), macroalgal cover (%) (c), and scatterplots of PSI values against hard coral (d) and macroalgal cover (e), and hard coral against macroalgal cover (f). Data are site-level estimates (i.e. UVC conducted by two divers) for the full dataset (n = 2,199).

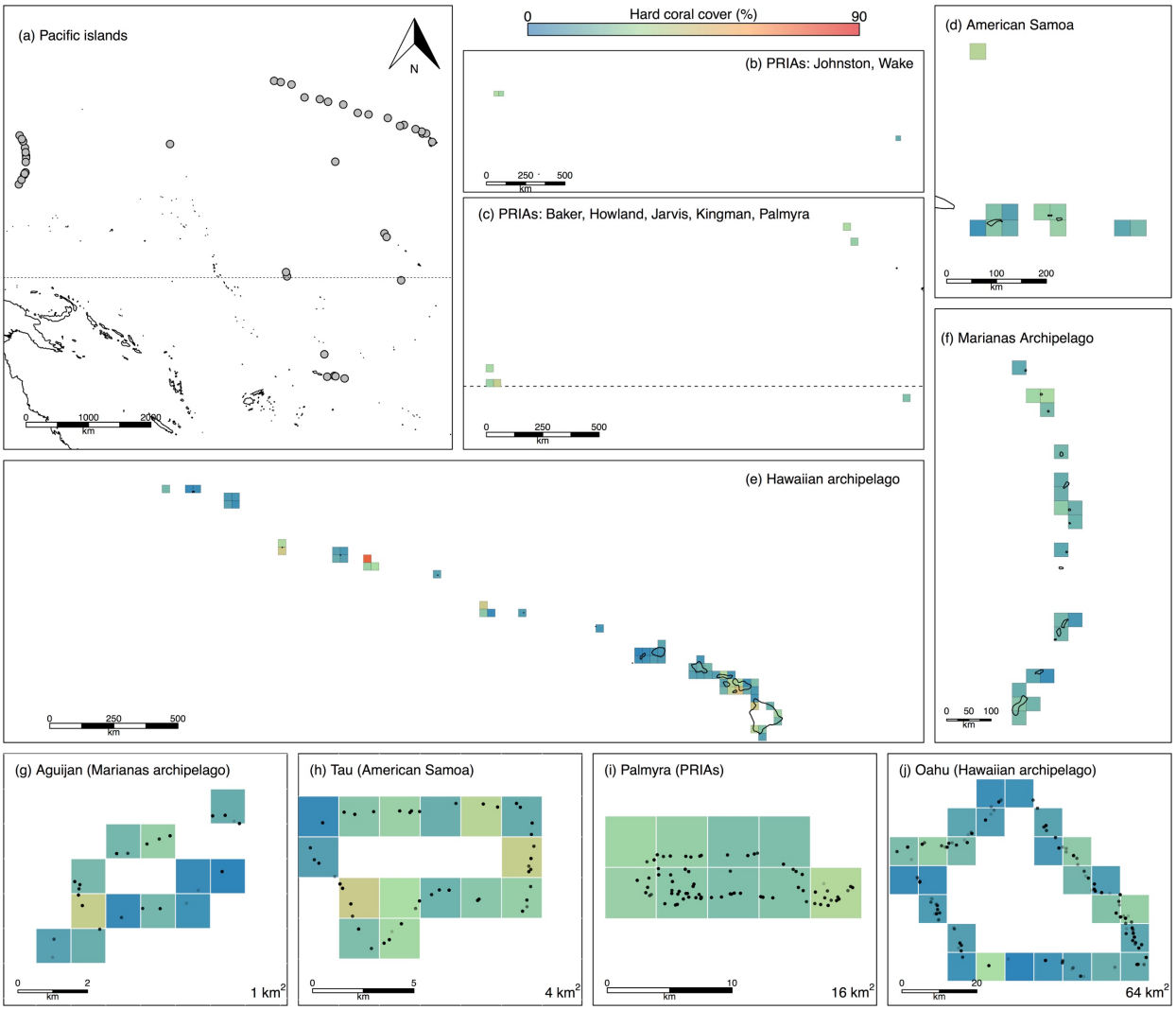

Figure A4.2 Spatial variation in reef benthic coral cover across 42 Pacific islands and atolls. For each island group (a), cells are coloured by its coral cover (%) value at the 1,024 km^2 grain scale for the Pacific Remote Island Areas (PRIAs, n = 7) (b,c), American Samoa (n = 5) (d), Hawaiian archipelago (n = 17) (e) and Marianas archipelago (n = 13) (f). Examples of smaller grain scales shown for Aguijan at 1 km^2 (g), Tau at 4 km^2 (h), Palmyra at 16 km^2 (i), and Oahu at 64 km^2 (j), overlaid by black points that indicate UVC site locations.

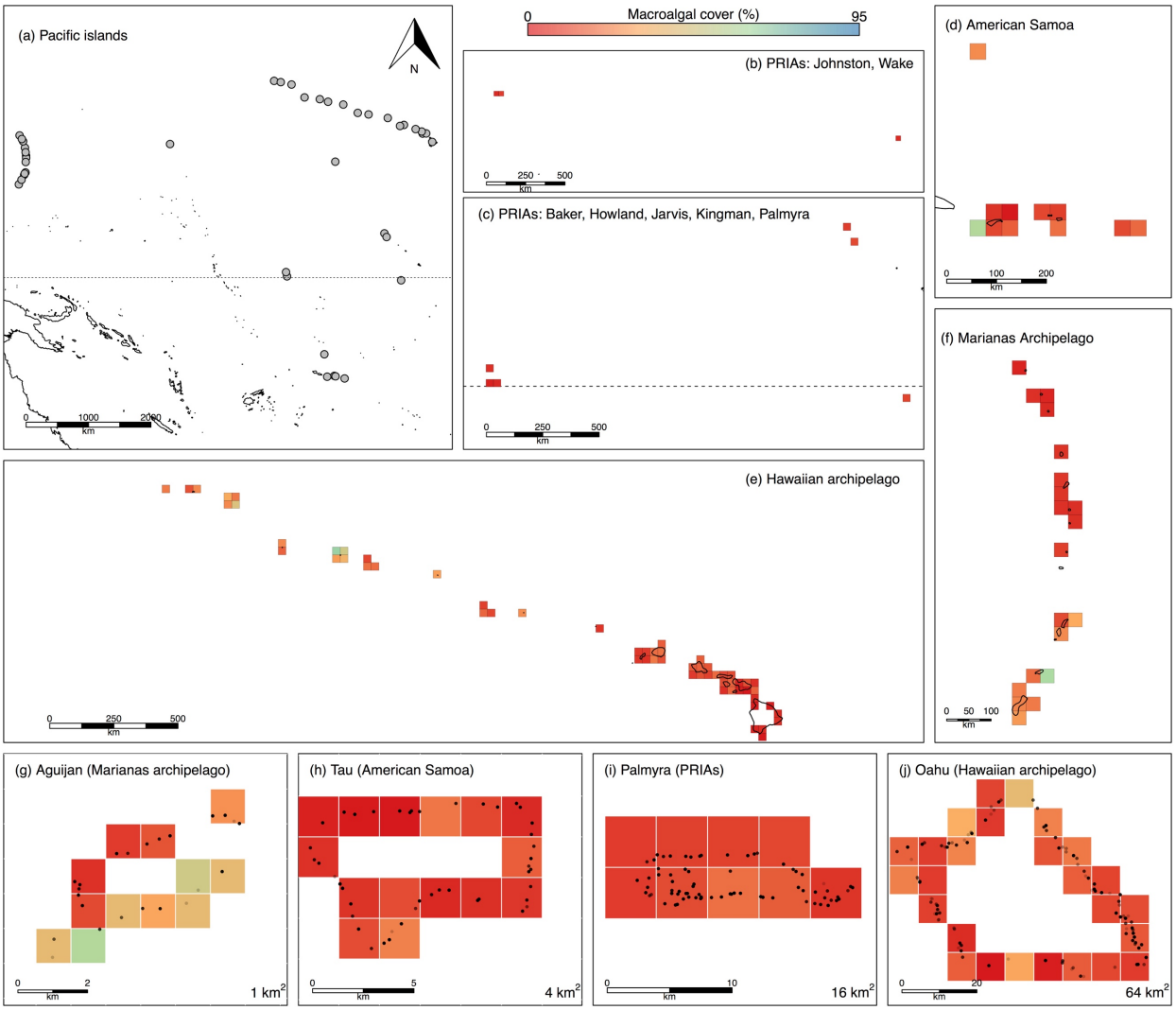

Figure A4.3 Spatial variation in reef benthic macroalgal cover across 42 Pacific islands and atolls. For each island group, cells are coloured by its macroalgal cover (%) value at the 1,024 km^2 grain scale for the Pacific Remote Island Areas (PRIAs, n = 7) (b,c), American Samoa (n = 5) (d), Hawaiian archipelago (n = 17) (e) and Marianas archipelago (n = 13) (f). Examples of smaller grain scales shown for Aguijan at 1 km^2 (g), Tau at 4 km^2 (h), Palmyra at 16 km^2 (i), and Oahu at 64 km^2 (j), overlaid by black points that indicate UVC site locations.

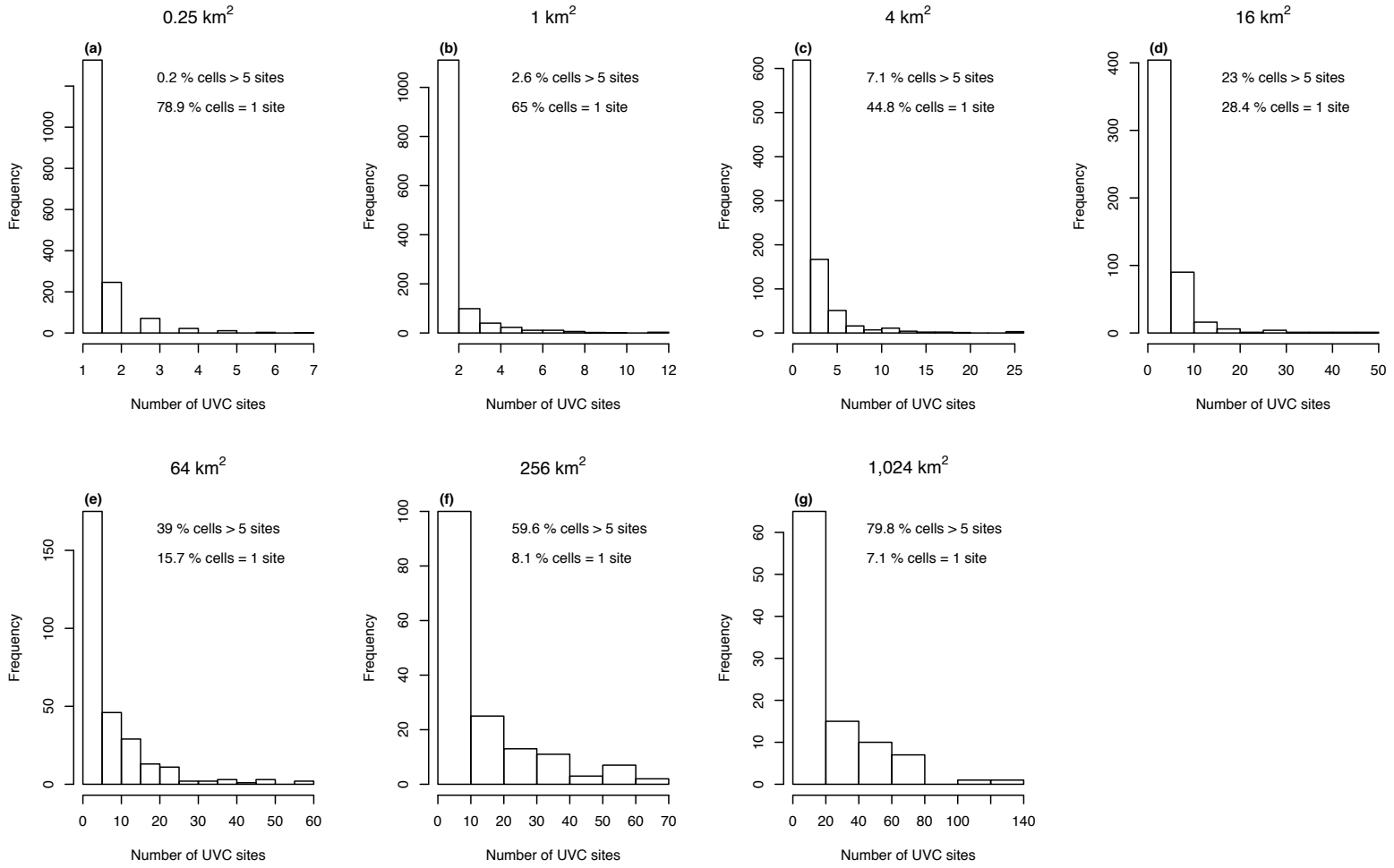

Figure A4.4 Histogram of the number of UVC sites included in each cell for each grain scale: 0.25 (a), 1 (b), 4 (c), 16 (d), 64 (e), 256 (f), and 1,024 km^2 (g). Panels are annotated with the proportion of cells containing more than 5 UVC sites and proportion of cells containing a single UVC site.

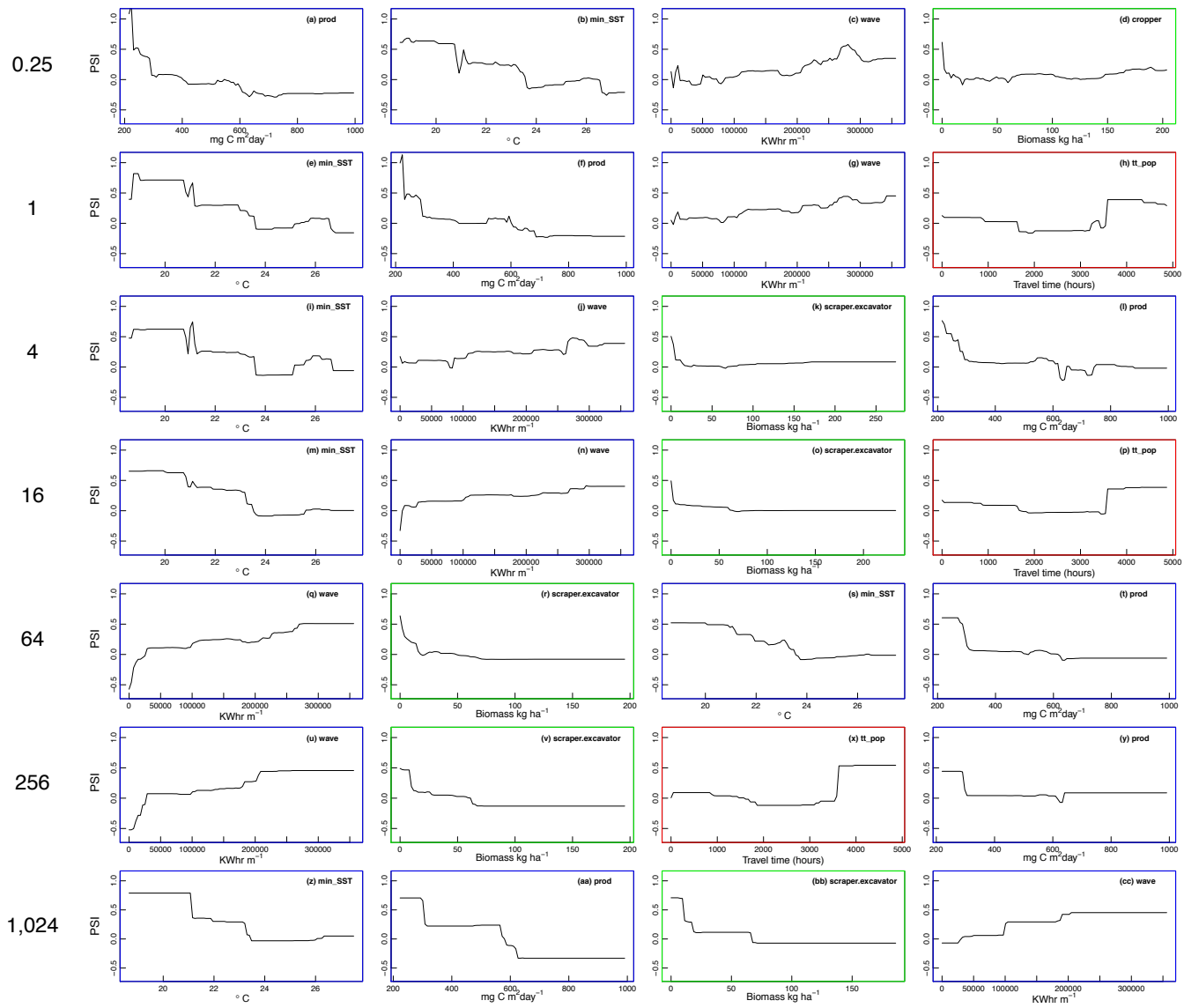

Figure A4.5 Partial dependence plots for the four most important covariates in predicting PSI values. Rows present each grain scale: 0.25 (a - d), 1 (e - h), 4 (i - l), 16 (m-p), 64 (q-t), 256 (u-y), and 1,024 km^2 (z - cc). At each scale (i.e. each row), covariate importance decreases across columns from left (most important covariate) to right (4th ranked covariate). Plots are coloured to distinguish between abiotic/bottom-up (blue), biotic (green), and anthropogenic (red) covariates, and annotated with each covariate name (min_SST = minimum SST; prod = oceanic productivity; wave = wave energy; total_herb = total herbivore biomass; cropper = cropper biomass; scraper.excavator = scraper and excavator biomass; tt_pop = travel time to nearest population centre).

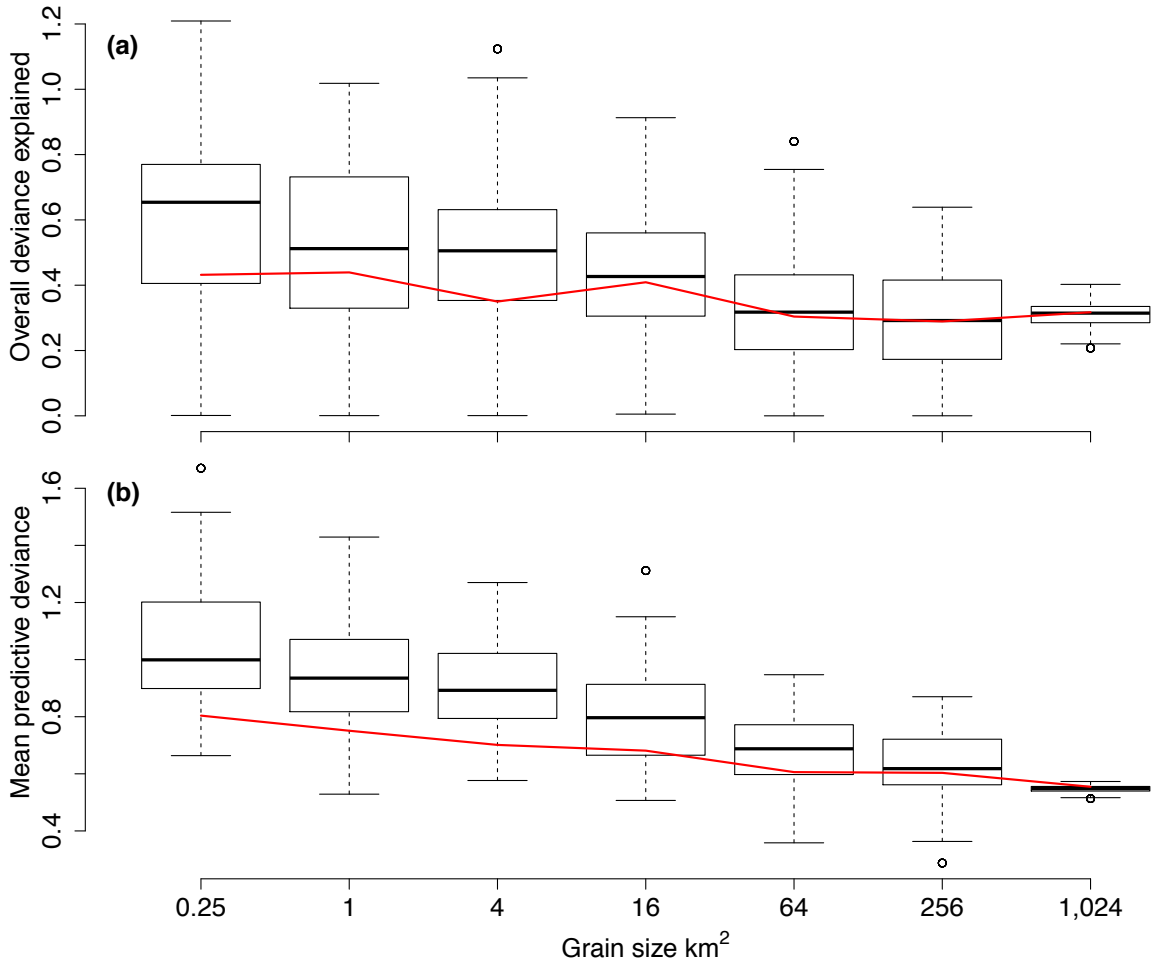

Figure A4.6 Model fit of boosted regression trees. Overall deviance explained (a) and mean predictive deviance (b) are plotted for each spatial grain for models built using the full dataset (red lines) and a reduced dataset fixed at 100 grids per grain (black boxplots). For the reduced dataset, boosted regression trees were fitted to data from 100 grids per grain, where grids were sampled randomly but equally across the four major island groups (25 grids per island group), and the process was repeated for 100 replicates. Boxplots show the median relative importance estimates with 25th and 75th quantiles, with whiskers that extend to 1.5 x the interquartile range and outliers as black circles.

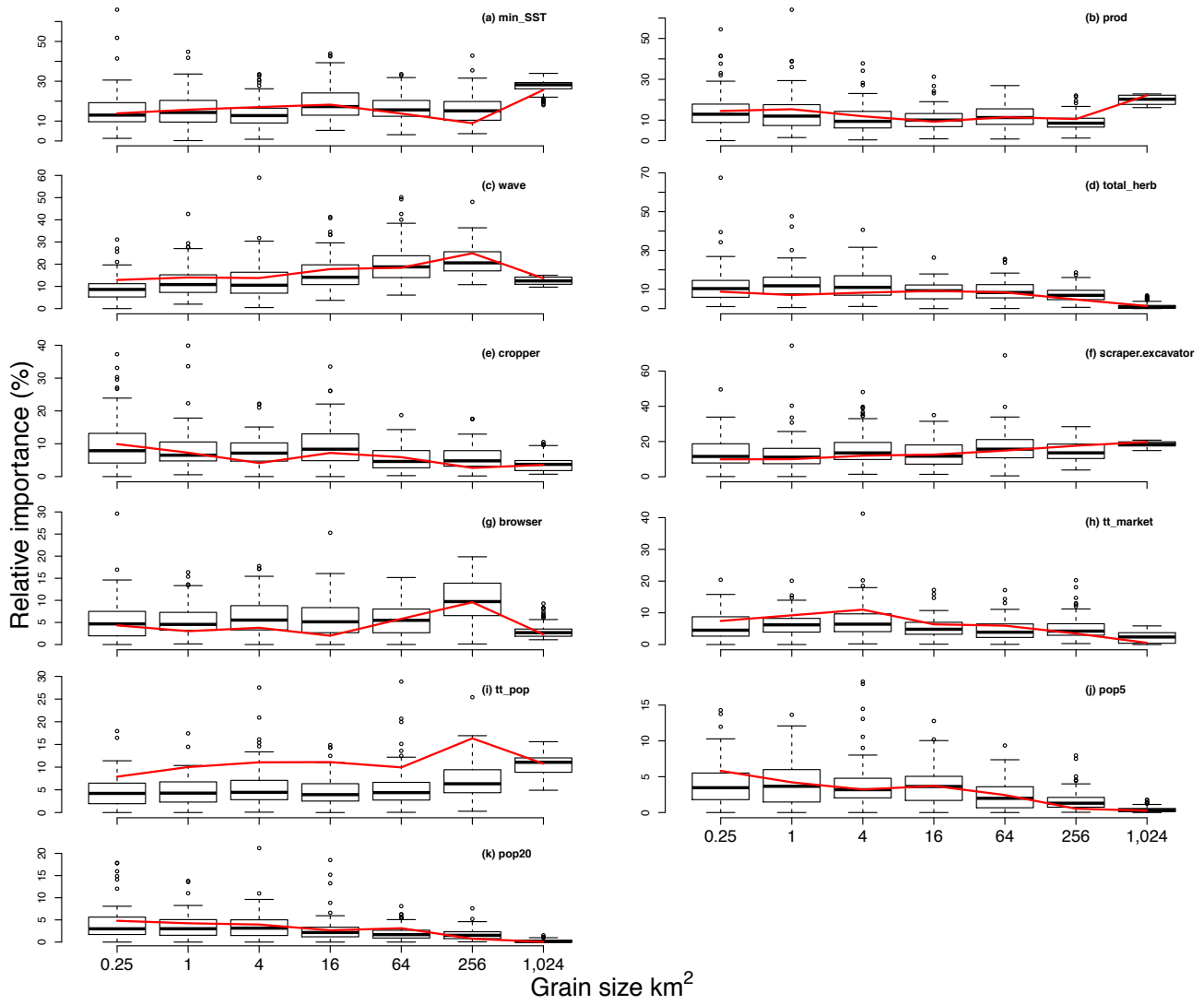

Figure A4.7 Boxplots of relative importance estimates (%) of abiotic/bottom-up (a - c), biotic (d - g) and anthropogenic (h - k) covariates in explaining variation in PSI values across 0.25 to 1,024 km^2 grain scales. Boosted regression trees were fitted using a reduced dataset of 100 grids per grain, where grids were sampled randomly but equally across the four major regions (25 grids per region), and the process was repeated for 100 replicates. Boxplots show the median relative importance estimates with 25th and 75th quantiles, with whiskers that extend to 1.5 x the interquartile range and outliers as black circles. Corresponding relative importance estimates from the main analysis are overlaid as red lines.

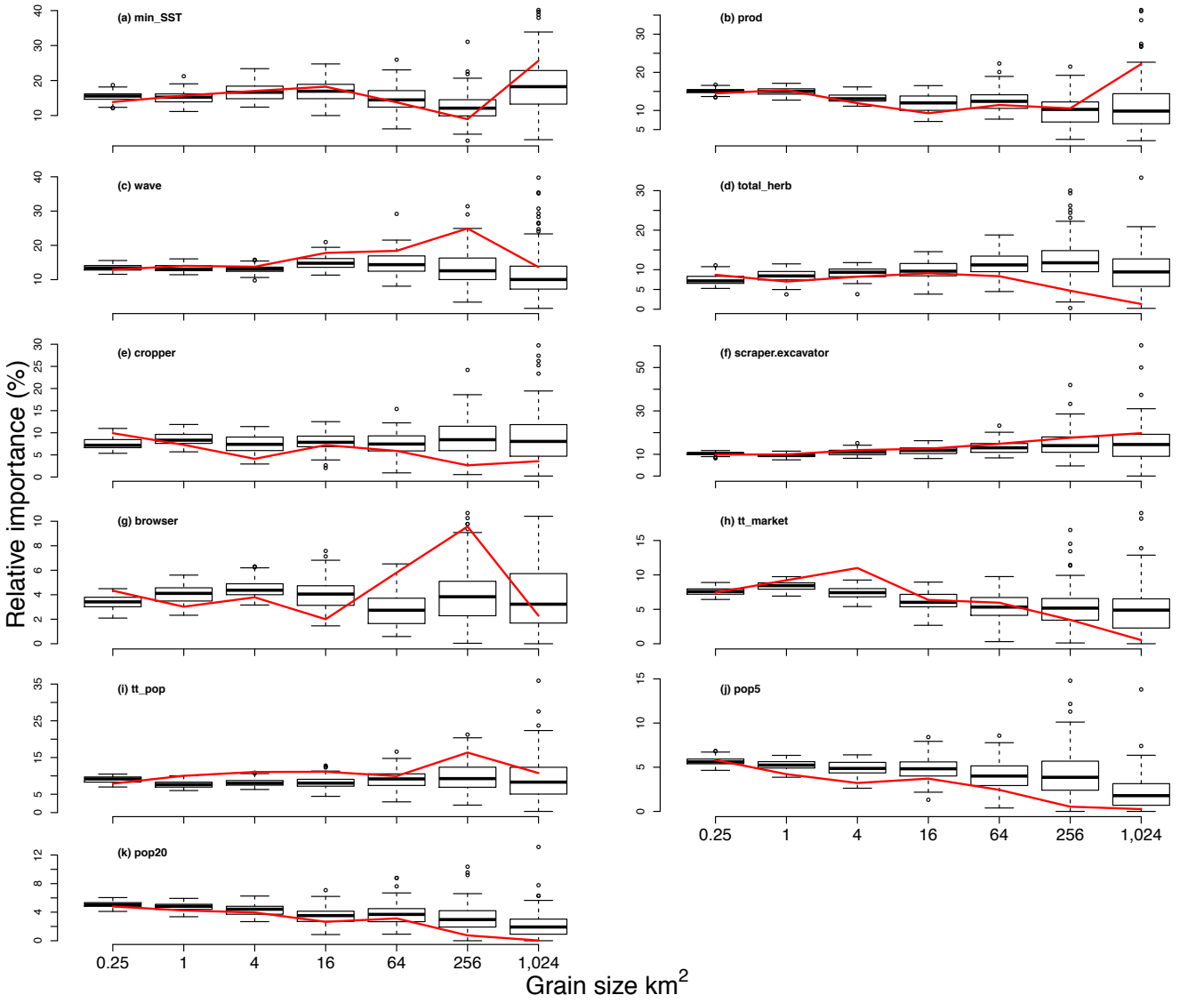

Figure A4.8 Boxplots of relative importance estimates (%) of abiotic/bottom-up (a - c), biotic (d - g) and anthropogenic (h - k) covariates in explaining variation in PSI values across 0.25 to 1,024 km^2 grain scales. Boosted regression trees were fitted using a reduced dataset generated from a random sample of 1 UVC site from each grid cell, and the process was repeated for 100 replicates. Boxplots show the median relative importance estimates with 25th and 75th quantiles, with whiskers that extend to 1.5 x the interquartile range and outliers as black circles. Corresponding relative importance estimates from the main analysis are overlaid as red lines.